

Suchart Siengchin

Natural Fiber Reinforced Thermoplastics

Suchart Siengchin

Natural Fiber Reinforced Thermoplastics



TECHNISCHE UNIVERSITÄT
CHEMNITZ

**Universitätsverlag Chemnitz
2017**

Impressum

Bibliografische Information der Deutschen Nationalbibliothek

Die Deutsche Nationalbibliothek verzeichnet diese Publikation in der Deutschen Nationalbibliografie; detaillierte bibliografische Angaben sind im Internet über <http://dnb.d-nb.de> abrufbar.

Titelfoto: Sabrina Dennise Möckel
Satz/Layout: Anja Bochmann, Ricarda Künzel-Ripp

Technische Universität Chemnitz/Universitätsbibliothek
Universitätsverlag Chemnitz
09107 Chemnitz
<http://www.tu-chemnitz.de/ub/univerlag>

readbox unipress
in der readbox publishing GmbH
Am Hawerkamp 31
48155 Münster
<http://unipress.readbox.net>

ISBN 978-3-96100-019-7

<http://nbn-resolving.de/urn:nbn:de:bsz:ch1-qucosa-222094>

Natural Fiber Reinforced Thermoplastics

Von der Fakultät für Maschinenbau der
Technischen Universität Chemnitz

genehmigte

HABILITATION

zur Erlangung des akademischen Grades

Doktoringenieur habilitus

(Dr.-Ing. habil.)

vorgelegt

Von: Dr.-Ing. Suchart Siengchin

Geboren am: 13.11.1971 in Bangkok, Thailand

Verteidigt am: 21.10.2016

Gutachter: Univ.-Prof. Dr.-Ing. habil. Prof. E. h. Prof. Lothar Kroll

Univ.-Prof. Dr.-Ing. habil. Thomas Lampke

Univ.-Prof. Dr.-Ing. André Wagenführ

Acknowledgement

First and foremost, I would like to express my special gratitude to my supervisor Prof. Dr.-Ing. habil. Lothar Kroll for his scientific support, guidance, enthusiastic encouragement and useful critiques during the planning and development of this habilitation work. Also a special thanks go to the reviewer Prof. Dr.-Ing. Thomas Lampke and Prof. Dr.-Ing. André Wagenführ and the assessors Prof. Dr.-Ing. Michael Groß, Prof. Dr.-Ing. Stephan Odenwald und Prof. Dr.-Ing. Thomas von Unwerth for their stand-by. I would like to express my special acknowledgement to Dr.-Ing. Jürgen Tröltzsch for our fruitful discussions on natural fiber composites knowledge, enlightened the perspectives of this field, also the help and friendship. Their assistance and scientific skills accelerated the progress of this habilitation significantly.

I am grateful thank to the King Mongkut's University of Technology North Bangkok (KMUTNB) for providing me the opportunity of working in an outstanding environment from the scientific and technical point of view. The support of the colleagues at the Material and Production Engineering (MPE), KMUTNB is grateful acknowledged during my stay. Many thanks to the students in my research group at Natural Composite Research Group for their kind help in the experiments.

I would like to convey my special thanks to my parents and my sisters and brother who constantly supported and encouraged me.

Suchart Siengchin

Bibliografische Beschreibung

Siengchin, Suchart

Natural Fiber Reinforced Thermoplastics

Habilitationsschrift an der Fakultät für Maschinenbau der Technischen Universität
Chemnitz, Institut für Strukturleichtbau, Chemnitz, 2016

190 Seiten

97 Abbildungen

15 Tabellen

131 Literaturzitate

Referat

Great research efforts are undertaken to produce lightweight, easy reprocessable all-polymeric composites and especially natural fiber thermoplastic polymer composites. At present natural fiber composite parts are mostly used in the automotive, and food packing, building sectors. Research activities target the production productivity, novel shaping technologies and ensuring their multifunctionality. Major aims of this work were to produce natural fiber reinforced thermoplastics and determine their structure-property relationships. Binary and hybrid composites composed of polyethylene (PE), polypropylene (PP) and polylactide (PLA), poly (hydroxybutyrate-co-hydroxyvalerate) (PHBV) with natural fibers were produced by different techniques. The dispersion of natural fibers and particles were inspected in SEM and μ CT. The thermal and mechanical properties of the related composites were determined and discussed. It was found that natural fiber worked as reinforcement in respect to most of the mechanical characteristics.

Schlagworte

Natural fiber, thermoplastic, reinforcement, hybrid composite, structure-property

Table of content

Abstract	XI
List of Abbreviations and Symbols	XVII
Chapter 1 Motivation	1
Chapter 2 Theoretical background	3
2.1 Classification of composites Polymers	3
2.2 Composite materials	4
2.2.1 Two main constituents of composite materials	4
2.2.2 Dispersion strengthened composites	5
2.2.3 Particle strengthened composites	5
2.2.4 Fiber strengthened composites	6
2.2.5 Characteristics of fiber-reinforced composites	7
2.2.6 Continuous fibers reinforcement	8
2.2.7 Discontinuous fibers reinforcement	9
2.2.8 Layered composites	10
2.2.9 Factors influencing the performance of biocomposites	11
2.3 Biocomposites	11
2.3.1 Biodegradable polymers	13
2.3.2 Natural fibers	15
2.3.3 Chemical modifications of natural fiber	21
Chapter 3 Binary composites	23
3.1 Polylactide (PLA)/flax mat composites	23
3.2 Polylactide (PLA)/woven flax textiles composites	30
3.3 Polyethylene and polypropylene/nano-silicon dioxide/flax composites .	42
3.4 Polylactide (PLA)/woven flax fiber textiles/boehmite alumina (BA)	
composites	58
Chapter 4 Hybrid composites	73
4.1 Polyethylene/nanoparticle, natural and animal composites	73

4.2 Polyethylene/Flax/SiO ₂ composites	88
4.3 Un- and Modified Polylactide (PLA) /woven Flax Fiber composites	100
4.4 Poly(butylene adipate-co-terephthalate)(PBAT)/woven flax composites	122
4.5 Poly(hydroxybutyrate-co-hydroxyvalerate)/sisal natural fiber/clay composites	140
5 References	155
Biography	167

Abstract

Biocomposites made from biodegradable polymer as matrix and natural fiber as reinforcement are certainly environmentally friendly materials. Both constituent materials are fully biodegradable and do not leave any noxious components on Earth. The natural fibers have been used as reinforcement due to their advantages compared to glass fibers such as low cost, high specific strength and modulus, low density, renewability and biodegradability. Major aims of this work were to produce natural fibers and/or nanoparticles with polyethylene (PE), polypropylene (PP) and polylactide (PLA), poly(hydroxybutyrate-co-hydroxyvalerate)(PHBV) matrices and determine their structure-property relationships. Following abstracts of the present research work are manifold:

Binary composites

Poly(lactide (PLA)/flax mat composites

The poly(lactide (PLA)/flax mat and modified PLA/flax mat composites were produced by hot press technique. Two additives of non-regulated wax/ethylene acrylate copolymer/butyl acrylate and acrylic were used as modifier for PLA. The dispersion of the flax mat in the composites was studied by scanning electron microscopy (SEM). The PLA composites were subjected to instrumented falling weight impact test. The mechanical and thermal properties of the composites were determined in tensile test, thermogravimetric analysis (TGA) and dynamic-mechanical thermal analysis (DMTA), respectively. It was found that the PLA based composites increased the impact resistance. The tensile strength value of modified PLA/flax mat composite decreased slightly compared to the PLA. The elongation at break data indicated that an improvement in ductility of modified PLA and its composites. Moreover, addition of thermal modifier enhanced thermal resistance below processing temperature of PLA and had a marginal effect on the glass transition temperature of PLA. The storage modulus master curves were constructed by applying the time-temperature superposition (TTS) principle. The principle of linear viscoelastic material was fairly applicable to convert from the modulus to the creep compliance for all systems studied.

Poly(lactide (PLA)/woven flax textiles composites

The poly(lactide (PLA)/woven flax textiles 2x2 twill and 4x4 hopsack composites were produced by interval hot press technique. Two weave styles of flax used to reinforce in PLA. The dispersion of the flax composite structures in the composites was inspected in scanning electron microscopy (SEM). The PLA composites were subjected to instrumented falling weight impact test. The mechanical properties (tensile, stiffness and

strength) of the composites were determined in tensile and dynamic-mechanical thermal analysis (DMTA) tests, respectively. SEM observed that the interfacial gaps around pulled-out fibers were improved when produced by the interval hot press. It was also found that the both styles of flax composites increased the impact resistance compared to the neat PLA. The tensile strength and stiffness value of PLA/flax composites were markedly higher than that of the neat PLA and reflect the effects of composite structures. The calculated storage creep compliance was constructed by applying the time-temperature superposition (TTS) principle. The calculated creep response of these flax composites was much lower than that of the neat PLA.

Polyethylene and polypropylene/nano-silicon dioxide/flax composites

Composites composed of polylactide (PLA), modified PLA and woven flax fiber textiles (Flax weave style of 2x2 twill and 4x4 hopsack) were produced by hot press technique. Two structurally different additives used to modify PLA. The dispersion of the flax composite structures in the composites was studied by scanning electron microscopy (SEM) and computed microtomography system (μ CT). The PLA composites were subjected to water absorption and instrumented falling weight impact tests. The thermomechanical and creep properties of the composites were determined in thermogravimetric analysis (TGA), dynamic-mechanical thermal analysis (DMTA) and short-time creep tests, respectively. It was found that the modified PLA and its composite increased the impact resistance compared to the unmodified PLA. Incorporation of flax decreased resistance to thermal degradation and increased water uptake. The impact energy and stiffness value of PLA/flax composites was markedly higher than that of PLA but reflect the effects of composite structures and flax content. The storage modulus master curves were constructed by applying the time-temperature superposition (TTS) principle. From the master curve data, the effect of modified PLA on the storage modulus was more pronounced in the low frequencies range.

Poly(lactide (PLA)/woven flax fiber textiles/boehmite alumina (BA) composites

The textile biocomposites made from woven and non-woven flax fibre reinforced poly(butylene adipate-co-terephthalate) (PBAT) were prepared by compression moulding using film stacking method. The mechanical properties (such as tensile strength and stiffness, flexural strength and modulus, and impact strength) of textile biocomposites were determined in tensile, flexural and impact tests, respectively. The PBAT-based composites were subjected to water absorption. The comparison of the mechanical properties was made between pure PBAT and textile composites. The influence of flax weave styles on the mechanical properties was also evaluated. The results showed that the strength of

the textile biocomposites was increased according to weave types of fibers, especially in the stiffness was significantly increased with the higher densification of the fibers. The 4x4-plain woven fibers (4-yard-wrap and 4-yard-weft weave direction) reinforced biocomposite indicated the highest strength and stiffness compared to the other textile biocomposites and pure PBAT. This was considered to be as the result of the character of weave style of 4x4-plain woven fibers. The aminopropyltriethoxysilane affected the mechanical properties and water absorption of the resulting composites laminates due to the surface compatibility between flax fiber and PBAT.

Hybrid composites

Polyethylene/nanoparticle, natural and animal composites

Binary and ternary composites composed of high-density polyethylene (HDPE), boehmite alumina (BA) and different kinds of natural-, animal fibers, like flax, sponge gourd (SG), palm and pig hair (PH) were produced by hot press technique. Aqueous BA suspensions were sprayed on the HDPE/flax mat to prepare nanoparticle/natural fiber reinforced ternary polymer composites followed by drying. The dispersion of the natural-, animal fibers and BA particles in the composites was studied by scanning electron microscopy (SEM) and discussed. The thermomechanical and stress relaxation properties of the composites were determined in thermogravimetric analysis (TGA), dynamic-mechanical thermal analysis (DMTA) and short-time stress relaxation tests (performed at various temperatures), respectively. The HDPE based composites were subjected to water absorption and instrumented falling weight impact tests. It was found that the all composites systems increased the stiffness, stress relaxation and reduced the impact toughness. The stress relaxation modulus of natural-, animal fiber composites were higher compared to that of the neat HDPE. This modulus increased greatly with in corporation of BA. The relaxation master curves were constructed by applying the time-temperature superposition (TTS) principle. The inverse of Findley power law could fairly applicable to describe the relaxation modulus vs. time traces for all systems studied. Incorporation of BA particles enhanced the thermal resistance which started to degrade at higher temperature compared to the HDPE/flax mat composite. The HDPE/flax mat/BA composite could reduce the water uptake.

Polyethylene/Flax/SiO₂ Composites

Composites composed of high-density polyethylene (HDPE), woven flax fiber textiles (Flax weave style of 2x2 twill and 4x4 hopsack) and silicon dioxide (SiO₂) were produced by hot press with nano spraying technique. The SiO₂ slurries were sprayed by a hand onto the both surface of the woven flax fiber. The HDPE /woven flax fibers composites with and without used nano-spraying technique were produced by hot pressing in a laboratory press. The dispersion of SiO₂ particles and flax in the composites was studied by scanning electron microscopy (SEM). The related HDPE based composites were subjected to instrumented falling weight impact test. The thermal resistance, stiffness and tensile strength properties of the composites were determined in thermogravimetric analysis (TGA), dynamic-mechanical thermal analysis (DMTA) and tensile tests, respectively. It was found that the impact energy and stiffness value of HDPE/flax composites was markedly higher than that of HDPE but reflect the effects of composite structures and flax content. Incorporation of SiO₂ particles enhanced resistance to thermal degradation. It was established that the linear viscoelastic material principle are fairly applicable to convert from the modulus to the creep compliance results.

Un- and Modified Polylactide (PLA) /woven Flax Fiber composites

Hybrid composites composed of polypropylene (PP) or high-density polyethylene (HDPE), different flax fibers (unidirectional-, biaxial and twill_{2x2}) and silicon dioxide (SiO₂) were produced by hot press technique. The ternary polymer composite was effectively fabricated by spraying SiO₂ solvents onto the surface of flax fiber. The dispersion of SiO₂ particles and flax in the composites was studied by scanning electron microscopy (SEM). The related PP and HDPE based composites were subjected to instrumented falling weight impact test. The thermal and mechanical properties of the composites were determined by thermogravimetric analysis (TGA), dynamic-mechanical thermal analysis (DMTA), creep and stress relaxation tests, respectively. It was found that thermal decomposition temperature of the PP or HDPE/flax composites increased by the addition of SiO₂ particles. The impact energy, stiffness, creep resistance and relaxation modulus value of all flax composites increased markedly compared to the PP and HDPE matrix. Time–temperature superposition (TTS) was applied to estimate the creep and relaxation modulus of the composites as a function of time in the form of a master curve. The activation energies for the all PP and HDPE composites systems studied were also calculated by using the Arrhenius equation. The generalized Maxwell model was fairly applicable to the stress relaxation results.

Poly(lactide (PLA)/woven flax fiber textiles/boehmite alumina (BA) composites

Composites composed of polylactide (PLA), woven flax fiber textiles (weave style of 2x2 twill and 4x4 hopsack) and boehmite alumina (BA) were produced by hot press. The spraying technique served for the pre-dispersion of the alumina nanoparticles. The aqueous alumina slurry was produced by mixing the water with water dispersible alumina. The dispersion of the flax structures and alumina particles in the composites was studied by scanning electron microscopy (SEM). The PLA composites were subjected to water absorption and instrumented falling weight impact tests. The creep and thermomechanical properties of the composites were determined in short-time creep tests (performed at various temperatures), thermogravimetric analysis (TGA) and dynamic-mechanical thermal analysis (DMTA), re

spectively. It was found that the incorporation of alumina particles reduced the water uptake compared to the PLA/flax blends. The impact energy and stiffness value of PLA/flax blends was markedly higher than that of PLA but reflected the effects of composite structures. Incorporation of alumina particles enhanced storage modulus and the creep resistance compared to the PLA/flax blends but slightly incremented thermal resistance at high temperature. No clear trend in the flax weave style- effect was found in the thermal behaviour. The creep master curves were constructed by applying the time-temperature superposition (TTS) principle. The Findley power law could satisfactorily describe the creep compliance vs. time traces for all systems studied.

Poly (hydroxybutyrate-co-hydroxyvalerate)/sisal natural fiber/clay composites

Poly(hydroxybutyrate-co-hydroxyvalerate)(PHBV) biocomposites different sisal containing with the fiber length of 0.25 and 5 mm, and addition of clay particles were prepared by hot compression technique. Silane (Bis(triethoxysilylpropyl)tetrasulfide) treatment has been used to modify in order to enhance the properties of related hybrid composites. The all composites were subject to water absorption test. The mechanical properties of hybrid composites such as tensile stiffness and strength, toughness and hardness determined in tensile, impact and hardness tests, respectively. It was found that tensile strength, stiffness and impact strength of long sisal fiber improved with increasing fiber content. Hardness of short sisal fiber improved with increasing fiber content. Treated Silane of long fibers at 20 wt.% loading was found to enhance the tensile strength fiber by 10% and impact strength by 750% as compared to the neat PHBV. Note that this feature was also confirmed by the appearance of a scanning electron microscopy. Moreover, the hardness and water resistance of the PHBV/sisal composites increased by the addition of clay particles. The diffusion coefficient for the PHBV and hybrid composites systems studied were also calculated.

List of Abbreviations and Symbols

Abbreviations

APS	Aminopropyltriethoxysilane
BA	Boehmite alumina
BPF	Bamboo pulp fiber
CNT	Carbon nanotube
DCP	Dicumyl peroxide
DMA	Dynamic mechanical analysis
DMTA	Dynamic mechanical thermal analysis
FH	Fluorohectorite
FRCs	Fiber reinforced composites
HDPE	High density polyethylene
IFWI	Instrumented falling weight impact
LDPE	Low density polyethylene
LVM	Linear viscoelastic material
MA	Maleic anhydride
MAA-PP	Maleic acid anhydride modified polypropylene
MFC	Microfibrillated cellulose
MFI	Melt flow index
μCT	Microtomography
NaOH	Sodium hydroxide
OMMT	Organomontmorillonite
pMDI	Diphenylmethane diisocyanate
PE	Polyethylene
PP	Polypropylene
PMMA	Poly(methyl methacrylate)
PH	Pig hair
PLA	Poly lactide
PLLA	Poly L-lactide acid
PHBV	Poly(hydroxybutyrate-co-hydroxyvalerate)
PGA	Polyglycolic acid
PBS	Polybutylene succinate
PES	Polyethylene succinate
PBAT	Polybutylene adipate-co-terephthalate
PHAs	Polyhydroxyalkanoates

PHB	Polyhydroxybutyrate
RSF	Rice straw fiber
RT	Room temperature
SEM	Scanning electron microscopy
SG	Sponge gourd
TGA	Thermogravimetric analysis
TTS	Time-temperature superposition
UD	Unidirectional
WLF	Williams-Landel-Ferry

Symbols

a_T	Shift factor
a_{cN}	Impact strength of notched specimens
B	Burger's vector of dislocations
b_n	Remaining width
C_1, C_2	Constant factors
D	Diffusion coefficient of water absorption
D', D''	Real and imaginary parts of creep compliance
D_e	Elastic creep compliance
D_v	Viscoelastic creep compliance
d	Diameter
E	Modulus of elasticity
E_c, E_m, E_p	Elastic modulus of composites
E_r	Stress relaxation modulus
E^*	Complex Young's modulus
E', E''	Storage and loss modulus
$E_a, \Delta H$	Activation energy
f	Frequency
G	Shear modulus
h	Thickness
l	Interparticle spacing
l_c	Critical length
M_t	Moisture absorption
R	Universal gas constant
SiO_2	Silicon dioxide
$\tan \delta$	Loss factor
T	Temperature
T_g	Glass transition temperature
t	Time
V_v	Void volume
V_m, V_p	Volume fraction
vol. %	Volume percent
W_f, W_m	Initial weights of components
wt. %	Weight percent
w	Energy absorbed

Greek Symbols

τ	Shear stress
σ_f, σ_m	Stress of composites
σ_0	Applied stress
ρ	Density
ε_0	Amplitude – and applied constant of strain
ω	Angular frequency
δ	Phase shift
$\alpha-, \beta-, \gamma$	Relaxation transitions
τ_{rk}	k-th relaxation time

1 Motivation

Biocomposite materials have been developed from biodegradable polymers as matrix and natural fiber as reinforcement, which have been a good alternative interest in the composite sciences because of their degradation in soil or regard to environmental condition and do not leave any pollution on the earth. In the last few years, biocomposite materials have gained a major issue that is to develop biopolymer materials reinforced with natural fibers for various applications such as marine, medical and especially automotive industries by completely considered on their mechanical properties, biodegradability and environmental impact.

For all thermoplastics, fossil fuel was used as feedstock for the thermoplastics, while plastics wasted generated each year which concern about the effects of petrochemical plastics on the environment and the increased dependence on oil and gas imports. Polymeric materials from renewable resources could become an important of solution. Over the last century, polymer matrices from renewable resources are gaining ground over conventional petroleum based matrices (e.g. polypropylene, polyethylene) because of environmental problems related to their disposal as well as concerns over petroleum availability. The raising environmental consciousness and awareness increase the using of natural fibers as reinforcements in polymer composites in order to replace synthetic fibers and reduce matrix content. The advantages of using natural fiber composite materials are lightweight, high strength, -stiffness, corrosion resistance, lower impact on the environment, and low abrasive wear for processing machinery. However, the main limitations of related composites are the most of natural fibers cannot disperse easily in thermoplastic, as well as, low compatibility between fibers and matrix polymer, which leads to lower mechanical and thermal properties of the final products, therefore the improvement of the interfacial adhesion is considered. In order to improve moisture resistance of natural fibers and interfacial adhesion between natural fibers and polymer matrices, chemical modifications of natural fibers were carried out to improve mechanical properties and interfacial adhesion of the natural fiber reinforced polymer composites. The action of a silane treatment is to create a chemical link between a reinforcement and matrix, as well as creating high fiber surface area that is necessary for optimization of fiber-matrix reinforcement and improvement of fiber-matrix-interfacial adhesion. Moreover, it is worthy note that a variety of composite structures is also associated with an increase in mechanical properties of composites. The mechanical behaviors of composite materials have a strong impact on the composite structures of the reinforcing phase.

This research work is mainly focused on the development of bio- and polymer composites using different types of natural fiber and/or nanoparticle including fiber composite structure as reinforcement and different thermoplastic and biopolymer as a matrix material. In this work the influence of the addition of natural fibers on the properties of different polyethylene (PE), polypropylene (PP) and polylactide (PLA), poly(hydroxybutyrate-co-hydroxyvalerate)(PHBV) are investigated. Based on this work the following state of art and conclusion can be drawn in separated chapters of related binary and hybrid composites.

2 Theoretical Background

2.1 Classification of composites

There are various ways of classifying composite materials the simplest may be classified as natural, and synthetic or man-made composite. The composites that occur in the nature are called naturally occurring composites. Typical examples of such composites include wood composed of cellulose and lignin, human or animal body composed of bones and tissues or even rocks and minerals. Sea shells and elephant tusk are also the examples composites provided by nature. Majority of composites materials used today are man-made. The microstructure of the man-made composites provides a convenient basis for classifying them for the purpose of study, processing and analysis. Generally composites are composed of two distinct materials. The two component materials can be combined by two ways, by inserting one material into the other called phase composition and another one is bonding them layer by layer called layered composition. The schematic of classes of composites is shown in figure 1.

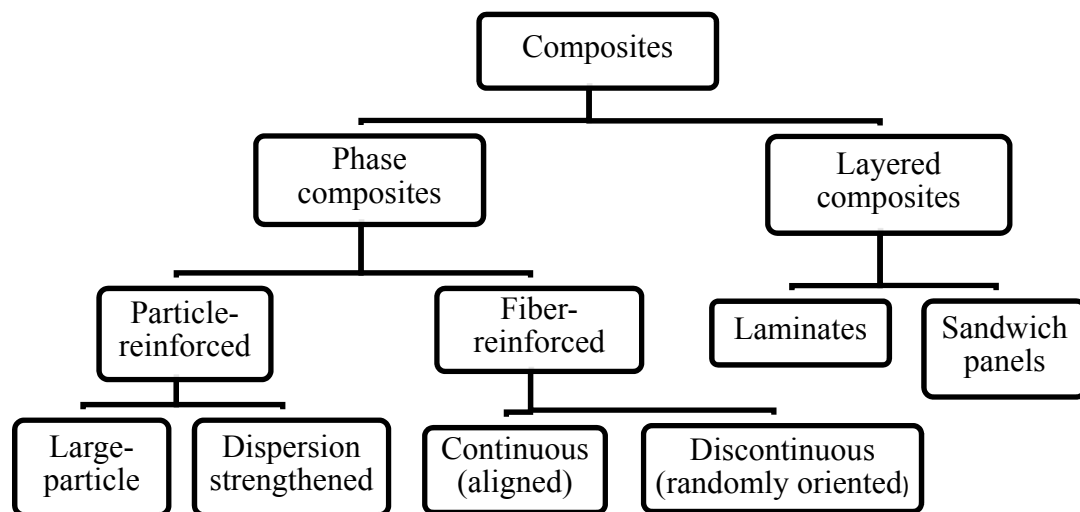


Figure 1: Schematic illustration of classes of composites.

In the phase composition, material that receives the insert is of continuous nature and is called matrix. The insert of discrete nature may be called reinforcement or filler. The multiphase composites are classed into subgroup as.

Filled composites

The primary function of insert phase is to reduce cost. In addition, the filler also alters some physical properties and even the mechanical properties in some instances for example carbon black filled natural rubber.

Reinforced composites

The primary function of insert is to improve the mechanical properties. If more than one type of material is inserted, the composite is called hybrid composite. The matrix may be a single phase or multiphase material.

2.2 Composite materials

A composite material is a combination of two or more materials that results in better properties than those of the individual components used alone. For each material retains its separate chemical, physical, and mechanical properties. The main advantages of composite materials are their high strength and stiffness. Both the matrix and reinforcement phase play an important role in the strength of composite. The matrix performs the following functions.

- a) Take the load and transfers to reinforcement.
- b) Binds or holds the reinforcement and protects the same from mechanical or chemical damage that might occur by abrasion their surface and from chemical attack by some extraneous source.
- c) Matrix also separates the individual fibers and prevents brittle crack from passing completely across the section of the composite.

The reinforcing phase is usually of low density, strong, stiff and thermally stable. The major load on composite is born by reinforcing phase. It impedes the motion of dislocations if it is in the form of dispersoids. The most common fibers are high strength, high modulus.

2.2.1 Two main constituents of composite materials

Matrices: there are three main types of man-made matrices, which are polymer, metal and ceramic. Matrices hold and protect the fibers from environmental and physical damage. Keeping the fibers separated decreases cracking and redistributes the load equally among all fibers. Therefore, the matrix contributes greatly to the properties of the com-

posites. The ability of composites to withstand heat or to conduct heat or electricity depends primarily on the matrix properties since this is the continuous phase. Thus, the matrix selection depends on the desired properties of the composite being constructed.

Reinforcements: the strength, stiffness and density of the composite materials are very dependent on the reinforcing material. The ultimate tensile strength of a composite is a result of the synergy between the reinforcement and the matrix. The matrix forces load sharing among all the fibers, strengthening the material. Furthermore, the efficiency of reinforcing materials depends on size and morphology of reinforcing materials that possibly have lump, particle or fiber form such as long, short, woven fibers.

2.2.2 Dispersion strengthened composites

Dispersion strengthened composites consist of a uniform dispersion of ultrafine refractory of oxides in a high melting metal or alloy matrix. The size of dispersion-strengthened material is containing particles 10 nm to 250 nm in a diameter as particulate composites. The concentration of particles varies from 1 to 15% by volume. The main effect of dispersoids is that it increases the work hardening of the matrix which is the major load bearing phase. Dispersoids strengthen the composite by impeding the motion of dislocations caused by the external stress. Strengthening primarily depends on the interparticle spacings in accordance with the following relationship (equation 1):

$$\tau = \frac{Gb}{l} \quad (1)$$

Where G is the shear modulus of the matrix, b is the Burger's vector of dislocations, l is the interparticle spacing and τ is the shear stress required to yield and cause dislocations to move. For effective strengthening, spacing of particle must be less than $0.1 \mu\text{m}$.

2.2.3 Particle strengthened composites

Particle strengthened composites or large-particle composites are unlike dispersion strengthened composites. The particles in particulate composites are larger in size 1 to $50 \mu\text{m}$ and their concentrations usually range from 15-40% by volume. The load is carried by both the matrix and particles. Because of their size, particles cannot impede the motion of dislocations. They enhance the strength of composites by hydrostatically restraining the movement of the matrix in their neighborhood is restricted from following freely, resulting in an increased in shear stress required to produce further deformation.

Normally the elastic modulus of the particulate composite follows the rule of mixture. Its value falls between the higher value given by equation 2 and the lower value given by equation 3 [1].

$$E_c = V_m E_m + V_p E_p \quad (2)$$

$$E_c = \frac{E_m E_p}{E_p V_m + E_m V_p} \quad (3)$$

Where E_c , E_m , E_p are represent the elastic modulus of composites, matrix and particle respectively and V_m , V_p are represent the volume fraction of matrix and particle respectively.

2.2.4 Fiber strengthened composites

The basic principle used in fiber reinforced composites (FRCs) is that materials are generally stronger in fiber form than in bulk form due to minimum number of defects contain by them. Most fiber reinforced composites provide improved strength, fatigue resistance, stiffness and strength to weight ratio by incorporating strong, stiff, but the brittle fibers into a softer, more ductile matrix. The matrix material transmits the force to the fibers, which carry most of the applied force. To achieve significant strengthening effect in the composite system, the fibers must possess not only greater elastic modulus but also greater tensile strength than the matrix. The strength of the FRCs is therefore primarily determined by the strength of fibers. The nature and type of the interfacial bond is also important. A weak interfacial bond may result in interfacial separation or fiber pull-out under applied tensile loads. In case of excessive fibers the matrix is unable to coat the fibers properly, leading to poor bonding and voids development at the interface.

2.2.5 Characteristics of fiber-reinforced composites

Many factors must be considered when designing a fiber-reinforced composite, including the length, diameter, orientation, amount, and properties of fiber.

a) Fiber length and diameter

Fiber can be short, long or even continuous. Their dimensions are often characterized by aspect ratio (l / d), where l is fiber length and d is diameter. Typical fibers have diameters varying from 10 microns to 150 microns. The strength of composite improves when the aspect ratio is large. Fibers often fracture because of surface imperfections. In many fiber-reinforced systems, discontinuous fibers with an aspect ratio are greater than some critical value used to provide an acceptable compromise between processing ease and properties. A critical fiber length (l_c) for any given fiber diameter (d), can be determined by equation 4 [2].

$$l_c = \frac{\sigma_f d}{2\tau_i} \quad (4)$$

Where σ_f is the strength of the fiber and τ_i is related to the stress which the matrix begins to deform. If the fiber length (l) is smaller than l_c , little reinforcing effect is observed, if l is greater than about $15l_c$, the fiber behaves almost as if it were continuous. The strength of the composite can be estimated from equation 5.

$$\sigma_c = f_f \sigma_f \left(1 - \frac{l_c}{2l}\right) + f_m \sigma_m \quad (5)$$

Where σ_m is the stress on the matrix when the fibers break.

b) Amount of fiber

A greater volume fraction of fibers increase the strength and stiffness of the composite, as expect from the rule of mixtures. However, the maximum volume fraction is about 80% beyond which fibers can no longer be completely surrounded by the matrix.

c) Orientation of fiber

The reinforcing fiber may be introduced into the matrix in a number of orientations. Short, randomly oriented fibers are having a small aspect ratio. Long or even continuous, uni-directional arrangements of fiber produce anisotropic properties, with particularly good strength and stiffness parallel to the fibers. One of the unique characteristics of fiber-reinforced composites is that their properties can be tailored to meet the different types of loading conditions. Long and continuous fibers can be introduced in several directions within the matrix and more complicated arrangements such as 0°/45°/90° piles provide reinforcement in multiple directions.

d) Fiber properties

In most fiber-reinforced composites, the fibers are strong, stiff and lightweight. If the composite is to be used at elevated temperatures, the fibers should also have a high melting temperature. Therefore, the specific strength and specific modulus of the fiber are important characteristics. The specific strength and specific modulus of fiber can be estimated by equation 6 and 7 respectively.

$$\frac{\sigma}{\rho} \quad (6)$$

$$\frac{E}{\rho} \quad (7)$$

Where σ is tensile strength, ρ is density and E is modulus of elasticity.

There are two types of fiber reinforcement are used, continuous fibers and discontinuous fibers.

2.2.6 Continuous fibers reinforcement

In order to express the elastic properties of the composites in terms of the matrix and the fiber properties it is desirable to consider the two extreme cases of tensile loading, longitudinal loading (isostrain) and transverse loading (isostress). In case of isostrain condition the load applied on the composite is parallel to the orientation of fibers both the components are strained equally provided there is no slippage between the fibers and matrix.

The elastic modulus of the composite is given as rule of mixture as equation 8.

$$E_c = E_m V_f + E_f V_m \quad (8)$$

Where E_c , E_f , E_m are elastic modulus of composite, fiber and matrix respectively. V_f , V_m are the volume fraction of fibers and matrix respectively.

Under transverse loading, under isostress condition the rule of mixtures expressed in the same way as equation 8. Thus,

$$E_c = \frac{E_m E_f}{E_f V_m + E_m V_f} \quad (9)$$

A comparison of equation 8 and 9 shows the tensile failure in composites loaded transversely occur at very low stresses approximated to half that of the matrix strength. This may be due to the stress concentrations at the fiber-matrix interface. In the case of continuous fiber reinforced composites maximum strengthening effect is realized only if the load applied is parallel to the orientation of fiber while it is the lowest in the normal direction. Thus, the properties of continuously aligned fibers are anisotropic in nature. If fibers are aligned in multi directions such as $0^\circ/45^\circ/90^\circ$ one can obtain more isotropic composite [1].

2.2.7 Discontinuous fibers reinforcement

The discontinuous fibers behave like broken fibers and their ends carry fewer loads than their middle part. Because of the bonds between the matrix and fibers are broken at their ends. Therefore the stress in a discontinuous fiber will vary along its length. The tensile stress is zero at the ends and increases along the length and reaches a maximum at a critical length from either end. The length of the discontinuous fibers must be larger than critical length (l_c). The critical fiber aspect ratio (l_c/d) which is more important term than simply critical fiber length.

It is given as equations 10 and 11

$$\frac{l_c}{d} = \frac{\sigma_f}{2\tau} \quad (10)$$

$$\frac{2l_c\tau}{d} = \sigma_f \quad (11)$$

Thus, for the effective strengthening, the critical aspect ratio must be high enough (a minimum of 10) or else the matrix will continue to flow around the fibers and will be unable to transfer load to them.

2.2.8 Layered composites

Layered composites are composed of two or more different layers or sheets bonding together. The layers can differ in material, form and orientation. By proper combination of constituting layers one can achieve a balance of such properties as light weight, high strength, high stiffness, wear resistance, unusual thermal expansion characteristics, etc. Properties of layered composites tend to be anisotropic and may vary from one side of the composite to other. Each layer may perform separate and distinct function. The individual itself can be a reinforced composite which is bonded by another resin. Layered composites are broadly grouped into two categories, a) laminated or laminar, b) sandwich composites

Laminar composites: Laminar composite materials also include very thin coatings, thicker protective surfaces, claddings, and many others. Laminated are generally produced by joining sheets or layers through and adhesive.

Sandwich composites: Sandwich composites generally consist of a thick low density core between thin facing layers of comparatively higher density. The primary aim of producing sandwich composite is to improve structural performance by improving strength-to-weight ratio.

2.2.9 Factors influencing the performance of biocomposites

There are two basic factors influencing the properties of composite materials:

Fiber architecture

Fiber architecture, which includes fiber geometry, fiber orientation, packing arrangement and fiber volume fraction, is responsible for many composite properties, especially mechanical properties. The fiber volume fraction (V_f) is probably one of the most important factor. Most of the mechanical properties are increased with increasing V_f up to a certain point.

Fiber-matrix interface

The interface between fiber and matrix is crucial in terms of composite performance. The interface serves to transfer externally applied loads to the reinforcement via shear stresses over the interface. Controlling the strength of the interface is necessary. Clearly, good adhesion is essential to adequately transfer stresses to the reinforcement and provide a true reinforcing function. Another important mechanical property is toughness; resist the propagation of cracks, which occurs in composites due to their heterogeneous structure. It is important that under certain circumstances interfacial adhesion breaks down as to allow various toughening mechanisms to become operative.

2.3 Biocomposites

Biocomposites are composite materials comprising one or more phase(s) derived from biological origin. Matrices may be polymers, ideally derived from renewable resources such as vegetable oils or starches. They are also called biopolymer. In terms of the reinforcement, this could include plant fibers (or natural fibers) such as cotton, flax, hemp or fibers from recycled wood or even by-products from food crops. Cellulose is also included, since it comes from a renewable resource.

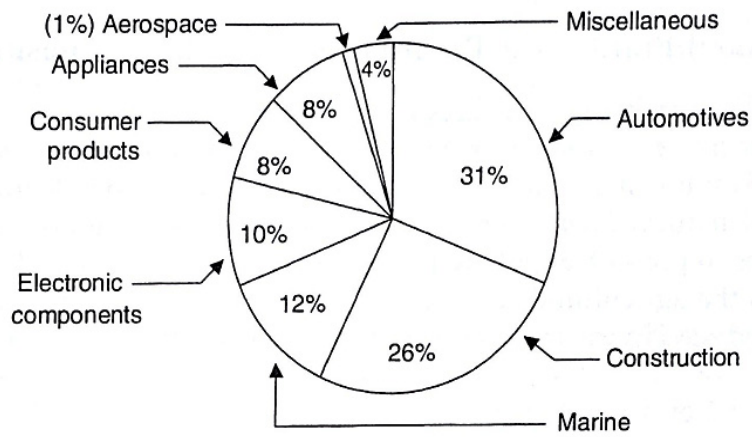


Figure 2: Fiber-reinforced plastic composites used [3].

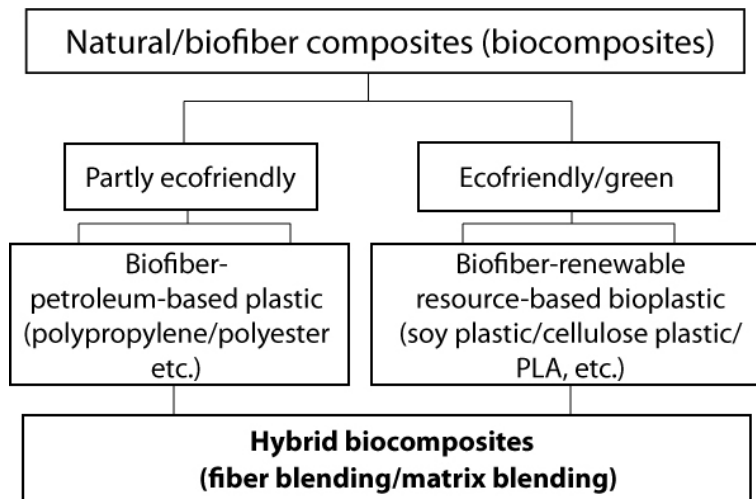


Figure 3: Classification of bio-based polymer composites [3].

2.3.1 Biodegradable polymers

Biodegradable polymers can be degraded by biological system. They can be degraded by such as microbial degradation. Biodegradable polymers can be distinguished: synthetic and natural polymers. The synthetic polymers derived from petroleum resources (non renewable resources) and the natural polymers derived from biological resources (renewable resources). Therefore, biodegradable polymers can be completely biodegradable, renewable and environment-friendly.

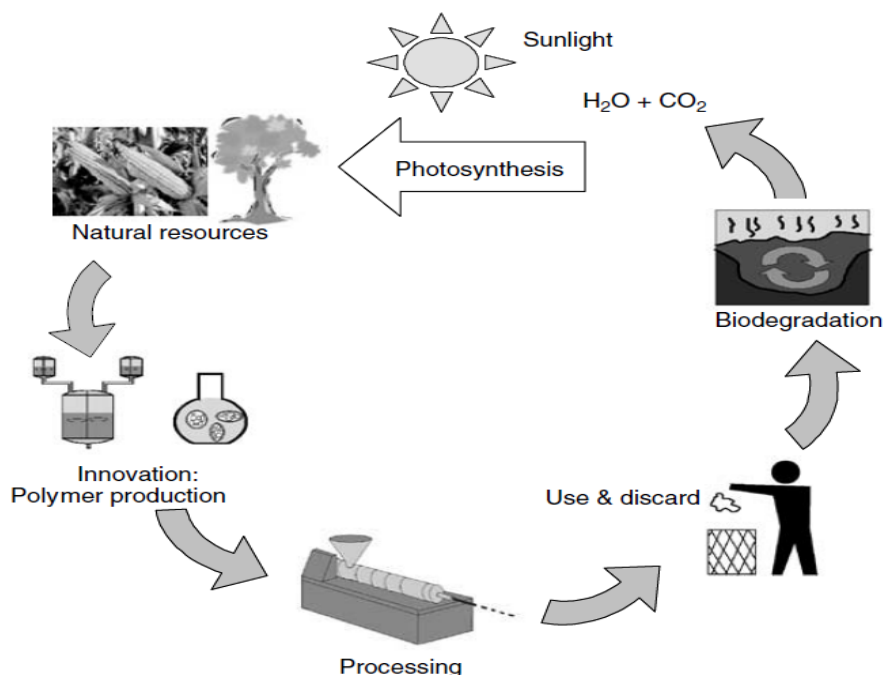


Figure 4: Life cycle of biodegradable polymers can maintain CO₂ balance in the environment [3].

Biodegradable polymers derived from Petroleum Resources

These are synthetic polymers with hydrolysable functions, such as ester, amide and urethane, or polymer with carbon backbones, in which additives like antioxidants are added. Some example of synthesis, properties and biodegradability of main classes are discussed below [4].

Aliphatic polyesters

This is most extensively studied class of biodegradable polymers, because of their important diversity and its synthetic versatility. A large variety of monomer can be used. The aliphatic polyesters are almost the only high molecular weight biodegradable compounds. Their hydrolysable ester bonds make them biodegradable. Aliphatic polyesters can be classified into two types according to the bonding of constituent monomers. The

first class consists of the polyhydroxyalkanoates. These are polymers synthesized from hydroxyacids, HO-R-COOH. For instance, poly(glycolic acid) (PGA) and poly(lactic acid) (PLA). Poly(alkene dicarboxylate) represent the second class. They are prepared by polycondensation of diols and dicarboxylic acids. For instance, poly(butylene succinate) (PBS) and poly(ethylene succinate) (PES).

Aromatic copolyesters

Aromatic polyesters are insensitive to hydrolytic degradation and to enzymatic or microbial attack. However, mechanical properties of such polyesters are lower than those of non-biodegradable polymers. To improve them, aliphatic-aromatic copolyesters were made. Aliphatic-aromatic copolyesters consist in mixture of aliphatic and aromatic monomers. They are often based on terephthalic acid. For instance, poly(butylene adipate-co-terephthalate) (PBAT).

Biodegradable polyesters or bacterial polymers

They are polyesters obtained by polymerization of monomers prepared by fermentation process or produced by a range of microorganisms, cultured under nutrient and environmental conditions (microbial polymer). These materials are accumulated in microorganisms as storage materials

Polyhydroxyalkanoates

Polyhydroxyalkanoates (PHAs) are a family of intracellular biopolymers synthesized by many bacteria as intracellular carbon and energy storage granules. PHAs are mainly produced from renewable resources by fermentation. PHAs are generally classified into short-chain-length PHA (sCL-PHA) and medium-chain-length PHA (mCL-PHA) by different number of carbons in their repeating units. For instance, sCL-PHAs contain 4 or 5 carbons in their repeating units, while mCL-PHAs contain 6 or more carbons in their repeating units. The term mCL is coined because the number of carbons in the monomers roughly corresponds to those of medium-chain-length carboxylic acids. PHA nomenclature and classification may still evolve as new structures continue to be discovered. The main biopolymer of the PHA family is the polyhydroxybutyrate homopolymer (PHB), but also different poly(hydroxybutyrate-co-hydroxyalkanoates) copolyesters exist such as poly(hydroxybutyrate-co-hydroxyvalerate) etc.

Poly(hydroxybutyrate-co-hydroxyvalerate)

Poly(hydroxybutyrate-co-hydroxyvalerate) (PHBV) is the most common members in the PHA family. Depending on the monomer units, PHAs can be homopolymers or

copolymers, and exhibit behavior varying from rubbery to rigid plastic. When composed, bacteria that naturally occur in the soil grow on PHA and turn into water and carbon dioxide. PHBVs can be used to produce a wide range of products from grocery bags, biomedical applications, but the major problem in applications are brittleness and lack of superior mechanical properties. Therefore, several modifications have been proposed to improve their mechanical properties.

2.3.2 Natural fibers

Plant based natural fibers are lignocelluloses in nature and are composed of cellulose, hemicelluloses, lignin, pectin and waxy substances. The chemical compositions of fibers are presented in table 1. Cellulose is considered the major framework component of the fiber structure. It provides strength, stiffness and structural stability of the fiber.

Table 1: Chemical composition of some of natural fibers [5].

Fiber	Cellulose (wt%)	Hemicellulose (wt%)	Lignin (wt%)	Waxes (wt%)
Bagasse	55.2	16.8	25.3	-
Bamboo	26-43	30	21-31	-
Flax	71	18.6-20.6	2.2	1.5
Kenaf	72	20.3	9	-
Jute	61-71	14-20	12-13	0.5
Hemp	68	15	10	0.8
Sisal	65	12	9.9	2
Ramie	68.6-76.2	13-16	0.6-0.7	0.3
Abaca	56-63	20-25	7-9	3

The chemical structure of cellulose (cf. figure 5a) consists of three hydroxyl groups (OH). Two of them form hydrogen bonds within the cellulose macromolecules (intramolecular) at the same time as the rest of the group forms hydrogen bond with other cellulose macromolecule. Hemicellulose occurs mainly in the primary cell wall and has branched polymers containing five and six carbon sugars (cf. figure 5b) of varied chemical structures. Lignin is amorphous and has an aromatic structure (cf. figure 5c). Pectin comprises of complex polysaccharides. Their side chains are cross-linked with the calcium ions and arabinose sugars. In addition to small amounts of organic (extractives) and inorganic (ash) components are present in the fiber structure. Organic extractives are responsible for

color, odor and decay resistance whilst inorganic constituents enhance the abrasive nature of the fiber. Figure 6 shows a schematic structure of a natural fiber and figure 7 presents the model of the structural organization of the three major structural constituents of the fiber cell wall. In accordance with a specific type of fiber, cellulose microfibrils have their own cell geometry which is a factor responsible for the properties of the fiber. Each fiber cell wall consists of primary and secondary layers of cellulose microfibrils. The fiber structure develops in the primary cell wall and is deposited during its growth. The secondary wall consists of three layers and each layer has a long chain of helical cellulose microfibrils. The cellulose content increases steadily from primary to secondary layers and the hemicelluloses amount are similar in each layer. However, lignin content decreases in this sequence. Hemicellulose molecules are hydrogen bonded with cellulose fibrils and they form cementing materials for the fiber structure. Lignin and pectin are coupled with the cellulose–hemicellulose network and provides an adhesive quality to hold the molecules together.

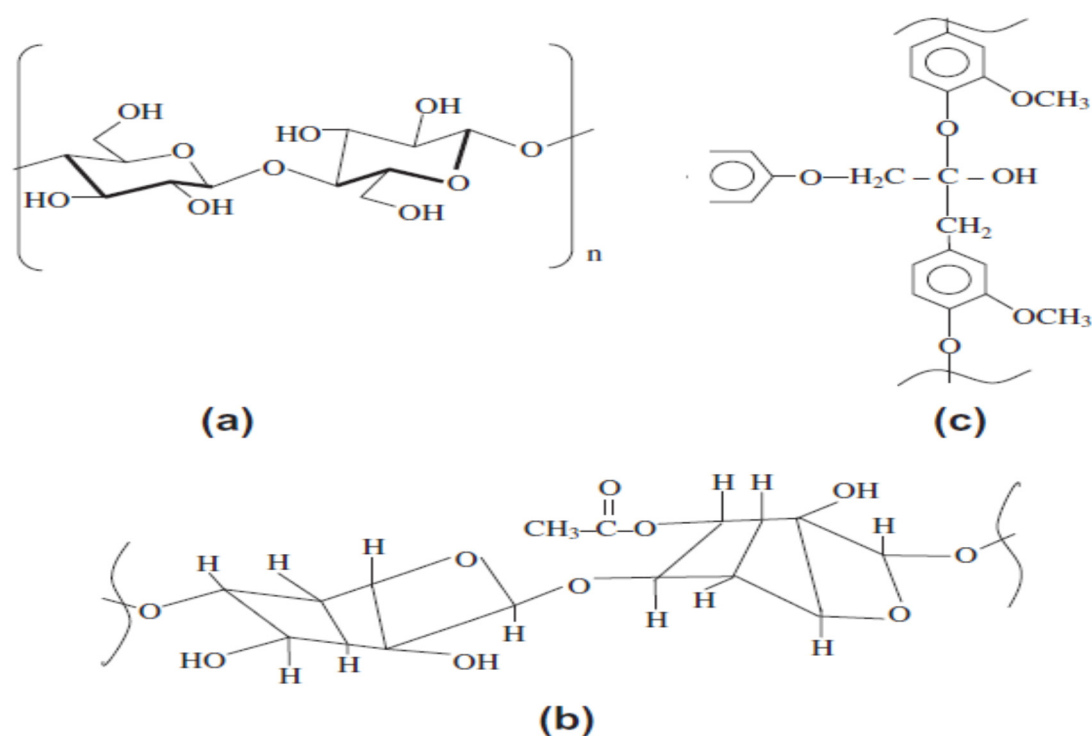


Figure 5: Chemical structure of (a) cellulose (b) hemicelluloses and (c) lignin [5].

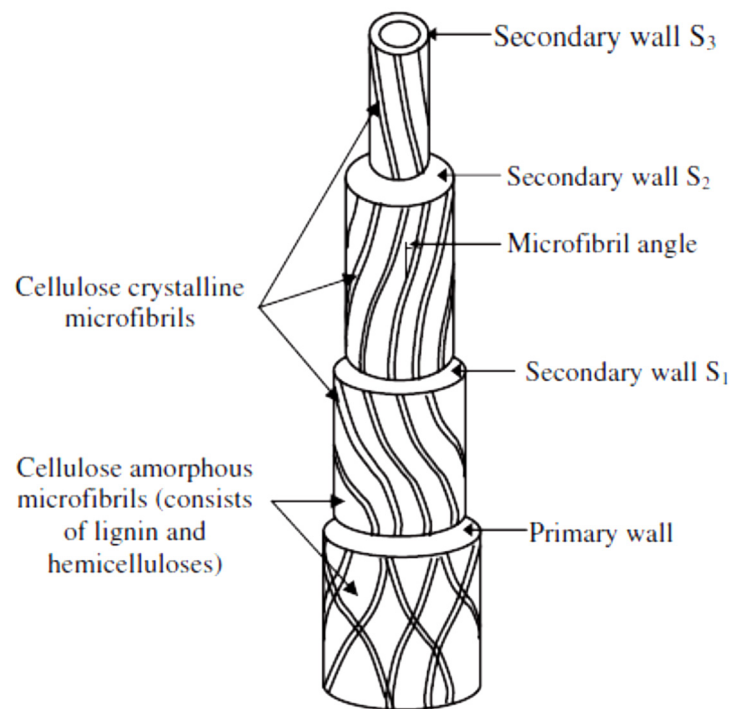


Figure 6: Structure of natural fiber [5].

Table 2: Compare between natural fiber and glass fiber [8].

	Natural fibers	Glass fibers
Density	Low	Twice that of natural fibers
Cost	Low	Low, but higher than natural fiber
Renewability	Yes	No
Recyclability	Yes	No
Energy consumption	Low	High
Distribution	Wide	Wide
CO ₂ neutral	Yes	No
Abrasion to machines	No	Yes
Health risk when inhaled	No	Yes
Disposal	Biodegradable	Not biodegradable

This adhesive quality is the cause for the strength and stiffness properties of the fiber. Secondary thick layer (S_2) determines the mechanical properties of the fiber. Generally, fibers with a higher cellulose content and a lower microfibrillar angle (the angle between the fiber axis and cellulose microfibrils) have better strength properties. Mechanical properties of natural fiber over synthetic fiber are presented in table 2. Although natural fibers have relatively lower strength properties compared to the synthetic fibers, the specific modulus and elongation at break signifies the potentiality of these fibers to replace synthetic fibers in engineering polymer composites.

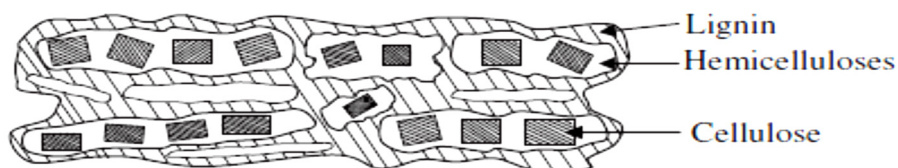


Figure 7: Structural organization of the three major constituents in the fiber cell wall [5].

There has been growing interest in the use of natural fibers as reinforcements for biodegradable polymers because natural fibers have the functional capability to substitute glass fibers that are currently being used in the industry today and also have advantages such as low cost, high specific strength and modulus, low density, ease of fiber surface modification, relative non-abrasiveness and wide availability. Note that natural fibers

are subdivided based on their origins, coming from plants, animals or minerals. All plant fibers are composed of cellulose while animal fibers consist of proteins (hair, silk, and wool). Plant fibers include bast (or stem or soft sclerenchyma) fibers, leaf or hard fibers, seed, fruit, wood, cereal straw, and other grass fibers. The reinforcing efficiency of natural fiber is related to the nature of cellulose and its crystallinity. The main components of natural fibers are cellulose (α -cellulose), hemicelluloses, lignin, pectin and waxes [6-7].

Textile fiber composites

The development of textile technologies such as weaving, knitting and braiding has resulted in the formation of composites that have superior mechanical properties, as continuous orientation of fibers is not restricted at any point. In applications where more than one fiber orientation is required, a fabric combining 0° and 90° fiber orientations is useful. Woven fabrics are produced by the interlacing of warp (0°) fibers and weft (90°) fibers in a regular pattern or weave style. The fabric's integrity is maintained by the mechanical interlocking of the fibers. Drape (the ability of a fabric to conform to a complex surface), surface smoothness and stability of a fabric are controlled primarily by the weave style [7]. The following is a description of some of the more commonly weaves styles:

Plain

Each warp fiber passes alternately under and over each weft fiber. The fabric is symmetrical, with good stability and reasonable porosity. However, it is the most difficult weaves for draping, and the high level of fiber crimp imparts relatively low mechanical properties compared with the other weave styles. With large fiber, this weave style gives excessive crimp and therefore it is not generally used for very heavy fabrics.

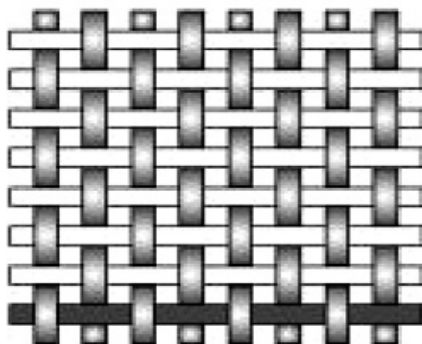


Figure 8: Plain weave structure.

Twill

One or more warp fibers alternately weave over and under two or more weft fibers in a regular repeated manner. This produces the visual effect of a straight or broken diagonal “rib” to the fabric. Superior wet out and drape is seen in the twill weave over the plain weave

with only a small reduction in stability. With reduced crimp, the fabric also has a smoother surface and slightly higher mechanical properties.

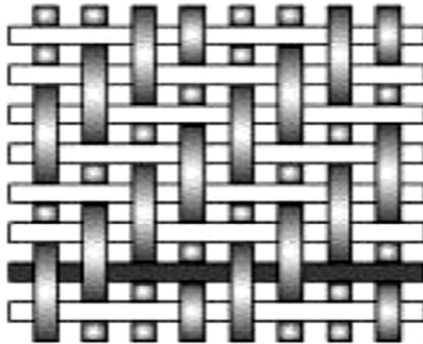


Figure 9: Twill weave structure.

Satin

Satin weaves are fundamentally twill weaves modified to produce fewer intersections of warp and weft. The “harness” number used in the designation (typically 4, 5 and 8) is the total number of fibers crossed and passed under, before the fiber repeats the pattern. A “crowfoots” weave is a form of satin weave with a different stagger in the repeat pattern. Satin weaves are very flat, have good wet out and a high degree of drape. The low crimp gives good mechanical properties. Satin weaves allow fibers to be woven in the closest proximity and can produce fabrics with a close “tight” weave. However, the style’s low stability and asymmetry needs to be considered. The asymmetry causes one face of the fabric to have fiber running predominantly in the warp direction while the other face has fibers running predominantly in the weft direction.

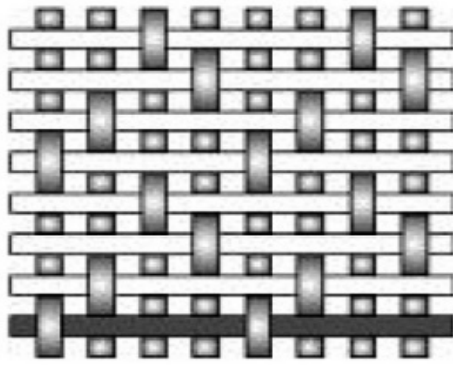


Figure 10: Satin weave structure.

2.3.3 Chemical modifications of natural fiber surfaces

Natural fibers are suitable reinforcement materials for composites due to a combination of good mechanical properties and environment advantages such as renewability, eco-friendliness and biodegradability. Due to natural hydrophilic character resulting in high water absorption that leads to low compatibility with hydrophobic polymer matrices, poor dimension stability as water absorption swells fibers and poor adhesion between fibers and matrices. Chemical treatments on reinforcing fiber can reduce its hydrophilic tendency and thus improve compatibility with the matrix. The improvement of matrix/fibers composite adhesion leads to increase the mechanical properties. Many research activities have been conducted to improve the interfacial adhesion of composites by treating fibers by chemical treatments such as sodium hydroxide (NaOH) and silane [9]. Chemical treatments on reinforcing fiber can reduce its hydrophilic tendency and thus improve compatibility with the matrix. The improvement of matrix/fibers composite adhesion leads to increase the mechanical properties. Many research activities have been conducted to improve the interfacial adhesion of composites by treating fibers by chemical treatments such as sodium hydroxide (NaOH) and silane.

Silane treatment

Silane is a chemical compound with chemical formula SiH_4 . Silane is used as coupling agents to let fibers adhere to a polymer matrix, stabilizing the composite material. Silane coupling agents may reduce a number of cellulose hydroxyl group in the fiber matrix interface. In the presence of moisture, hydrolysable alkoxy group leads to the formation of silanols. The silanol then reacts with the hydroxyl group of the fiber. The formed stable covalent bonds to the cell wall that are chemisorbed onto the fiber surface. Therefore, the hydrocarbon chains provided by the application of silane restrain the swelling of the

fiber by creating a crosslink network due to covalent bonding between the matrix and the fiber. The reaction schemes are given as in figure 11.

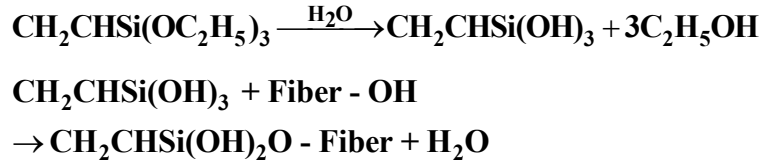


Figure 11: The reaction schemes between silane and fiber [10].

Note that the composition of silane forms a chemical link between the fibre surface and the matrix through a siloxane bridge. It undergoes several stages of hydrolysis, condensation and bond formation during the treatment process of the fibre. Silanols form in the presence of moisture and hydrolysable alkoxy groups. During condensation process, one end of silanol reacts with the cellulose hydroxyl group (Si–O–cellulose and other end reacts (bond formation) with the matrix (Si–Matrix) functional group. This co-reactivity provides molecular continuity across the interface of the composite. It also provides the hydrocarbon chain that restrains the fibre swelling into the matrix. As a result, fibre matrix adhesion improves and stabilizes the composite properties.

3 Binary composites

3.1 Polylactide (PLA)/flax mat composites

State of the Art

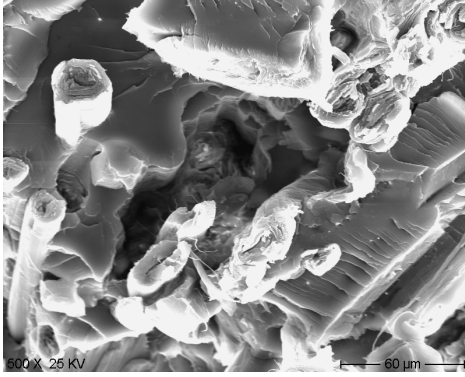
Research on the most promising polylactide (PLA) became under spot of interest and has increased substantially using in medical and automotive applications [11-12], due to its high mechanical strength, biodegradability and simple process ability compared to other biopolymers [13-14]. However, the insufficient impact strength and low thermal stability of PLA are the limiting factors of its applications. In order to improve the mechanical and thermal properties of PLA are considered an addition of fibers or filler materials [15-16]. In the related area of PLA -based natural composites have attracted considerable interest because they often exhibit remarkable property improvements when compared to the neat PLA. Kumar et al. [16] reported that mandelic acid and dicumyl peroxide (DCP) acted as efficient additives for flax fabric reinforced PLA composites and introduction of DCP in composites can be improved the mechanical properties. A variety of natural fibers, such as flax fabric, cellulose, kenaf and abaca [16-19] have already been checked as possible reinforcements in PLA. Roussi re et al. [20] studied the mechanical properties of poly L-lactide acid (PLLA) matrix biocomposites that were reinforced with randomly scattered flax fibers in the lamination plane. They reported an improved tensile strength as well as elastic modulus of PLLA/flax composites at the cost of the elongation at break. Siengchin et al. [21] reported the mechanical properties of flax/PLA composites depend on the weave style which plays an important role with respect to reinforcing efficiency. They observed a marked improvement in stiffness and impact energy value of PLA/ woven flax fiber textiles It was also reported that the impact and tensile properties of cordanka 30 wt.% containing PLA composites increased markedly when compared to the neat PLA. [22]. Moreover, Das et al. [23] investigated the thermal properties of PLA/clay nanocomposite films. They found that the glass transition temperature of the composite films increased markedly compare with unreinforced PLA film. This is associated with hindered chain mobility in presence of dispersed clay platelets. In order to enhance the interactions between the components with preformed natural fibers, various strategies have been recommended. The benefit based on the knowledge gained with traditional natural fiber (e.g. surface treatment by zirconium oxychloride and alkali [24-25]. The use of conventional compounding techniques to modify thermoplastics matrix is a promising route compared and usually more practical and economical than surface modification of natural fibers. The advantage of direct modified polymers is an effective process being simple and cost efficient for producing natural fiber composite with an

additional toughness. A further beauty of this approach is that a modification of matrix polymer may guarantee the compatibility with the selected commercial additives. The present work addresses the toughening and thermal reinforcing polylactide (PLA) via a modification of PLA matrix using compounding technique. Flax mat was used as reinforcement. A further aim of this work was to demonstrate the feasibility of the production of un- and modified PLA/flax mat composites and compare the structures impact, thermal and mechanical properties of the related composites. One of the criteria for selecting this flax fiber was that the automotive industry is leading in the development use of composite materials based on flax and undergone comprehensive researches for new fiber reinforced composites. Note that due to its excellent strength and toughness. Flax is one of most interesting plants that have long been produced in useful structural composite materials. Numerous studies have confirmed that flax is a promising reinforcement widely used in commercial and biodegradable polymer matrices [16, 20-21, 26]. Arbelaiz et al. [26] reported that flax fiber reinforced polypropylene with maleic anhydride treatments resulted in an increment of about 8% the interfacial shear strength value and displayed the optimum tensile properties.

Materials and preparation of composites

Non-woven flax fibers (flax mat; 220 gm⁻²) were supplied by Dittrich Vliesstoffe GmbH (Ramstein-Miesenbach, Germany). The nonwoven textile was made of individual fibers. One can observe the randomly orientation of flax fiber which had diameter in between 15-25 µm and displayed fiber lumina in the cross section corresponding section SEM analysis (cf. Figure 12a-b). PLA (Polylactide 2002 D, NatureWorks, Minnetonka, MN, USA) was utilized as polymeric matrix for composite systems. Its melt flow rate (MFI at 210 °C/2.16 kg) was 6 g/10min). Two commercial additives were used as modifier for PLA. Biomax Thermal 300 (composition of non-regulated wax/ethylene acrylate copolymer/butyl acrylate) and Palaroid BPM-500 served as thermal and acrylic impact modifier, respectively.

a)



b)

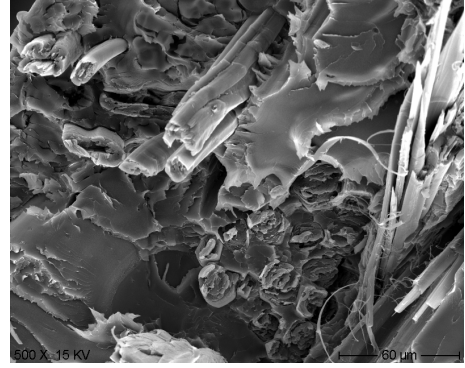


Figure 12: SEM pictures taken from PLA/flax a) and modified/PLA b) composites.

PLA and modified PLA sheets were prepared by twin-screw extruder (Leistritz, Nürnberg, Germany). The modified PLA was compounded by setting the barrel temperatures between 100 (zone 1) and 190-200 °C (from zone 2 to 9), rotor speed of 225 rpm and pressure of 50 bar. The thermal and impact modifier - contents in the PLA systems investigated were set for 5 and 3 wt.%, respectively (according to suppliers' recommendation). The additives and PLA granulates were charged in feeder in the first zone of the extruder using the above conditions. The PLA composite sheets were produced by hot press methods. The flax mat was set for 20 wt.%. The PLA and modified PLA containing flax mat composites were placed by hand laying-up a layer of flax mat and then by a layer of PLA sheet. The composites based on PLA were compression molded into 1-mm thick sheets at $T = 210$ °C using the hot press (P/O/Weber, Maschinen und Apparatebau, Remshalden, Germany).

$$\sigma(t) = \sigma_0 \sin(\omega t + \delta) \quad (12)$$

A complex Young's modulus (E^*) reflects the contribution of both storage (E') and loss (E'') components to the stiffness of material, as follows:

$$E^* = \frac{\sigma_0}{\varepsilon_0} = E' + iE'' \quad (13)$$

According to schematic of DMA, the stress and modulus at these two points can be calculated from equations 13 and 14, respectively. The storage modulus (E') gives directly:

$$E' = E^* \cos \delta \quad (14)$$

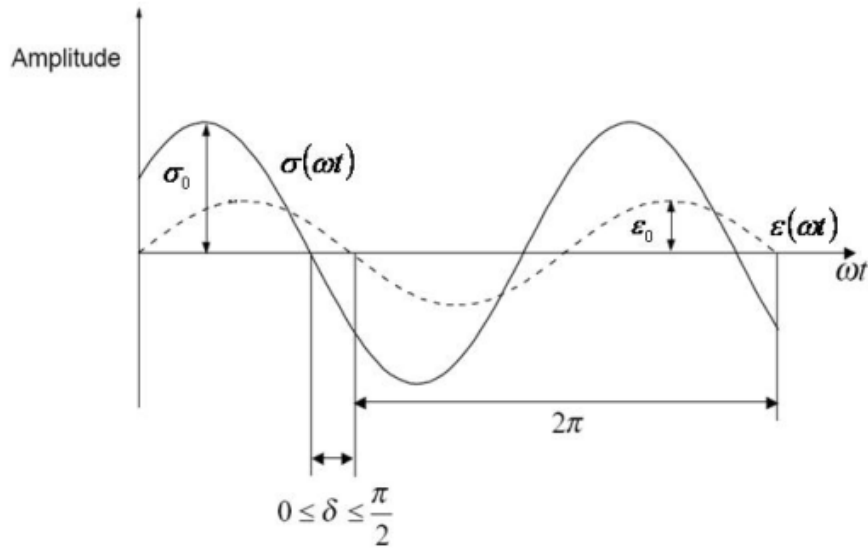


Figure 13: Schematic of the DMA experiment [20].

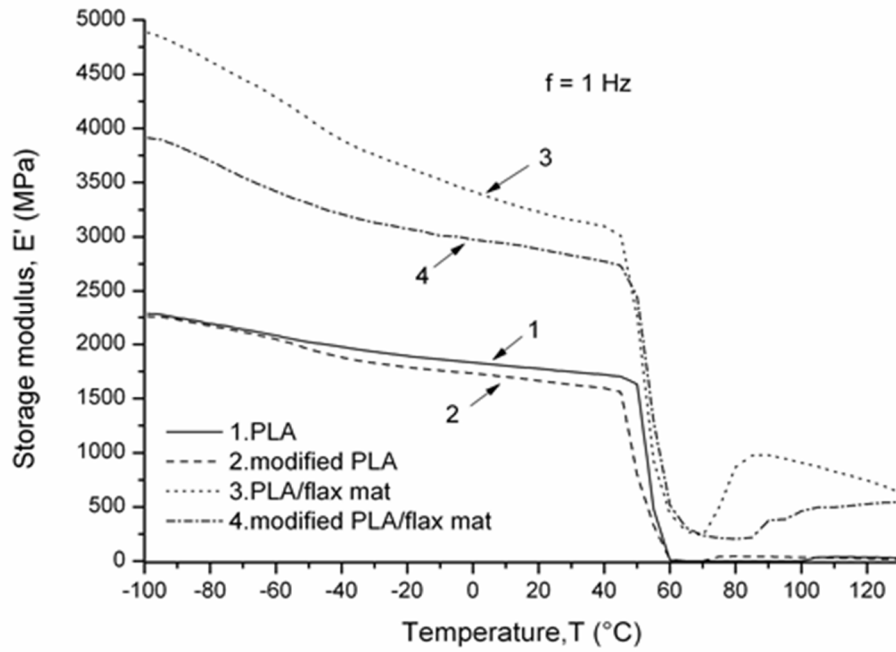


Figure 14: E' vs. T traces for the PLA, modified PLA and its composites.

Figure 14 shows the storage modulus as function of temperature for the PLA, modified PLA and its composites. It is clearly seen that the storage modulus of un- and modified PLA/flax mat composites was higher than that of the neat PLA. It denotes that the mobilization of PLA macromolecules was restricted due to the addition of flax. However, the modified PLA and its composite resulted a decrease in the storage modulus below glass transition temperature (T_g at ca. 60 °C), compared to the based on unmodified one. An addition with flax mat was marginal on the effect of T_g . A rapid increasing region of E' at higher temperature can be seen for PLA systems studied, due to the cold crystallization of the amorphous PLA [27, 31]. Figure 15 shows the variation of storage modulus in the range of temperatures between -100 and 130 °C for the modified PLA and modified PLA/flax mat composite tested at 0.1, 1 and 10 Hz, respectively. A remarkable of frequency - influence was observed for the stiffness. An increase of frequency shifted the position of the E' to higher temperatures at whole temperature range.

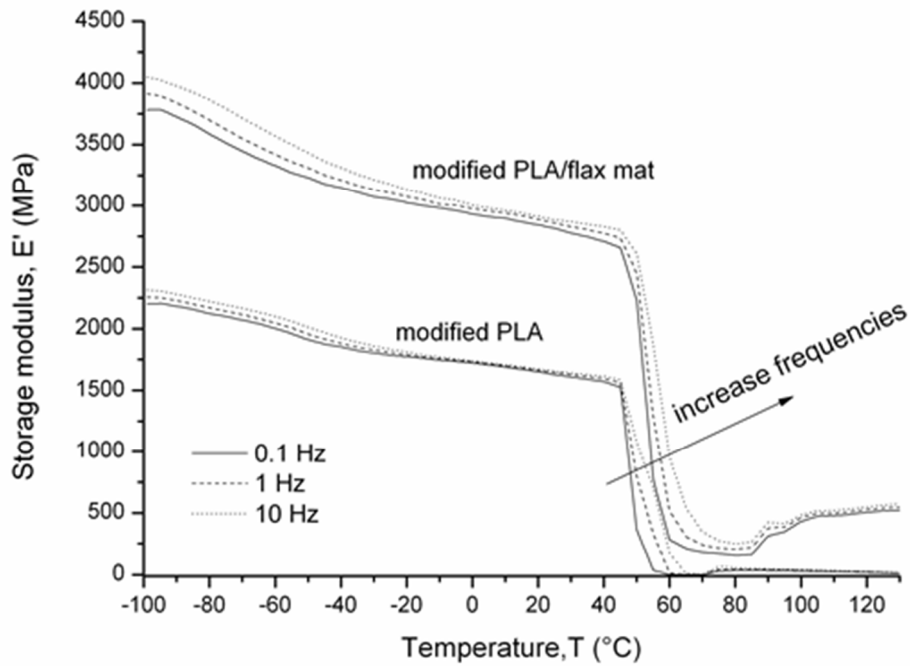


Figure 15: Storage modulus versus temperature for a range of frequencies.

Master curves in the form of storage modulus versus frequency were produced by superimposing the storage modulus versus frequency traces using the time-temperature superposition (TTS) principle. A reference temperature ($T_{ref} = 25$ °C) was used for this superposition (shifting) process. The related shift factor (aT) used for the generation of storage modulus master curve is $aT = E'(T)/(E'(T_{ref}))$. Master curves of the storage modulus against frequencies created at a reference temperature of 25 °C are shown in figure

16 for the PLA systems studied. From E' master curves have been shown that the storage modulus data approached a similar plateau value at high frequency, but applying the modified PLA for composite was reflected in shifting the curve position horizontally, along the frequency axis (terminal region at lower frequencies). One can conclude that the structure of the modified PLA and its composites were more strong on the thermal effect. Note that the master curve provided a useful prediction of the storage modulus for large time scales (from 10^{-14} to 10^{26} Hz). Furthermore, use of an Arrhenius function fit [32], the activation energies are calculated for the PLA systems studied. These two activation energies of PLA and modified PLA were obtained 165.7 and 195.5 kJ/mole, respectively. The activation energy for the composites was found to be higher than un- and modified PLA. It is likely that this activation energy can be described a complex combination of effects, since the TTS is only directly applicable to the restricted with amorphous PLA.

Generally, simple rule of linear viscoelastic material (LVM) principle can be very useful in helping to understand the effect of creep properties on the frequency. The conversion method from the modulus to the creep compliance based on the correspondence LVM principle [33] can then be shown simply to be given by equation 15.

$$D' = \frac{E'}{(E')^2 + (E'')^2} \quad (15)$$

where D' is storage creep compliance.

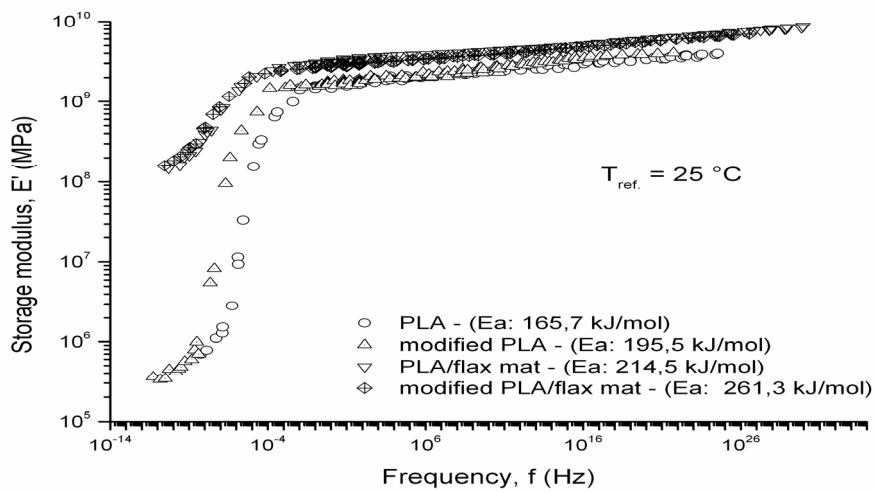


Figure 16: Storage modulus master curves (E' vs. f) constructed by considering the TTS and selecting $T_{ref} = 25 \text{ }^{\circ}\text{C}$ the PLA, modified PLA and its composites. E_a was calculated by the Arrhenius equation, i.e.: $aT = E_r(t, T)/(E(t, T_{ref}))$.

An influence of flax mat and modified PLA on the storage creep compliance is demonstrated in figure 17. As expected to the flax mat reinforcement, the storage creep resistance of PLA/flax mat and modified PLA/flax mat composites increased markedly compared to the PLA for all over loading frequencies. A convert model was fairly applicable to the modulus results and offers good insight into the nature of changes of creep response with frequency decrease. It can be seen that the slope of composites curves changed at below 10^{-4} Hz. The flax mat/modified PLA composite was accompanied with a shift in the slope of PLA towards lower frequency and delayed the creep rate. The related composite may fail even subsequent to that of the PLA matrix. This can be confirmed to the effects of the modified PLA with enhanced creep stability at the low frequencies.

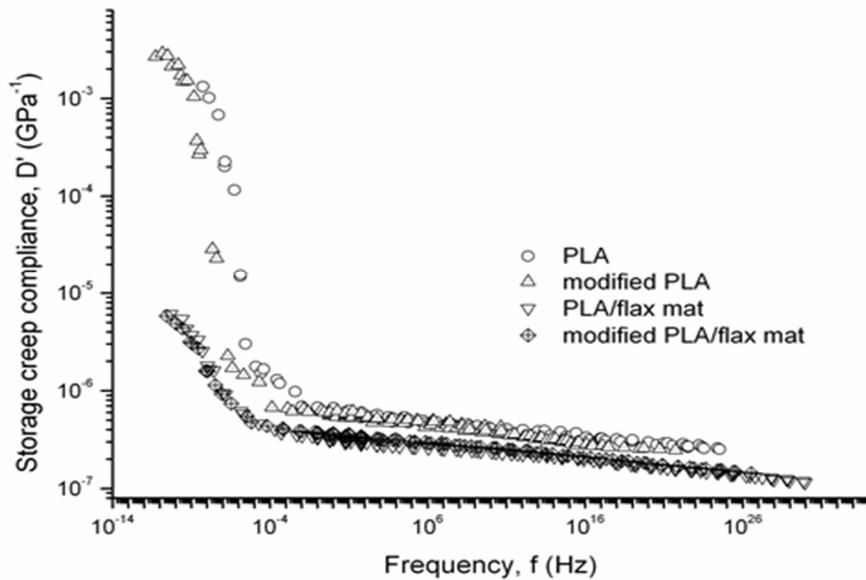


Figure 17: Conversion from the modulus to creep compliance for the PLA system studied.

Conclusion

In this work has examined the effect of thermal and acrylic impact modifier, in a PLA/flax mat composites. The work devoted to study the morphology, impact, thermal and mechanical properties of the PLA system studied. Toughened PLA and its composites have been successfully produced by direct modified matrix. The modified PLA based composite hints for smooth fracture surface in which indicated a ductile deformation. This was demonstrated by SEM investigation. The impact resistance of PLA was highly enhanced by the addition of flax mat and acrylic impact modifier. The tensile strength and storage modulus value of modified PLA were slight lower than the neat PLA. Incorporation of flax

mat increased markedly the stiffness of PLA. The modified PLA was associated with a considerable increase in the thermal resistance of TGA test. The storage modulus master curves were constructed by applying the time-temperature superposition (TTS) principle.

The linear viscoelastic material principle was fairly applicable to convert from the modulus to the creep compliance results which could describe on the thermal effect of modified PLA. The proposed of direct modified PLA was an effective way being simple and cost efficient for producing PLA/flax mat composite.

3.2 Polylactide (PLA)/woven flax textiles composites

State of the Art

Nowadays, an increase of plastic demand, coupled with awareness in economics and environment which are tremendous stimulants in procuring materials to replace polymer of petroleum base. Therefore, the materials ranging from general thermoplastic to specific thermosetting resin are developed from bio-polymer and they are already used in various in medical and automotive applications. Note that research on biopolymer such poly(lactic acid) (PLA) became under spot of interest due to its good biocompatibility, biodegradability and mechanical properties (tensile strength and stiffness) [34]. Considerable efforts are being made to increase the thermal and mechanical properties of PLA by reinforcing it with natural fibers [18, 31]. Moreover, PLA reinforced with natural fiber is another eco-friendly material with its potentiality to be adequately used in automotive industry with significance. For industry application, Toyota has proposed to apply bio composites such PLA/jute in its manufacturing of spare wheel cover and transparent sunroof. However, the end properties of natural reinforced composites depends on an adhesion of fiber-matrix which play an important role with respect to reinforcing efficiency. The problem of weak interfacial adhesion is insufficient wetting of natural fibers by the non-polar polymer matrices, resulted in stress transfer efficiency from the matrix to the reinforcing fibers is reduced. Different surface chemical modifications such as silane and isocyanate treatment [35-36], have achieved tremendous success in improving the interfacial properties in natural fibre composites. Out of these methods, composite structure has attracted considerable attention in the recent years due to the achieved improvements in mechanical characteristics of PLA. This is a most preferred method because of its simple and cost effectiveness. Recently reported, the composite structures are associated to an increase in mechanical properties of composites. Liu and

Hughes [37] investigated the fracture behaviour and toughness of epoxy matrix composites reinforced with woven flax fibre textiles. They found that the addition of woven textile resulted improvement in fracture toughness. However, toughness is dominated by the fibre volume fraction, rather than the reinforcement structure.

The processing of thermoplastic composite materials is characterized by a wide variety of distinct methods or techniques (Vacuum bagging-, consolidation and compression moulding). The process selection depends on many factors including: the quantity and production rate, the form and details of the product, the size of final product, the dimensional accuracy and surface finishing, the nature of material and the process costs. According to the defined structural applications and the use of large fabrics, the most suitable processing techniques will be in continuous compression moulding. It is feasible to use the continuous compression moulding press for small and medium-sized production series. Thermoforming continuous fibre reinforced thermoplastic composite sheets can be shaped into complex structures as it can be seen in figure 18. In order to do such material is heated in a heating field. After reaching the desired thermoforming temperature the sheet is transported into the press. The press is then closed applying a pressing force during a fixed time. The continuous system operates always in a sequential manner. The system is closed during the compression moulding phase, and a surface pressure that varies with the component's dimensions is applied on the materials to be manufactured.



Figure 18: Interval hot press technique.

The main objective of this project is to promote the utilization of natural fibres in structural applications where traditionally glass fibres have been used until now. A further aim of this work was to demonstrate the feasibility of the production of PLA/flax composites with various flax structures using the interval hot press technique. As a result, aligned textiles from flax fibres that are suitable for use as high-strength reinforcing fabrics will be studied in order to obtain structural composite materials and influenced of composite structures.

These flax textiles with greater added-value from completely renewable sources will comprise all the possibilities for a broad range of applications and components.

Materials and preparation of composites

Two types of the woven flax fiber textiles (weave style of 2x2 twill and 4x4 hopsack) were used as reinforcement. The flax had a yarn size of 250 tex. Biotex Flax was supplied by Composites Evolution (Chesterfield, UK). The density was 1.24 g/cm³ (according to suppliers' information). Figure 19 shows the example of woven flax textiles. Note the undulation of corresponding composites was assumed to follow it crosses over. PLA (Polylactide 2002 D, NatureWorks, Minnetonka, MN, USA) was utilized as polymeric matrix for composite systems. Its melt flow rate (MFI at 210 °C/2.16 kg) was 6 g/10min.

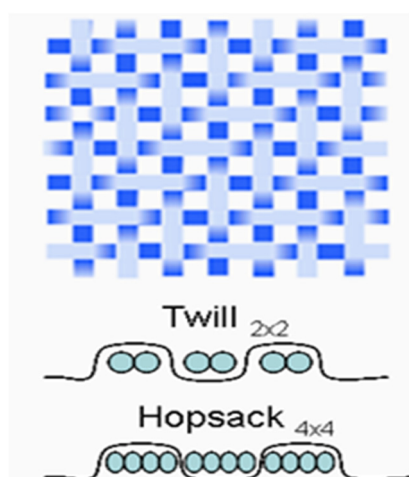


Figure 19: Schematic representation of woven flax textiles 2x2 twill and 4x4 hopsack.

PLA/twill_{2x2} and PLA/hopsack_{4x4} composites were produced by interval hot press (Advanced Composites Machines, PLA 1500 S, Markdorf, Germany). The woven flax fiber textiles were dried for 6 h at 80 °C in an oven. The layer of woven flax fibers and then by layer of PLA sheet were compressed at an infeed of 10 m/hour (h). The heating section of the interval hot press machine was set at 200 °C and the compression pressure was 20 bar. The interval hot press was performed as follows. First, The composite material transport phase took place before the pressing phase. During the transport phase the press was opened quickly (no pressure was applied on the layers to be laminated). Thus, the complete of press cycle comprised the following steps: closing, pressing, opening, and transporting. A schematic view of a continuous compression unit system and pressure/ temperature were showed in figure 20.

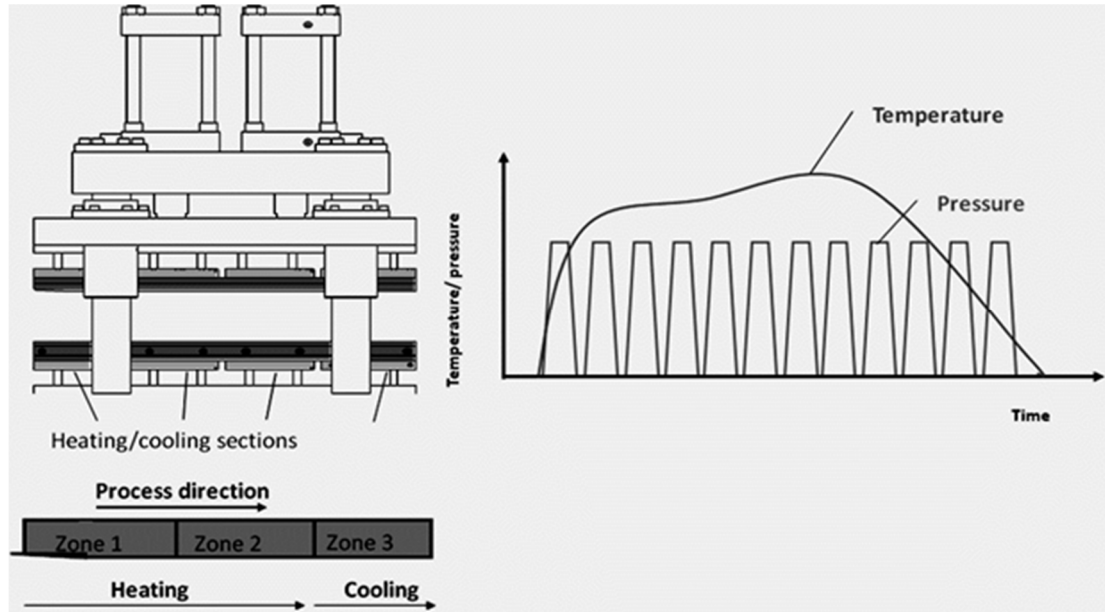


Figure 20: Schematic description of the interval hot press and representative temperature/pressure vs. time curves [43].

The density of the composites was calculated according to the obtained total volume V_c and the initial weights of flax fiber and PLA matrix components W_f and W_m , respectively. However, due to the same condition of compression force in the mould, it can be assumed that a void volume (V_v) of those composites is similar.

$$V_c = V_f + V_m + V_v \quad (16)$$

The density equation of composites (ρ_c) using the obtained total volume V_c is:

$$\rho_c = \frac{W_f + W_m}{V_c} \quad (17)$$

So that the calculated densities of the PLA/flax_{4x4} and PLA/flax_{2x2} composites were 1.12 and 1.09 g/cm³, respectively and used to compare the mechanical and impact behaviors of related composites.

Characterization and testing

Morphology detection

The fracture surface was subjected to scanning electron microscopy (SEM) inspection in a JSM 5400 device of Jeol (Tokyo, Japan). The surface was gold coated prior to SEM inspection performed at low acceleration voltage.

Instrumented Falling Dart Impact

Instrumented falling weight impact (IFWI) test was performed on a Fractovis 6785 (Ceast, Pianezza, Italy) using the following settings: incident impact energy, 20 J; diameter of the dart, 20 mm; diameter of the support rig, 40 mm; weight of the dart, 10.357 kg; drop velocity, 1.97 m/s. IFWI tests were performed on quadratic specimens of 60x60 mm² at room temperature.

Tensile response

Tensile test was performed on dumbbell-shaped specimens (DIN-ISO-527) on a Zwick 1474 (Ulm, Germany) universal testing machine. Tests were run at room temperature at $v=2$ mm/min crosshead speed and the related stress-strain curves were registered.

Thermomechanical response

Dynamic mechanical thermal analysis (DMTA) was performed in tensile mode at frequencies of 0.1, 1 10 Hz at all isothermal temperatures, using a DMA Q800 apparatus (TA Instruments, New Castle, NJ). The storage modulus (E') was determined as a function of the temperature ($T = -100^{\circ}\text{C} \dots +130^{\circ}\text{C}$). The strain applied was 0.1%. The specimens were cooled to -100°C . The temperature was allowed to stabilize and then increased by 5°C , kept 2 min isothermal until 130°C .

Result and Discussion

Impact weight test

Figure 21 shows the force as functions of the time for the neat PLA, PLA/flax_{4x4} and PLA/flax_{2x2} composites. For the neat PLA a value of 97 N was determined for the peak force. One can recognize that in all cases the addition of fabric resulted in an improvement of impact resistance fracture over the unreinforced PLA. In those composites with a fiber waviness would tend to be suppressed and it has an effect of inhibiting the ability of flax fibers to pullout from the PLA matrix. The abrupt rise from initial to maximum force was believed that this was due to the flax fabric debonding from the PLA matrix. Note that closer to the maximum force, the macro-crack growth could be observed. After this point, the main crack continued to propagate and the force was decreased. Moreover,

the crack growth was sudden extension producing a gradual failure (in case of the composites only). It could also clearly demonstrate for advantage of composite_{4x4} with fewer undulations, the maximum peak force of flax_{4x4} composites increased markedly compared to the composite of flax_{2x2} and PLA. As pointed out by schuermann [38], this could be the effects of fiber waviness due to the fiber crossing (weft crossover points) lead to a reduction of the in-plane properties of a cross-ply composite laminate. Since the density and the properties of the reinforcing fiber both composites were similar, the results suggested that the impact resistance of PLA was related to the organization of the microstructure. The temperature dependence on the force versus time curves is demonstrated on example of the PLA/flax_{4x4} and PLA/flax_{2x2} composites in figure 22. It is clear from this figure that a decrease of temperature, the fracture time was decreased, and paralleled to reduce of the peak force. For the flax composite_{4x4}, the peak force was reduced by approx. 38 % when evaluated at -30 °C. The largest change in the fracture time occurred in the flax composite_{4x4}. This is probably due to the fact that the lower fiber waviness of flax composite has been surpassed at the low testing temperature. Whether the related change may be traced to the weave type of the corresponding flax requires further investigations.

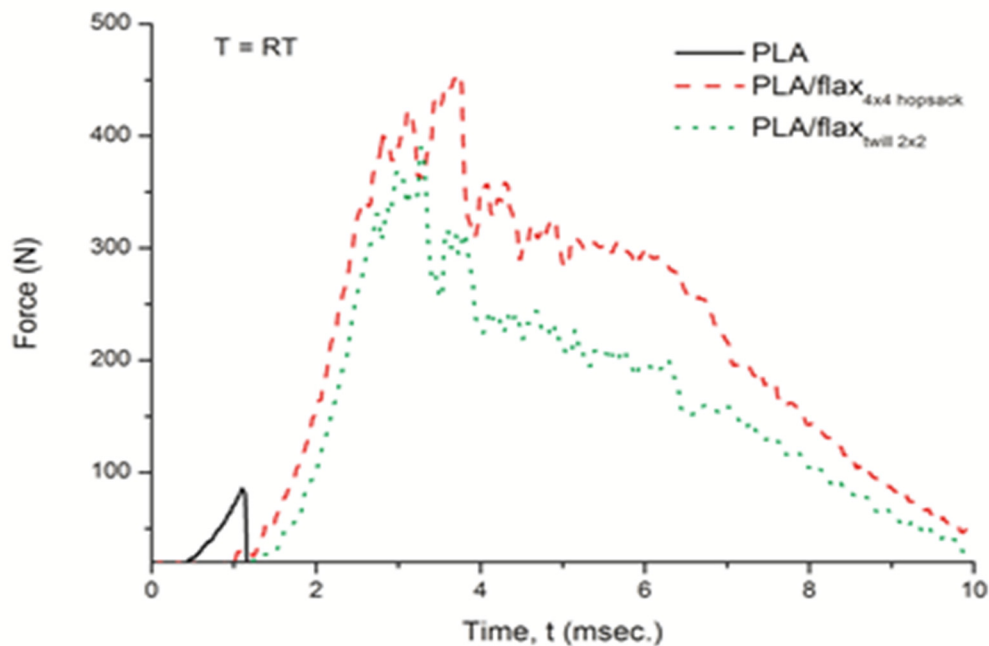


Figure 21: Representative force vs. time curves for the PLA, PLA/flax_{4x4} hopsack and PLA/flax_{2x2} twill.

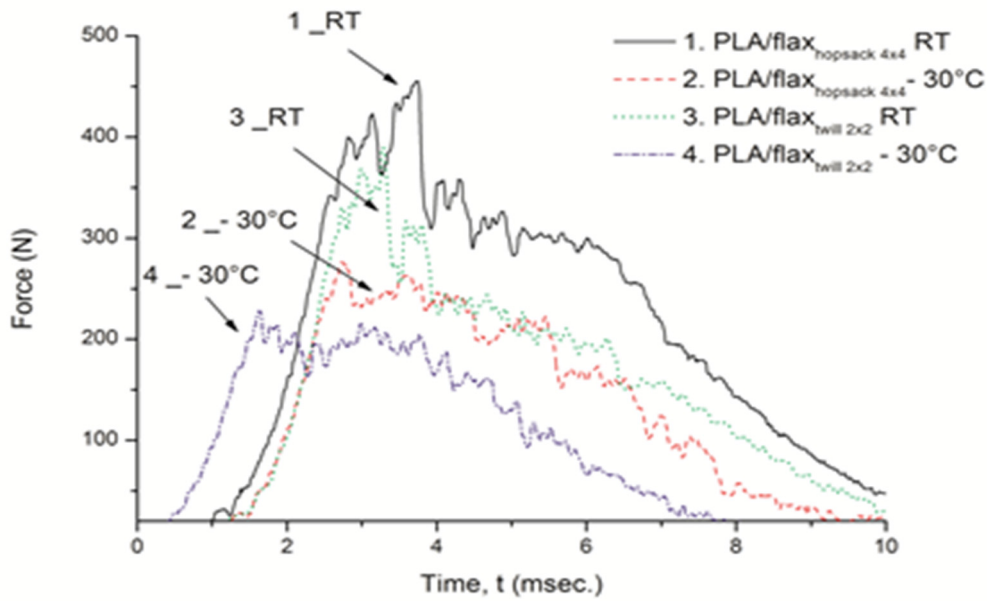


Figure 22: Effect of temperature on the force vs. time of the PLA/flax_{4x4} hopsack and PLA/flax_{2x2} twill.

The photographs of typical failure behavior of the related composites after the falling dart impact tests are shown in figures 23a and b for PLA/flax_{4x4} and PLA/flax_{2x2} composites, respectively. As shown in figure 23, the brittle fracture was rough and the whitened zone could be clearly discerned around the crack zone. The degree of stress whitening appeared to be dependent upon the type of fiber weave and evaluated temperature. Note that the stress whitened region for the samples with low temperature tested was lost from crack growth. A further decrease in the temperature of -30 °C, the impact resistance was found to decrease markedly and the crack did not propagate along the fabric direction but it was occurred suddenly fracture. Failure of flax_{2x2} composite, debonding of flax fibres from the PLA matrix (cf. Figure 23b) and brittle fracture of matrix were the main fracture mechanisms. Although it was clear that micro-cracking extends some way into the laminate from the crack face.

It was recognized in the literature that the failure mechanisms for natural fiber-reinforced polymers have been identified such as matrix failure, fiber fracture, and fiber–matrix interfacial failure [39]. The latter grouping has a strong impact on the interface characteristics between fiber and the bio-based matrix. SEM pictures taken from the PLA/flax_{4x4} and PLA/flax_{2x2} composites are shown in figures 24a and b, respectively. It was observed that the interfacial gaps around pulled-out fibers were smaller when produced by the interval hot press (as previous studies by conventional compression molded technique

[21]). The pressure step of interval hot press technique used to open slightly the tool which was supported to reduce a void content of related composites. This also allowed concluding that the flax fiber pull-out enables dissipation of high energy along the interface, which was consistent with further related properties. Note that the interface gap for composite_{4x4} revealed a similar interface gap as its composite_{2x2}. Furthermore, it can be seen that the holes and roughness of a fracture surface were visible in both composites.

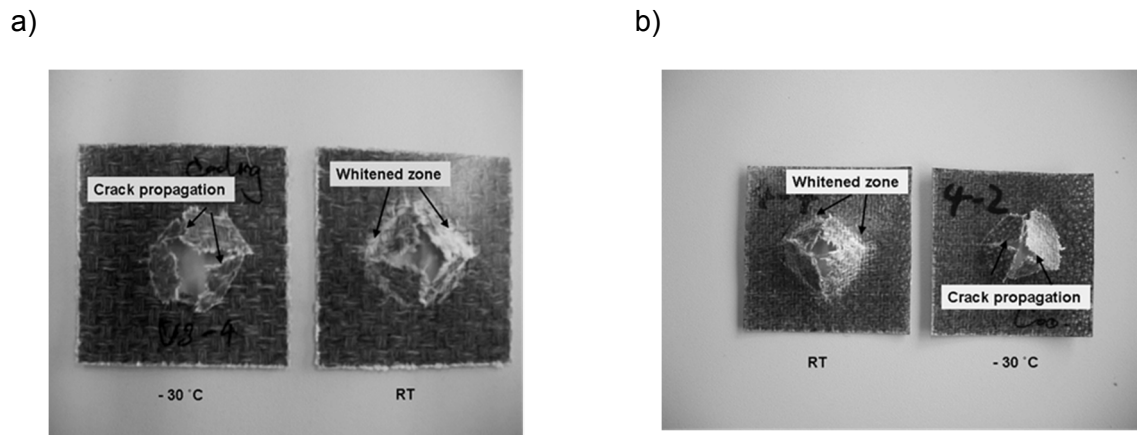


Figure 23: Typical failure of the specimens of PLA/flax4x4 a) and PLA/flax2x2 b) composites after IFWI.

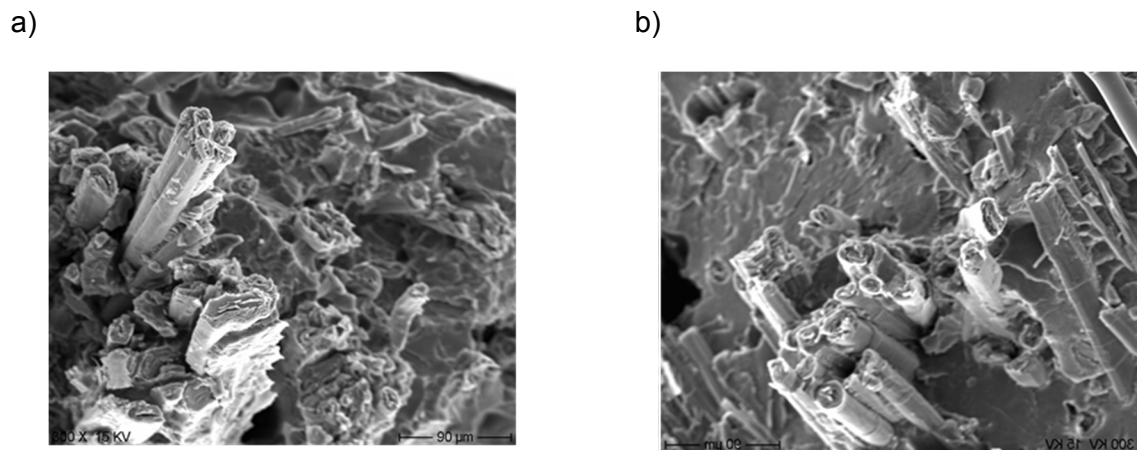


Figure 24: SEM pictures taken from PLA/flax4x4 a) and PLA/flax2x2 composites b).

Tensile response

It has been reported that the stiffness and strength properties of composites are depended on weave architecture and fiber undulation [40]. Note that the interlacing of fibers in fabric leads to fiber undulation. This is in accordance with tensile test - observations. Results of the tensile strength, modulus and elongation at break are given in figure 25.

It is clearly seen that the incorporation of different weave types strongly affected the tensile mechanical behavior of PLA. For the both woven composites, the tensile stiffness and strength of the corresponding composites increased at the cost of elongation at break (slightly reduction) compared to the neat PLA. The increase of the tensile strength with adding flax weave textiles was largely due to an increase the axial stiffness of the composites. For example, the stiffness of the flax_{4x4} and flax_{2x2} composites was improved by approx. 118 % and 102 %, respectively, compared to the neat PLA. It is interesting to note that the flax_{4x4} composite exhibited higher tensile modulus and strength than the composite_{2x2}. The decrease of the tensile mechanical data has to be attributed to the undulation effect of woven flax textile_{2x2}. An increase in flax undulation of composite_{2x2} led to a decrease strength and stiffness during tension loading, thus accounting for some of drop in impact strength when compared to flax composite_{4x4}. This observation is in accord with experimental result of impact weight test (cf.-figure 21). Similar conclusion was drawn also for the mechanical behavior of flax reinforced HDPE in former work [41].

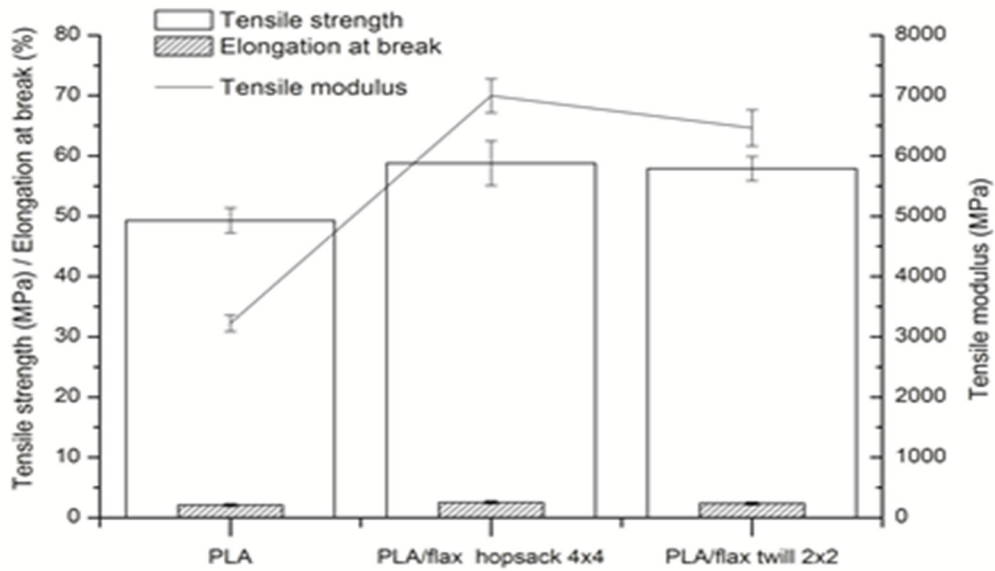


Figure 25: Tensile mechanical characteristics of the systems studied.

Dynamic mechanical response

Figure 26 demonstrates the effect of increased frequencies on the storage modulus as a function of temperature for the PLA, PLA/flax_{2x2} and flax_{4x4} composites. It is clear from figure 26 in whole temperatures investigated that the storage modulus decreased markedly with increasing temperature and decreasing frequency. Due to the cold crystalliza-

tion of the amorphous chains which was typical of PLA [31], increased the storage modulus above 100 °C. Surprisingly, the reinforcing effect of the weave textiles was increased stiffness of cold crystallization phenomenon backwards lower temperature. The composite with flax_{4x4} exhibited the highest stiffness at the whole evaluated frequency range. It can be attributed to the reinforcing effect of this weave structure_{4x4} in the PLA matrix. This is in harmony with the tensile test results which increased tensile stiffness of composite_{4x4}.

It is also striking for PLA that, the course of the modulus as a function of temperature was quite similar with increasing frequency, i.e. the related traces are running more or less parallel to one another. Note that the modification with flax weave textiles affected the storage modulus but its change with the frequency was governed by the PLA/flax composites itself.

The relationship between the storage modulus and the creep compliance was proved to be capable of predicting the nonlinear viscoelastic behaviors of the system studied. Creep compliance is defined as the inverse quantity of modulus by the following equation which was already successfully adapted to estimate the storage creep behavior of a natural reinforced PLA [21].

$$D' = \frac{E'}{(E')^2 + (E'')^2} \quad (18)$$

where D' and E' are the real parts of the creep compliance and modulus, respectively. E'' is the imaginary part of the modulus.

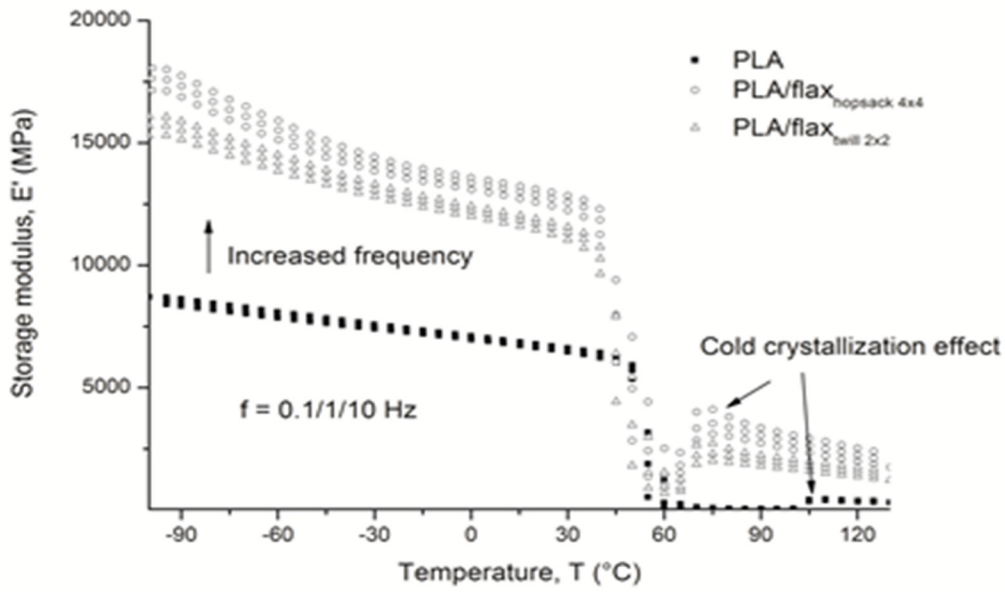


Figure 26: E' vs. T trace at different frequencies for the PLA, PLA/flax_{4x4} hopsack and PLA/flax_{2x2} twill.

The storage creep compliance as a function of temperature for PLA, PLA/flax_{2x2} and PLA/flax_{4x4} composites are depicted in figure 27. It can be clearly seen that an increase of temperature, the calculated creep compliance increased for the PLA. The creep compliance indicated the temperature active softening of the PLA as a result of the highly increased mobility of polymer chains at the glass transition of PLA (approx. 60 °C). Observations of temperature clearly indicate that the creep response of these flax composites was much lower than that of neat PLA. Strikingly, the results showed that the time-temperature superposition (TTS) method is superior to the existing methods ($aT=f_0/f_T$) [42], by normalizing the effects of the frequency on the calculated creep behaviors. Since the creep value of PLA at closer to T_g dramatically increased, when the temperature above T_g , the flax composites had less softer rubbery properties which dependent greatly on the loading frequency from low to high scanning range. Note that the molecular chains of flax composites_{4x4} had a very limited freedom of movement and its free volume decreases slower with the frequency, when compared to the PLA and flax composite_{2x2}. This finding is agreed with the impact resistance test. The lower temperature as well as lower frequency showed less rubbery properties, due to slow chain mobility, likely in the interphase regions. The stretching of the amorphous and entangled chains PLA occurs with considerable time delay under the high frequency in presence of low undulation of flax_{4x4} composite.

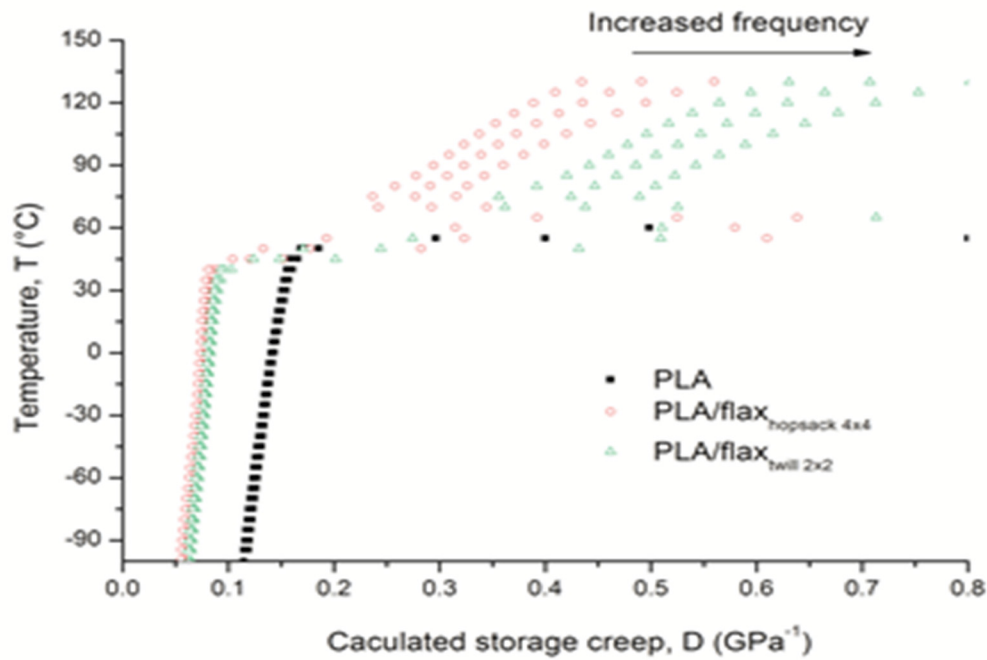


Figure 27: Conversion from the modulus to creep compliance for the PLA, PLA/flax4x4 hopsack and PLA/flax2x2 twill.

Conclusion

This work devoted to study the morphology, falling weight impact and mechanical properties of a PLA (Polylactide) and its flax_{2x2} and flax_{4x4} reinforced composites. SEM results have shown that the interfacial gaps between flax and PLA matrix became small when using the interval hot press. Flax reinforcement in PLA matrix increased markedly the impact resistance. The impact value of PLA/flax_{4x4} composite was higher than that of PLA/flax_{2x2} composite. A decrease in temperature reduced the peak force. The degree of stress whitening appeared to be dependent upon the types of fiber weave according to photograph observations. The presence of flax was associated with an increase stiffness and slightly tensile strength of related composites. Clear trend in the effect of composite structures was found in the stiffness at the whole evaluated frequency range. The calculated storage creep compliance could be well described by an applicability of the conversion method from the modulus. Observations of temperature clearly indicated that the calculated creep response of these flax composites was much lower than that of the neat PLA. A benefit of this proposed interval hot press technique is a very effective process for the production of flax reinforced PLA composite.

3.3 Un- and Modified Polylactide (PLA) /Woven Flax Fiber Composites

State of the Art

Natural fibers have been receiving considerable attention as substitutes for synthetic fiber reinforcement. Their advantageous properties compared to other materials are low cost and density, acceptable specific strength, good thermal insulation properties and renewable resources [44]. The expanded use of natural thermoplastic composites has attracted considerable attention in R&D activities due to the promise of simultaneous improvements in stiffness and toughness characteristics of the corresponding thermoplastic composites [41, 45]. Poly(lactic acid) (PLA) has been widely used in medical and automotive applications, due to its good biocompatibility, biodegradability and mechanical properties, PLA is often modified with natural fibers, such as cellulose, kenaf and abaca fibers to improve the thermal and physical–mechanical properties [18-19, 31, 46] (e.g. impact, stiffness at a high temperature and strength properties). Although natural fibers have outstanding properties, major problem of using them with PLA is the poor interracial bonding between the natural fiber and thermoplastic. However, though the modification of PLA with natural fibers results in enhanced strength and stiffness [47-48]. It was shown recently that rice straw fiber (RSF) coated with poly(methyl methacrylate) thin film showed better compatibility with the PLA matrix [48]. The significantly improved thermal and mechanical properties were attributed to the interfacial adhesion improvement between treated RSF and PLA. The tensile strength and thermal stability of treated RSF-PLA was improved compared with untreated RSF-PLA composite.

Flax fibers are tough and are found to be a potential reinforcement in PLA because they are inexpensive and environmentally friendly. The flax reinforcement indicated a better improvement of the modulus of PLA [22]. PLA/flax composite became an ecologically beneficial alternative to natural reinforced composites with petrochemical matrices in the future. It is worthy note that a variety of composite structures is also associated with an increase in mechanical properties of composites [37]. The mechanical behaviors of composite materials have a strong impact on the composite structures of the reinforcing phase. The goal of this study was to demonstrate the feasibility of the production of un- and modified PLA with different flax composite structures and compare the morphology, water absorption, impact, thermal and mechanical properties of the related composites. The woven flax fiber was used as reinforcement. The dispersion of woven flax fiber in

PLA was assessed by scanning electron microscopy (SEM) and computed microtomography system (μ CT). The un- and modified PLA/flax composites were compression molded and compare the structure-property relationships of the resulting composites.

Materials and preparation of composites

Woven flax fiber textiles (weave style of 2x2 twill and 4x4 hopsack) were used as reinforcement which had a yarn size of 250 tex. Biotex flax was supplied by Composites Evolution (Chesterfield, UK). Figure 28 shows the two woven flax textiles that were used to study the effect of weave type. The density was 1.24 g/cm^3 (according to suppliers' information). PLA (Polylactide 2002 D, NatureWorks, Minnetonka, MN, USA) was utilized as polymeric matrix for composite systems. Its melt flow rate (MFI at $210^\circ\text{C}/2.16 \text{ kg}$) was $6 \text{ g}/10\text{min}$). Two commercial additives were used as modifier for PLA. Biomax Thermal 300 (composition of non-regulated wax/ethylene acrylate copolymer/butyl acrylate) and Palaroid BPM-500 served as thermal and acrylic impact modifier, respectively.

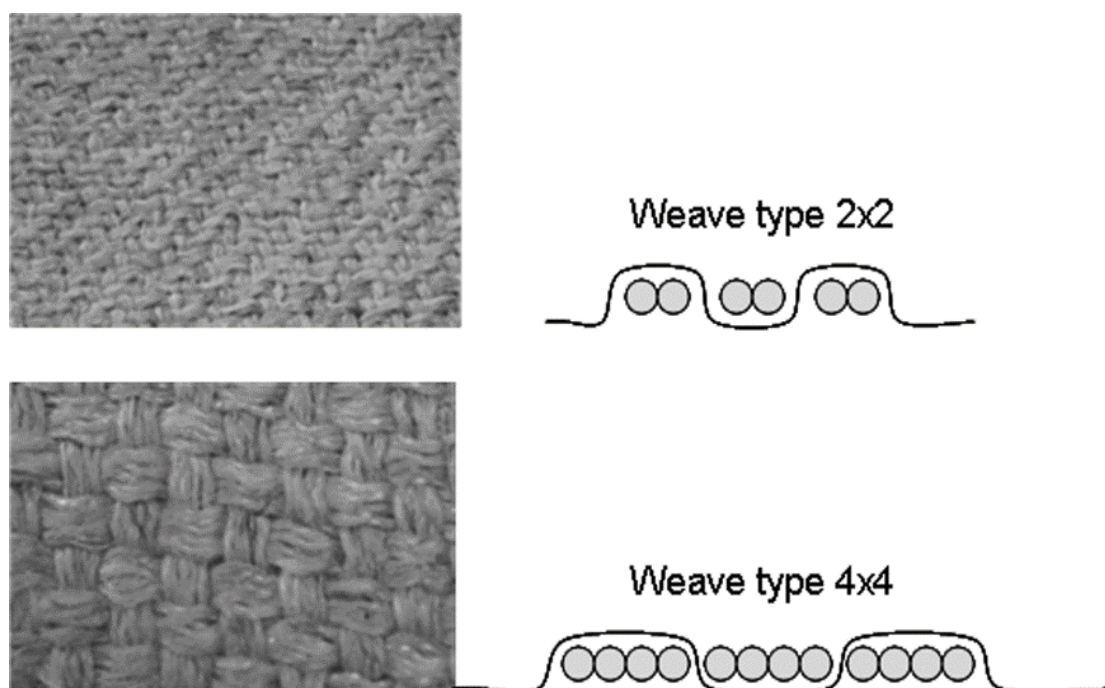


Figure 28: Schematic representation of weave style 2x2 twill and 4x4 hopsack.

PLA and modified PLA sheets were prepared by twin-screw extruder (Leistritz, Nürnberg, Germany). The modified PLA was compounded by setting the barrel temperatures between 100 (zone 1) and $190\text{--}200^\circ\text{C}$ (from zone 2 to 9), rotor speed of 225 rpm and pressure of 50 bar . The thermal and impact modifier contents in the PLA system investigated were set for 5 and $3 \text{ wt.}\%$, respectively (according to suppliers' recommendation). The additives and PLA granulates were charged in feeder in the first zone of the extruder

using the above conditions. The PLA composites were produced by hot press methods. The PLA composites placed by hand laying-up a layer of woven flax fibers and then by a layer of PLA or modified PLA sheet. The PLA /woven flax fibers composites were produced into 1-mm thick sheets by hot pressing in a laboratory press (P/O/Weber, Maschinen und Apparatebau, Remshalden, Germany) at a temperature of 200 °C with a fixed holding time of 7 min. under a pressure of 10 MPa. The composites produced are listed in table 3.

Table 3: Recipe and designation of the un- and modified PLA-based systems studied.

Sample Designation	Flax _{2x2} twill (wt.%)	Flax _{4x4} hopsack (wt.%)
PLA	-	-
modified PLA	-	-
PLA/flax _{2x2} twill (l)	35	-
PLA/flax _{2x2} twill (h)	65	-
PLA/flax _{4x4} hopsack (l)	-	35
PLA/flax _{4x4} hopsack (h)	-	65
modified PLA/flax _{2x2} twill (l)	35	-
modified PLA/flax _{4x4} hopsack (l)	-	35

Characterization and testing

Morphology detection

The fracture surface was subjected to scanning electron microscopy (SEM) inspection in a JSM 5400 device of Jeol (Tokyo, Japan). The surface was gold coated prior to SEM inspection performed at low acceleration voltage.

Water absorption

Water absorption of the composites was investigated over a period of 30 days. The composites were cut into specimens (20x20 mm²) and then, they were immersed in water in a bath at room temperature. Weight gains were recorded by periodic removal of the specimens from the water bath and weighing on a balance. The percentage gain at any time t (M_t) as a result of moisture absorption was calculated from the following equation:

$$M_t = \frac{W_w - W_d}{W_w} \cdot 100\% \quad (19)$$

where W_d and W_w denote the weight of dry material (initial weight of materials) and weight of materials after exposure to water absorption, respectively.

Instrumented Falling Dart Impact

Instrumented falling weight impact (IFWI) test was performed on a Fractovis 6785 (Ceast, Pianezza, Italy) using the following settings: incident impact energy, 20 J; diameter of the dart, 20 mm; diameter of the support rig, 40 mm; weight of the dart, 10.357 kg; drop velocity, 1.97 m/s. IFWI tests were performed on quadratic specimens of 60x60 mm² at room temperature.

Thermal and thermomechanical response

Thermogravimetric analysis (TGA) was performed on a DTG-60 SHIMADAZU device (Kyoto, Japan). TGA experiments were conducted in the temperature range from 30 to 500 °C under nitrogen at a heating rate of 10 °C/min.

Dynamic mechanical thermal analysis (DMTA) was performed in tensile mode at frequencies of 0.1, 1 10 Hz at all isothermal temperatures, using a DMA Q800 apparatus (TA Instruments, New Castle, NJ). The storage modulus (E') was determined as a function of the temperature ($T = -100^\circ\text{C} \dots +130^\circ\text{C}$). The strain applied was 0.1%. The specimens were cooled to -100°C . The temperature was allowed to stabilize and then increased by 5°C , kept 2 min isothermal until 130°C .

Creep response

Short time creep test was made in tensile mode at different temperatures using the above DMA apparatus. The applied stress was 3 MPa. The temperature dependence of the creep response of the composites was studied in the range from 15 to 50°C . Isothermal tests were run on the same specimen in the above temperature range by increasing the temperature stepwise by 5°C and equilibrating the specimen at each temperature for 2 min. During the isothermal tests the duration of the creep testing was 15 min.

Result and Discussion

Morphology

The SEM pictures in figures 29 a-b present the morphological characteristics of the PLA/flax_{2x2} and PLA/flax_{4x4} composites. One can see that composites containing flax_{2x2}

and flax_{4x4} displayed slightly different fracture surface appearances. While the flax structures prevented from spreading out of the molted PLA during hot pressing. The molten PLA could spread out uniformly in the related composites. Note that the flax had diameter of 15-25 μm . The cross-section of the flax fibers displayed clear lumina which were not filled with PLA. The μCT micrographs of the unmodified PLA/flax_{4x4} and modified PLA/flax_{4x4} composites are shown in figure 30. It can be seen that the impregnation quality of PLA and modified PLA composites were similar due to their small difference in voids. The porosities of unmodified and modified PLA composites were between 8-9 %, and there was no obvious dependence on the type of the matrices modification. This was a fairly to compare the observed change in the thermal and mechanical properties of both un- and modified PLA composites in further investigations.

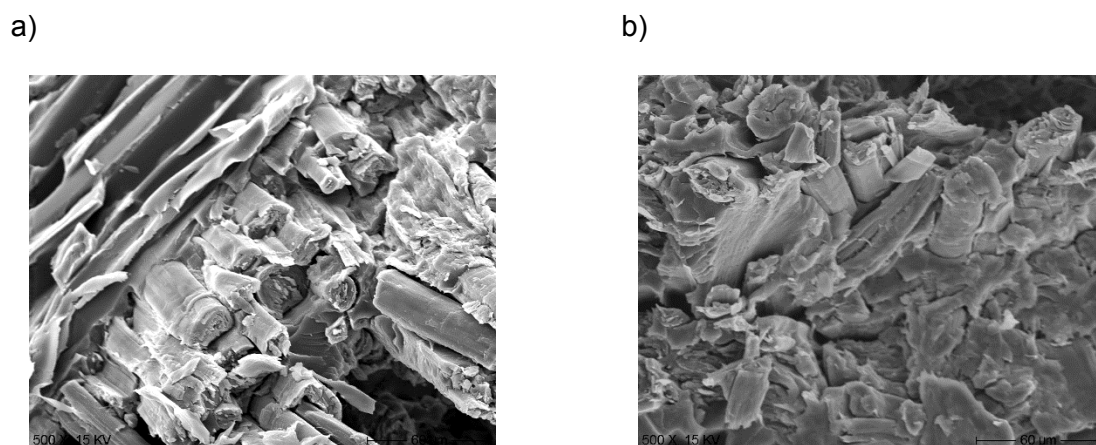


Figure 29: SEM pictures taken from PLA/flax_{2x2} a) and PLA/flax_{4x4} b) composites.

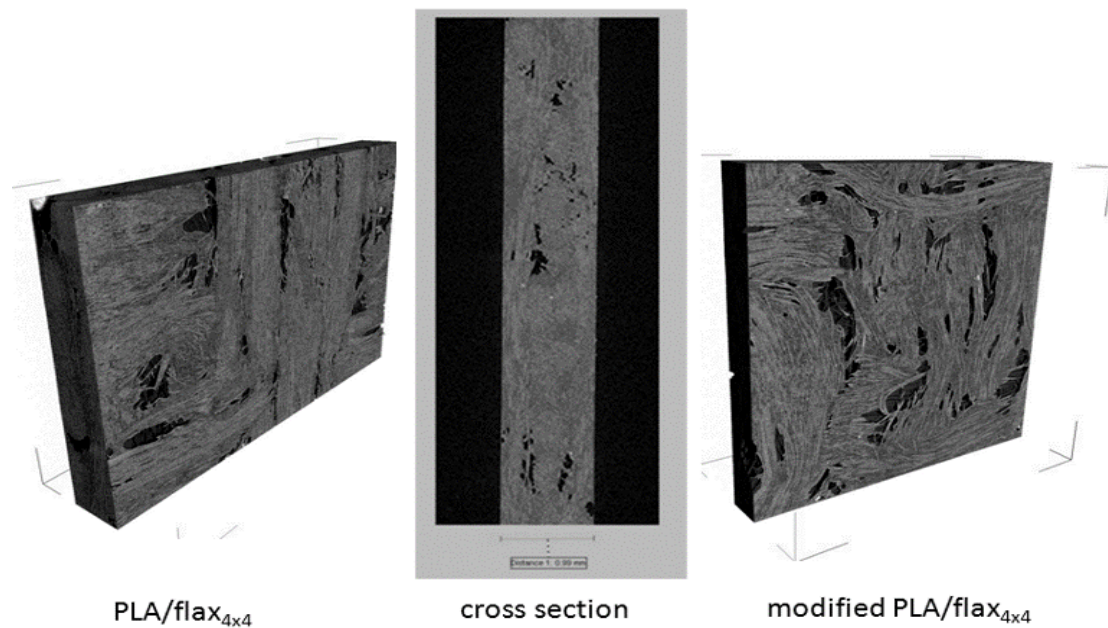


Figure 30: μ CT scans of the PLA/flax_{4x4} and modified PLA/flax_{4x4} composites.

Falling dart impact response

Results of the falling dart impact tests and data are given in figure 31 and table 4, respectively. One can recognize that the impact resistance of the modified PLA increased markedly compared to the PLA. This toughness modification of PLA was accompanied with a shift of the force peak toward higher force and longer time (cf. table 4). It is clearly seen that the incorporation of flax structures strongly affected the impact behavior of PLA. Note that the resistance to impact increased with increasing amount of flax content. The reinforcing effect of the structures of PLA containing 65 wt.% of flax_{2x2} and flax_{4x4} indicated an increase impact energy by approx. 9.7 % and 39.7 %, respectively, compared to the neat PLA. The related change suggested enhanced energy absorption in the fiber orientation but indicated for the character of flax fiber weave style. It is also well resolved that the impact resistance of the modified PLA composites in both flax structures was always inferior to that of the PLA composites. The modified PLA/flax_{2x2} composite specimen recorded the peak force value at ca. 232 N upon 2.2 msec. This peak force was increased by approx. 23 % compared to the unmodified PLA/ flax_{2x2} composite. This can be explained by the consideration of the highly increased mobility of the flexible chains in the modified PLA matrix. The photograph of typical failure behavior of the related composites after the falling dart impact tests is clearly shown in figure 32 that the change in the matrix failure occurred in the modified PLA/flax composites compared to the unmodified PLA/flax composites. This is the typical feature of tough fracture in the

modified PLA/flax composites. The fracture surface became a whitened zone around the crack.

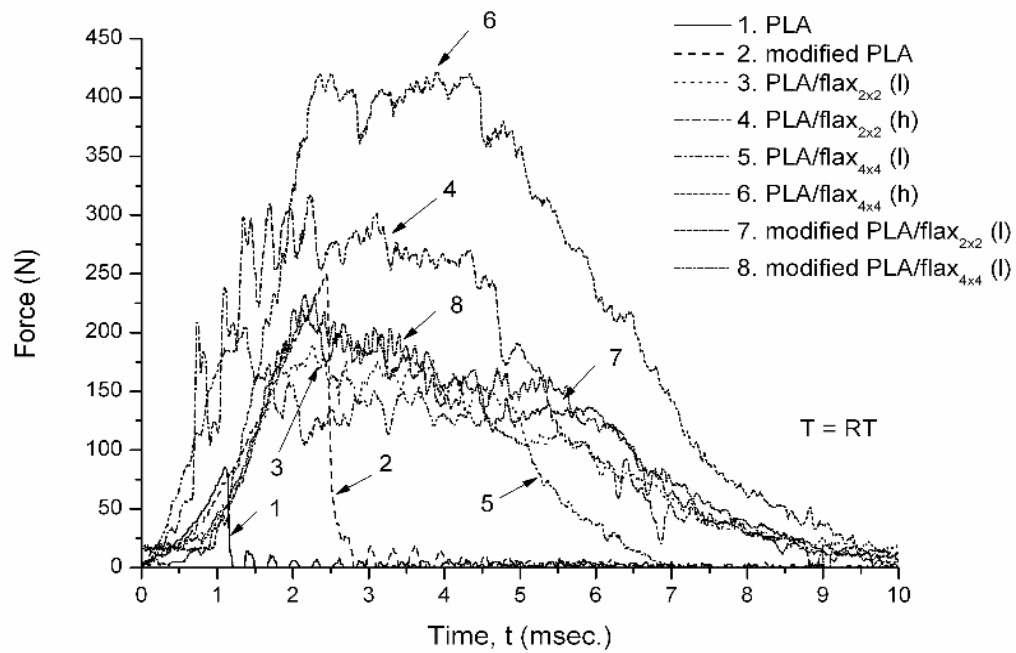


Figure 31: Characteristic force-time curves for the un- and modified PLA-based systems.

Table 4: Impact characteristic of the un- and modified PLA-based systems studied.

Sample Designation	Force (N)	Time (ms)	Energy (J)
PLA	85.6	1.1	0.075
modified PLA	250	2.4	0.49
PLA/flax _{2x2} twill (l)	190.2	2.3	0.36
PLA/flax _{2x2} twill (h)	316.7	2.2	0.77
PLA/flax _{4x4} hopsack (l)	204.6	1.4	0.29
PLA/flax _{4x4} hopsack (h)	422	3.9	1.94
modified PLA/flax _{2x2} twill (l)	231.9	2.2	0.36
modified PLA/flax _{4x4} hopsack (l)	220.5	2.1	0.3

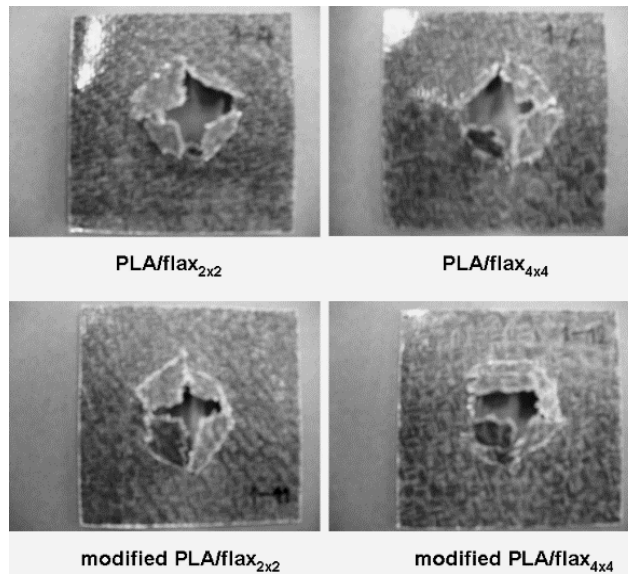


Figure 32: Failure of the specimens of the un- and modified PLA composite systems studied after IFWI.

Water uptake

The water uptake as a function of time for the PLA, modified PLA and its composites, are demonstrated in figure 33. It is interesting to note that the PLA recorded water absorption value at 0.8 % upon 30 days while the modified PLA did not absorb water within a month. The flax composites exhibited remarkably large amount of water absorption within in first 3 days. This is attributed due to the chemical nature of cellulose content in flax composites. The water sorption behavior was considered to depend on the flax content. The water uptake of composites increased with increasing flax content in PLA. The water uptake of the PLA/flax_{2x2} 65 wt.% composite was 14 % whereas the composite containing 35 wt.% flax_{2x2} was 9% after 30 days of immersion. Other studies also have reported a similar trend for pineapple-leaf fiber reinforced low density polyethylene (LDPE) composites. It was found that the moisture absorption increases linearly with the fiber loading [49]. On other hand, the effect of modified PLA in composites on the water uptake value was marginal.

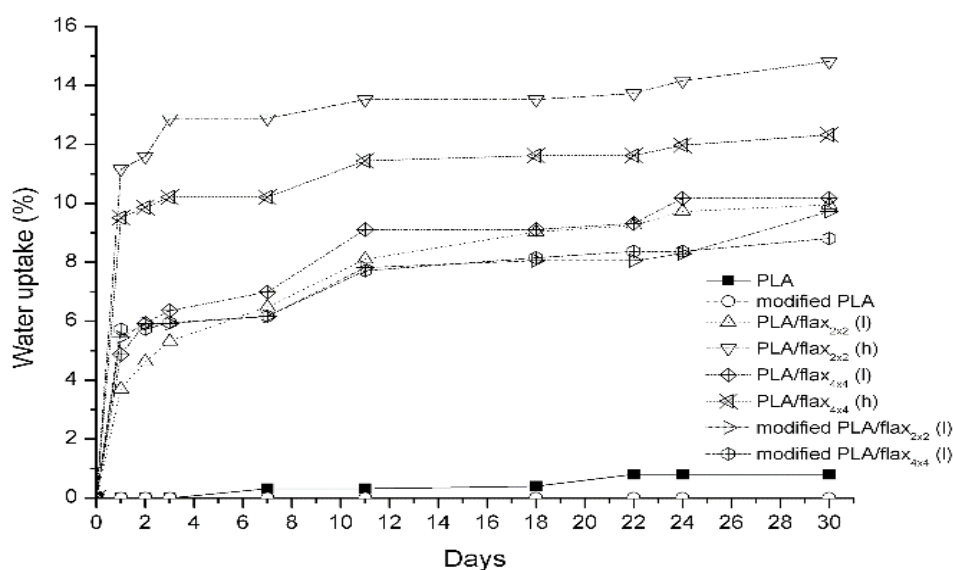


Figure 33: Water uptake on the un- and modified PLA systems studied.

Thermogravimetric analysis

Figure 34 presents the overall of the thermogravimetric decomposition process for the PLA, modified PLA, flax and its composites at a heating rate of 10 °C/min. The TGA data are listed in table 5. It is well known that the thermal stability effects in natural fiber and the natural composites exhibited three stages from its TGA spectra. Initially stage at low temperature is usually due to the removal of absorbed moisture. The second and third stages observed at high temperature are usually attributed to the degradation of hemicelluloses and non-cellulosic materials [50]. This is in accordance with flax - TGA observation. It is clearly seen in figure 33 that that thermal decomposition process of all PLA composites had similar characteristics as a result of one step procedure representing depolymerization. Due to the thermal decomposition of hemicelluloses and the degradation of lignin, the weight loss of flax composites decreased markedly. As shown in table 5, resulted mainly from the thermal decomposition of modified PLA and its composites, was observed with an improve slightly in thermal resistance at least below 250 °C, compared to PLA and PLA composites, respectively. This is indicate that the effect of thermal mo

difier in PLA. One can conclude in figure 33 that the thermal stability of composites decreased with increasing amount of flax content. The resistance of thermal effect was better with the modified PLA.

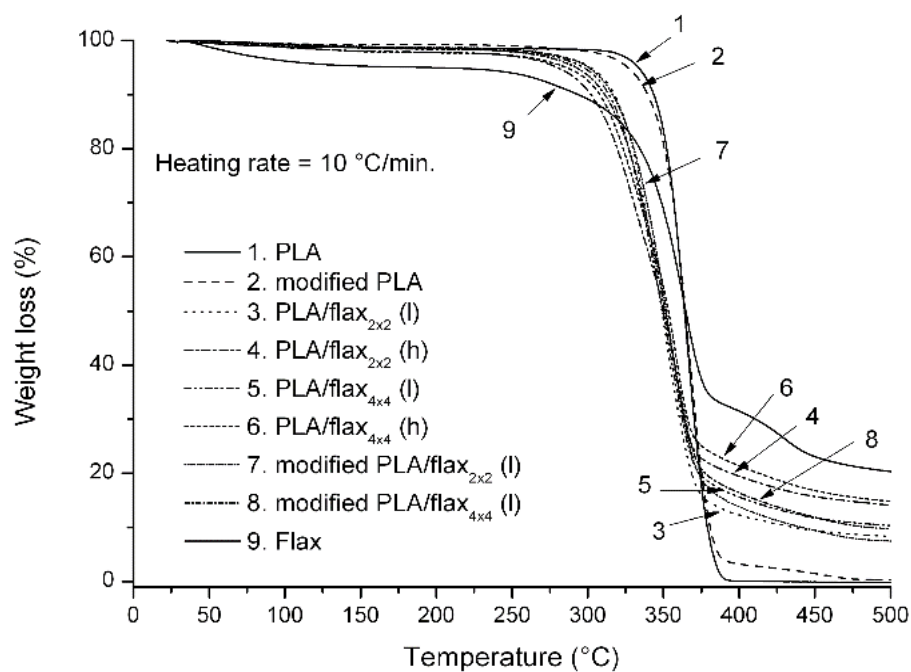


Figure 34: Weight loss versus temperature for the un- and modified PLA systems studied.

Table 5: TGA characteristic of the un- and modified PLA-based systems studied.

Sample Designation	Td 150 °C (%)	Td 250 °C (%)	Td 350 °C (%)
PLA	98.71	98.49	83.30
modified PLA	99.28	99.02	80.89
PLA/flax _{2x2} twill (l)	98.63	98.21	48.18
PLA/flax _{2x2} twill (h)	98.08	97.15	50.23
PLA/flax _{4x4} hopsack (l)	98.66	98.03	49.01
PLA/flax _{4x4} hopsack (h)	97.99	97.24	54.24
modified PLA/flax _{2x2} twill (l)	98.93	98.35	53.12
modified PLA/flax _{4x4} hopsack (l)	98.69	97.93	51.54
Flax	95.29	94.01	68.62

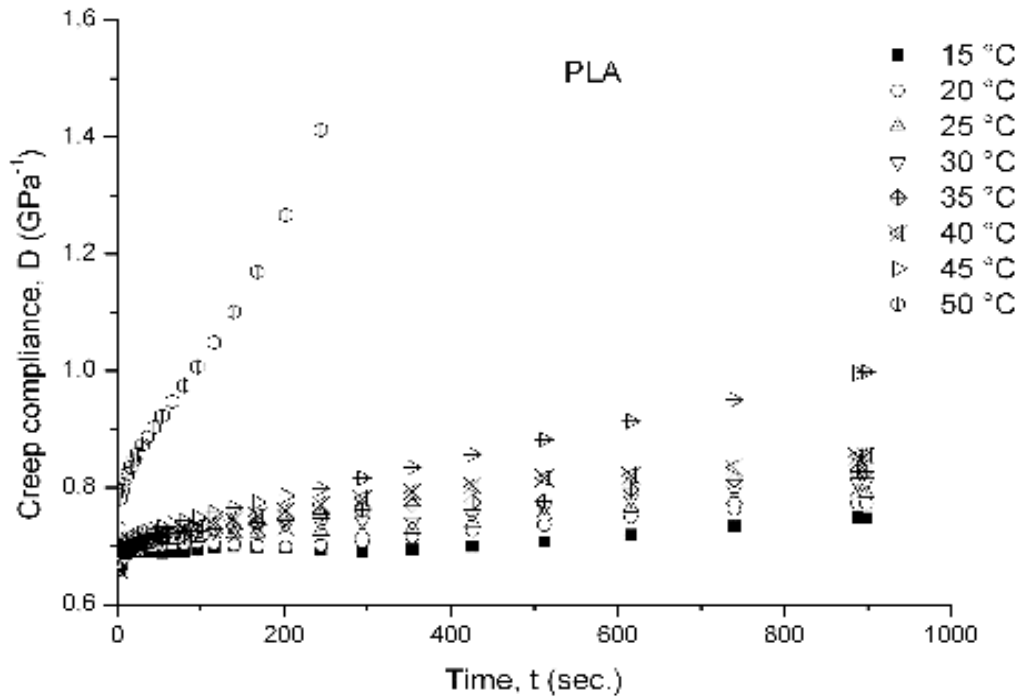
Creep response

Figure 35a and 35b demonstrates the effects of increased temperature on the creep compliance of PLA and modified PLA. One can recognize that the modified PLA exhibited higher creep compliance than the PLA one, especially at high temperature. This was due to the enhancement of the mobility of PLA chains with the toughness agent, which would make the PLA softer and the orientation movement of amorphous chains easier. Note that a tertiary range of modified PLA (fracture creep) has been achieved at temperature of 50 °C. In practical term, the creep compliance is generally expressed as consisting of two components, the elastic (D_e , instantaneous, time-independent) and the viscoelastic (D_v , reversible, time-dependent) [51].

$$D(t, \sigma_0, T) = D_e(\sigma_0, T) + D_v(t, \sigma_0, T) \quad (20)$$

where σ_0 is the applied stress, T is the temperature and t is the time.

a)



b)

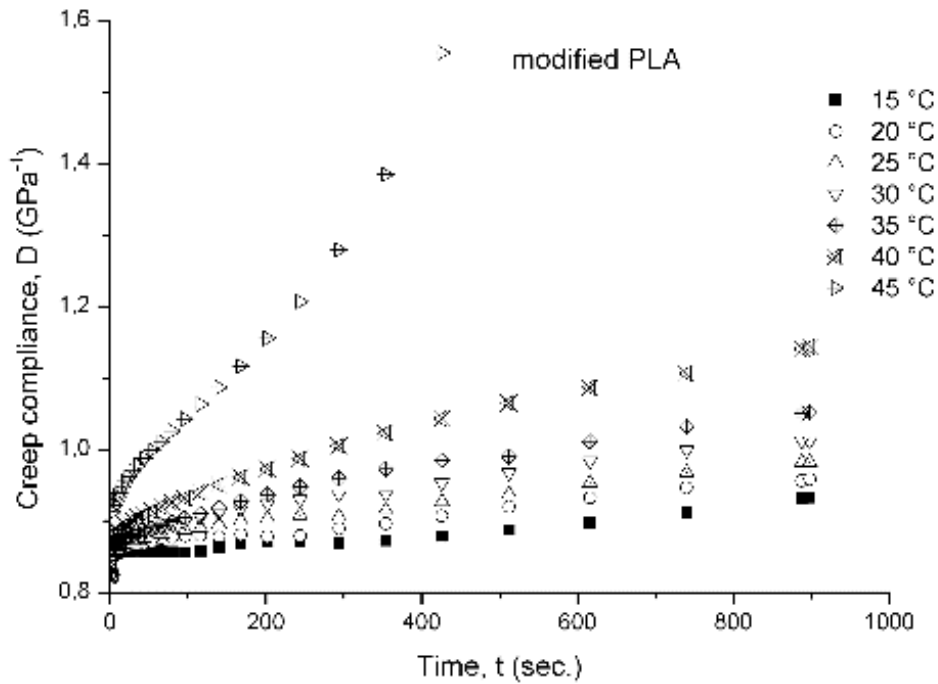


Figure 35: Effect of temperature on the creep compliance of the PLA a) and modified PLA b).

The results of the elastic (D_e) and viscoelastic (D_v) parts of creep compliance data with increased temperature are listed in table 6. The D_e and D_v have been associated with the stiffness and flow of amorphous polymer chains in the short term creep, respectively. The results in table 6 for the PLA and modified flax composites system studied showed that D_e and D_v increased with an increase in temperature. This was due to the softening of the bulk materials at elevated temperature. With the introduction of flax, it was observed that D_e and D_v decreased under each condition. One can notice that the effect of flax reinforcing structures on the D_e and D_v value was marginal. However, the both D_e and D_v of creep compliance were enhanced markedly with an increase amount of reinforcing flax.

Table 6: Elastic (De) and viscoelastic (Dv) parts of the creep response of the un- and modified PLA-based systems studied.

		15 °C	20 °C	25 °C	30 °C	35 °C	40 °C	45 °C	50 °C
PLA	elastic	0.66	0.66	0.66	0.66	0.66	0.66	0.66	0.73
	Visco	0.75	0.77	0.79	0.81	0.83	0.85	1.00	55.70
modified PLA	elastic	0.82	0.82	0.82	0.83	0.83	0.84	0.87	
	Visco	0.93	0.96	0.98	1.01	1.05	1.14	7.89	
PLA/flax2x2 twill (l)	elastic	0.46	0.46	0.47	0.48	0.49	0.50	0.52	0.69
	Visco	0.55	0.57	0.58	0.59	0.60	0.61	0.80	4.09
PLA/flax2x2 twill (h)	elastic	0.18	0.18	0.18	0.19	0.19	0.21	0.25	0.37
	Visco	0.26	0.26	0.27	0.27	0.27	0.29	0.38	1.54
PLA/flax4x4 hopsack (l)	elastic	0.40	0.41	0.42	0.43	0.44	0.46	0.48	0.74
	Visco	0.51	0.51	0.53	0.53	0.54	0.56	0.94	5.06
PLA/flax4x4 hopsack (h)	elastic	0.23	0.23	0.23	0.23	0.24	0.24	0.24	0.38
	Visco	0.34	0.33	0.33	0.33	0.32	0.31	0.31	0.93
modified PLA/flax2x2 twill (l)	elastic	0.50	0.51	0.52	0.53	0.54	0.56	0.60	1.00
	Visco	0.62	0.63	0.64	0.65	0.67	0.70	1.46	7.52
modified PLA/flax4x4 hopsack (l)	elastic	0.31	0.31	0.32	0.32	0.33	0.34	0.36	0.66
	Visco	0.41	0.42	0.42	0.43	0.43	0.44	0.98	3.38

The time temperature superposition (TTS) method can be used in order to obtain the polymeric material lifetime. This method can be used to shift in a short time results under normal application conditions and the results obtained can be extrapolated to longer times. According to the TTS principle, the response time (t) or frequency (f) as function of creep (D) or storage modulus (E') at one temperature T₀, is similar in shape to the same functions at neighbouring temperatures (T). The curve of D or E' at one temperature, can be horizontally shifted along the t or f axis then overlapped on the curves at neighbouring temperatures.

$$a_T = \frac{D(t, T)}{D(t, T_0)} = \frac{E'(f, T)}{E'(f, T_0)} \quad (21)$$

The Arrhenius equation is generally acknowledged as suitable to describe the relationship between the shift factors using TTS of master curve and the reference temperature. The Arrhenius equation generally used to calculate the activation energy (ΔH) via [32]:

$$\ln a_T = \frac{\Delta H}{R} \left(\frac{1}{T} - \frac{1}{T_0} \right) \quad (22)$$

where R is the universal gas constant.

In Figure 36, the creep master curves of the PLA, modified PLA and its composites at the reference temperature of 25 °C, are plotted as a function of the creep time, t. One can see in figure 36 that the creep master curves of PLA and modified PLA covered only a period of 14 h and 8 h, respectively. However, the curve of the flax composites reached duration of 50 h. The creep behavior of flax composites increased sharply at first, and then almost kept constant. For pure PLA and modified PLA, the creep also increased sharply at first, and then the rapid creep was observed with the increase of time. For the master curves from short-term creep TTS in figure 36, the PLA and modified PLA exhibited the primary, secondary and tertiary stages of creep (initial, steady state and fracture creep respectively) whereas only primary and secondary creep stages were observed for flax composites. Recall, the onset of the tertiary creep stage of PLA and modified PLA was detected at approximately 14 h and 8 h, respectively, of creep time.

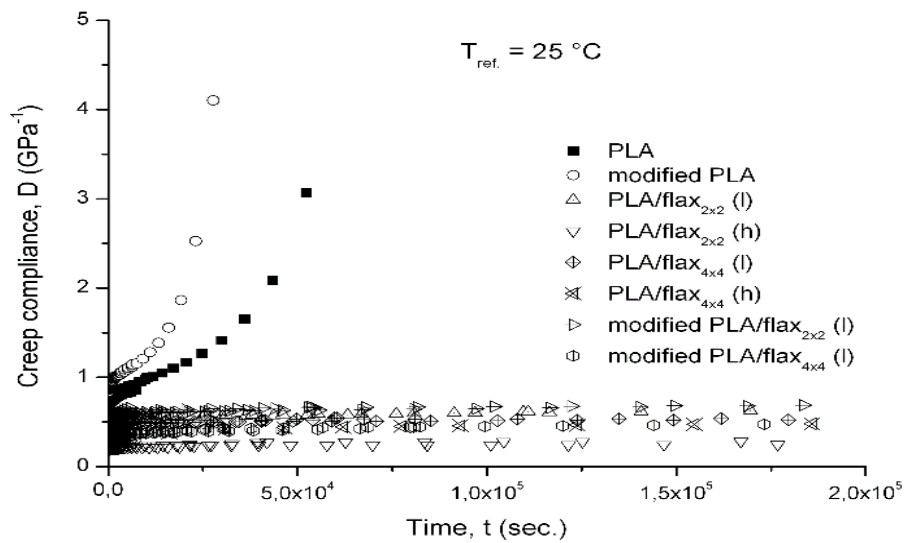


Figure 36: Creep master curves (compliance vs. time) constructed by considering the TTS and selecting Tref= 25 °C.

Dynamic mechanical thermal response

Figure 37 displays the traces of storage modulus (E') as function of temperature for the PLA, modified PLA and its composites. One can notice that the modified PLA showed a lower storage modulus in the whole temperature range investigated compared to the unmodified PLA. The presence of flax increased the storage modulus and with a shift in the T_g of PLA towards higher temperature. The storage modulus of PLA/flax_{4x4} 65 wt.% composite was increased by approx. 150% at least below the T_g compared to the neat PLA. On the other hand, the E' decreased with increasing temperature. Note that due to the cold crystallization of the amorphous PLA, the E' of composites was increased above 100 °C, as expected. Regarding to the effect of composite structures, the incorporation of flax_{4x4} led to enhance in the E' compared to the composite containing flax_{2x2}, while the E' also increased by increasing the flax content. Difference change in the stiffness occurred between the PLA/flax_{2x2} and PLA/flax_{4x4} composites due to the effect of fiber undulation. According to the literature and reported by Paessler et al. that the effects of fiber waviness due to the fiber crossing such as warp and weft crossover points, lead to a reduction of the in-plane properties of such a laminate. Clear differences regarding strength and stiffness of the laminates without and with undulations could be observed for carbon fiber/epoxy composites [38, 52].

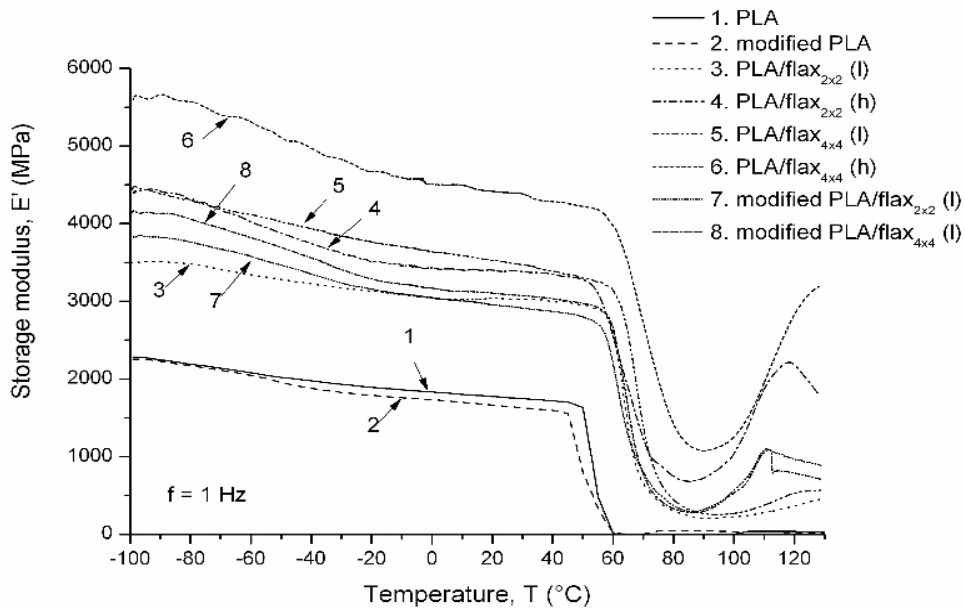


Figure 37: E' and $\tan \delta$ vs. T traces for the un- and modified PLA systems studied.

A remarkable difference influence of frequencies is observed for the storage modulus of the PLA and its composites. An increase in frequency was accompanied with a shift on the E' towards higher temperature (not reported here). DMA master curves were performed to study how the stiffness of PLA/flax composites and modified PLA are affected

by exposure at elevated frequencies. The shift factor (a_T) using the time temperature superposition (TTS) principle for the generation of storage modulus master curve is according to equation 21. A reference temperature ($T_{ref} = 25\text{ }^{\circ}\text{C}$) was used for this shifting process. The values of storage modulus (E') for the PLA, modified PLA and flax composites are compared in figure 38. It is seen from this figure that pure PLA had a lower E' than PLA/flax composites at whole over loading frequencies. It was also demonstrated that the addition of flax improved the stiffness of PLA and modified PLA. Note that in the terminal region at lower frequencies, the storage modulus master curve was more dependent on the reinforcement effect of the flax. In this analysis, the stress can be transferred from PLA matrix to flax, so the chain mobility of the matrix is reduced. From the master curve data, the effect of modified PLA on the storage modulus was more pronounced in frequencies range from 10^{-4} to 10^{-13} Hz. The E' shifted to lower frequencies when the modified PLA was used. This can be attributed to the heat-stabilizing effect of the modified PLA. The combined thermal modifier PLA which was formed relative steady-free radicals produced in low frequency process, could improve the progression of thermal resistance. By comparing the activation energies (cf. Figure 38), one may conclude that the E_a increased with modified PLA. This result suggests that E_a may be sensitive to the thermal modifier. Incorporation of flax into the PLA matrix yielded also an increase in E_a that can be traced to the restricted PLA chains.

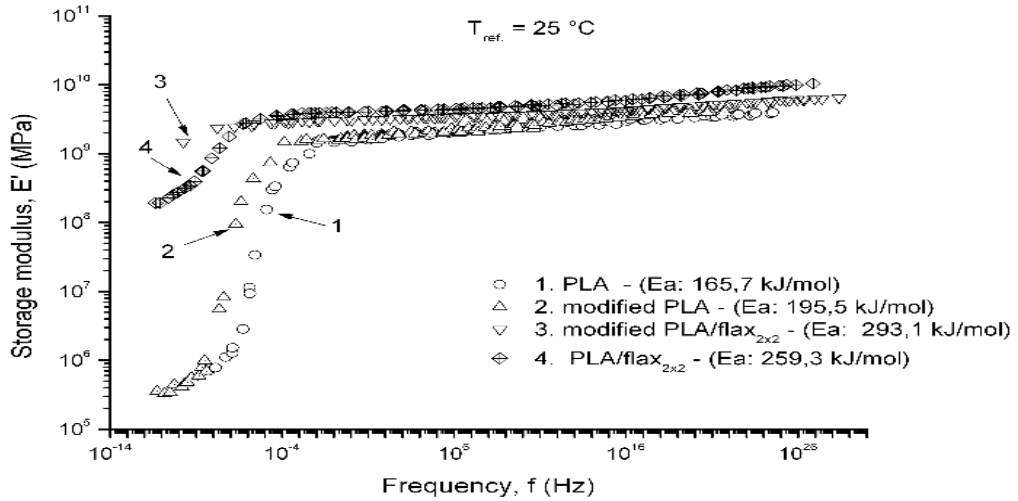


Figure 38: Storage modulus master curves were constructed by considering the TTS and selecting $T_{ref} = 25\text{ }^{\circ}\text{C}$. E_a was calculated by the Arrgenius equation, i.e.: $aT = E_r(t, T)/(E(t, T_{ref}))$.

Conclusion

This work devoted to study the morphology, water absorption, falling weight impact, thermal and mechanical properties of a PLA (Polylactide) and its flax_{2x2} and flax_{4x4} reinforced composites. Toughened PLA and composite have been successfully produced by direct modified matrix. The flax fibers displayed clear lumina which were not filled with PLA. This was demonstrated by SEM investigation. The impact resistance of PLA was highly enhanced by the addition of flax composite structures and acrylic impact modifier. The storage modulus value of modified PLA was slight lower than that of neat PLA. Incorporation of flax increased markedly the stiffness and water uptake of PLA. However, increase in storage modulus had a strong impact on the composite structures. The thermal degradation of PLA/flax composites decreased markedly compared to the neat PLA. The creep and storage modulus master curves were constructed by applying the time-temperature superposition (TTS) principle. The calculated data indicated that an improvement in the creep compliance and stiffness can be achieved with incorporation of flax. From the master curve data, the effect of modified PLA on the storage modulus was more pronounced in the low frequencies range. The proposed of direct modified PLA is an effective way being simple and cost efficient for producing PLA/flax composite.

3.4 Poly(butylene adipate-co-terephthalate) (PBAT)/woven flax composites

State of the Art

Eco-friendly biocomposite materials have been developed from biodegradable polymers as matrices and natural fibers as reinforcement, which have been a good alternative interest in the composite science because of their degradation in soil or regard to environmental condition and do not emit and leave any noxious components on the earth. Great research efforts are undertaken to produce lightweight, easy reprocessable, especially biocomposites, which may compete with traditional composites in various application fields based on their favored recycling and beneficial performance/cost balance [53]. Although biopolymer can offer the resulting composites many advantages. A large body of research works was already dealing with different bio-based polymers such as polylactide (PLA) and poly(butylene adipate-co-terephthalate) (PBAT), and the related knowegde is well summerized in recent reviews (e.g. [54-55]). Because PLA is highly brittle, PBAT has been a commercially interested polymer because of its high toughness (strain at break ~ 710%) and complete biodegradability. However, the commercial large scale applications of this biodegradable polymer are limited. This is because of its

relatively high cost and certain limitations in mechanical properties, like low tensile strength and modulus due to its low crystallization [56]. To date a large body of research & development works was denoted to clarify the process-structure-property relationships in reinforced polymers with natural fibers in order to be applied for various applications, especially in buliding and automotive industries by completely considered on their mechanical properties, biodegradability and environmental friendliness. Note that natural fibers have been used as reinforcement for biodegradable polymers due to their advantages compared to glass fibers, such as low cost (lower than glass fibers), high specific strength and modulus, low density, renewability and biodegradability [57]. Many researchers have reported the use of flax fibers, which is in form of short fibers, non-woven mat or woven fabric in order to reinforce thermoplastic polymers [16]. Note that flax is a high quality plant fiber, flexible and strong, can adapt to the changing environment as well. Bodros et al. [39] investigated the mechanical properties of biopolymers reinforced flax fiber composites. They found that the tensile strength and modulus increased with the increased in flax fiber content. The investigation of the mechanical properties of biopolymer and flax fiber composites was also made by Oksman et al. [58]. It was found that the composite strength and stiffness were improved by adding flax fiber up to 40 wt%. Anyway, only few works used to study their structures of woven fibers, which can behave as better reinforcement in term of mechanical behavior than short or unidirectional fibers [59]. From literatures, the incompatibility between polymer and natural fiber has to be mentioned. Incorporation of silane coupling agents could improve the compatibility of natural fiber/polymer compsoites [35].

In this research work was mainly focused on the development of textile biocomposites by using different types of flax fibers as a reinforcement and biodegradable polymer PBAT as a matrix material. A further aim of this work was to check the effects of the silane coupling agent and composite structure of the flax fiber. The mechanical properties such as tensile strength and modulus, impact strength, flexural strength and flexural modulus of these composites laminates were investigated.

Materials and preparation of composites

Poly(butylene adipate-co-terephthalate) (PBAT) pellets were purchased from Ecoflex-FBX7011-BASF. PBAT has a density of 1.25-1.27 g/cm³, a melting temperature of 110-120 °C and transparency of 82% (according to suppliers' information). Woven and non-woven flax fibers used as reinforcement were supplied by Composites Evolution (Ches-terfield, UK) and Tilsatec Advanced Materials, Tilsatec Ltd., (Wakefield, UK), respectively.

To prevent void formation, the PBAT pellets and flax fibers were dried at 60 °C for 24 h before processing to remove all absorbed moisture. The granulated PBAT was first converted into a film approximately 0.2 mm in thickness using a chill-roll cast film extruder (LE 25-30/C model, Labtech Engineering, Thailand). The temperature of the six extruder barrel zones was set at 160, 160, 170, 180, 190 and 200 °C, respectively, and the temperature of the die was set at 200 °C. The PBAT film was collected on rolls and stored in the laboratory under ambient conditions prior to use to manufacture the laminated biocomposites. The surface of flax fibers was modified with a 3-Aminopropyltriethoxysilane (APS) coupling agent (Dynasylan® AMEO, Evonik Industries AG, Germany). Surface modification of flax fibers with APS coupling agents was carried out in solution. The solution consisted of 3 wt% three-aminopropyltriethoxysilane (compared to the weight of flax fibers) added in 100 wt% ethanol. The solution was continuously stirred for 30 min to let silane hydrolysis. Afterwards, the fibers were immersed in the solution for 4 h followed by drying in an oven at 60 °C for about 24 h.

The technique of film stacking for woven fabrics reinforcing thermoplastics is necessary when need to bonded different entities. The films are formed from thermoplastic with quenching in order to guarantee the necessary temperature window during hot pressing [2]. As reinforcing fabrics usually woven flax and PBAT are used. PBAT composites laminates containing different weave types of woven flax fibers which are 2x2 twill and 4x4 plain woven, and non-woven mat as shown in Fig. 39. The laminates were produced by a compression molding using film stacking method. The composites laminates were prepared in which two layers of fibers were placed alternately between three layers of PBAT films in parallel arrays shown in Fig. 40. The composites were subjected to compressed consolidation at the specified temperature of 150 °C with constant pressure of 1500 psi for 5 min followed by cooling under pressure. When the mold temperature reached 60 °C, the composites samples were removed and cut to desired shapes for mechanical properties testing. The density of the composite laminates is shown in Table 5.

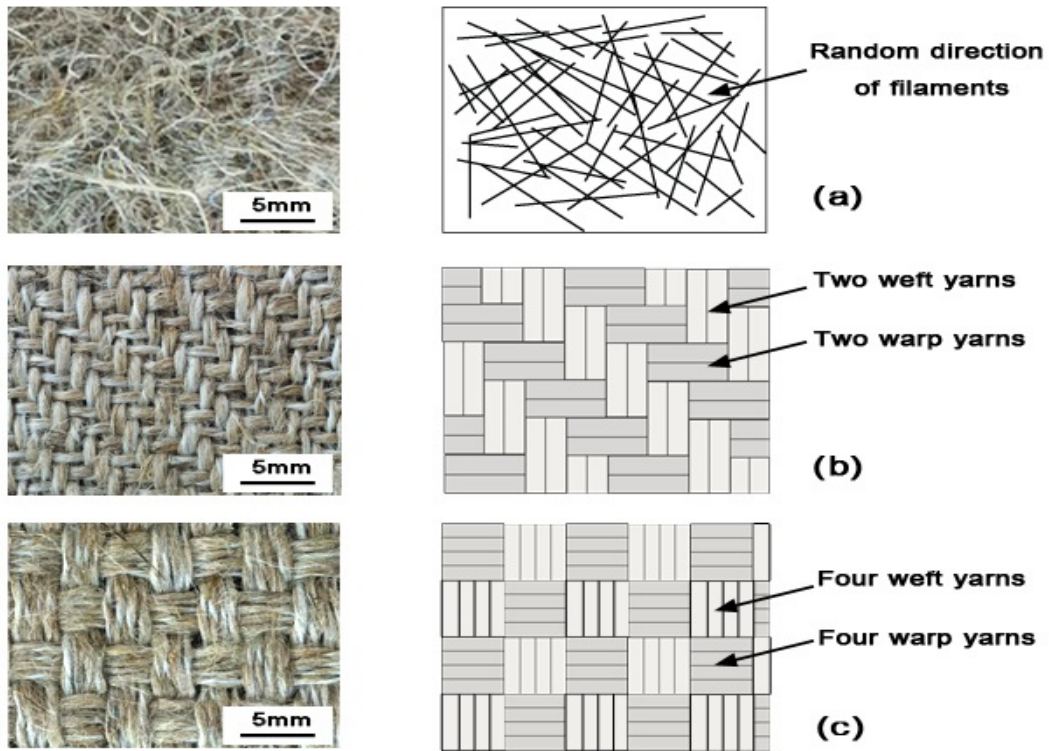


Figure 39: Used of different woven flax fibers; (a) non-woven flax, (b) 2x2 twill woven flax, and (c) 4x4 plain woven flax.

Table 7: Density of composite laminates.

Composites	Density (g/cm ³)
PBAT/non-woven flax	1.29
PBAT/2x2 twill woven flax	1.31
PBAT/4x4 plain woven flax	1.32

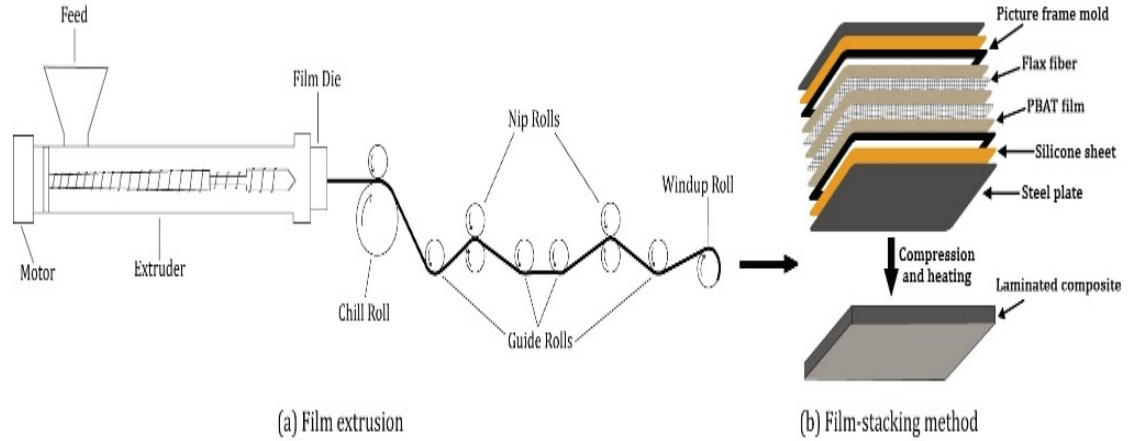


Figure 40: Schematic representation of fabrication procedure of the laminated biocomposite.

Characterization and testing

Morphology detection

The fracture surface was subjected to scanning electron microscopy (SEM) inspection in a JSM 5400 device of Jeol (Tokyo, Japan). The surface was gold coated prior to SEM inspection performed at low acceleration voltage.

Tensile response

Tensile test was performed on dumbbell-shaped specimens (DIN-ISO-527) on a Zwick 1474 (Ulm, Germany) universal testing machine. Tests were run at room temperature at $v=2$ mm/min crosshead speed and the related stress-strain curves were registered.

Impact response

The impact resistance was determined on notched Charpy test specimens according to EN ISO 179-1 and using a universal testing machine with a single swing of a pendulum energy of 25 J. Five specimens were tested and at least three replicate specimens were presented as an average of tested specimens. The Charpy impact strength of notched specimens, a_{cN} , was calculated with the following equation:

$$a_{cN} = w \times 10^3 / h \times b_N \quad (23)$$

where; w is the corrected energy absorbed by the specimen in joules, h is the thickness of the test specimen in millimeters, b_N is the remaining width at the notch base of the test specimen in millimeters.

Flexural response

A three-point flexural test was carried out according to ASTM D790. Flexural samples were performed on universal testing machine QC-506M1 (Cometech, Taiwan) at a cross-head speed of 4 mm/min and span length of 74 mm. At least five specimens were tested and the averaged value was analyzed.

Water absorption

Water absorption of the composites was investigated over a period of 30 days. The composites were cut into specimens (20x20 mm²) and then, they were immersed in water in a bath at room temperature. Weight gains were recorded by periodic removal of the specimens from the water bath and weighing on a balance. The percentage gain at any time t (M_t) as a result of moisture absorption was calculated from the following equation:

$$M_t = \frac{W_w - W_d}{W_w} \cdot 100\% \quad (24)$$

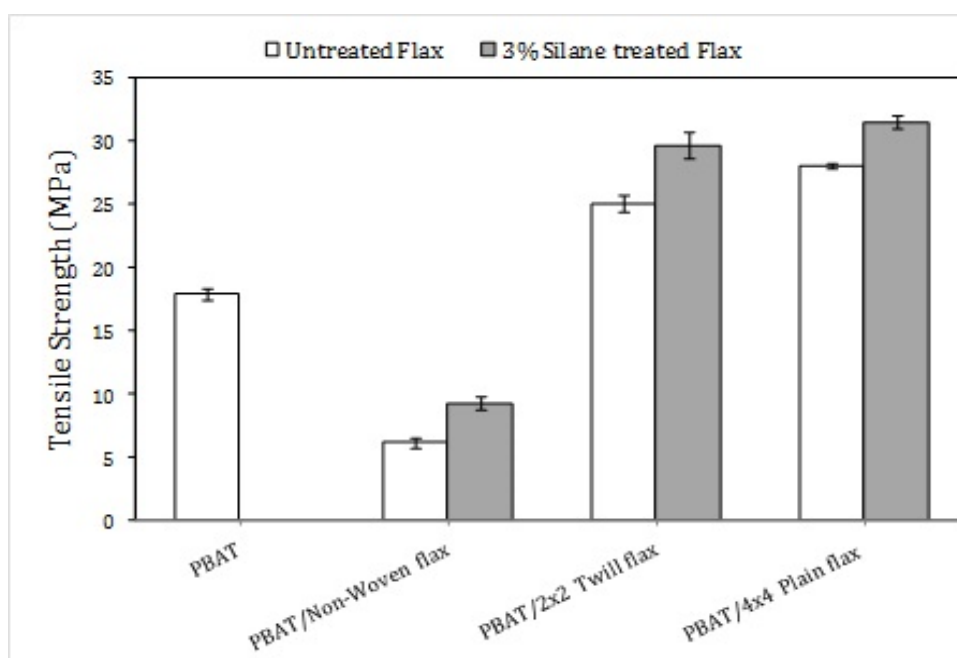
where W_d and W_w denote the weight of dry material (initial weight of materials) and weight of materials after exposure to water absorption, respectively.

Result and discussion

Tensile properties

Figures 41a and b show the tensile strength and modulus of PBAT/2x2 twill, 4x4 plain woven flax, and PBAT/non-woven flax composites compared to pure PBAT. It can be observed that textile composites of 2x2 twill and 4x4 plain woven fibers provided a better tensile strength than that of pure PBAT. This is due to the reinforced character of woven-flax structure and a higher densification of fibers. However, the PBAT/non-woven flax composite has the lowest tensile strength of 6.16 MPa compared to 17.91 MPa of pure PBAT. This can be observed that the matrix is impermeable into the structure of non-woven flax fiber contributing to poor adhesion between the matrix and fiber. Note that Fig. 42 (a) demonstrates the impermeability of PBAT into the non-woven flax structure.

a)



b)

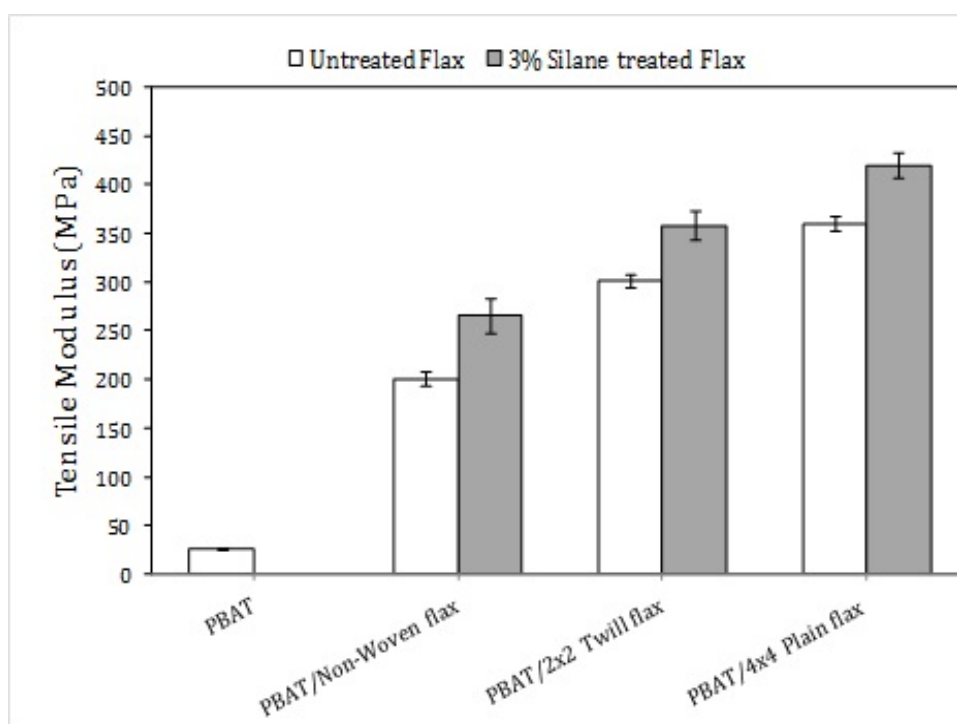


Figure 41: Tensile properties of biocomposites laminates: (a) Tensile strength and (b) Tensile modulus.

The tensile modulus value of the textile biocomposites compared to pure PBAT can be also seen in figure 41b. All the textile biocomposite showed a great increase in tensile stiffness compared to pure PBAT. This suggested that the low stiffness character of PBAT is improved by adding the relatively high stiffness character of the flax fibers. Similar result was observed by John et al. for flax fiber/biopolymer composites [60]. The stiffness of the composite increases due to the addition of fibers allows effective stress transfer at the interface, which consequently increases the modulus. In contrary, figure 42 (b) and (c) shows the agglomeration of the PBAT/2x2 twill and 4x4 plain flax structure contributing to good adhesion between matrix and fiber. It is mainly attributable to the reinforcing effect imparted by the combination of the flax/entangled molecular chains of PBAT, which allows for a greater degree of stress transfer from the PBAT matrix to the flax fiber. This is the results of better tensile strength and modulus of 2x2 twill and 4x4 plain flax /PBAT composites than that of non-woven flax /PBAT composite. From Figures 41a and b, it can be observed that the tensile properties of PBAT/all flax composites was affected by the incorporation of APS. For 3% of APS treated-fiber composites showed a reactive coupling effect that resulted in higher tensile strength and modulus compared to the untreated ones. The enhancement of tensile strength and modulus with APS treatment can be attributed to the better adhesion between fibers and matrix.

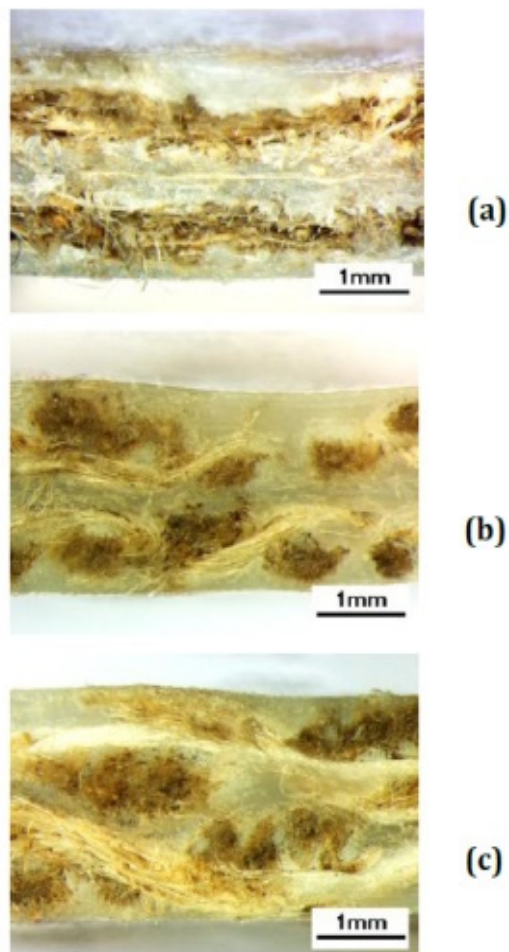


Figure 42: Cross section of (a) non-woven flax, (b) 2x2 twill woven flax, and (c) 4x4 plain woven flax/PBAT biocomposite laminates.

Impact response

The results of impact strength of pure PBAT and textile/PBAT composites laminates are shown in figure 43. It can be found that the pure PBAT has the highest impact strength. This is probably due to a high toughness character of PBAT matrix. The addition of fibers in the PBAT matrices composites decreased the impact strength compared to pure PBAT. Note that the mobility of PBAT chains decreased with the addition of flax fiber. This can be also explained by the addition of fibers which have the brittle behavior can reduce the toughness of PBAT. Sdrobis et al. [61] investigated composite containing cellulose pulp fibers. The result recorded a decrease in impact strength of neat LDPE from 75.1 kJ/m² to 52.8 KJ/m² for LDPE/pulp fibers. However, 4x4 plain woven flax/PBAT composites have the highest impact strength compared to non-woven and 2x2 twill flax/PBAT composites. This enhancement is likely to be the higher densification of the fibers. The main factor to improve the impact strength of 2x2 twill and 4x4 plain woven

flax was sufficient flow of the molten PBAT which caused bigger diffusion at the interface (cf. figures 42b and c) and obtained higher impact strength compared to non-woven. Observed lower undulation in 4x4 plain woven structure indicated an increase in the impact strength by approximately 15% compared with the laminates PBAT/2x2 twill flax. This is an indication that the undulation changed for an effect of the flax reinforcement in the corresponding composites laminates. Note that the undulation of composites laminates was higher in the shear stress, and it would produce extra a stress concentration which decreased the impact strength of laminates. The effect of the APS addition on the impact strength is also reported in figure 43 for the PBAT/2x2 twill, 4x4 plain woven flax, and PBAT/non-woven flax composites. One can recognize that the impact strength of 2x2 twill, 4x4 plain flax and non-woven flax biocomposites increased markedly with additional of 3% APS treated flax composite compared to the untreated all flax composites laminates. Recall that an increase of impact strength for all flax composites is due to the improved compatibility and interfacial bonding of the phases.

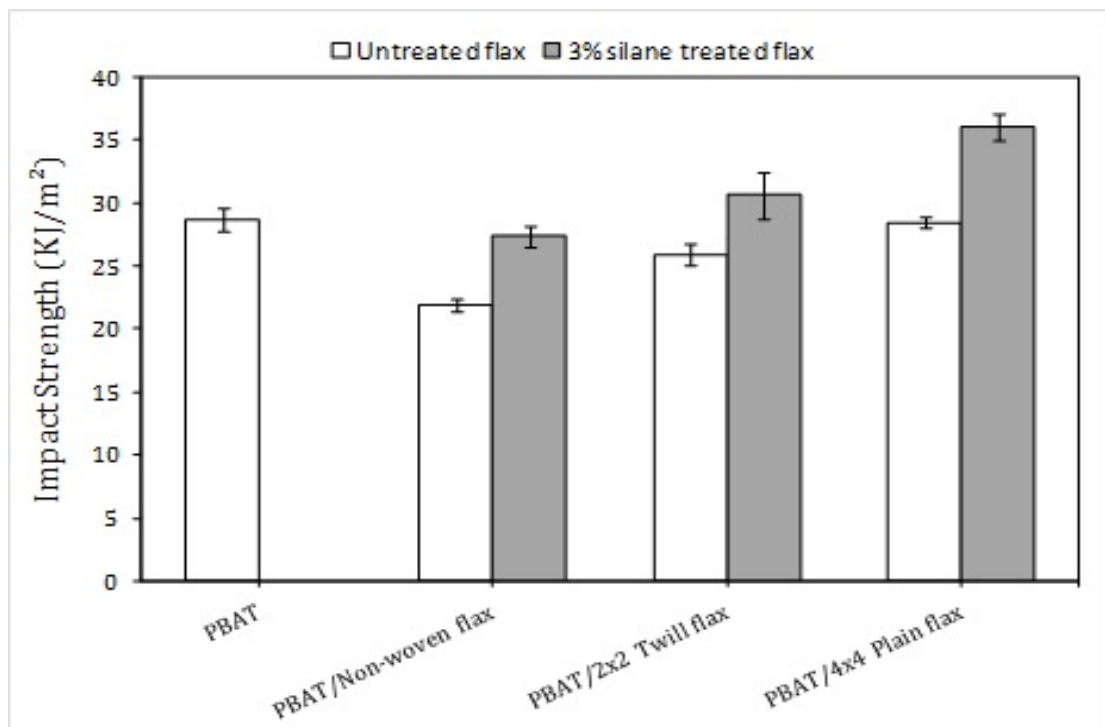
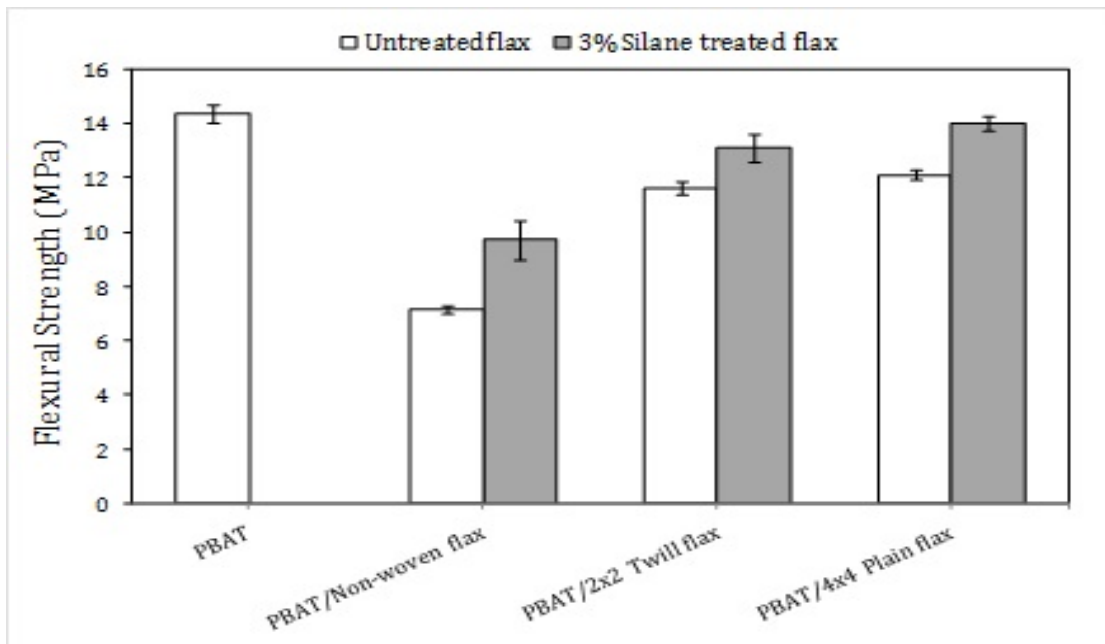


Figure 43: Impact resistance properties of biocomposites laminates.

Flexural properties

The flexural strength and modulus of pure PBAT and PBAT/textile composites laminates are shown in Figures 44a-b. It can be found that adding fibers in the PBAT decreased the flexural strength compared to pure PBAT. This can be explained by the addition of fibers reduced the toughness of PBAT. Besides, [62] the brittle behavior of fibers limited the plasticity of the composites. Note that the same statement holds for the PBAT/flax laminates system studied with tensile test. The flexural modulus of pure PBAT and PBAT/textile biocomposite was also made a comparison. It can be observed that the textile biocomposites greatly enhanced the flexural modulus, particularly in the PBAT/2x2 twill and PBAT/4x4 plain flax/PBAT composites compared to pure PBAT. The addition of 2x2 twill and 4x4 plain woven flax fibers in PBAT biocomposite provided a significantly better improvement in flexural modulus than did non-woven flax fibers. This means that the weave structures and densification of fibers gives positive effect to the flexural modulus of the PBAT based composites. Due to the effect of fiber undulation in ref. [52] observed clear differences in strength and stiffness of the laminates. For 3% APS treated flax of whole composites, it was found to increase the flexural strength and modulus compared to the untreated ones. This is attributed to the better adhesion between matrix and fiber. On the other hand, the APS treated flax composites is still lower strength than that of pure PBAT, while flexural strength decrease, showing a stiffening effect.

a)



b)

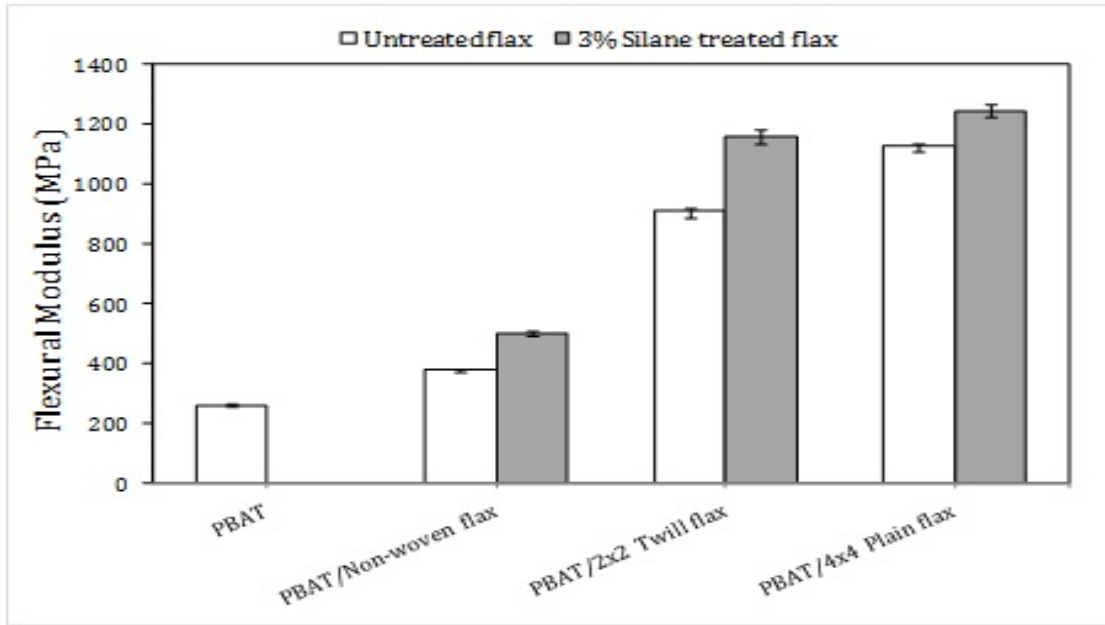


Figure 44: Flexural Properties of biocomposites laminates: (a) Flexural strength and (b) Flexural modulus.

Water absorption

Figure 45 shows the water absorption of pure PBAT and PBAT/textile composites laminates as a function of time. It is obvious that adding flax fiber into PBAT increased water absorption. The rapid water absorption was observed for all woven flax laminates within a few hours of immersion. The high water absorption occurred in PBAT/woven flax laminates. This is attributed to the hydrophilic character of flax fibers. Recently reported by Wu [63] also indicated that the water uptake of PBAT/Peanut husk fibers increased with increasing the PH content. The highest water uptake was found in the PBAT/non-woven flax laminates. This could explained that the non-woven flax fibers weakly adheres to the hydrophobic PBAT. The neat PBAT exhibited the highest resistance to water absorption because the hydrophobic nature of PBAT, which demonstrated weak interaction with water. One could also recognize that low resistance to water uptake was due to poor adhesion between the matrix and fiber. This suggestion is in accord with demonstrated on examples of the flax/furan bio-composites in ref. [64] which had negative influence in the water absorption. The reduction of water uptake is due to the improved interfacial bonding of the phases. Poor adhesion between fiber and matrix also causes cracks and voids between them. This causes easy penetration and storage of water through the voids. After the treatment of flax fiber with 3% APS, it obviously reduced the water absorption of the composites. It is considered to be due to the APS coupling agents form

hydrogen or covalent bonds with some of free hydroxyl group of cellulose, which reduce the water absorption capacity of cellulose. Another reason for the decrease in water absorption capacity of composites would be the enhancement of adhesion between fiber and matrix resulting in a decrease in voids between fiber and polymer matrix.

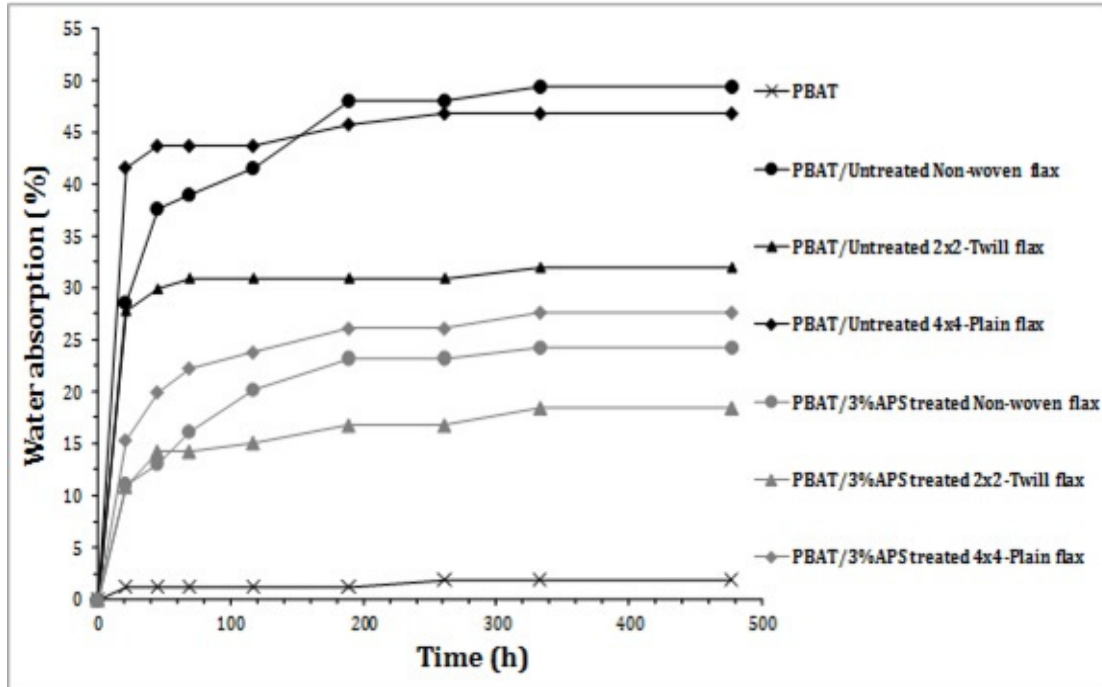
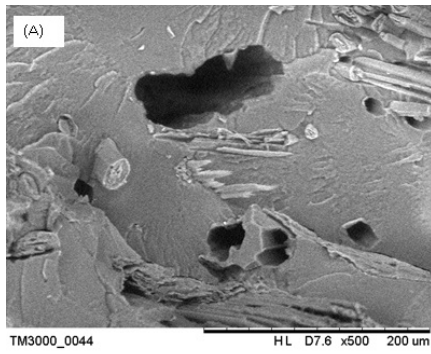


Figure 45: Water absorption of pure PBAT and PBAT/woven flax laminates biocomposites.

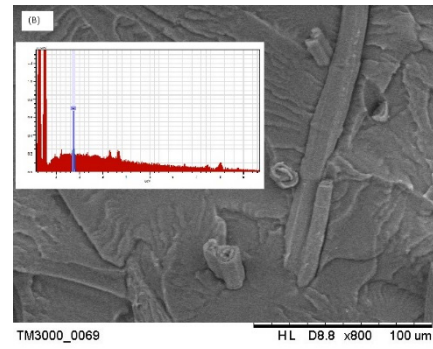
Morphology

SEM micrographs of the fracture surface of the untreated and treated flax composites are shown in figures 46a-f. SEM micrographs of figures 46(a), (c) and (e) indicates that there are voids between fiber and matrix which is an evidence of poor adhesion. Poor adhesion seems to facilitate debonding of the fiber. This was also confirmed by the mode of fracture in the untreated composites. SEM micrographs of the 3% APS treated flax composite clearly indicated that the treatment facilitates better adhesion between fiber and matrix than that of untreated one. This is evident that the treatment of flax fiber with APS improves the interfacial adhesion attributing to better strength and stiffness. Note that for selected spots of specimen, an elemental analysis was performed. EDS revealed the major constituents of silane (Si), as indicated in figure 46b. This finding confirms that the APS emerged from the flax fiber.

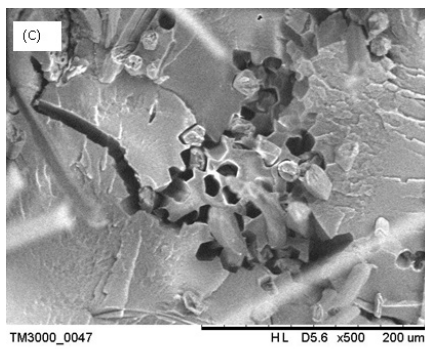
a)



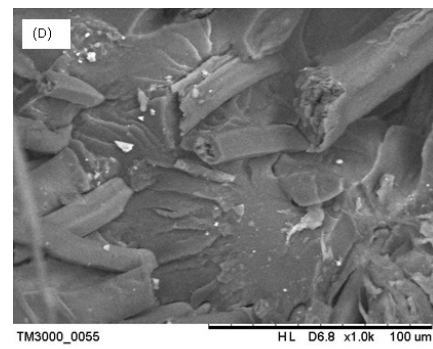
b)



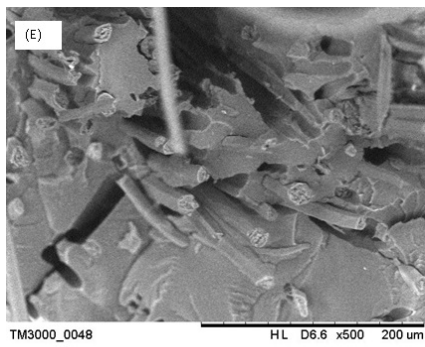
c)



d)



e)



f)

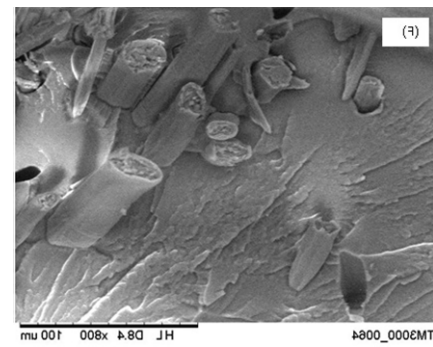


Figure 46: SEM micrographs of the fracture surface of PBAT-flax fiber composites: (a) Untreated and (b) 3% APS treated non-woven flax; (c) Untreated and (d) 3% APS treated 2x2 twill weave flax; (e) Untreated and (f) 3% APS treated 4x4 plain weave flax.

Conclusion

This work investigated the effects of 3-Aminopropyltriethoxysilane (APS) coupling agent on the mechanical properties and water absorption of the composites laminates made of PBAT and woven flax fibers. The textile composites exhibit promising mechanical properties, especially in the tensile strength and modulus, and flexural modulus. The PBAT biocomposites reinforced with two types of woven flax fibers and the higher fiber densification can improve the tensile and flexural modulus of the laminates. Incorporation of all flax decreased the water resistance of the PBAT based composites. However, increase in mechanical properties and water resistance had a strong impact on the APS which improved an interface of the reinforcement and PBAT matrix. This was demonstrated by SEM investigation. The PBAT/woven flax fiber biocomposites laminates have potential to become an ecologically beneficial alternative to glass fibers reinforced composite with petrochemical polymer matrices in the future. Possible fields of application could be the automotive parts, food packaging and agricultural applications. But a development of modeling of the structure-property relationships in this biocomposite is a further task to be solved.

4 Hybrid composites

4.1 Polyethylene/nanoparticle, natural and animal composites

State of the Art

The use of polymer composites has increased substantially used in engineering applications due to the outstanding properties compared to pure polymers. Polyethylene (PE) is one of the most widely used polyolefin polymers. High density polyethylene (HDPE) was used as the matrix for nano and natural composite materials, has attracted increasing interest recently due to its excellent chemical resistance, high impact strength, good thermal and mechanical properties [65-67]. The utilizing of the good thermal and mechanical properties of boehmite alumina (BA) nanoparticles in the HDPE composites has been studied [68-69]. BA incorporation increased in thermal stability and stiffness of HDPE and enhanced the elongation at a break obviously at the same time, while impact resistance of the HDPE/BA systems was reduced with increasing BA content. To achieve a fine nano-scale dispersion of the fillers is a great challenge. Beside of traditional nanocomposite techniques, for thermoplastics the water-mediated dispersion of suitable nanofillers has been recommended [70]. It was early noticed that this preparation technique of the nanocomposites has a strong impact on the remarkable property improvements [32].

A variety of natural fibers such as rice husk [71], jute [28], flax [72] and banana [73] fibers have been tested for use in HDPE/fiber composites. Natural fiber is straightforward not only from the viewpoint of the offer significant cost advantages and benefits associated with processing compared to synthetic fibers but also in respect to the reduction of the dependency on foreign and domestic petroleum oil. Several research papers deal with the optimization of natural fiber-reinforced HDPE composites. Some investigations look for ways to improve the interactions between polymer matrix and natural fibers. The use of HDPE based maleated coupling agents was helpful to increase the strength properties of HDPE-wood-flour composites, due to the increased interaction between the wood flour and HDPE matrix [74]. Choudhury [75] demonstrated that the tensile and flexural properties of ionomer-treated sisal/HDPE composites were strongly improved compared to neat HDPE. Mulinari et al. [24] studied the effect of modification of sugarcane bagasse cellulose with zirconium oxychloride/HDPE composites. The modified bagasse reduced the composites elongation. The increase in stiffness is associated to fibers reinforcement at the cost of the tensile strength and ductility. This reduction is associated to defects generated in the material after cellulose fibers insertion. The plant- and animal-based fibres were attracted much attention to the engineering, and bioengineering industries

such automotive and medical applications and undergone comprehensive researches for new composites. The goal of this study was to explore the potential of the water-mediated technique using nanospraying to disperse suitable fillers on nanoscale and investigate the potential of flax, sponge gourd (SG), palm and pig hair (PH) fibers produced reinforced HDPE composites. A further aim of this work was to demonstrate the feasibility of the production of HDPE/flax mat/BA composites. Accordingly, binary and ternary composites composed of high-density polyethylene (HDPE), boehmite alumina (BA) and different kinds of natural-, animal fibers were produced by hot press technique and the structure–property relationships of the resulting compounds were evaluated.

Materials and preparation of composites

Non-woven flax fibers (flax mat; 220 gm⁻²) were supplied by Dittrich Vliesstoffe GmbH (Ramstein-Miesenbach, Germany). The flax fibers in the non-woven textile are randomly orientated. The nonwoven textile is made of individual fibers. Pig hair (PH) and oil palm empty fruit bunch fiber are the by products obtained from 2 food processing plants in Thailand, Batagro Safety Meat Packing Co., Ltd. and Asian Palm Oil Co., Ltd. Sponge gourd (SG) fibers are commercially available in Thailand. The natural and animal fibers were used as reinforcing fillers. The water dispersible boehmite alumina (BA; AlO(OH); Dispal®11N7-80 of Sasol GmbH, Hamburg, Germany) served as filler for all composite systems. The nominal particle size of alumina in water was 220 nm though that of the alumina powder as delivered was 40 µm. Alumina has Al₂O₃ content of 80 wt.% and specific surface area is 100 m²/g. High-density polyethylene sheet (HDPE) (Finck&Co, Krefeld, Germany) was used as polymeric matrix for all composite systems. Its density was 0.95 g/cm³.

The HDPE binary and ternary composites were prepared by nano-spraying and/or hot press methods, respectively. First, the HDPE/flax mat/BA ternary composites were produced by a hot press using nano-spraying technique. The BA particles were dispersed in water at ambient temperature under continuous mechanical stirring for 30 minutes to obtain aqueous BA slurry. The BA slurry was sprayed into the non-woven flax fibers by a hand spraying-up and dried for 48 h at room temperature (RT) and then for 24 h at 80 °C in oven. The flax mat contents in the binary composites were set for 20 and 40 wt.%. The flax mat and alumina/or pork, SG, palm contents in the ternary composites were set for 20 and 10 wt.%, respectively. The composites produced are listed in Table 8. The HDPE containing flax mat or, pork/bob and palm followed by hand laying-up a layer of natural –or animal fibers and then by a layer of HDPE sheet. The binary and ternary composites based on HDPE, after the BA particles spraying on the flax mat and dried,

were compression molded into 1-mm thick sheets at $T = 190\text{ }^{\circ}\text{C}$ using the hot press (P/O/Weber, Maschinen und Apparatebau, Remshalden, Germany).

Table 8: Recipe and designation of the HDPE-based systems.

Sample Designation	Flax mat (wt.-%)	Boehmite alumina (BA) (wt.-%)	Pig hair (PH) (wt.-%)	Palm (wt.-%)	Sponge-gourd (SG) (wt.-%)
HDPE	-	-	-	-	-
HDPE/flax mat(l)	20	-	-	-	-
HDPE/flax mat(h)	40	-	-	-	-
HDPE/flax mat/BA	20	10	-	-	-
HDPE/flax mat/PH	20	-	10	-	-
HDPE/flax mat/Palm	20	-	-	10	-
HDPE/flax mat/SG	20	-	-	-	10

Characterization and testing

Morphology detection

The fracture surface was subjected to scanning electron microscopy (SEM) inspection in a JSM 5400 device of Jeol (Tokyo, Japan). The surface was gold coated prior to SEM inspection performed at low acceleration voltage.

Thermal and thermomechanical response

Thermogravimetric analysis (TGA) was performed on a DTG-60 SHIMADAZU device (Kyoto, Japan). TGA experiments were conducted in the temperature range from 30 to 500 $^{\circ}\text{C}$ under nitrogen at a heating rate of 10 $^{\circ}\text{C}/\text{min}$.

Dynamic mechanical thermal analysis (DMTA) was performed in tensile mode at frequencies of 0.1, 1 10 Hz at all isothermal temperatures, using a DMA Q800 apparatus (TA Instruments, New Castle, NJ). The storage modulus (E') was determined as a function of the temperature ($T = -100^{\circ}\text{C} \dots +130^{\circ}\text{C}$). The strain applied was 0.1%. The specimens were cooled to -100 $^{\circ}\text{C}$. The temperature was allowed to stabilize and then increased by 5 $^{\circ}\text{C}$, kept 2 min isothermal until 130 $^{\circ}\text{C}$.

Stress relaxation response

Short-time (duration 30 min) stress relaxation tests were made in single cantilever mode at different temperatures, ranging from 5 to 45 °C, using above DMA apparatus. The strain applied was 0.5%. In the temperature range 5–45 °C isothermal tests were run on the same specimen by increasing its temperature stepwise by 5 °C. Prior to the stress relaxation measurement, the specimen was equilibrated for 3 min at each temperature step. The specimen dimensions were 30x10x1 mm³ (length x width x thickness).

Water absorption

Water absorption of the composites was investigated over a period of 30 days. The composites were cut into specimens (20x20 mm²) and then, they were immersed in water in a bath at room temperature. Weight gains were recorded by periodic removal of the specimens from the water bath and weighing on a balance. The percentage gain at any time *t* (*M_t*) as a result of moisture absorption was calculated from the following equation:

$$M_t = \frac{W_w - W_d}{W_w} \cdot 100\% \quad (25)$$

Instrumented Falling Dart Impact

Instrumented falling weight impact (IFWI) test was performed on a Fractovis 6785 (Ceast, Pianezza, Italy) using the following settings: incident impact energy, 20 J; diameter of the dart, 20 mm; diameter of the support rig, 40 mm; weight of the dart, 10.357 kg; drop velocity, 1.97 m/s. IFWI tests were performed on quadratic specimens of 60x60 mm² at room temperature.

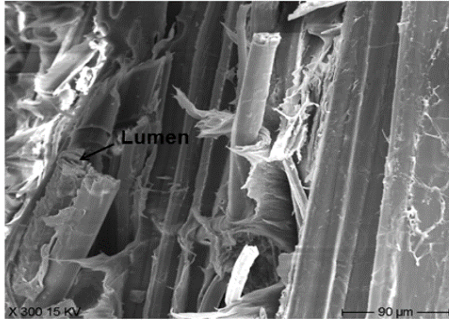
Result and discussion

Morphology

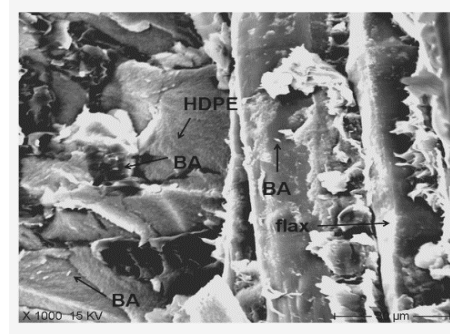
The SEM pictures in figures 47a-e present the morphological characteristics of the HDPE-based systems studied. It can be seen in figures 47a-b, that the BA particles were homogeneously dispersed in the HDPE/flax mat composite. The individual flax fiber had diameter in the range of 30-60 µm and displayed clear fiber lumina. However, the lumina were not filled with HDPE matrix. Considering the present image of figure (47c), it can be concluded that due to the very smooth surface was present a poor adhesion between the HDPE matrix and pig hair. The latter was present in the form of large fibers and broad fibers size distribution. Furthermore, one may conclude in figures 47d-47e that fiber surfaces of palm and SG were rough. This seems to be better stacked with the related

HDPE composites which may indicate an enhanced adhesion of HDPE/flax mat/palm and HDPE/flax mat/SG ternary composites. It was the first hint for an upgrade property in the corresponding composites.

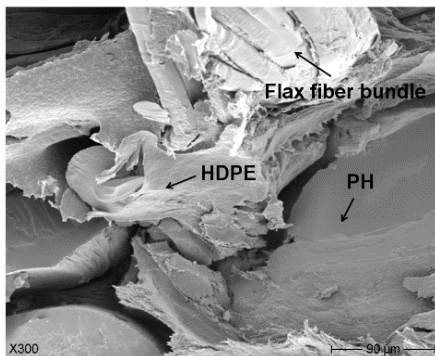
a)



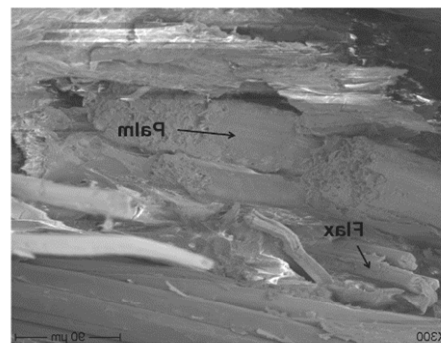
b)



c)



d)



e)

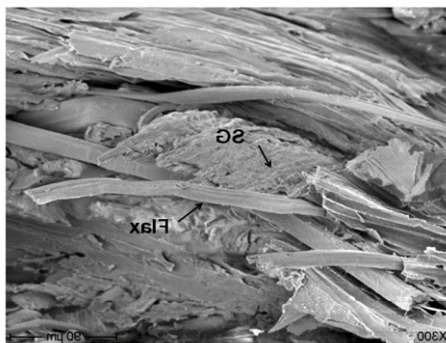


Figure 47: SEM picture from the fracture surfaces of HDPE/flax mat (a), HDPE/flax mat/BA (b), HDPE/flax mat/PH (c), HDPE/flax mat/Palm (d) and HDPE/flax mat/SG (e), composites.

Thermogravimetric analysis

The effects of BA particles and natural-, animal fibers on the thermal stability of HDPE systems are displayed in figure 48. One can be recognized that thermal degradation of HDPE was a one-step procedure representing depolymerization. The binary and ternary composite systems exhibited two-step-like transitions. Due to the dehydration from cellulose unit and thermal cleavage of glycosidic, the decomposition temperature of HDPE/fibers composites was comparatively lower than that of the HDPE as reported for jute/HDPE composites [9]. One can recognize that the thermal stability decreased remarkably with increasing of flax mat content in the HDPE at whole temperature range. For the composites contain 20 wt.% flax mat, the weight loss as reaching 370 °C, was enhanced by approx. 15 % compared to the HDPE/flax mat 40 wt.%. The incorporation of BA particles strongly improved the thermal degradation of the HDPE/flax mat composite. It has also to be mentioned that BA for improving the thermooxidative stability has been reported for PEs and POM [68, 76]. The HDPE/flax mat/BA composite started to degrade at higher temperature compared to the HDPE/flax mat composite. Note that the resistance to thermal degradation of the HDPE/flax mat/PH composite was slightly higher than those of composites containing palm and SG. One possible explanation is that the high moisture content of natural fibers also caused a great problem for thermal properties. The change in the TGA values shows the moisture difference between pig hair- and natural composites. This finding is in agreement with reported by Cheung et al. that composite with animal fibre provided also better thermal properties [77].

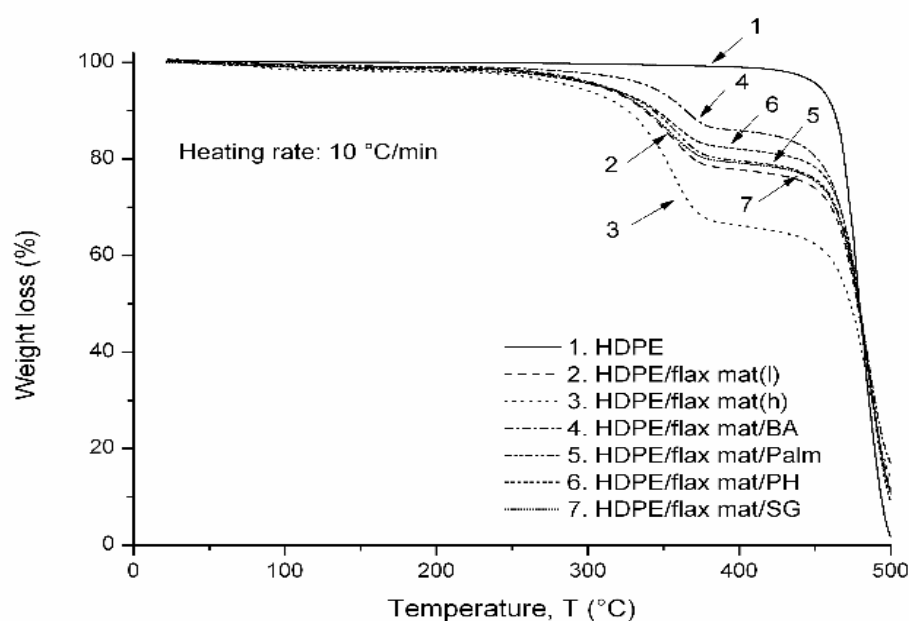
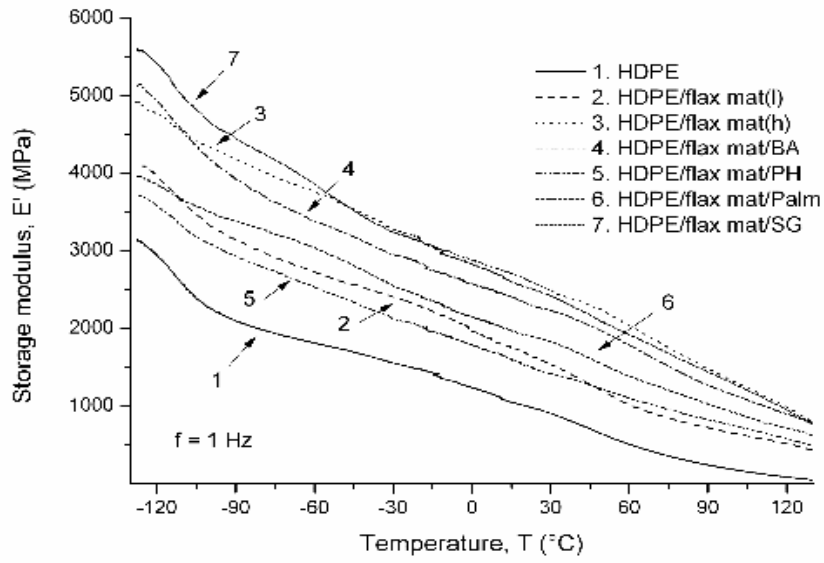


Figure 48: Weight loss versus temperature for the HDPE systems studied.

Dynamic mechanical response

Figures 49a and b depict the storage modulus (E') and loss factor ($\tan \delta$) as functions of the temperature for the binary and ternary composites systems containing different amounts of flax mat. It can be observed in figure 49a that the all composites exhibited markedly higher stiffness than the neat HDPE. This can well be explained by the reinforcing effect of the natural fibers leading to increased stiffness. The storage modulus increased remarkably with increasing the flax mat content. For the binary composites contain 40 wt.% flax mat, the E' is improved by approx. 25 % compared to the HDPE/flax mat 20 wt.%. The incorporation of BA into HDPE/flax mat resulted in a pronounced stiffness enhancement at the whole temperature range. Poorly adhesion of large PH fibers in the HDPE/flax mat matrix act as stress concentrations (cf. figure 47c) and cause premature interfacial debonding which accompanied by low storage modulus. It is also well resolved that the stiffness of those composites containing palm and SG was always inferior to that of HDPE/flax mat composite. This can be explained by the consideration of the surface roughness of the natural fibers in the related composites, as discussed earlier. Concerning, previous studies on the relaxation processes in pure HDPE describe three transitions, namely α -, β - and γ -relaxations from higher to lower temperature [78-79]. The relaxation transition (γ) located at -110°C was assigned to the glass transition temperature. The β transition of HDPE was invisibly because its absence the chain branches. The latter peak in HDPE (α -relaxation at approx. 80°C) was usually attributed the chain segment mobility in the crystalline phases and reoriented defect in crystalline phases. One can notice that the γ relaxation peak of HDPE also exhibited a shift to high temperature regions with the incorporation of BA particles. The shift of this peak toward higher temperatures due to alumina indicates for the reinforcing effect. On the other hand, the effect of natural and animal fibers on the relaxation transitions was marginal.

a)



b)

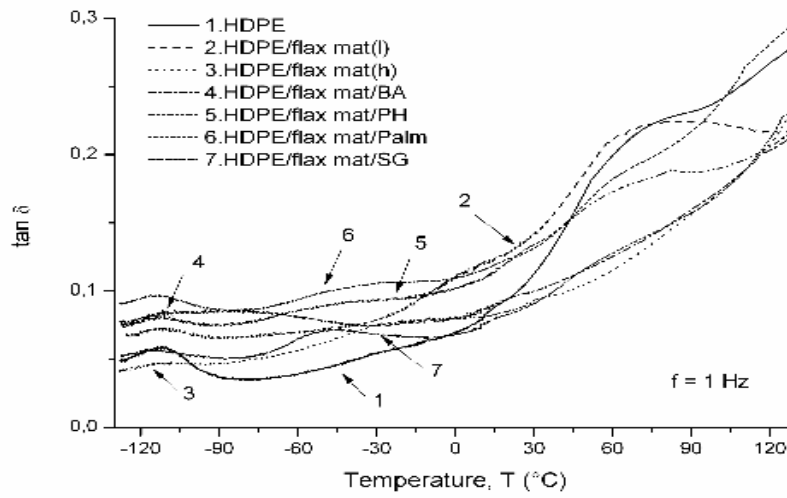


Figure 49: E' (a) and $\tan \delta$ (b) vs. T traces for the HDPE systems studied.

Stress relaxation response

Theoretical background

Stress relaxation phenomenological models, which provide another route to study the time dependence and gain understanding on viscoelastic behavior of reinforcing composite materials. For stress relaxation under applied constant strain (ε_0) the material response is given by:

$$E_r(t) = \frac{\sigma(t)}{\varepsilon_0} \quad (26)$$

where $E_r(t)$ is the stress relaxation modulus, and $\sigma(t)$ is stress, both as a function of time (t).

In the nonlinear range the dependence upon the level of the applied deformation can be expressed by multiplying the linear parameters by so-called nonlinearity factors, which are deformation-, time- and temperature-dependent. The nonlinear stress relaxation modulus is given by:

$$E_r(t, \varepsilon(t), T) = \frac{\sigma(t, \varepsilon(t), T)}{\varepsilon_0} \quad (27)$$

Generally, the basis of the conversion method from the modulus to the creep compliance can be determined by using a linear viscoelastic material principle [33]. Relaxation modulus is defined as the inverse quantity of creep compliance (D) by the following equation:

$$E_r = \frac{1}{D} \quad (28)$$

Accordingly, the stress relaxation and creep behaviors of material are predicted by empirical model, such the Findley power law can well describe the creep compliance vs. time traces. Therefore, in order to obtain a deeper insight into the effect of the natural fiber and nanoreinforced HDPE systems on the temperature and the long-term stress relaxation behavior, the applicability of the inverse of the Findley equation has been investigated following the correspondence relationship.

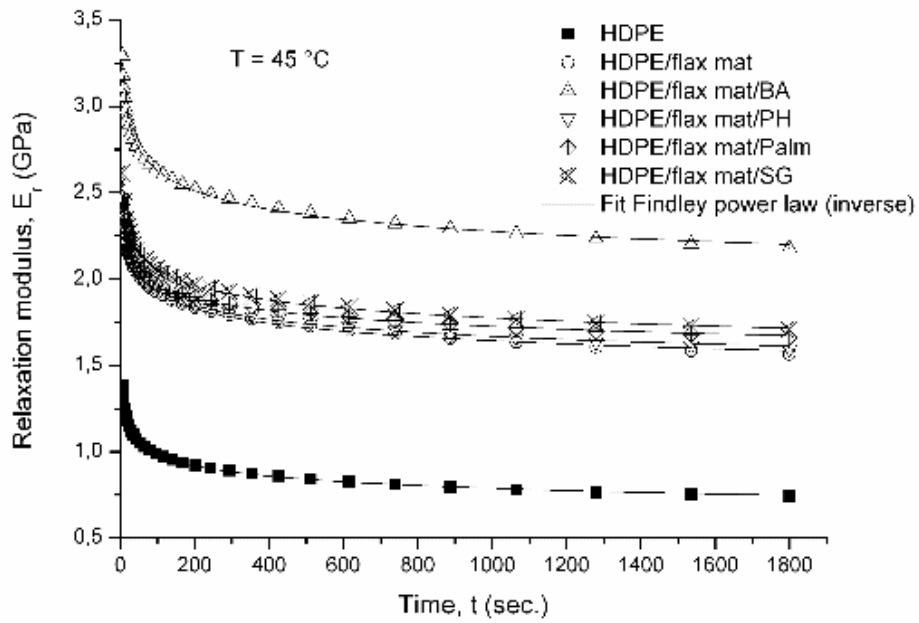
Accordingly, for the time dependency of the relaxation modulus, the inverse of the Findley power law equation is given by [80]:

$$E_{rF} = (E_{rF0} + E_{rF1} * t^n)^{-1} \quad (29)$$

where the subscript F indicates that the parameters are linked with the Findley power law, n is a constant independent of strain, E_{rF0} is the time-independent relaxation modulus and E_{rF1} is coefficient of the time-dependent term.

Figures 50a-b displays the stress relaxation modulus (E_r) as a function of time for the binary and ternary composites systems containing different amounts of flax mat at temperature of 5 °C and 45 °C, respectively. The solid lines appearing in each curve represents the calculated data using the inverse of the Findley power law model. It is clear from figure 50 that the relaxation modulus decreased with increasing temperature. The E_r values of the all composites systems were higher compared to the HDPE. For the relaxation modulus of HDPE/flax mat/BA ternary composite after the relaxation time of 1800 s was increased by 25% and 40% at $T = 5$ and 45 °C, respectively, compared to the HDPE/flax mat binary composite. This relaxation modulus increased greatly with incorporation of BA particles due to the development of a restricted molecular mobility. This phenomenon, observed also in DMA test and reported in PS [81], is associated with a pronounced increase in the stiffness. One can also recognize that the HDPE/flax mat/SG composite exhibited higher relaxation modulus value than the composites containing PH and palm. The DMA corroborated this fact by indicating that the storage modulus of roughness surface SG was shifted towards higher values (cf. figure 49a). However, the difference in the relaxation modulus between natural and animal fibers diminishes with increasing temperature. Figure 51 demonstrates the effect of increased temperature on the relaxation modulus response of HDPE/flax mat composite. One can recognize that the shape of relaxation curves of the composites was similar at all test temperature. The time-independent relaxation modulus (E_{rF0}) increased remarkably with increasing temperature.

a)



b)

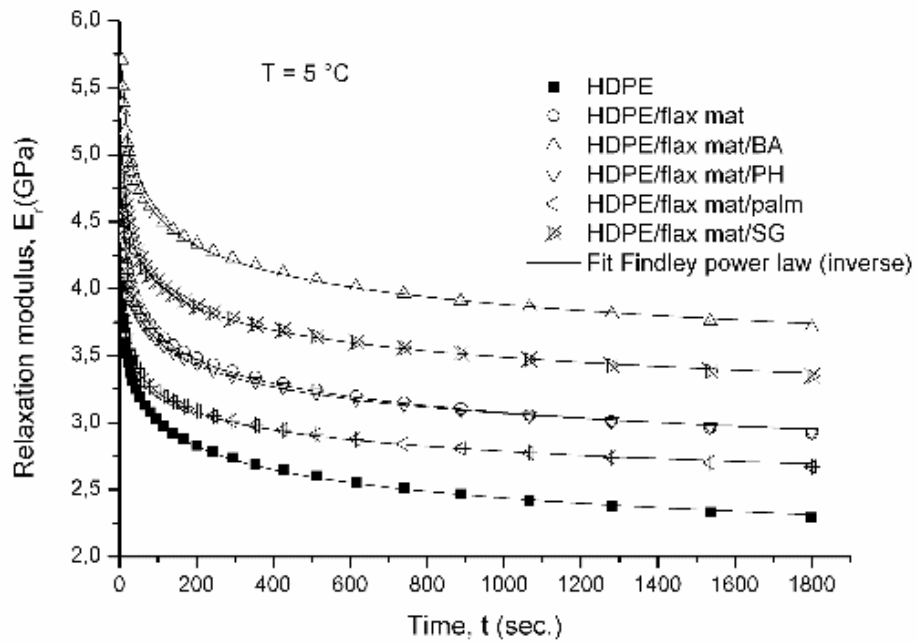


Figure 50: Characteristic relaxation modulus -time curves registered for the HDPE systems studied at testing temperature of $5\text{ }^{\circ}\text{C}$ (a) and $45\text{ }^{\circ}\text{C}$ (b).

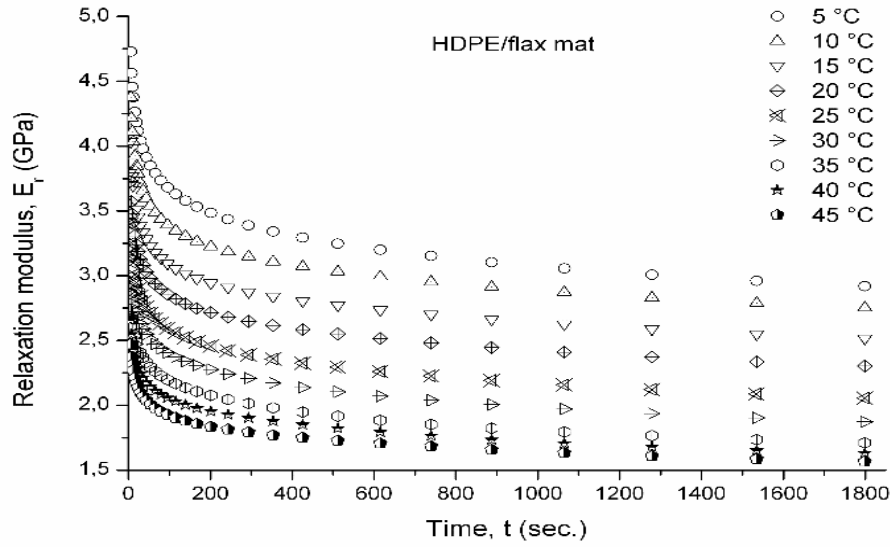


Figure 51: Characteristic relaxation modulus -time curves registered on HDPE/flax mat composite at different testing temperatures.

Master curves of the relaxation modulus produced by superimposing the relaxation modulus versus time traces using the time-temperature superposition (TTS) principle. A reference temperature ($T_{ref} = 25\text{ }^{\circ}\text{C}$) was used for this superposition (shifting) process. The related shift factor (a_T) used for the generation of relaxation modulus master curve is $a_T = E_r(T)/(E_r(T_{ref}))$. Master curves of the relaxation modulus against time created and simulated fits according to the inverse of the Findley power law at a reference temperature of $25\text{ }^{\circ}\text{C}$ are shown in figure 52 for the HDPE, HDPE/flax mat and HDPE/flax mat/BA composite. The shift factors are linked with TTS via the Arrhenius function. From the shift factors for the relaxation modulus of the HDPE, the activation energy of 200 kJ/mole can be calculated. The activation energy of the HDPE/flax mat and HDPE/flax mat/BA binary-, and ternary composites was calculated as 157 and 153 kJ/mole, respectively. One can notice that the relaxation modulus increased with decreasing activation energy and addition of flax and BA reinforcements. On other hand that the related curves show a good fit between the experimental and the simulated results according to the Findley power law. This power law fits very well to the relaxation modulus data for all systems up to approx. 1333 min.

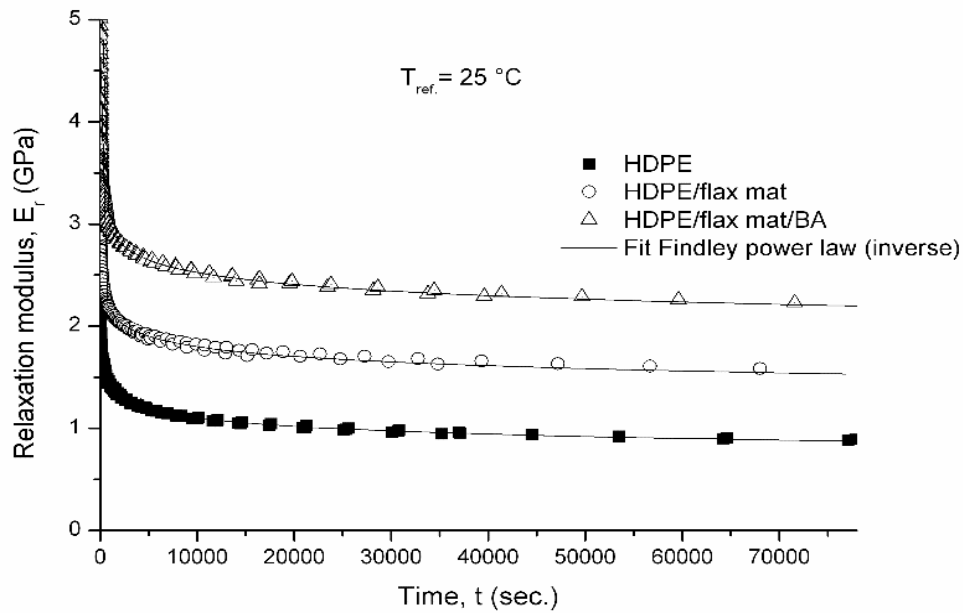


Figure 52: Relaxation modulus master curves constructed by considering the TTS and selecting $T_{ref} = 25\text{ }^{\circ}\text{C}$ and their fitting by the Findley power law equation (inverse).

Water absorption

Figure 53 depicts the water uptake as a function of time for the binary and ternary composites systems containing different amounts of flax mat. Due to the light interaction with water of HDPE was present a low diffusion of water about 0.93 % of the water uptake after subjected to water absorption for 30 days. A rapid water uptake was observed for all binary and ternary composites within the first 7 days of immersion. The water absorption of composite systems was reached quasi-equilibrium state after 18 days. One can also recognize that the penetration of water increased markedly with increasing flax mat content in HDPE matrix. Note that the incorporation of BA particles in the HDPE/flax mat composite could reduce the water uptake. The HDPE/flax mat/BA composite, recorded water absorption value at 4.87 % upon 30 days. This is in accordance with recent reports claiming that the water absorption was reduced by adding nanofillers. For polyester and polyesterimide with SiO_2 , TiO_2 and ZnO composites when compared to standard compounds, showed better water resistance [82]. On the other hand, the water sorption behavior was slightly considered to depend on the types of reinforcing fibers. The water uptake of HDPE/flax mat/PH composite was reduced by approx. 33 and 14 % as reaching 30 days compared to the composites containing SG and palm, respectively. Fick's law was adopted to calculate the diffusion coefficient (D) of water absorption values. It is

well resolved that there is a fair agreement between the water uptake and those calculated by the Fick's law. By comparing the diffusion coefficient (cf. Figure 53), one may conclude that the D of HDPE/flax mat composite decreased with incorporation of BA. This result suggests that D may be sensitive to the nanoparticles barrier effect. It has also been observed that these nanofillers reacted with water lead to decrease the rate of diffusion [83-84]. Additional of SG and palm fibers into the HDPE/flax mat yielded also an increase in diffusion coefficient of water absorption.

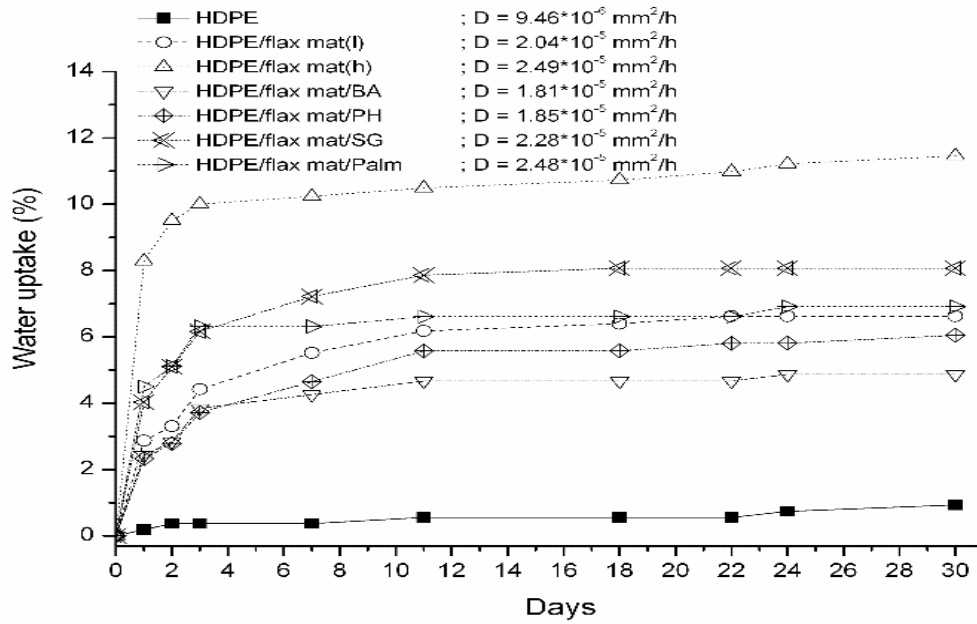


Figure 53: Water uptake on the binary and ternary composites systems containing different amounts of flax mat. Fick's law was used to calculate the diffusion coefficient of water absorption (D) after 30 days immersed in water, i.e.: $D = \pi (kb/4\mu_0)^2$.

Falling dart impact response

The reinforcing effects of the BA particles and natural-, animal fibers on the force versus time curves are demonstrated on the HDPE systems in figure 54. Observation of impact energy indicates that the natural- and animal fibers enhanced the stiffness and reduced the toughness of the related composites at the same time. With addition of the BA in HDPE/flax mat composite was accompanied with a shift of the force peak toward higher force and longer time. This is due to the nanoparticle character of the reinforcing effects. Note that the BA reinforcing the matrix in HDPE/flax mat system leads to increased stiffness and accompanied with reduced ductility. This is in qualitative agreement in accordance with the DMA results (cf. figure 49a) and the reduction of impact toughness of HDPE by BA particles was also discussed in Ref. [69]. The presence of SG fibers was

associated with a reduction in the maximum force peak compared to the PH and palm reinforcements. Accordingly, the observed impact resistance is likely less due to the BA particles themselves, but more due to their amount of flax fibers.

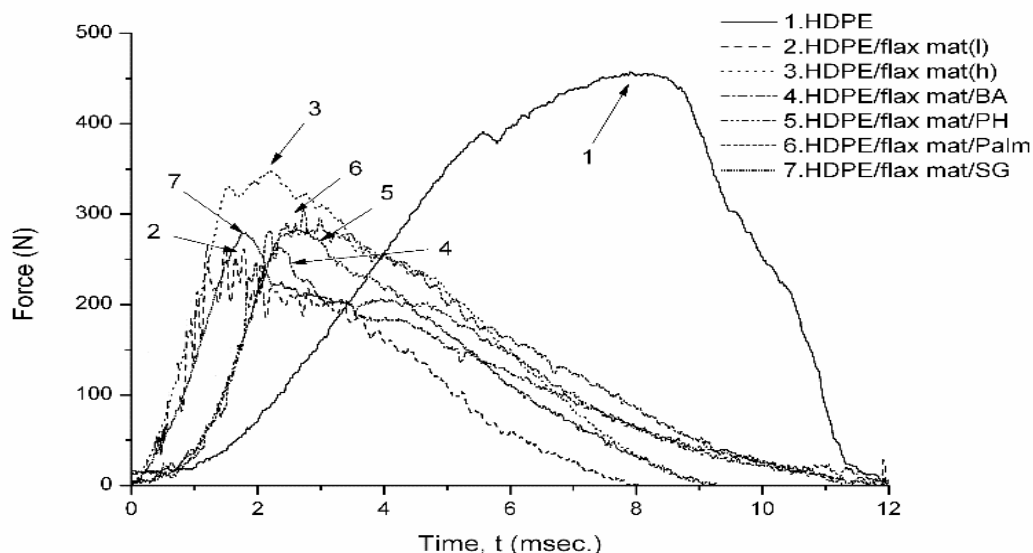


Figure 54: Characteristic force-time curves for the HDPE systems studied.

Conclusion

This work devoted to study the morphology, thermal, mechanical, stress relaxation, water absorption and falling weight impact properties of a high-density polyethylene (HDPE) and its pig hair (PH), palm, sponge gourd (SG) fibers and boehmite alumina (BA) reinforced binary and ternary composites. The BA was introduced in the HDPE/flax mat in 10 wt.% via spraying method. Based on this work the following conclusions can be drawn:

- Nanospraying technique resulted in homogeneously BA dispersed in the HDPE/flax mat composite. The flax mat, palm and SG fibers seem to be better stacked with the related composites compared to the PH.
- Incorporation of BA particles improved the thermal degradation and water uptake of the HDPE/flax mat composite.
- The storage modulus of the all composites was higher than the neat HDPE at the cost of the ductility (impact toughness). The stiffness increased with increasing the flax mat content. Poorly, adhesion of PH fibers in the HDPE/flax mat matrix accompanied by low stiffness.
- The stress relaxation values of the all composites systems were higher compared to the HDPE. This relaxation modulus increased greatly with incorporation of BA

particles due to the development of a restricted the molecular mobility. With addition SG exhibited higher relaxation modulus value than the composites containing PH and palm. Based on isothermal short-term stress relaxation experiments master curves in form of stress relaxation modulus vs. time were constructed by time-temperature superposition (TTS) principle. The related master curves could be well described by the inverse of the Findley power law.

4.2 Polyethylene/Flax/SiO₂ Composites

State of the Art

Nowadays, the R&D on polymer composites has particularly focus on natural fibers reinforcements. It is known that natural fibers display a low density, and yielding relatively lightweight with high specific properties. Natural fiber is becoming more and more important because of a cost advantages and benefits associated with processing compared to synthetic fibers. The use of the natural fiber is considered more practical and economical with great application potential than others tradition micro-scale reinforced polymer composites. The special attention focused on natural composites is due to their excellent physical and mechanical properties [85-88]. High density polyethylene (HDPE) is one of the most widely used plastic materials. The highly crystalline nature of HDPE is responsible for its higher density and stiffness, as well as its low permeability and high chemical resistance. HDPE was already used as the matrix for natural composite materials, with a range of interesting properties. The natural composites show potential to be used in a variety of structural and technological applications. Many works indicated that with adding the natural fibers, such as jute, flax and sisal fibers [28, 72, 75] into HDPE matrix exhibited an effective approach to improving the impact strengths, tensile and flexural of HDPE. The tensile and flexural properties of ionomer-treated sisal/HDPE composites were strongly improved compared to neat HDPE [75]. Liu et al. [73] investigated the mechanical properties of banana fiber filled composites based on HDPE/PA-6 blends. They found that the modulus and flexural strength increased with the increase in banana fiber loading up to 48.2 wt.%, while impact toughness was lowered gradually. For the nanoclay/wood/HDPE combinations were used to obtain a ternary composite [67]. It was found that the flexural properties of HDPE/wood composites could be significantly improved with a combination of the coupling agent content and nanoclay. The reinforcement of recycled HDPE with bagasse and pine fibers has been done by Lei et al. [89]. The mechanical properties of the fiber reinforced recycled HDPE compared well with those of virgin HDPE/fiber composites and the coupling agents had slightly influence on

the thermal degradation but enhanced the modulus and impact strength of the related composites.

Generally, incorporation of silicon dioxide (SiO_2) particles in polymers resulted in excellent mechanical, thermal, and other properties. Note that SiO_2 particles have been already checked as possible reinforcements in polymer matrices. Rosso et al. [90] employed the dispersed silica in the epoxy resin for tensile and fracture tests, indicated that the addition of 5 vol.% silica nanoparticles could improve the stiffness and fracture energy. Tsai et al. demonstrated that the compressive strengths of the glass/epoxy composites can be improved with the silica contents [91]. The enhancement in compressive strength could be attributed to the enhanced interfacial bonding modified by the dispersed silica nanoparticles. However, only few investigations have been carried out the influence of composite structures and importance of SiO_2 particles on the properties of flax fiber composites based on HDPE. The goal of this study was to demonstrate the feasibility of the production of HDPE/flax/ SiO_2 composites with various flax structures using the nanospraying technique and compare the structures impact, thermal and mechanical properties of the different flax reinforced HDPE composites. One of the criteria for selecting this nano-spraying technique was that many nanoparticles are available in solvent form and this technique is very simple and more economical compared to conventional nanostructuring technologies such as in situ polymerization.

Materials and preparation of composites

The solubility of silicon dioxide (SiO_2) with 40 wt.% SiO_2 concentration (Nanopol XP of Nanoresins AG, Geesthacht, Germany) served as filler. Figures 55a-b shows the SEM images of the SiO_2 particles and HDPE/flax_{2x2} composite, respectively. It can be seen in figure 55a that the SiO_2 nanoparticles were spherically shape with diameter of approx. 20 nm. Two types of the woven flax fiber textiles (weave style of 2x2 twill and 4x4 hopsack) were used as reinforcement which had a yarn size of 250 tex. Biotex Flax was supplied by Composites Evolution (Chesterfield, UK). The density was 1.24 g/cm³ (according to suppliers' information). Characteristic SEM picture taken from the HDPE/flax_{2x2} composite in figure 55b shows the flax fiber had diameter in the range of 15-25 μm and displayed fiber lumina in the cross section. High-density polyethylene sheet (HDPE) (Finck&Co, Krefeld, Germany) was used as polymeric matrix for all composite systems. Its density was 0.95 g/cm³.

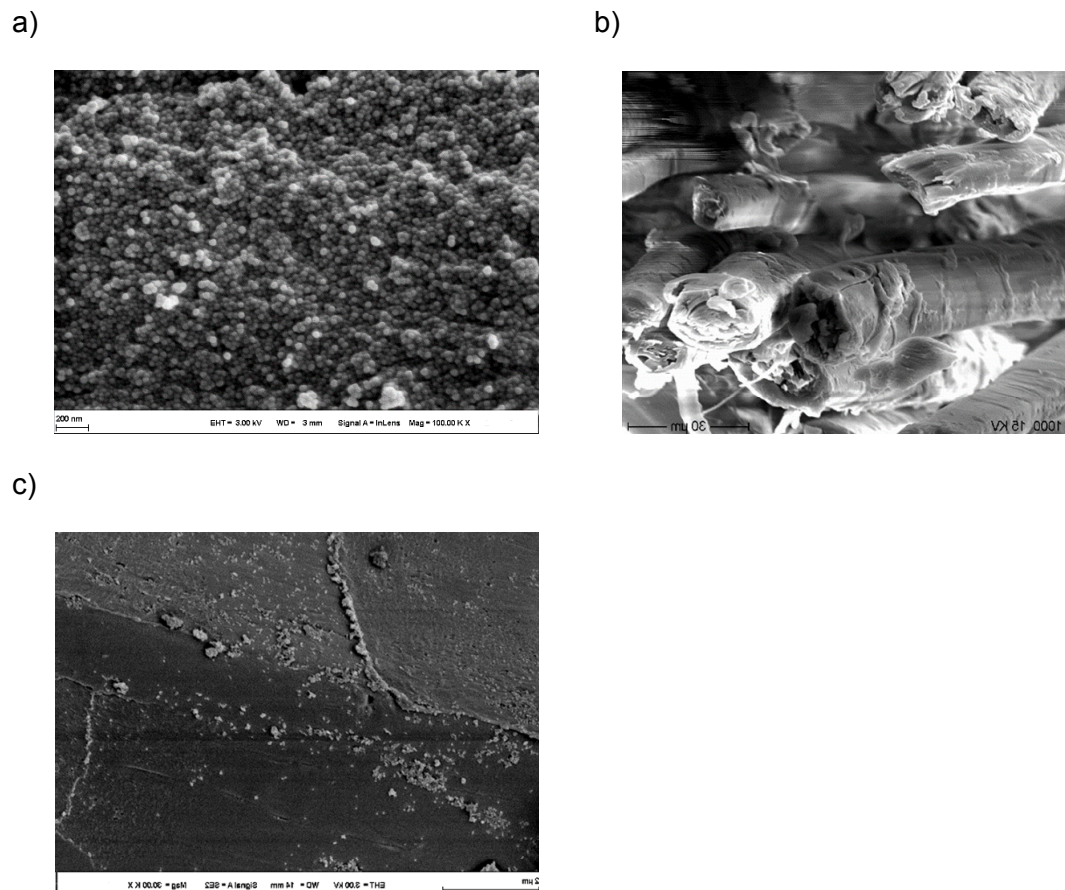


Figure 55: SEM picture of silicon dioxide particles (a), from the fracture surfaces of HDPE/flax2x2 (b) and HDPE/flax4x4/SiO₂ (c), composites.

The HDPE binary and ternary composites were prepared by nano-spraying and/or hot press methods, respectively. First, the HDPE/flax4x4 hopsack /SiO₂ ternary composites were produced by a hot press using nano-spraying technique. For the SiO₂ spray technique, the woven flax fiber was positioned on a dish and the SiO₂ slurries were sprayed by a hand onto the both surface of the woven flax fiber. The distance between the sample and the nozzle was approx. 10 cm. The amount of SiO₂ was set for 8 wt.% by weight control. After the nano-spray system, the samples were dried for 48 h at room temperature (RT) and then for 24 h at 80 °C in oven. The HDPE binary and ternary composites placed by hand laying-up a layer of woven flax fibers and then by a layer of HDPE sheet. The HDPE /woven flax fibers composites with and without used nano-spraying were produced into 1-mm thick sheets by hot pressing in a laboratory press (P/O/Weber, Maschinen und Apparatebau, Remshalden, Germany) at a temperature of 190 °C with a fixed holding time of 8 min. under a pressure of 10 MPa. The composites produced are listed in Table 9.

Table 9: Recipe and designation of the HDPE-based systems.

Sample Designation	Flax _{2x2} twill (wt.%)	Flax _{4x4} hopsack (wt.%)	Silicon dioxide (SiO ₂) (wt.%)
HDPE	-	-	-
HDPE/flax _{2x2} twill (l)	35	-	-
HDPE/flax _{2x2} twill (h)	60	-	-
HDPE/flax _{4x4} hopsack (l)	-	35	-
HDPE/flax _{4x4} hopsack (h)	-	60	-
HDPE/flax _{4x4} hop- sack/SiO ₂	-	35	8

Characterization and testing

Morphology detection

The fracture surface was subjected to scanning electron microscopy (SEM) inspection in a JSM 5400 device of Jeol (Tokyo, Japan). The surface was gold coated prior to SEM inspection performed at low acceleration voltage.

Instrumented Falling Dart Impact

Instrumented falling weight impact (IFWI) test was performed on a Fractovis 6785 (Ceast, Pianezza, Italy) using the following settings: incident impact energy, 20 J; diameter of the dart, 20 mm; diameter of the support rig, 40 mm; weight of the dart, 10.357 kg; drop velocity, 1.97 m/s. IFWI tests were performed on quadratic specimens of 60x60 mm² at room temperature.

Thermal and thermomechanical response

Thermogravimetric analysis (TGA) was performed on a DTG-60 SHIMADAZU device (Kyoto, Japan). TGA experiments were conducted in the temperature range from 30 to 500 °C under nitrogen at a heating rate of 10 °C/min.

Dynamic mechanical thermal analysis (DMTA) was performed in tensile mode at frequencies of 0.1, 1 10 Hz at all isothermal temperatures, using a DMA Q800 apparatus (TA Instruments, New Castle, NJ). The storage modulus (E') was determined as a function of the temperature (T = -100°C . . . +130°C). The strain applied was 0.1%. The specimens were cooled to -100 °C. The temperature was allowed to stabilize and then increased by 5 °C, kept 2 min isothermal until 130 °C.

Tensile response

Tensile test was performed on dumbbell-shaped specimens (DIN-ISO-527) on a Zwick 1474 (Ulm, Germany) universal testing machine. Tests were run at room temperature at $v=2$ mm/min crosshead speed and the related stress-strain curves were registered.

Result and discussion

Falling dart impact response

Figure 56 depicts the force as functions of the time for the HDPE, HDPE/Flax binary composites and PLA/flax/SiO₂ ternary composite. It can be seen that the peak force of all binary and ternary composites increased markedly compared to the HDPE. One can recognize that the impact resistance enhanced with increasing flax content in HDPE matrix. With increase of woven flax fibers in HDPE was accompanied with a shift of the force peak toward higher force and longer time. For example, the peak force of HDPE containing 60 wt.% flax_{4x4} was improved by 95 % compared to the same composite structure containing 35 wt.%. The difference in the impact energy occurs between the HDPE/flax_{2x2} and HDPE/flax_{4x4} composites due to the fact that the impact resistance increased in the flax fiber orientation but reduced in the fiber undulation of flax_{2x2}. The addition of SiO₂ particles into HDPE/flax matrix exhibited two-step-like fracture transitions and resulted in a considerable decrease in the fracture toughness. The reinforcing effect of SiO₂ was act a localized crack growth accompanied with reduced ductility. The outcome is reduced impact energy, as schematically illustrated in figure 57. Note that the matrix related crazing and shear yielding deformations are suppressed by the presence of SiO₂ particles. The failure mechanisms, the occurrence of which depends on the dispersion state of the particles in respect to the loading. The SiO₂ particles may act as induced void formation via internal cavitations debonding that supports a final fracture plane. A similar trend has been reported for PA-6/HNBR/ FH or BA nanoparticles [92]. The photographs of typical failure behavior of the related composites after the falling dart impact tests are shown in figure 58. One can see that Incorporation of SiO₂ in HDPE/flax_{4x4}, the specimen was able to crack sideways during impact, allowing the dart to pass through the large opening of the specimen holder. With additional of composite structure of flax_{2x2} and flax_{4x4}, the delamination became less pronounced when the specimens break.

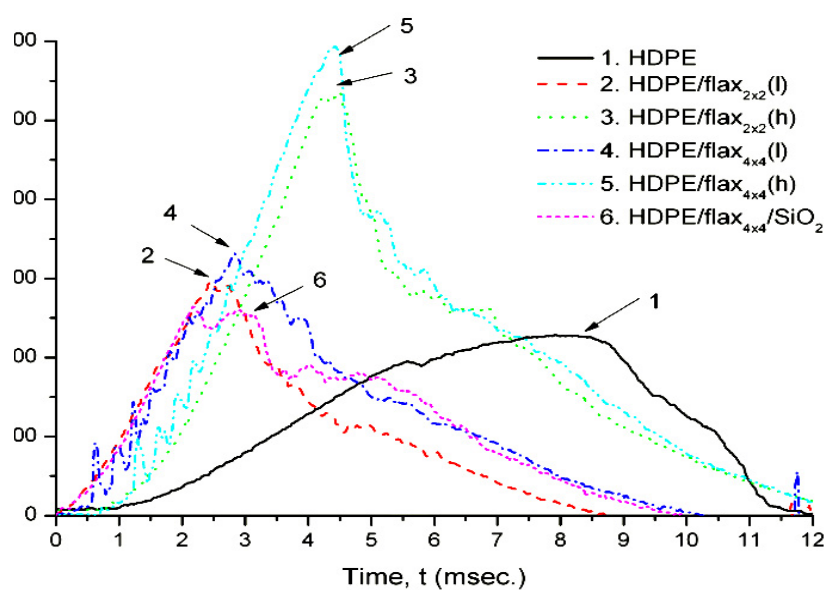


Figure 56: Characteristic force-time curves for the HDPE systems studied.

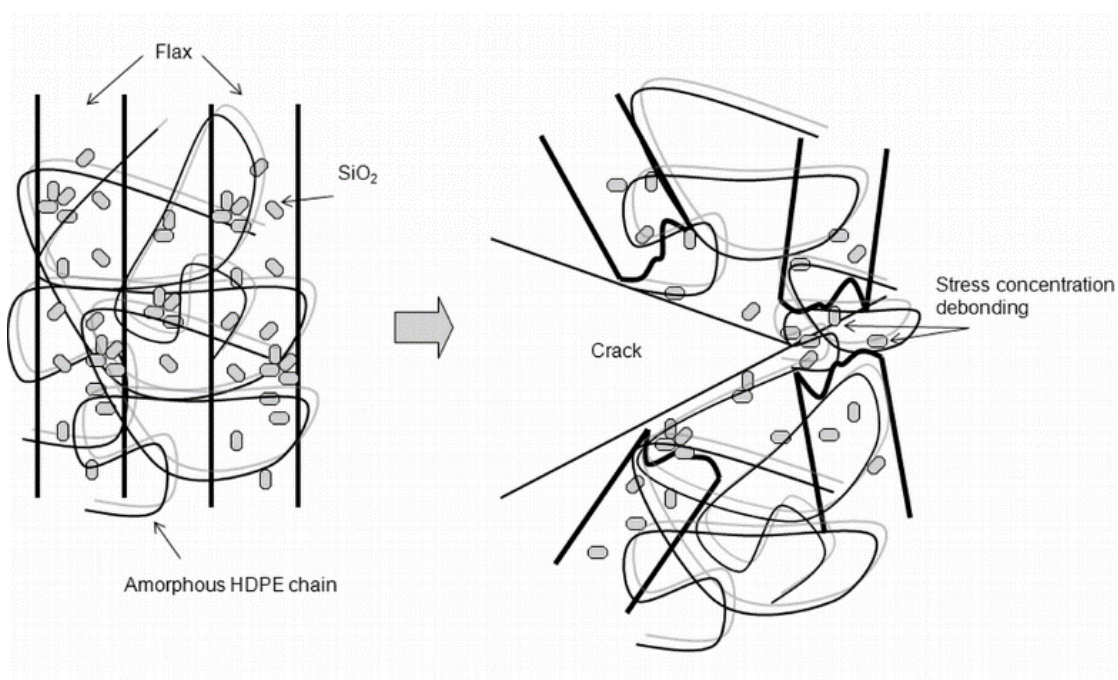


Figure 57: Schemes of the failure mechanisms in HDPE/flax4x4/SiO2 composite.

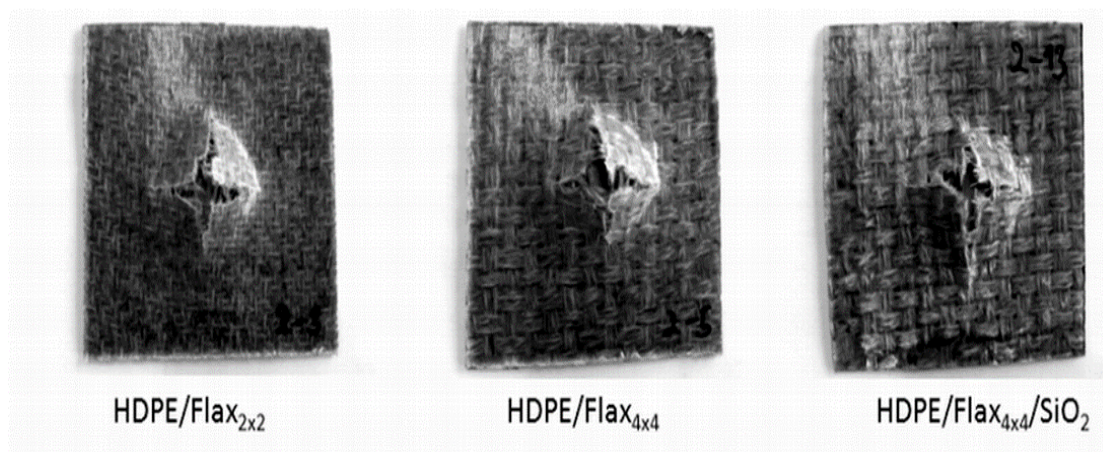
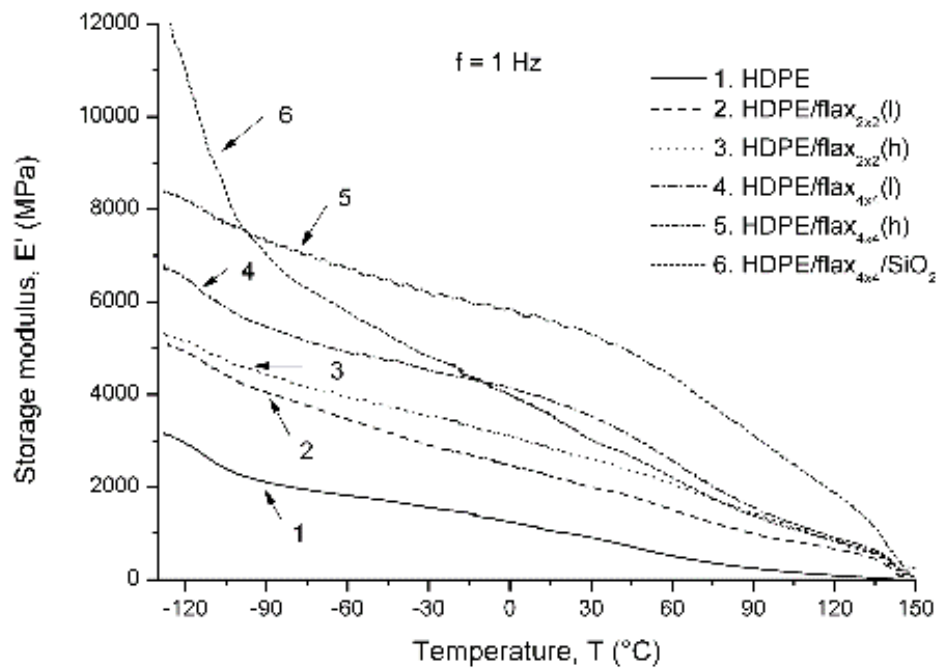


Figure 58: Typical failure of the specimens of HDPE/flax2x2, HDPE/flax4x4 and HDPE/flax4x4/SiO₂ composites after IFWI.

Dynamic mechanical thermal response

DMTA spectra in form of storage- (E') and loss modulus (E'') as function of temperature are demonstrated in figure 59. It is clear from figure 59a that the storage modulus of composite system studied increased with increasing the flax content at the whole temperature range and exhibited markedly higher stiffness than the neat HDPE. It is interesting to note that the stiffness of composites was considered to depend on the flax composite structures. For the HDPE/60 wt.% flax_{4x4} composite, the storage modulus was enhanced by approx. 70 % compared to the HDPE at the same amount of flax_{2x2} content. This can be well explained by reinforcing effect of composite structure of flax weave style 4x4 leading to an increased stiffness. The incorporation of SiO₂ into HDPE/flax_{4x4} resulted in a pronounced stiffness enhancement only in the low temperature range (below -15 °C). The plots of loss modulus vs. temperature in figure 59b reveal the E'' at -110 °C (γ transition) which was assigned to the glass transition temperature of HDPE. The loss modulus peak at approx. 60 °C (α transition) was usually attributed the chain segment mobility in the crystalline phases and reoriented defect in crystalline phases [78-79]. One can notice that the α peak of HDPE exhibited a shift to high temperature regions and no clear change with the incorporation of flax fiber was found in the β transition. The invisible β peak of HDPE/flax_{4x4}/SiO₂ composite at low temperature maybe due to SiO₂ indicates for the reinforcing effect. Whether the related change may be traced to the corresponding SiO₂ requires further investigations.

a)



b)

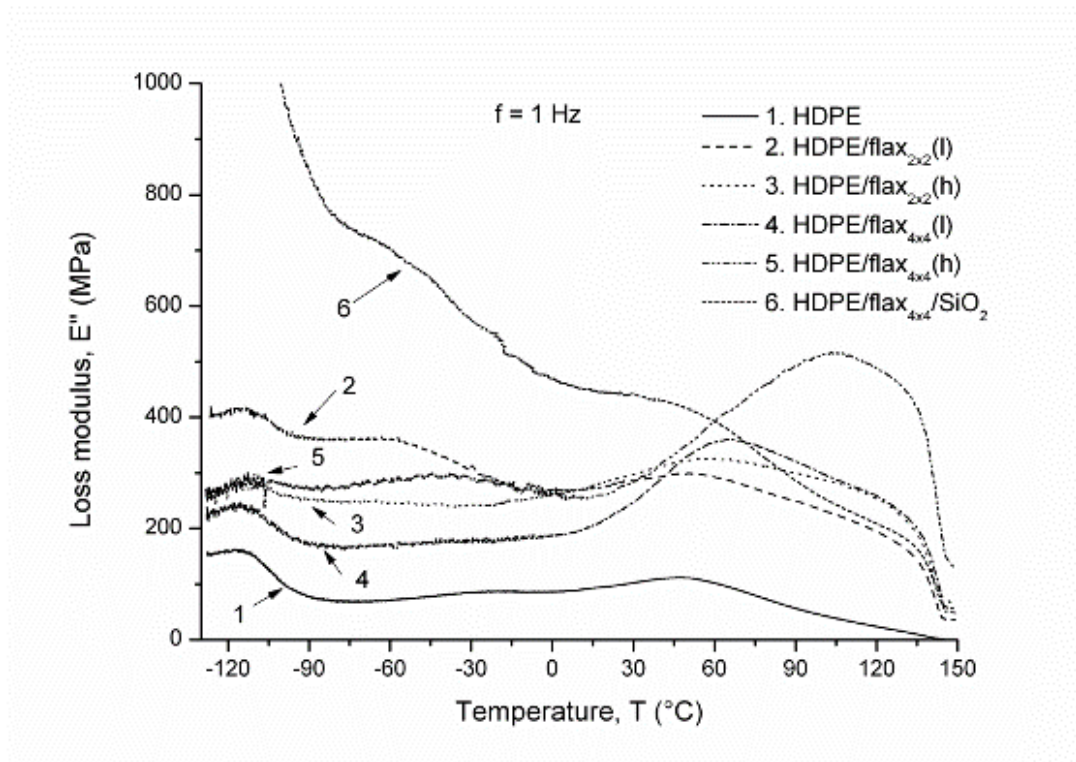


Figure 59: E' (a) and E'' (b) vs. T traces for the HDPE systems studied.

Creep behavior is of interest in materials science and engineering. A linear viscoelastic material (LVM) principle is causally linked to a basis of the conversion method from the modulus and can be used as an experimental probe [33]. LVM is generally assumed that the material does not change its structure. Therefore the applicability of the conversion method from the modulus to the creep compliance can be adopted. Creep compliance is defined as the inverse quantity of modulus by the following equation:

$$D' - iD'' = \frac{1}{E' + iE''} = \frac{E'}{(E')^2 + (E'')^2} - i \frac{E''}{(E')^2 + (E'')^2} \quad (30)$$

where D' and E' are the real, and D'' , E'' the imaginary parts of creep compliance and modulus, respectively.

For the following relationship between storage creep compliance and the modulus is given by:

$$D' = \frac{E'}{(E')^2 + (E'')^2} \quad (31)$$

Figure 60 demonstrates that the simple converted method adequately describes the temperature dependence of the storage creep compliance of the HDPE systems studied. The general trend was that the storage creep compliance increased with increasing temperature. As expected owing to this woven flax fiber reinforcement, the creep resistance of the all composites increased markedly compared to the HDPE. The most interesting result was that the D' curves of binary and ternary composites lay parallel to one another, at least until a given threshold. This means that the creep response in this stable temperature range was matrix dominated. The major effect of the flax reinforcement structure of flax_{4x4} was the reduction of the storage creep compliance. The increase of the creep resistance with increasing flax content was because of the development of an interphase of the reduced molecular mobility.

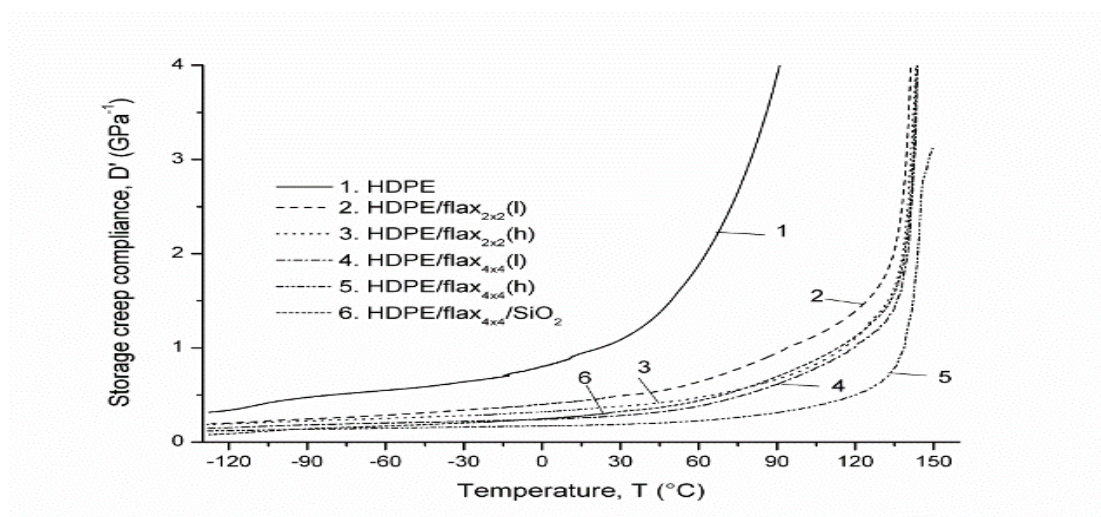


Figure 60: Conversion from the modulus to storage creep compliance for the HDPE systems studied.

Thermogravimetric analysis

Figure 61 shows the traces of the weight loss as a function of temperature for the HDPE, flax, HDPE/Flax binary composites and PLA/flax/SiO₂ ternary composite. It is clear from figure 61 that TGA curves were clearly two step thermal degradation of weight loss between 300 and 500 °C of binary and ternary composites. The decomposition temperature of all-HDPE/flax composites was comparatively lower than that of the HDPE as reported for jute/HDPE composites [28], due to the dehydration from cellulose unit and thermal cleavage of glycosidic. The second decomposition in between 450 and 500 °C was attributed to aromatization, involving dehydration reactions [93]. The thermal stability decreased remarkably with increasing the flax content. Note that the resistance to thermal degradation of the HDPE/flax_{2x2} composite was slightly higher than that of composite containing flax_{4x4}. The incorporation of SiO₂ resulted in a pronounced thermal stability enhancement at the whole temperature range. This can well be explained by the reinforcing effect of the SiO₂ particles leading to increased thermal resistance, due to restrict of SiO₂ particles with partly amorphous polymer segments and stack flax fiber surface (cf. figure 57). This fact can be enabling act a delay heat transfer between the SiO₂ and the PS matrix. The phenomenon, often observed in polymer nanocomposites, was associated with a pronounced increase in the thermal stability.

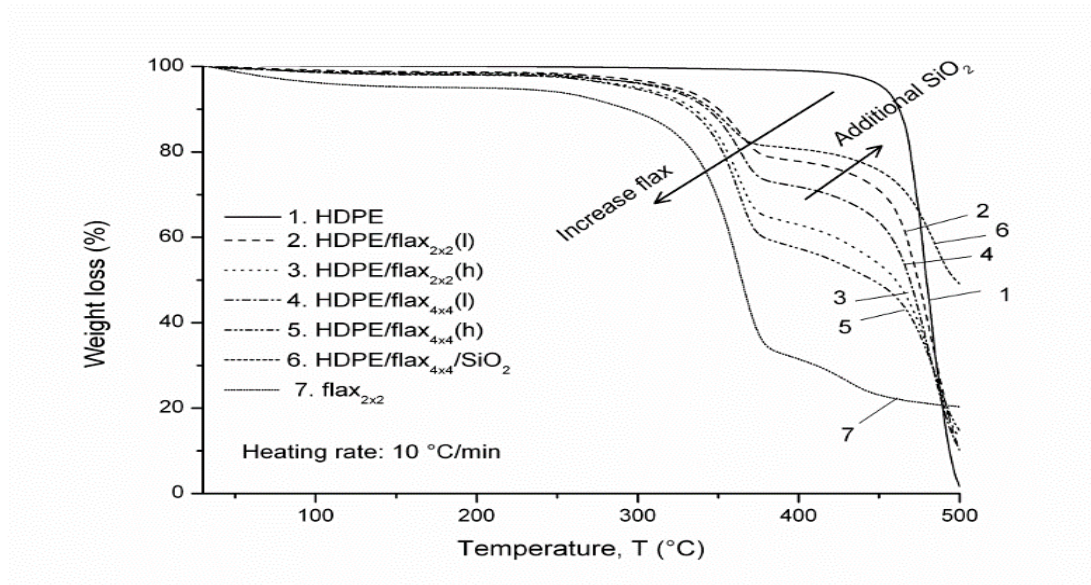


Figure 61: Weight loss versus temperature for the HDPE systems studied.

Tensile response

Results of the tensile mechanical tests are given in figure 62. One can notice that the tensile strength of the composites was strongly enhanced by adding woven flax fiber. The strength of the composites was more than 100% higher than that of the reference HDPE. Adding SiO₂ particles slightly reduced the tensile strength and elongation at break compared to the HDPE/flax_{4x4} composite. This is due to the partly aggregated SiO₂ particles act as stress concentrations. It is in accordance with our SEM observation (cf. figure 55c). On the other hand, the SiO₂ particles were nano-scale dispersed but still in smaller aggregates in the related nanocomposites. The weave style of woven flax had also a great impact on the tensile strength. The strength value was more than 15% higher for the flax_{4x4} than for the flax_{2x2} composites at the same flax content. The elongation at break was less sensitive for the composite structures than the strength. Nevertheless the flax fibrous and SiO₂ particles reinforcements enhanced the strength and reduced the ductility loss of the related nanocomposites at the same time.

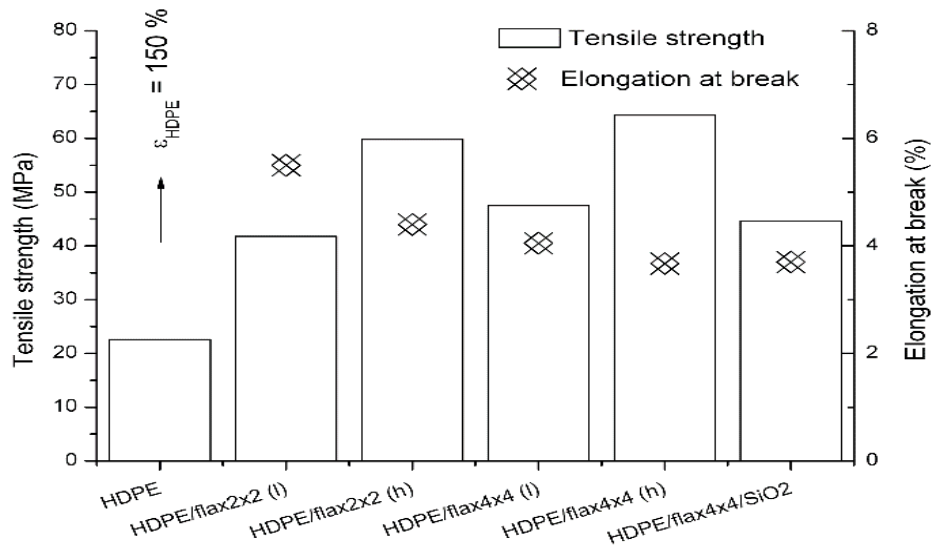


Figure 62: Tensile mechanical characteristics of the systems studied.

Conclusion

This work devoted to study the morphology, falling weight impact, thermal and mechanical properties of a high-density polyethylene (HDPE) and its flax_{2x2}, flax_{4x4} and silicon dioxide (SiO₂) reinforced binary and ternary composites. The SiO₂ was introduced in the HDPE/flax in 8 wt.% via spraying method. Nanospraying technique resulted in nano-scale dispersed but partly aggregation of SiO₂ dispersed in the HDPE/flax. This was demonstrated by SEM investigation. The stiffness value of HDPE/flax composites increased markedly compared to the neat HDPE. However, increase in storage modulus had a strong impact on the composite structures. The presence of SiO₂ particles was associated with a reduction in the maximum force peak of impact test. The stiffness and tensile strength increased with increasing the flax content at the cost of the ductility. Incorporation of SiO₂ particles increased the thermal stability which was considered to depend on the flax content and weave style. The applicability of the conversion method from the modulus to the creep compliance could be well adopted. The calculated data indicated that an improvement in the storage creep compliance can be achieved with increased flax content and depended on the reinforcement composite structure.

4.3 Polyethylene and polypropylene/nano-silicon dioxide/flax composites

State of the Art

Polypropylene (PP) and high density polyethylene (HDPE) have attracted interest of the most industrially successful thermoplastic polymers, due to its excellent cost-to-performance of mechanical properties. Nowadays great efforts are undertaken to improve the mechanical and thermal properties of thermoplastic polymer further, particularly through reinforcement with using natural fibers of various shape factors. HDPE and PP based on natural fiber composites have received great interest in academic and automotive industry sectors to make parts such as body panels, underbody structures, dashboards, front ends, and bumpers. For example, the door panels of the Ford Mondeo are manufactured by kenaf/PP composites [94-95]. The study of Zampaloni et al. [96] concluded that the kenaf/PP composites manufactured had a higher ratio of modulus/cost and a higher specific modulus than E-glass. Wambua et al. [97] demonstrated an overview of several different natural fiber–polypropylene composites in order to evaluate as replacements for glass fiber–reinforced materials. They found that the natural fiber composites have a potential to replace glass in many applications. The tensile strengths of most natural fiber composites compared well with glass fiber ones. An increase of fiber weight fraction increased the impact strength and stiffness. Note that the natural fibers have been receiving considerable attention as substitutes for synthetic fiber reinforcement. Their advantageous properties compared to other materials are low cost and density, acceptable specific strength, good thermal insulation properties, reduced tool wears, thermal and respiratory irritation and renewable resources. Although natural fibers have outstanding properties, major problem of using them with thermoplastic is the poor interfacial bonding between the natural fiber and thermoplastic. The reinforcing action is given when good adhesion between the natural fiber surface and matrix exists. Džalto et al. [64] demonstrated that the porosity of flax/furan bio-composites had negative influence in the stiffness and strength as well as the impact resistance and water absorption. The improvement of the mechanical properties such as impact strength to prepare toughened PP and HDPE have been widely studied both in R&D, e.g. chemical functionalization and modification, addition of synthetic fiber and filler, blending with both PP and HDPE etc. [98-100]. Haque et al. [101] studied a chemical treatment with several fiber types and observed an improvement in mechanical properties of polypropylene (PP) composites. Palm and coir fibers were chemically treated with benzene diazonium salt to increase

their compatibility with PP matrix. Chemically treated palm/coir composites yielded improved impact, flexural and hardness properties compared to the raw ones while coir fiber composites yielded better mechanical properties, except tensile strength increased with fiber loading. They also suggested that the 30% palm and coir fiber reinforced composites had the optimum set of mechanical properties. van de Velde and Kiekens used treated or untreated flax fibers for maleic acid anhydride modified polypropylene (MAA-PP). It was observed that the apparent shear stress of treated flax with MAA-PP composites were higher than that of untreated fiber composites [102]. A similar method was also applied to improve the composite properties of flax fiber and MAA-PP matrix [103]. Moreover, hybridization of fiber with fillers often exhibited better physical and mechanical properties compared to that of PP and HDPE. Example of plastic hybrid composites includes HDPE/wood flour/organoclay [104], PP/hemp fiber/nanoparticles [105] and PP/reed flour/nanoclay [106].

Flax fibers are tough and found to be a potential reinforcement in polymer. Flax fiber was used as the reinforcing material since they are abundant in nature and have minimal effect on the environment because of their biodegradable properties. Many researchers have reported the use of flax fibers, which is in form of short fibers in order to reinforce polymers [35, 107]. Arbelaiz et al. [107] indicated that the mechanical strength for unmodified flax fiber bundle/PP composites decreased with flax fiber bundle, due to a poor interfacial adhesion. However, while the modified with maleic anhydride-polypropylene copolymer as compatibilizer in related composites, the opposite trend was observed. Only few works used continuous flax fibers, which can behave as better reinforcement than short fibers. Recently, the addition of flax structures reinforcement is being given more attention because of their cost effectiveness for producing thermoplastic composites compared to the chemical modification method and can dramatically improve selected properties of the related composites. The potential of using continuous natural fiber for composites to improve the toughness of natural flax reinforced HDPE was demonstrated by Siengchin [41]. Previous work has shown that the impact energy and stiffness value of woven flax fiber composites increased markedly compared with HDPE matrix but reflect to the weave styles. The goal of this study was to demonstrate the feasibility of the production of various flax reinforcing PP and HDPE composites with silicon dioxide (SiO_2) using the hot press technique and compare the structures, impact, thermal and mechanical properties of the related composites. It can be noticed that SiO_2 became under spot of interest and has increased substantially used for binary and ternary composites in construction and automotive applications, due to its high stiffness fracture energy and compressive strengths [90-91].

Materials and preparation of composites

Silicon dioxide (SiO_2) solubility with 40 wt.% SiO_2 concentration (Nanopol XP of Nanoresins AG, Geesthacht, Germany) was used as the filler. Two types of the flax fiber structures (unidirectional-, +/- 45° biaxial and twill_{2x2} flax) were supplied by Composites Evolution (Chesterfield, UK), used as reinforcement which had a yarn size of 250 tex. The density of unidirectional (UD)- and biaxial flax was 1.5 g/cm³ and 1.24 g/cm³ for twill_{2x2} flax (according to suppliers' information). High-density polyethylene (HDPE - Finck&Co, Krefeld, Germany) and polypropylene (PP - Borealis AG, Vienna, Austria) sheets were used as polymeric matrix for all composite systems which had the density of 0.95 g/cm³.

There are many possibilities to produce polymer composites. Accordingly, the reinforcement composites can be introduced into polymer films with quenching in order to guarantee the necessary temperature window during hot press process, as demonstrated in ref [54]. This is the principle of hot press technique has been practiced so far. Therefore, the PP and HDPE binary and ternary composites were prepared by nano-spraying and hot press technique. For the SiO_2 spray technique, the flax fiber structures were positioned on a dish and the SiO_2 slurries were sprayed by a hand onto the both surface of the flax fiber. The distance between the sample and the nozzle was approx. 10 cm. The amount of SiO_2 was set for 8 wt.% by weight control. After the nano-spray system, the samples were dried for 48 h at room temperature (RT) and then for 24 h at 80 °C in oven. PP or HDPE/flax/ SiO_2 composites were prepared by using hand-layup technique. The binary and ternary composites placed by hand lay-up a layer of flax fibers and then by a layer of PP or HDPE sheet. The laminates were then produced into 1-mm thick sheets by hot pressing in a laboratory press (P/O/Weber, Maschinen und Apparatebau, Remshalden, Germany) at a temperature of 190 °C with a fixed holding time of 8 min. under a pressure of 10 MPa. The composites produced are listed in Table 10.

Table 10: Recipe and designation of the PP and HDPE-based flax composites systems studied.

Sample Designation	Unidirectional flax (wt.%)	Biaxial flax (wt.%)	Flax_{2x2} twill (wt.%)	Silicon dioxide (SiO₂) - (wt.%)
HDPE	-	-	-	-
HDPE/unidirectional	38	-	-	-
HDPE/unidirectional/SiO ₂	38	-	-	8
HDPE/biaxial	-	40	-	-
HDPE/biaxial/SiO ₂	-	40	-	8
HDPE/twill _{2x2}	-	-	35	-
HDPE/twill _{2x2} /SiO ₂	-	-	35	8
PP	-	-	-	-
PP/unidirectional	38	-	-	-
PP/unidirectional/SiO ₂	38	-	-	8
PP/biaxial	-	40	-	-
PP/biaxial/SiO ₂	-	40	-	8
PP/twill _{2x2}	-	-	35	-
PP/twill _{2x2} /SiO ₂	-	-	35	8

Characterization and testing

Morphology detection

The fracture surface was subjected to scanning electron microscopy (SEM) inspection in a JSM 5400 device of Jeol (Tokyo, Japan). The surface was gold coated prior to SEM inspection performed at low acceleration voltage.

Impact response

The impact resistance was determined on notched Charpy test specimens according to EN ISO 179-1 and using a universal testing machine with a single swing of a pendulum energy of 25 J. Five specimens were tested and at least three replicate specimens were presented as an average of tested specimens. The Charpy impact strength of notched specimens, a_{cN} , was calculated with the following equation:

$$a_{cN} = w \times 10^3 / h \times b_N \quad (32)$$

where; w is the corrected energy absorbed by the specimen in joules, h is the thickness of the test specimen in millimeters, b_N is the remaining width at the notch base of the test specimen in millimeters.

Thermal and thermomechanical response

Thermogravimetric analysis (TGA) was performed on a DTG-60 SHIMADAZU device (Kyoto, Japan). TGA experiments were conducted in the temperature range from 30 to 500 °C under nitrogen at a heating rate of 10 °C/min.

Dynamic mechanical thermal analysis (DMTA) was performed in tensile mode at frequencies of 0.1, 1 10 Hz at all isothermal temperatures, using a DMA Q800 apparatus (TA Instruments, New Castle, NJ). The storage modulus (E') was determined as a function of the temperature ($T = -100^\circ\text{C} \dots +130^\circ\text{C}$). The strain applied was 0.1%. The specimens were cooled to -100°C . The temperature was allowed to stabilize and then increased by 5°C , kept 2 min isothermal until 130°C .

Creep response

Short time creep test was made in tensile mode at different temperatures using the above DMA apparatus. The applied stress was 3 MPa. The temperature dependence of the creep response of the composites was studied in the range from 15 to 50°C . Isothermal tests were run on the same specimen in the above temperature range by increasing the

temperature stepwise by 5°C and equilibrating the specimen at each temperature for 2 min. During the isothermal tests the duration of the creep testing was 15 min.

Stress relaxation response

Short-time (duration 30 min) stress relaxation tests were made in single cantilever mode at different temperatures, ranging from 5 to 45 °C, using above DMA apparatus. The strain applied was 0.5%. In the temperature range 5–45 °C isothermal tests were run on the same specimen by increasing its temperature stepwise by 5 °C. Prior to the stress relaxation measurement, the specimen was equilibrated for 3 min at each temperature step. The specimen dimensions were 30x10x1 mm³ (length x width x thickness).

Result and discussion

Morphology

SEM pictures taken of the HDPE/UD-flax, HDPE/UD-flax/SiO₂, PP/UD-flax and PP/UD-flax/SiO₂ composites are shown in figures 63a-63d, respectively. One can observe from figures 63a and 63c that the flax fibers were better embedded in the PP matrix compared to the HDPE matrix. This well boding can be supported the enhancement of mechanical and thermal properties. The SEM images permit also the evaluation of the quality of the SiO₂-dispersion, and this was apparently better for PP than for HDPE. For the PP composites, there appeared to be a more uniform distribution of SiO₂. Note that the location and its dispersion of the SiO₂ is mostly controlled by their surface energetics and the driving force for the migration of the particles during preparation. However, this aspect was not addressed in this work and requires further investigations.

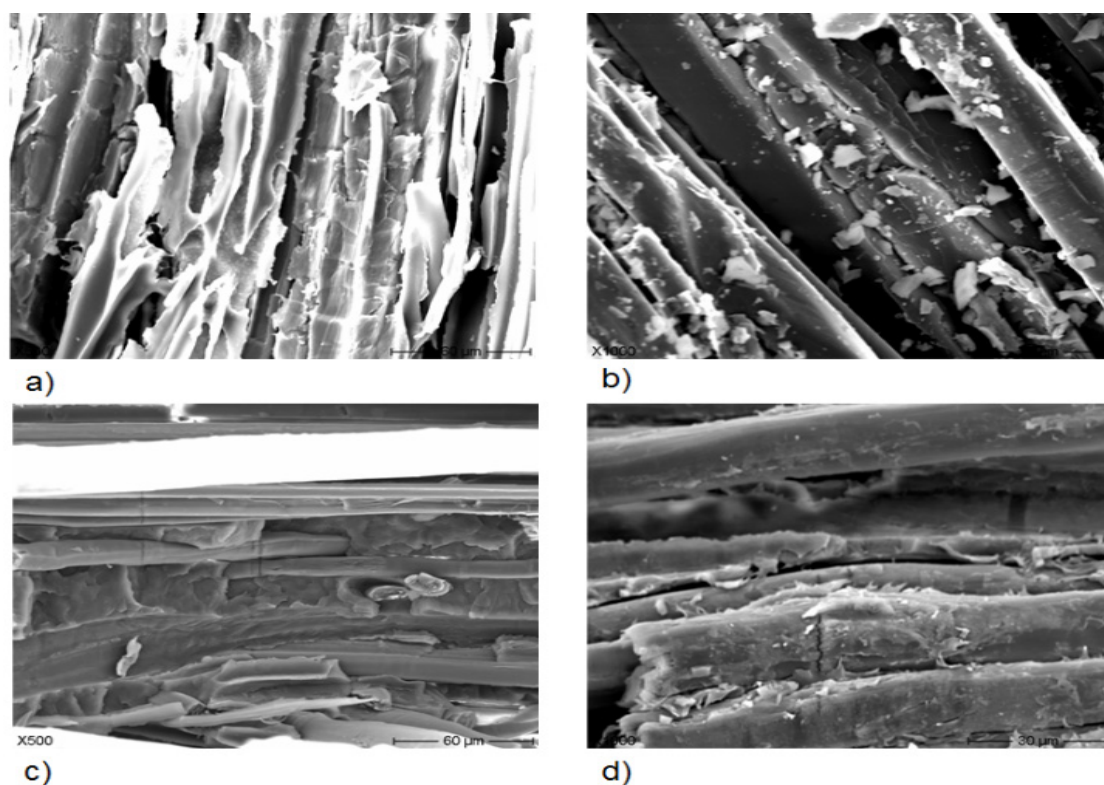


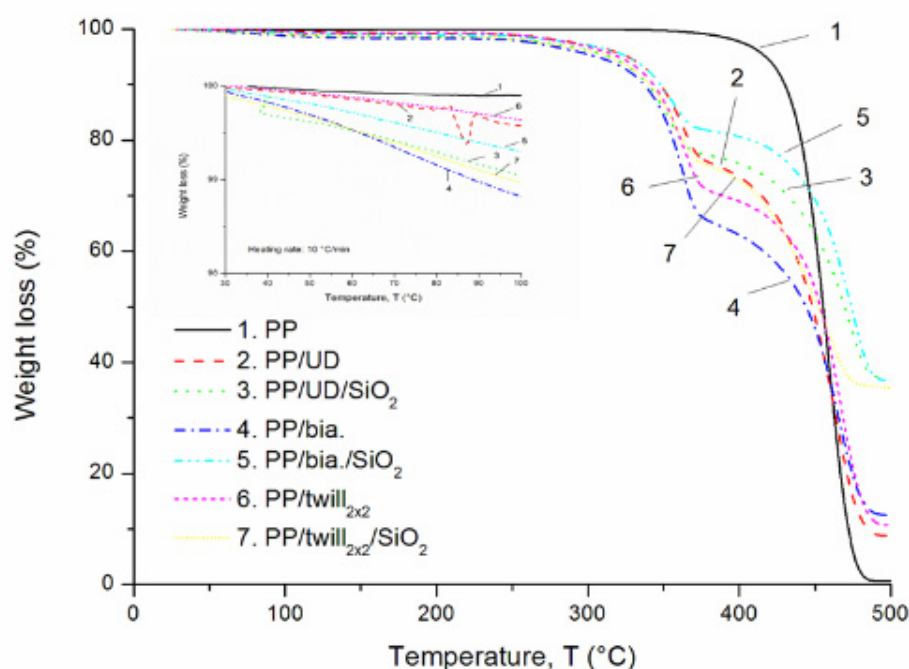
Figure 63: SEM pictures taken from HDPE/UD-flax a), HDPE/UD-flax/SiO₂ b), PP/UD-flax c), PP/UD-flax/SiO₂ composites d).

TGA response

TGA spectra in form of weight loss as function of temperature for the PP and HDPE-based flax composites systems studied are demonstrated in figure 64a and 64b, respectively. It can be seen from the figures 64a-b that the thermal degradation of the neat PP and HDPE started at 356 °C and 455 °C, and 100% degradation was noticed at 487 °C and 500 °C, respectively. Note that degrade of neat PP and HDPE was in only one step without residue. Clearly, two-step thermal degradation of weight loss for flax composites resulted in the temperature range of 300 °C-500 °C. The all flax composites showed lower onset temperature for the thermal degradation than that of even the neat PP. It is well known that the thermal stability of flax composites exhibited three stages from its TGA spectra, with an initial degradation decomposition peak was due to the moisture removal and further decompositions at high temperature was usually attributed to the degradation of hemicelluloses and non-cellulosic materials, respectively [93]. It can be noticed that all the investigated flax composites showed reduced thermal stabilities as the flax content increased. This was the result of low thermal stability of the flax compared to that of the PP and HDPE matrixes. However, there was no direct relation between the thermal stability and flax structures, as similar to our previous work on flax

structures based on PLA composites [21] However, incorporation of SiO_2 was substantial enhancement in the thermal stability of the all flax/PP and HDPE composites. The increase in the thermal stability of ternary composites was attributed to an interaction between the polymer and silica, where the SiO_2 delays volatilizations of the products generated at the temperature of $-\text{C}-\text{C}-$ scission of the polymer matrix. This indication of physical interaction between polymers and silica is probably related to the increase of the cross-linking density. Recall, these SiO_2 particles serve as a bridge to make more molecules of PP and HDPE interconnected. The overall melting temperature of PP and HDPE in the related systems is shown in figure 65. One can see that the melting point of the PP/UD/ SiO_2 composite was about 3 °C higher than that of the neat PP while the melting point of HDPE/UD binary- and HDPE/UD/ SiO_2 ternary composites showed slightly reduction compared with that of the neat HDPE. This change in the melting point may be assigned to some SiO_2 composite effect which was expected from the quality of nano-dispersion. Recall, that SiO_2 was mostly better dispersed in the PP matrix cf. figure 63d.

a)



b)

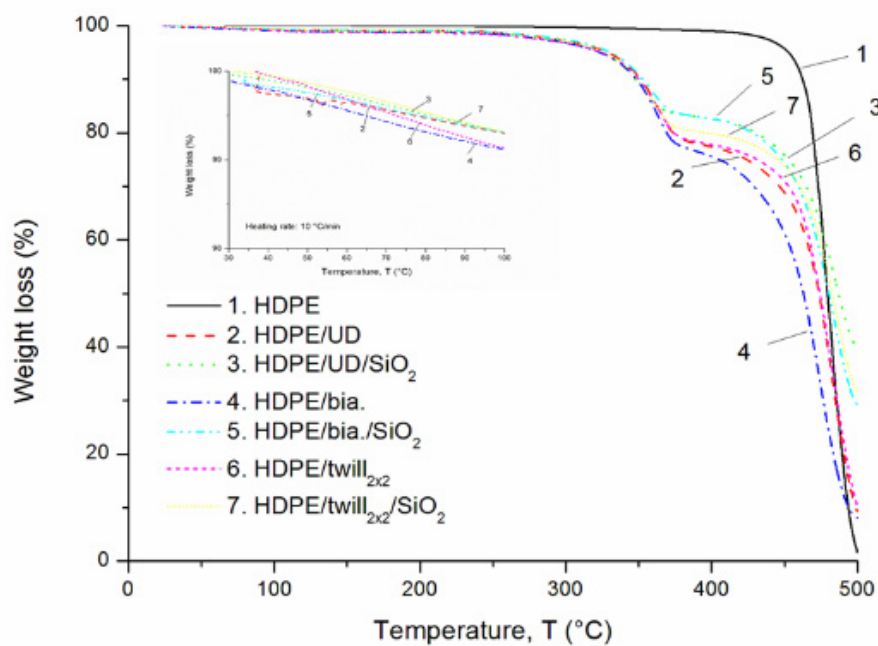


Figure 64: Weight loss versus temperature for the PP- a) and HDPE-based flax Figure sites systems studied b).

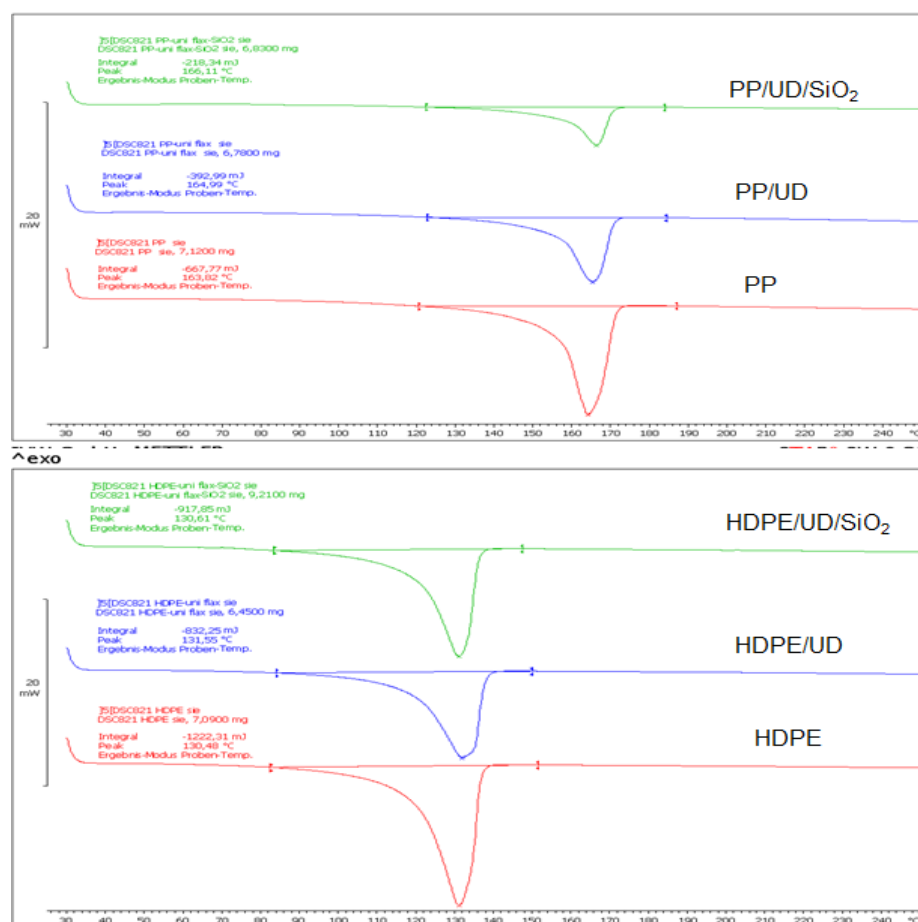


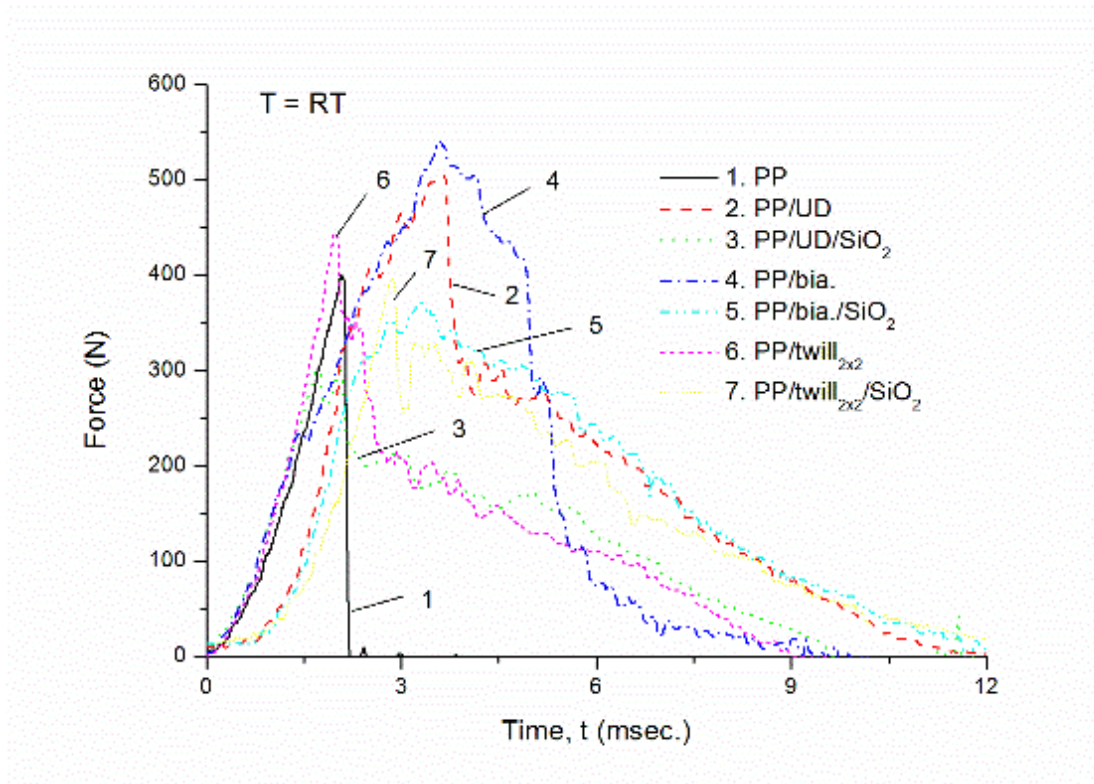
Figure 65: Characteristic DSC curves for the PP and HDPE-based flax composites systems studied.

Impact performance

Figures 66a-b display characteristic fractograms (force as a function of time) for the PP- and HDPE-based flax composites systems studied, respectively. One can recognize that incorporation of bia. flax showed a dramatic increase in the force peak and toward higher the fracture time of the neat PP and HDPE. The maximum load for the bia. flax binary composites increased by approximately 50% and 80% as compared PP and HDPE matrix, respectively. This can be assigned to the higher flexible deformation of bia. flax which was able to diffuse into the matrix contributing to the mechanical impact continuity of the composites system. Note that in comparison with the PP- and HDPE/UD flax composites, this maximum of force peak of PP- and HDPE/bia. composites indicated a marginal decrease from 539 to 504 N and 850 to 769 N, respectively. The slightly reduction can be assigned to some containing of the flax in related composites (cf. table 10). The impact strength were directly influenced by the weight fraction of related composites.

This suggestion is in accord with previous experimental result, as recently demonstrated on examples of the HDPE/flax mat and PLA/woven flax composites in ref. [108-109]. Moreover, the force peak of twill_{2x2} flax/ PP and HDPE composites was 445 N and 580 N, respectively, which were nearly comparable to the force peak of PP and HDPE matrix. An increment in the fracture time revealed that flax fibers had the capability to support effective mechanical loading transformation in the matrix. This relative increment of force peak and fracture time should be traced to the difference in the flax structure characteristics of bia., UD and twill_{2x2} flax (cf. figures 66a-b). Additional SiO₂, the fracture toughness decreased for all PP and HDPE flax composites systems. A decrease in peak force and fracture time at SiO₂ loading could be a reflection of decreased segmental motion in the boundary amorphous layers of the crystals between SiO₂ and matrix as well as SiO₂ agglomeration. Meanwhile, numerous cavitation sites can be created at the interface between the SiO₂ particles and the amorphous layers which promoted micro-crack formation. Similar investigations have also been our early reported in Ref. [41].

a)



b)

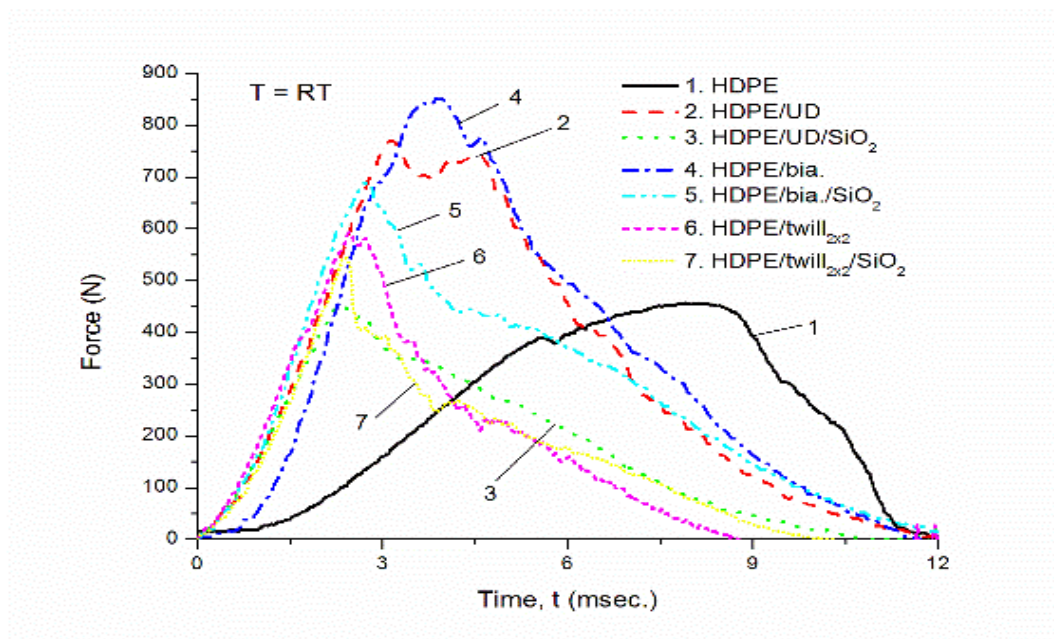


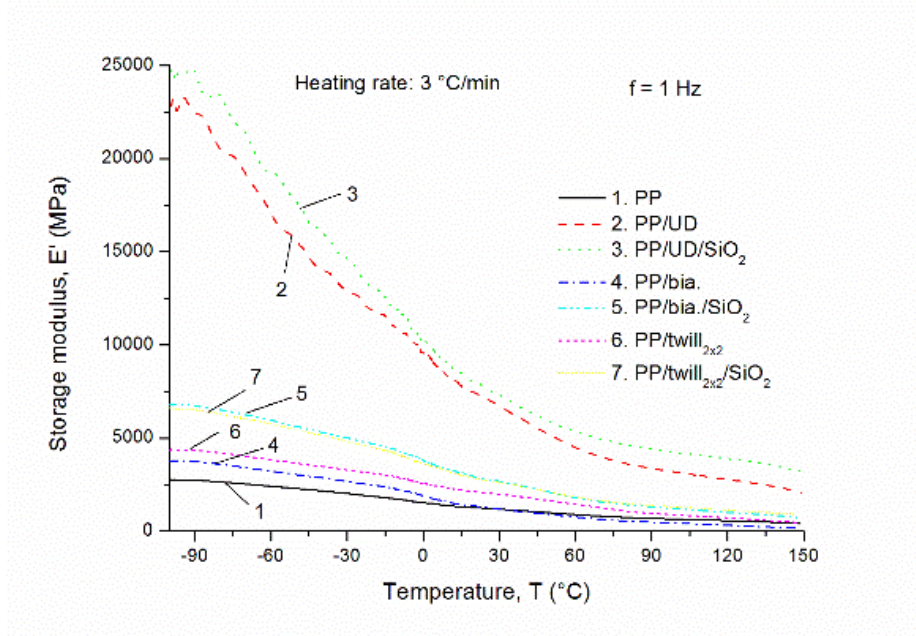
Figure 66: Characteristic force-time curves for the PP- a) and HDPE-based flax composites systems studied b).

Dynamic mechanical thermal response

Figures 67a-b depict the storage modulus (E') as a function of temperature for the PP- and HDPE based flax composites systems studied. It is clear from figures 67a-b that PP and HDPE showed the lowest storage modulus. The storage modulus increased with addition of flax in PP and HDPE at all evaluated temperatures. The reinforcing effect of composite structure twill_{2x2} and bia.-flax resulted in a pronounced stiffness slightly enhancement compared to the matrix. Interestingly, the storage modulus of the PP- and HDPE/UD flax composites at the between temperature -100 °C to 60 °C was in the range of 5–25 GPa. This was due to the preferential reinforced direction of unidirectional flax. Note that this stiffness value was very high for any meaningful structural applications of the bio-composites. Incorporation of SiO₂ particles in PP/bia.-, PP/UD-, HDPE/bia.- and HDPE/twill_{2x2} composites resulted in increase the stiffness, while PP/twill_{2x2} and HDPE/UD composites showed an SiO₂ influence slightly in the storage modulus. This improvement of modulus was probably due to the reduction of chain mobility and deformation within the polymer matrix. It can be notice that the addition of SiO₂ showed the highest increase in storage modulus for PP/UD flax composite. Unlike the incorporation of all flax and flax/SiO₂ had a marginal effect on the overall primary and secondary glass

transitions and reoriented defect in crystalline phases of PP and HDPE in the related systems (tan delta - not reported here).

a)



b)

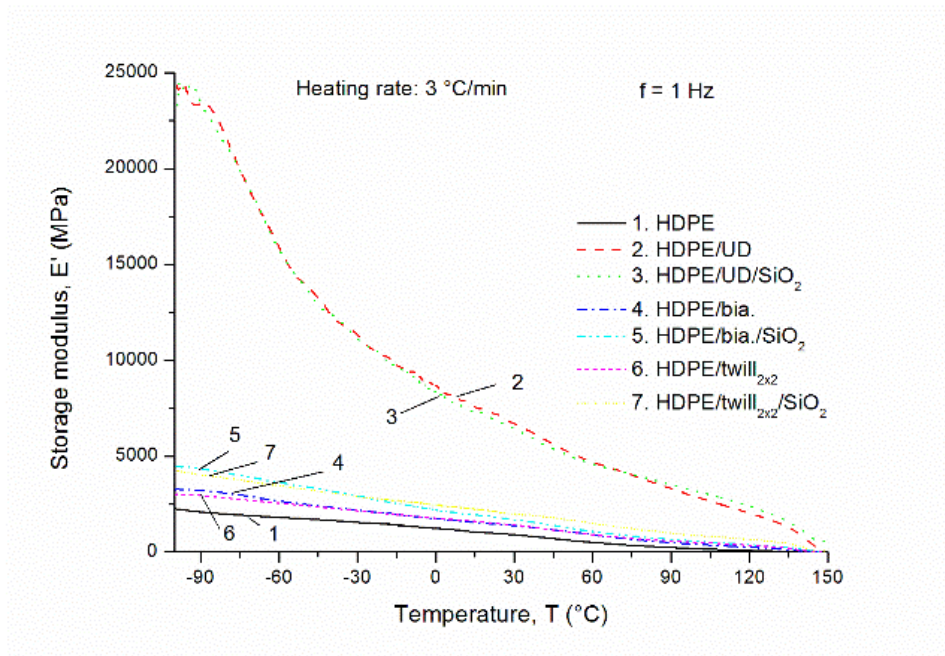


Figure 67: E' vs. T traces for the PP- a) and HDPE-based flax composites systems studied b).

Creep and stress relaxation response

Creep behavior is one of the most fundamental considerations of the physical properties critical to product acceptance in many engineering applications. Generally, viscoelastic properties of creep and stress relaxation response depend on the composite structure and applying temperature. The mobility of the chains of polymer decreases with decreasing the temperature [110]. Figure 68 displays the creep compliance values at 30 °C for the PP based flax composites. One can notice that the presence of flax fiber and SiO₂ particles decrease the creep compliance compared to the neat PP. The principle of the total creep compliance of a polymer composite is expressed as the sum of elastic- (De) and viscoelastic (Dv) components [111]. The total creep compliance (D) is:

$$D(t, \sigma, T) = D_e(\sigma, T) + D_v(t, \sigma, T) \quad (33)$$

where σ is the applied stress, T is the temperature, and t is time.

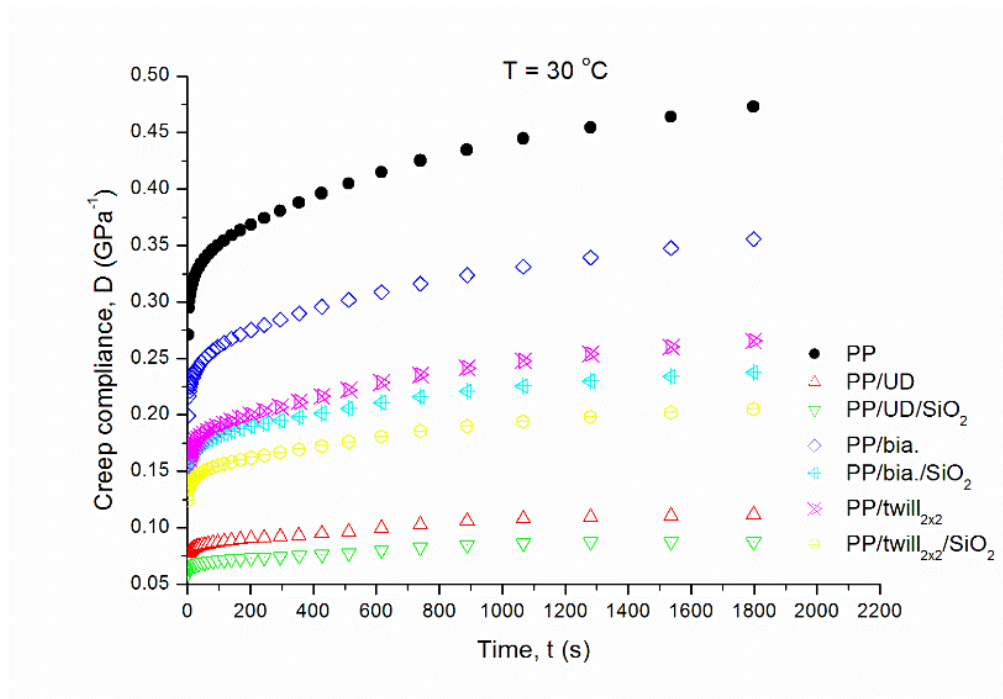


Figure 68: Compliance vs. time for the PP based flax composites systems studied.

With the addition of flax, it was observed that both D_e and D_v were lower than neat PP. For the flax composites containing SiO₂, the enhancement of the D_v was observed at all flax structure composites. Note that with the PP/UD-flax/SiO₂ composite resulted the most beneficial effect on D_e and D_v decreased. It can be also observed in figure 68 that the result of creep resistance was a suitable indicator for the flax fiber orientation. The

fiber orientation such as twill_{2x2} flax resulting in early force-deformation may increase substantially the creep resistance of PP composites previously subjected to bia. flax fiber. The ternary composite of PP/UD/SiO₂ showed lower creep compliance in the whole time investigated compared to the neat PP and all flax/PP with additional SiO₂. This suggests, which was as expected, whatever their geometry of unidirectional flax, had some effect in hindering the early viscoelastic deformation of the flax fiber reinforced composites. Moreover the SiO₂ particles can act as several aspects like to delay the stretching of molecular chain segments and enhanced friction polymer chains. This observation agrees with Siengchin et al [110] who reviewed that the nanoparticles influence was more significant on the instantaneous creep. This became more pronounced with increasing temperature.

The effect of testing temperature on the creep compliance, this is in accordance with our creep response observation that the creep resistance in the neat PP and its composites increased with increasing testing temperature and parallel to that also the De and Dv (not reported here). It is well know that according to the shift factors (aT) are linked with time-temperature superposition (TTS) via the Arrhenius and Williams-Landel-Ferry (WLF) functions. Temperature dependence of the shift factor is corrected by using the WLF or the Arrhenius equations [33]. The WLF former equation follows:

$$\log(a_T) = \frac{-C_1(T - T_0)}{C_2 + (T - T_0)} \quad (34)$$

where C1 and C2 are constants and T0 is the reference temperature in this case is 50 °C.

For the Arrhenius equation is:

$$\ln a_T = \frac{E_a}{R} \left(\frac{1}{T} - \frac{1}{T_0} \right) \quad (35)$$

where Ea is an activation energy, R is universal gas constant and T₀ is the reference temperature (= 50 °C).

Figure 69 displays the course of the experimentally determined aT values as a function of the temperature. One can recognize that the experimental aT data and their slope decreased with increasing temperature and addition of flax fiber. Note that this may be linked with the difference in flax structures. The decrease in slope of aT was mostly due

to the reinforcing effect of SiO_2 particles. The parameters of the Arrhenius (E_a) and WLF (c_1 , c_2) equations are listed in Table 11. One can observe that the practically results of activation energy (E_a) influenced by the structures of the flax composites. The most striking finding is that the unidirectional structure of the flax fiber likely affected the shift factors. Note that the E_a , C_1 and C_2 of PP/UD-flax composite decreased when compared to the bia. and $\text{twill}_{2 \times 2}$ composites. Moreover, the SiO_2 reinforcing effect was accompanied with a reduction in the experimentally determined E_a , C_1 and C_2 values. The creep master (followed by TTS - principle) as a function of time, selecting $T_{\text{ref.}} = 50^\circ\text{C}$ as reference temperature is depicted in figure 70. The aforementioned difference in the flax structures was well reflected and confirmed in the creep master curves. The same statement holds for the PP/UD/ SiO_2 composite with most increasing creep resistance. For example, the creep compliance of PP/UD/ SiO_2 ternary composite at 1800 sec. was reduced by approx. 5 time and 3 time compared to the PP/bia. and PP/ $\text{twill}_{2 \times 2}$ composites, respectively. Recall, studies on binary and ternary PP composites show that creep compliance at short term and calculated master curve was believed to be controlled by the deformation of the flax fiber phase.

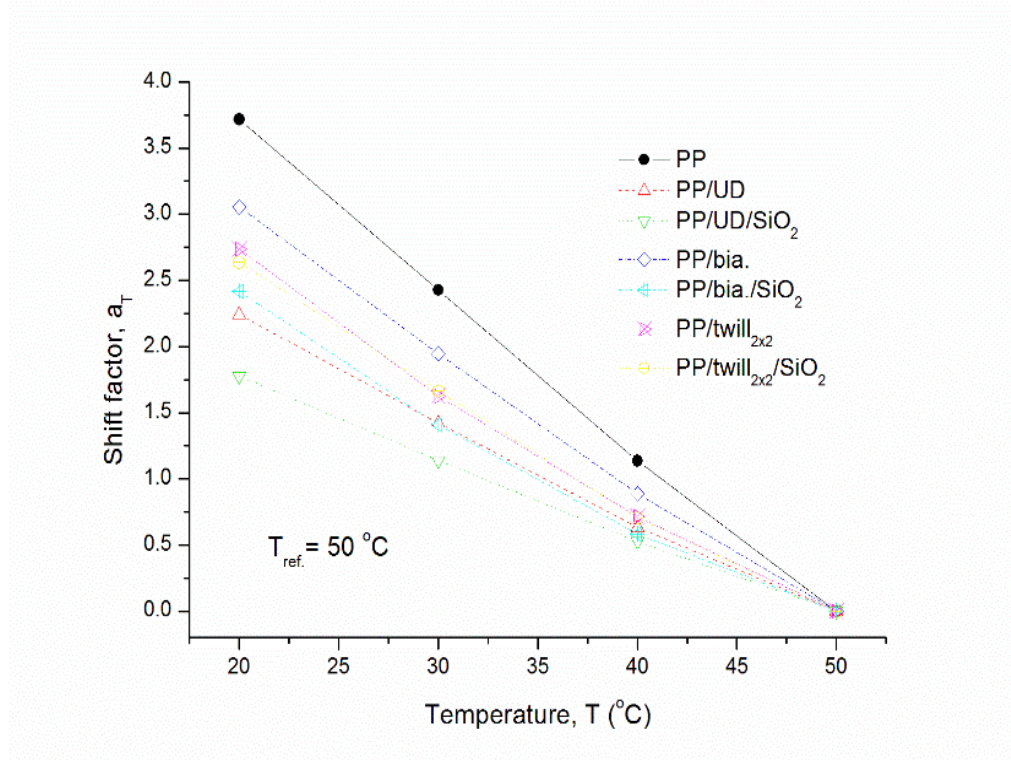


Figure 69: Experimental shift factors along with the related Arrhenius fits in the creep temperature.

Table 11: Fitting parameters of the generalized Maxwell model.

Sample Designation	Creep ref. 50 °C			Stress relaxation ref. 50 °C		
	Arrhenius	WLF		Arrhenius	WLF	
	Ea (kJ/mol)	C1	C2	Ea (kJ/mol)	C1	C2
PP	225.3	36.58	324.5	237	25.18	221.4
PP/unidirectional	134.2	10.79	174	157.8	17.21	226.7
PP/unidirectional/SiO ₂	106.9	11.67	226.8	125.1	7.414	135.2
PP/biaxial	183.3	16.96	196.1	194.5	22.49	238.7
PP/biaxial/SiO ₂	140.1	4.953	91.37	138.6	8.44	138.2
PP/twill _{2x2}	160.2	7.109	107.9	179.4	13.67	166.2
PP/twill _{2x2} /SiO ₂	157.1	10.21	145.7	169.7	10.34	138.2

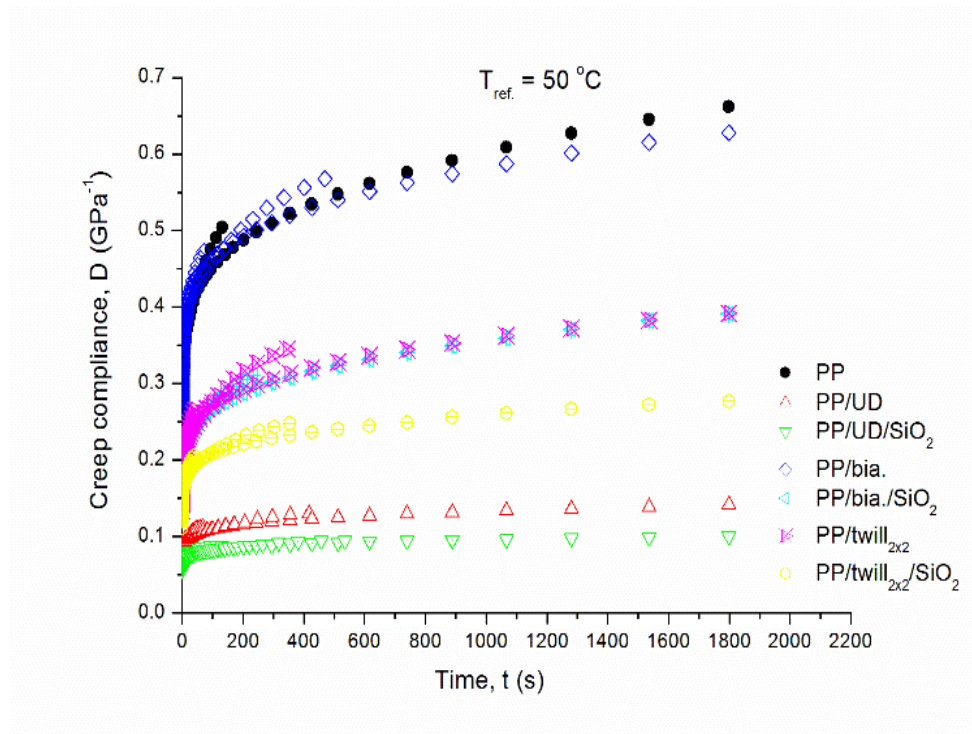


Figure 70: Creep master curves constructed by considering the TTS - selecting Tref.= 50 °C.

Similar to the creep response, the total stress relaxation used to gain deeper insight of PP and HDPE composites systems studied. The principle of the total relaxation modulus (E_r) is expressed as the sum of elastic- (E_{re}) and viscoelastic (E_{rv}) components. The stress relaxation of composite materials is separated in two stages. In the first stage of instantaneous relaxation, this starts at time closer to zero. In the next stage is time-dependent relaxation. Therefore, the total relaxation modulus can be followed:

$$E_r(t, \varepsilon, T) = E_{re}(\varepsilon, T) + E_{rv}(t, \varepsilon, T) \quad (36)$$

where ε is the applied stress, T is the temperature, and t is time.

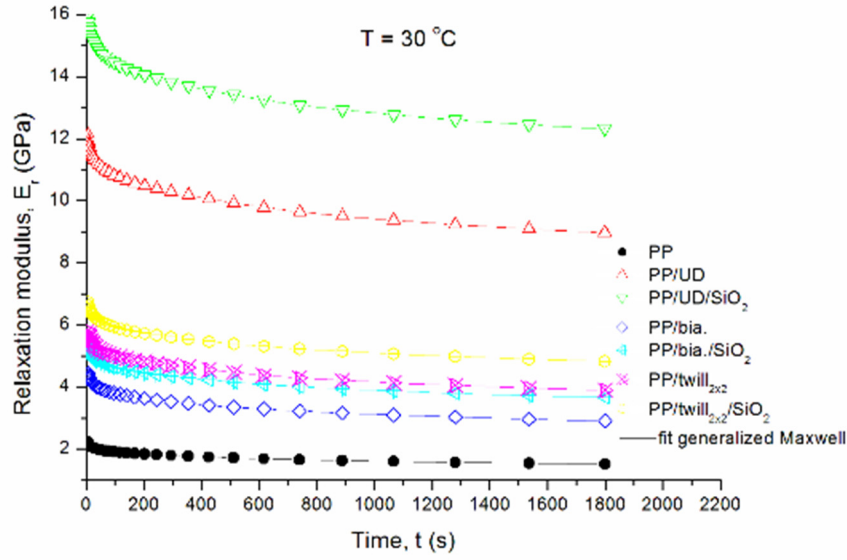
In additional, to describe the relaxation modulus versus time traces the generalized Maxwell model can well be used [80]. Consisting of an elastic spring and a viscous dashpot in series representing the generalized Maxwell model is

$$E_r(t) = E_{r0} + \sum_{k=1}^N E_{rk} \times e^{-t/\tau_{rk}} \quad (37)$$

where E_{r0} is the zero-time relaxation modulus, and τ_{rk} represents the k -th relaxation time with the corresponding relaxation modulus E_{rk} . To accurately predict the experiment data of stress relaxation, a four element Maxwell model was used for this work. Figures 71a and 71b depict the relaxation modulus as a function of time for binary- and ternary PP and HDPE composites systems studied and their fitting by the generalized Maxwell equation, respectively. It is well resolved that there was a good agreement between the relaxation curves and those predicted by the generalized Maxwell equation. The corresponding parameters of the generalized Maxwell model are summarized in table 12 using the related software of Rheology Advantage Data Analysis. To fit the data with the generalized Maxwell model, the experimental results can be assumed that the parameters of E_{rk} and τ_{rk} were independent on the structure of flax and SiO_2 particles but E_{r0} allowed varying. Note that the UD-flax composites of PP and HDPE showed a higher E_{r0} compared to the bia. and twill_{2x2} composites. It is evident from figures 71a-b that the instantaneous relaxation modulus (E_{re}) of all flax of both PP and HDPE composites was markedly higher than that of the matrix. The relaxation modulus of the ternary PP and HDPE composites was enhanced by adding SiO_2 particles compared to the flax/PP and HDPE binary composites. Moreover, the relaxation modulus versus time trace of the bia. and twill_{2x2} composites was always below that of the UD-flax version.

This can be attributed to the difference in the reinforcing stage of flax as discussed earlier.

a)



b)

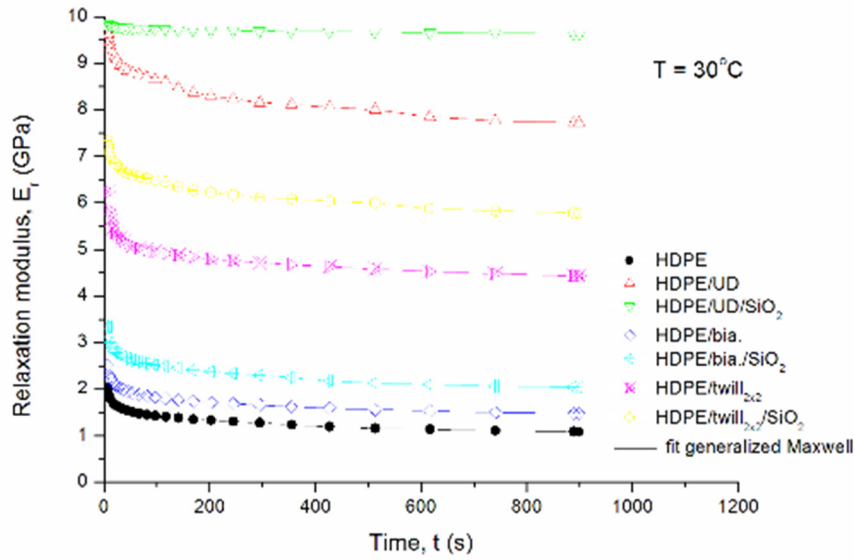


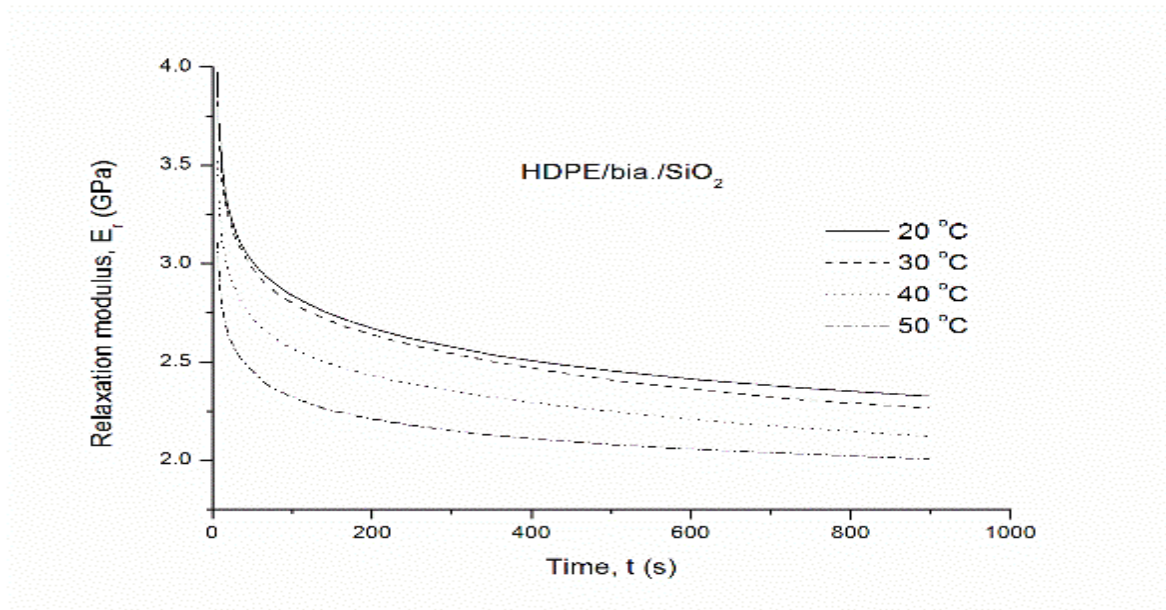
Figure 71: Relaxation modulus vs. time at $T = 30$ °C and their fitting by the generalized Maxwell equation for the PP- a) and HDPE-based flax composites systems studied b).

Table 12: The shift factor (aT) based on experimental results of the Arrhenius and Williams-Landel-Ferry (WLF) equations for creep and stress relaxation tests - selecting Tref= 50 °C.

Generalized Maxwell – Parameter	E_{r0} (GPa)	E_{rk1} (GPa)	τ_{r1} (s)	E_{rk2} (GPa)	τ_{r2} (s)	E_{rk3} (GPa)	τ_{r3} (s)	E_{rk4} (Pa)	τ_{r4} (s)
HDPE	2.02	1.28	5125	0.35	146	0.87	8.24	0.257	0.189
HDPE/unidirectional	9.79	8.57	7827	1.26	33.33	0.009	0.008	0.022	0.059
HDPE/unidirectional/SiO ₂	9.84	9.73	83160	0.13	29.29	0.066	0.016	0.034	0.057
HDPE/biaxial	2.52	1.74	5167	0.44	74.83	1.35	5.057	0.043	0.040
HDPE/biaxial/SiO ₂	3.34	2.54	3592	0.95	19.98	0.066	0.078	0.210	0.005
HDPE/twill _{2x2}	6.24	5.004	6588	1.92	13.27	0.189	0.181	0.320	0.657
HDPE/twill _{2x2} /SiO ₂	7.34	4.66	8587	0.58	50.97	0.002	0.013	0.015	0.008
PP	2.23	1.73	13100	0.28	289.1	0.3	15.09	0.391	0.434
PP/unidirectional	12.12	9.92	17640	1.31	325.4	1.25	16.71	0.226	0.285
PP/unidirectional/SiO ₂	15.98	13.43	20270	1.51	307.2	1.48	16.03	0.239	0.273
PP/biaxial	4.44	3.34	11330	0.63	272.1	0.58	16.23	0.047	0.003
PP/biaxial/SiO ₂	5.35	4.19	12800	0.65	292.8	0.68	16.28	0.527	0.487
PP/twill _{2x2}	5.82	4.45	13180	0.82	334	0.75	16.36	0.039	0.002
PP/twill _{2x2} /SiO ₂	6.74	5.45	14420	0.74	283	0.77	16.59	0.087	0.048

One can see from figures 72a-b that due to the softening of the PP and HDPE matrix, the E_{rv} decreased with increasing temperature. Note that the stiffness was decreased with diminished instantaneous relaxation modulus (E_{re}). The large $E_r(t)$ difference for the PP/bia./SiO₂ composite (cf. figure 72a) during temperature change suggests that the relaxation response was far more sensitive to the PP matrix in the related specimens than in the HDPE matrix. For the stress relaxation test of the PP and HDPE matrix, the activation energy of 237 kJ/mol and 167.5 kJ/mol, respectively (cf. figures 73a-b), can be calculated by using TTS. Incorporation of flax structures and SiO₂ particles decreased the E_a compared to both matrixes PP and HDPE. The obtained E_a was in the range of 125-195 kJ/mol for PP based composites and 29-142 kJ/mol for HDPE composites system studied. This depended upon the type of composite structures. Comparing these activation energies with those from stress relaxation and creep tests of PP composites system studied, similar trends to reduce E_a can be noticed when the SiO₂ particles added in all PP/flax composites. This can be confirmed to the reinforcing effect of SiO₂.

a)



b)

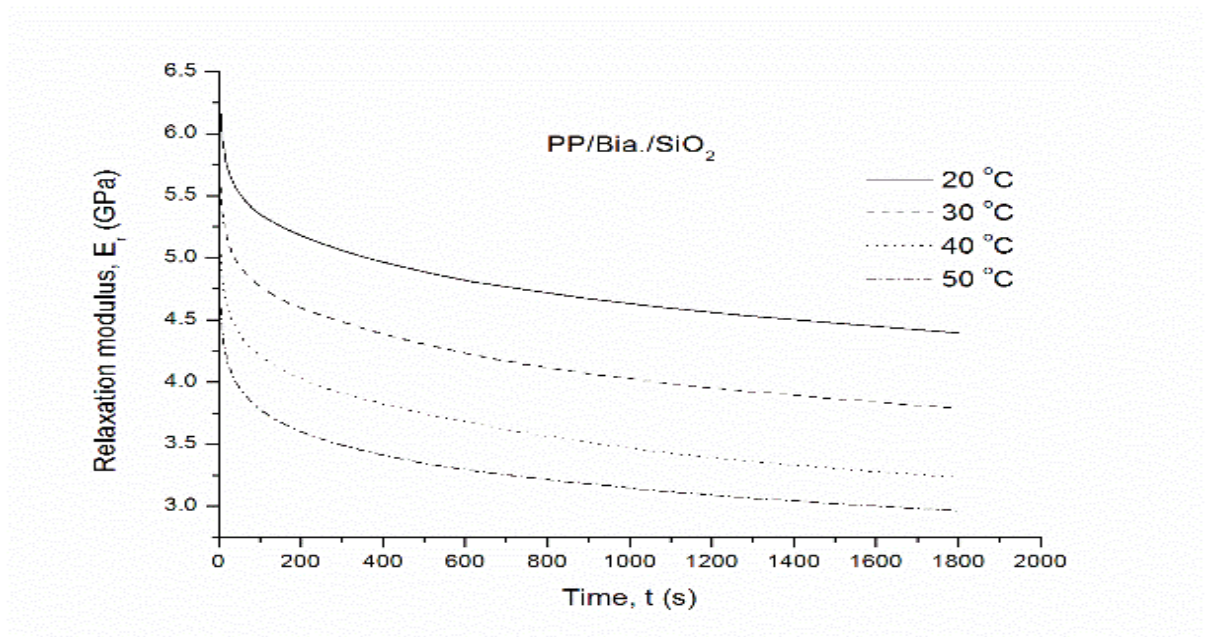
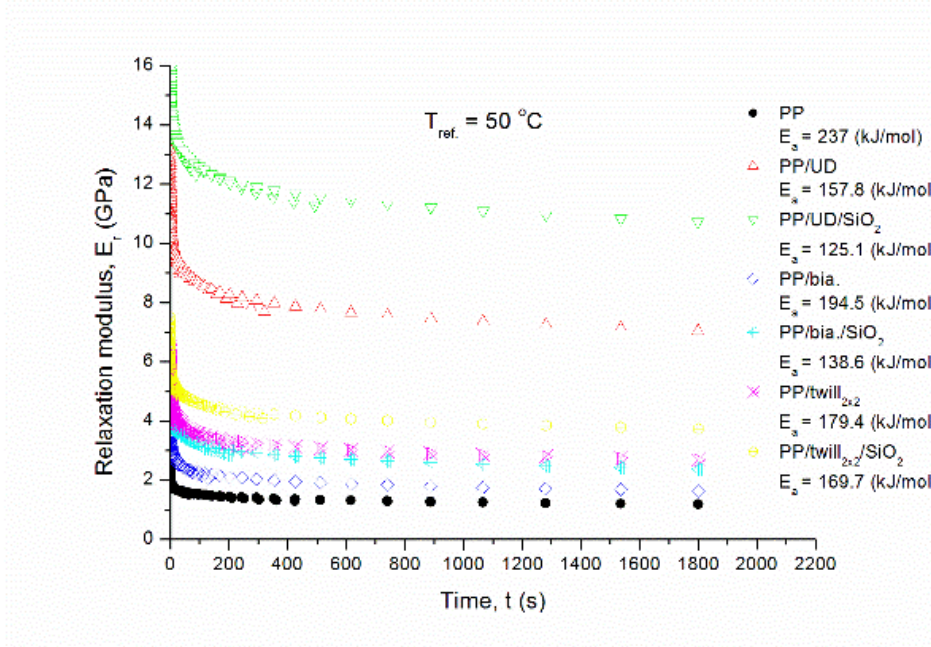


Figure 72: Effect of temperature on the relaxation modulus of the PP- a) and HDPE-based flax composites systems studied b).

The related master curves, viz. stress relaxation modulus as a function of time, selecting $T_{ref} = 50$ °C as reference temperature are depicted in figure 73a and 73b. One can recognize that according to the TTS principle satisfactorily fits to the stress relaxation data for all systems. Incorporation of UD flax enhanced markedly the relaxation modulus of PP and HDPE but less affected for bia. flax systems. This improvement in relaxation modulus was due to associate the arrest of segmental motion between at interfacial with

their neighborhood, thus increased in both elastic and viscoelastic components of the total stress relaxation. Recall, the improvement in relaxation modulus was more pronounced for the PP- and HDPE/UD/SiO₂ ternary composites.

a)



b)

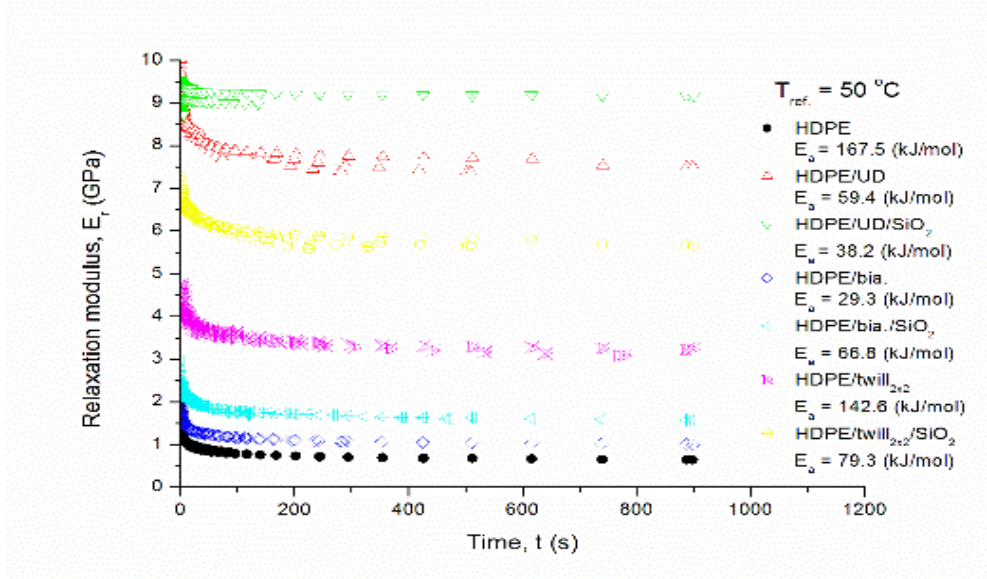


Figure 73: Relaxation modulus - master curves were constructed by considering the TTS and selecting $T_{ref} = 50\text{ }^{\circ}\text{C}$ for the PP- a) and HDPE-based flax composites systems studied b). E_a was calculated by the Arrhenius equation.

Conclusion

This work devoted to study the morphology, thermal, mechanical, creep and stress relaxation properties of polypropylene (PP) or high-density polyethylene (HDPE) hybrid composites based on different flax fiber (unidirectional-, biaxial and twill2x2) and silicon dioxide (SiO₂) The SiO₂ was introduced in the PP or HDPE/flax fiber in 8 wt.% using a hot press. Based on this work the following conclusions can be drawn:

Addition of SiO₂ significantly increased the thermal decomposition of PP-HDPE/all flax fiber composites. This can be attributed to the reinforcing effect of SiO₂.

The impact strength, stiffness and viscoelastic properties of PP-HDPE/all flax fiber laminates increased profoundly in the presence of SiO₂. However, this improvement of mechanical properties influenced strong on the flax structure characteristics.

Incorporation of SiO₂ particles and all flax fiber into the PP or HDPE matrix resulted in a considerable increase of the creep resistance and relaxation modulus. The improvement in creep and relaxation properties of PP and HDPE hybrid composites was attributed to the interfacial interaction of SiO₂ in the hybrid composites. Moreover, the improvement in creep compliance and relaxation modulus was more pronounced for the PP- and HDPE/UD/SiO₂ ternary composites.

Based on the TTS principle, experiments master-curves in form of creep compliance and relaxation modulus vs. time were constructed. The related master curves of relaxation modulus could be satisfactorily described by the generalized Maxwell model.

4.4 Polylactide (PLA)/woven flax fiber textiles/boehmite alumina (BA) composites

State of the Art

In the last years, composite materials based on biopolymers reinforced with natural fibers gained great attention due to their good physical-mechanical properties [86,112-113]. The advantages of natural fibers besides the environmental concern have led to the extensive development of composites reinforced with natural fibers. In general, natural fibers exhibit many advantageous properties as reinforcement for composites, showing low density, and yielding relatively lightweight composites with high specific properties. Natural fibers also offer significant cost advantages and benefits associated with processing compared to synthetic fibers. Moreover, they are renewable resources, which reduce the dependency on foreign and domestic petroleum oil. Different studies showed that polylactide (PLA) is one of the most promising biopolymers due to its good mechanical properties and biodegradability [34]. However, the insufficient impact strength and

low thermal stability of PLA are the limiting factors of its applications. In order to achieve the upgrade properties it has been recommended with nano-scale fillers and natural fibers, such as organoclay, carbon nanotube (CNT), cellulose, kenaf, abaca and hemp fibers [17-19, 23, 31, 114]. Das et al. [23] introduced a solvent casting method for PLA based composite films with nanoclays. The thermal degradation resistance of PLA was improved with clay loading because of barrier effects by the dispersed clay platelets. Suryanegara et al. showed that the use of microfibrillated cellulose (MFC) was helpful to increase the tensile modulus and strength due to the increased crystallization of PLA [31]. In addition, natural fiber reinforced biodegradable polymers, such PLA, are considered as novel reinforcements with great application potential compared to tradition micro-scale reinforcements. Bax et Mussig [22] investigated the impact and tensile properties of PLA with rayon fibers (Cordenka) and flax composites. They found that PLA containing 30 wt.% of Cordenka shows promising highest impact properties. Recently, reported by Kowalczyk et al. [27] that the mechanical properties of PLA can be improved by adding cellulose micro- and nanofibers. The nanofiber composite exhibited markedly higher stiffness compared to the cellulose microfibers composite. Moreover, Haq et al. [115] demonstrated that the balance of mechanical properties (stiffness and toughness) can be obtained by controlling the amount of bio-resin and nanoclay content in unsaturated polyester. Such multiphase hybrid biocomposites improved also barrier and thermal properties.

A variety of composite structures are associated to an increase in mechanical properties of composites [37]. With potential for the wider applications of bio-composite structures, these composites materials are growing interest in packaging, construction, medical and automotive industries. Usually, the mechanical behaviors of composite materials have a strong dependence on the composite structures of the reinforcing phase. The effect of woven composites on elastic properties and failure behavior of has been studied in the past [116-117]. Gupta et al. [117] investigated the effect of microstructural parameters on the tensile creep of woven composite. They reported that increase in crimp angle increased the instantaneous compliance and the magnitude of creep. It can be noticed that the composite structures are classified into structures with different fiber undulation. The mechanical properties of composite with fiber undulation will be different than mechanical properties of composite without fiber undulation [38, 52]. The viscoelastic and other mechanical properties may be linked with some fiber undulation effects in the composite structures. However, only few scientific works [16] have been carried out about the influence of composite structures and importance of nanofiller on the properties of natural fiber composites based on PLA. The object of this research work was to demonstrate the feasibility of the production of PLA/flax/alumina composites with various flax

structures using the nano-spraying/hot press techniques and compare the structures, water absorption, impact, thermal and mechanical properties of the different flax reinforced PLA composites. A further aim of this work was to explore the potential of the nano-spraying technique to disperse suitable fillers on nanoscale [40]. Note that many nanoparticles are available in solvent form and this technique is very simple and more economical compared to conventional nanostructuring technologies such as in situ polymerization. To get a clear picture on the effect of the nanofiller, the properties of the Biotex Flax 40%/PLA blend were also studied. Synthetic boehmite alumina was selected as nanofiller. It is noteworthy that alumina particles are water dispersible and have been already checked as possible reinforcements in thermoplastic. Khamalo et al. [68] reported that the addition of unmodified alumina nanoparticles could strongly the stability to thermooxidative degradation of the polyethylene matrices.

Materials and preparation of composites

Biotex Flax/PLA blend was supplied by Composites Evolution (Chesterfield, UK). The volume fraction of flax was 40 vol.%. Two types of woven flax fiber textiles (weave style of 2x2 twill and 4x4 hopsack – cf. Figure 74) were used as reinforcement which had a yarn size of 250 tex. The typical properties of Biotex Flax/PLA blend are listed in Table 10. The water dispersible boehmite alumina (BA; $\text{AlO}(\text{OH})$; Dispal®11N7-80 of Sasol GmbH, Hamburg, Germany) served as filler for all composite systems. The nominal particle size of alumina in water was 220 nm though that of the alumina powder as delivered was 40 μm . Alumina has Al_2O_3 content of 80 wt.% and specific surface area of 100 m^2/g (according to suppliers' information).

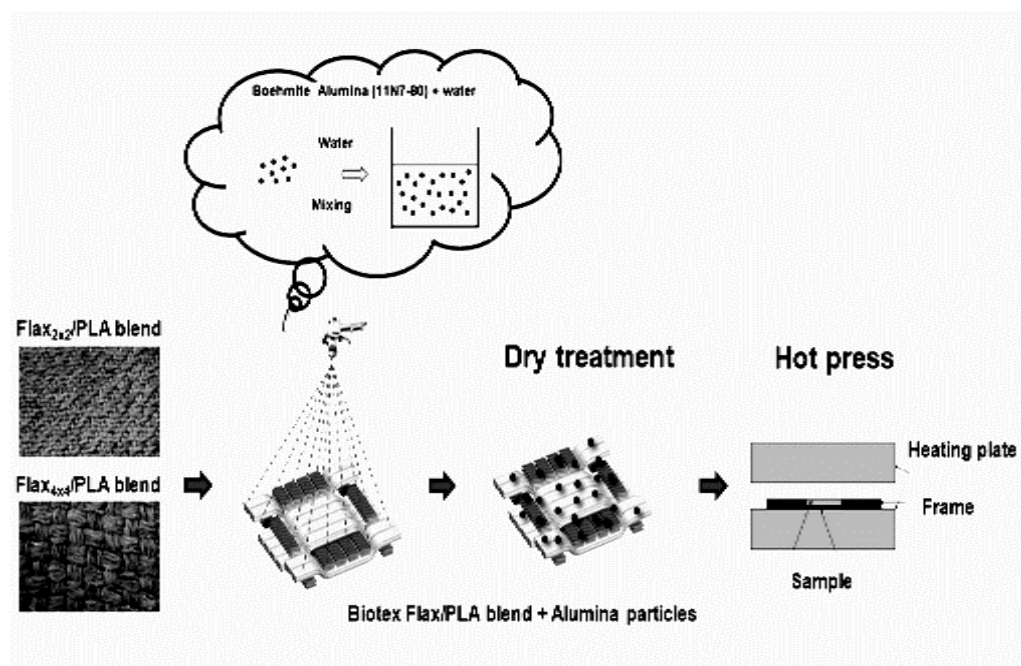


Figure 74: Scheme of the preparation of PLA/Flax blend/alumina composites via the nano-spraying method.

Table 13: Typical Properties of Biotex Flax/PLA blend as Delivered by Composites Evolution.

Density	1.33 g/cm ³
Tensile Strength	102 MPa
Tensile Elongation	1.6 %
Flexural Modulus	7.8 GPa
Flexural Strength	131 MPa
Charpy Impact (flat)	32.8 kJ/m ²

The PLA/flax/alumina composites were prepared by a hot press using nano-spraying technique. A scheme of the hand nano-spraying technique is given in figure 74. The alumina particles were dispersed in water at ambient temperature under continuous mechanical stirring for 30 minutes to obtain aqueous alumina slurry. For the alumina spray technique, the flax 40%/PLA sample was positioned on a dish and the alumina slurries were sprayed by a hand onto the both surfaces of the flax 40%/PLA sample. The distance between the sample and the nozzle was approx. 10 cm. The amount of alumina was set for 8 wt.% by weight control. After the nano-spray system, the samples were dried for 48 h at room temperature (RT) and then for 24 h at 70°C in oven. The blends

and composites, after the alumina particles spraying on the Biotex Flax40%/PLA blend and dried, were compression molded into 1-mm thick sheets under pressure of 10 MPa at $T = 210^{\circ}\text{C}$ using the hot press (P/O/Weber, Maschinen und Apparatebau, Remshalden, Germany). Although this technique is straightforward for PLA systems, the press conditions did not result in prominent thermal degradation of PLA. This claim is based on inspection of the fracture surfaces of the specimens where no burned flax/PLA was seen.

Characterization and testing

Morphology detection

The fracture surface was subjected to scanning electron microscopy (SEM) inspection in a JSM 5400 device of Jeol (Tokyo, Japan). The surface was gold coated prior to SEM inspection performed at low acceleration voltage.

Water absorption

Water absorption of the composites was investigated over a period of 30 days. The composites were cut into specimens (20x20 mm²) and then, they were immersed in water in a bath at room temperature. Weight gains were recorded by periodic removal of the specimens from the water bath and weighing on a balance. The percentage gain at any time t (M_t) as a result of moisture absorption was calculated from the following equation:

$$M_t = \frac{W_w - W_d}{W_w} \cdot 100\% \quad (38)$$

where W_d and W_w denote the weight of dry material (initial weight of materials) and weight of materials after exposure to water absorption, respectively.

Impact response

The impact resistance was determined on notched Charpy test specimens according to EN ISO 179-1 and using a universal testing machine with a single swing of a pendulum energy of 25 J. Five specimens were tested and at least three replicate specimens were presented as an average of tested specimens. The Charpy impact strength of notched specimens, a_{cN} , was calculated with the following equation:

$$a_{cN} = w \times 10^3 / h \times b_N \quad (39)$$

where; w is the corrected energy absorbed by the specimen in joules, h is the thickness of the test specimen in millimeters, b_N is the remaining width at the notch base of the test specimen in millimeters.

Creep response

Short time creep test was made in tensile mode at different temperatures using the above DMA apparatus. The applied stress was 3 MPa. The temperature dependence of the creep response of the composites was studied in the range from 15 to 50°C. Isothermal tests were run on the same specimen in the above temperature range by increasing the temperature stepwise by 5°C and equilibrating the specimen at each temperature for 2 min. During the isothermal tests the duration of the creep testing was 15 min.

Thermal and thermomechanical response

Thermogravimetric analysis (TGA) was performed on a DTG-60 SHIMADAZU device (Kyoto, Japan). TGA experiments were conducted in the temperature range from 30 to 500 °C under nitrogen at a heating rate of 10 °C/min.

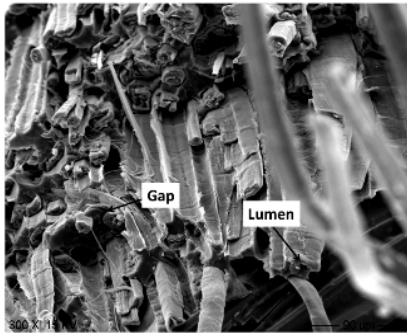
Dynamic mechanical thermal analysis (DMTA) was performed in tensile mode at frequencies of 0.1, 1 10 Hz at all isothermal temperatures, using a DMA Q800 apparatus (TA Instruments, New Castle, NJ). The storage modulus (E') was determined as a function of the temperature ($T = -100^\circ\text{C} \dots +130^\circ\text{C}$). The strain applied was 0.1%. The specimens were cooled to -100 °C. The temperature was allowed to stabilize and then increased by 5 °C, kept 2 min isothermal until 130 °C.

Result and discussion

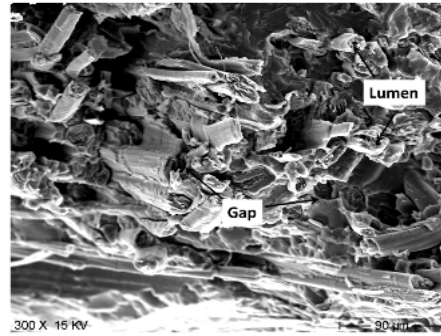
Morphology

The SEM pictures in figures 75a-d present the morphological characteristics of the PLA-based systems studied. SEM taken from the fracture surfaces revealed slight differences in the morphology of the PLA – based systems depending on their composite structures (cf. Figures 75a-75b). It can be seen that the flax had diameter in the range of 15-25 μm and displayed fiber lumina in the cross section. The small gap can be related to an insufficient flax-PLA adhesion due to the kinetic wetting and moisture of flax. SEM pictures taken from the PLA/flax2x2/alumina composites are shown in figures 75c-d. It can be observed that the alumina particles were homogeneously distributed in the related composites. On the other hand, the alumina particles were still partly aggregated in the flax and flax/PLA interphase (cf. Figure 75d). The reason for this aggregation was due to some reordering of the alumina particles during the drying treatment, when combining alumina particles with the water from the alumina slurries. It could be shown that the alumina particles were relocated. This finding is in agreement with the experimental results achieved mostly on the clay modified natural rubber and polystyrene lattices [70, 118].

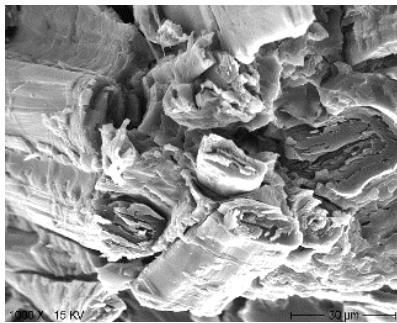
a)



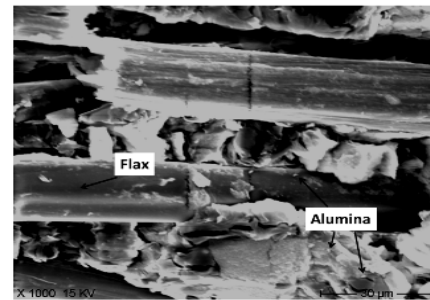
b)



c)



d)



e)

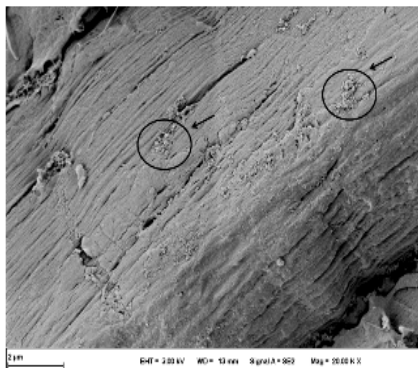


Figure 75: SEM pictures taken from PLA/flax2x2 blend a), PLA/flax4x4 blend b), PLA/flax2x2blend c) –x1000, PLA/flax2x2blend/alumina composite d) –x1000 and e) –x20000.

Water absorption

Figure 76 depicts the water uptake as a function of time for the PLA, PLA/Flax blends, and PLA/flax/alumina composites. The PLA/flax/alumina composite specimens after exposure to water absorption were more translucent than those of the initial PLA/flax blend and neat PLA (cf. Figure 76). This was the first hint for an effect of the alumina reinforcement in the corresponding composites. It can be seen that the water uptake of PLA was about 0.8% after subjected to water absorption for 30 days. The low water uptake occurs in PLA was attributed to the nature of the polymer which showed weak interaction with water. One can also recognize that the rapid water uptake was observed for all of the blends and composites within the first 3 days of immersion. Flax reinforcement in PLA matrix increased the penetration of water in blends. Note that the water absorption behavior was slightly considered to depend on the flax composite structures. However, the incorporation of alumina particles in the PLA/flax blends reduced the water uptake. The PLA/flax_{4x4}/alumina composite specimen recorded water absorption value at 10.23% upon 30 days. This water uptake was reduced by approx. 30% compared to the PLA/flax blend. Leu et al. indicated also that the incorporation of organomontmorillonite (OMMT) in to PLA matrix decreased the rate of diffusion [119]. Other authors reported that the water uptake of epoxy resin was decreased by adding organoclay particles. Major reason the reducing water uptake is that the nanoclay surface can be reacted with water molecules which decreased the diffusion process during immersion [83-84].

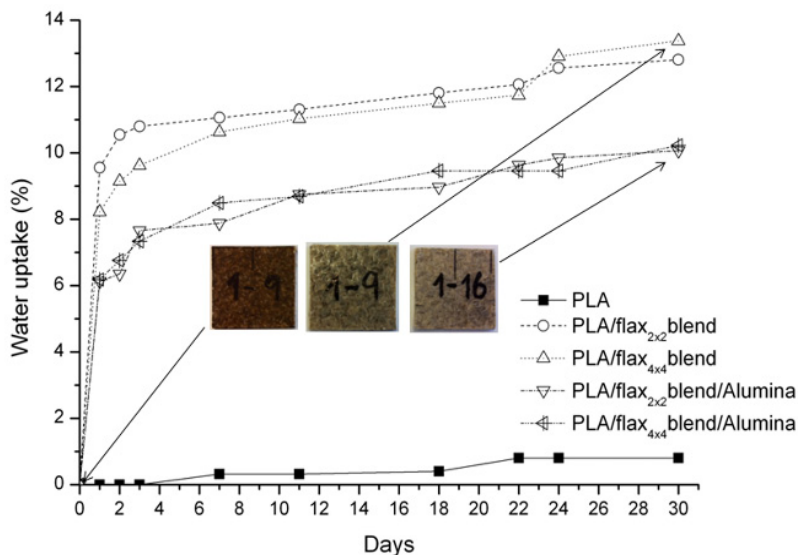


Figure 76: Water uptake of the PLA, PLA/flax blends and PLA/flax/alumina composites.

Impact weight test

The effect of the woven flax and alumina reinforcement in PLA on the force versus time curves is demonstrated on the PLA studies systems in figure 77. With addition of the woven flax fiber textiles in PLA was accompanied with a shift of the force peak toward higher force and longer time. This already suggests that the woven flax fiber textiles worked as major energy absorption mechanism. The presence of alumina particles was associated with a reduction in the maximum force peak. This alumina reinforcing in the PLA/flax matrix, induced a void formation via debonding events and acted a localized crack growth accompanied with reduced ductility. This finding was in analogy with reported for a HNBR-Toughened polyamide 6 composite containing sodium fluorohectorite (FH) and alumina nanoparticles [92]. It is clear that the weave style of flax was also a critical factor of the reinforcing phase in the composites. The impact energy was enhanced markedly with the reinforcing flax 4x4 compared to the flax 2x2. One can notice for the largest change of fracture toughness (fracture time) occurred between the PLA/flax2x2 and PLA/flax4x4 blends due to the high fiber undulation of the composite structures (weave style 2x2). However the fracture toughness still increased in the fiber weave style of 4x4. According to the reported by Paessler et al. [52] that clear differences regarding mechanical properties of the laminates without and with undulations could be observed for carbon fiber/epoxy composite. The effects of fiber waviness due to the fiber crossing such as warp and weft crossover points, lead to a reduction of the in-plane properties of such a laminate. [38, 52].

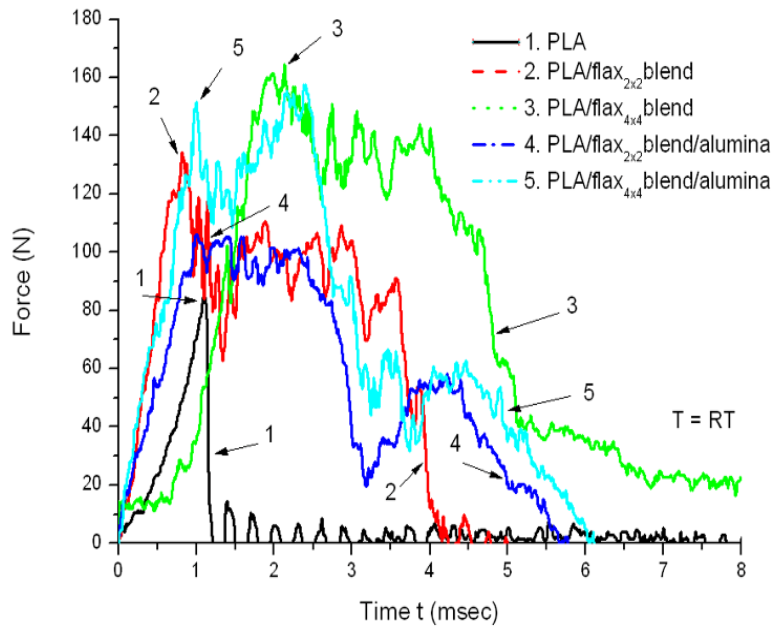
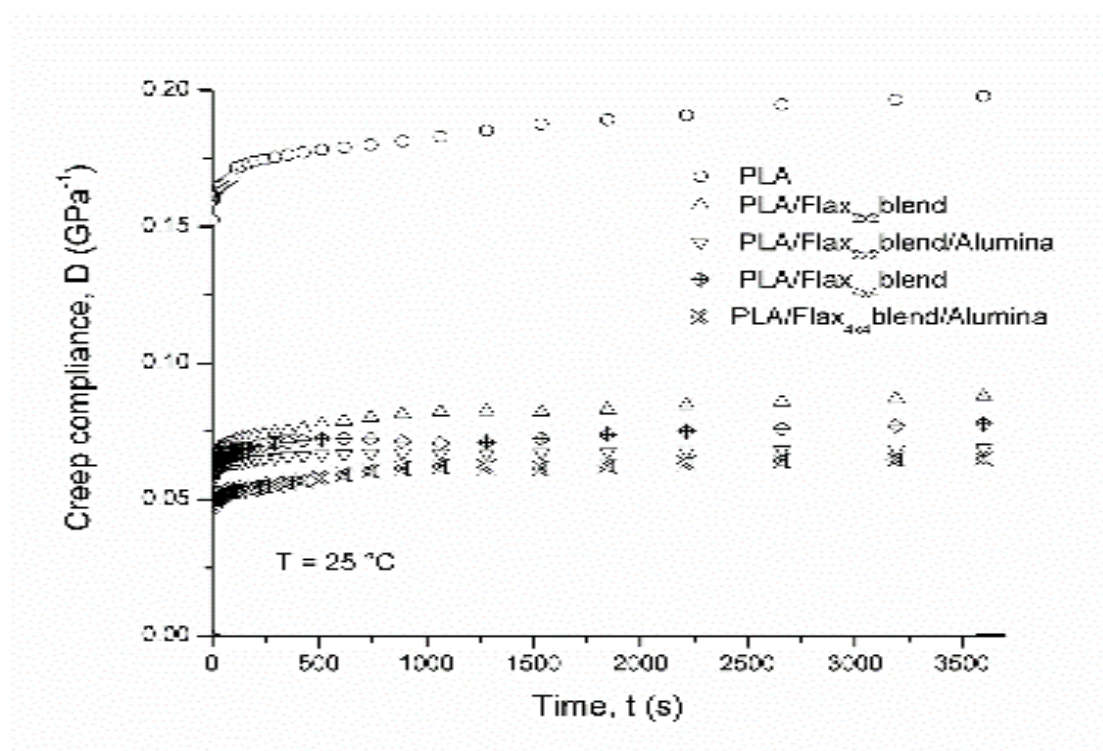


Figure 77: Representative force vs. time curves for PLA, PLA/flax blends and PLA/flax/alumina composites.

Creep response

Figures 78a-b display the traces of the creep and recovered compliance as a function of time for the PLA, PLA/flax blends, and the alumina-containing composites at $T = 25^{\circ}\text{C}$, respectively. As expected owing to this woven flax fiber reinforcement, the creep and recovered compliance resistance of the PLA/flax blends increased markedly compared to the PLA. For example, the compliance values of the PLA/flax2x2 and PLA/flax4x4 blends were reduced by approx. 225 and 290%, respectively, showing the reinforcing effect of the flax structures. The addition of alumina particles into PLA/flax matrix resulted in a decrease slightly in the creep and recovered compliance.

a)



b)

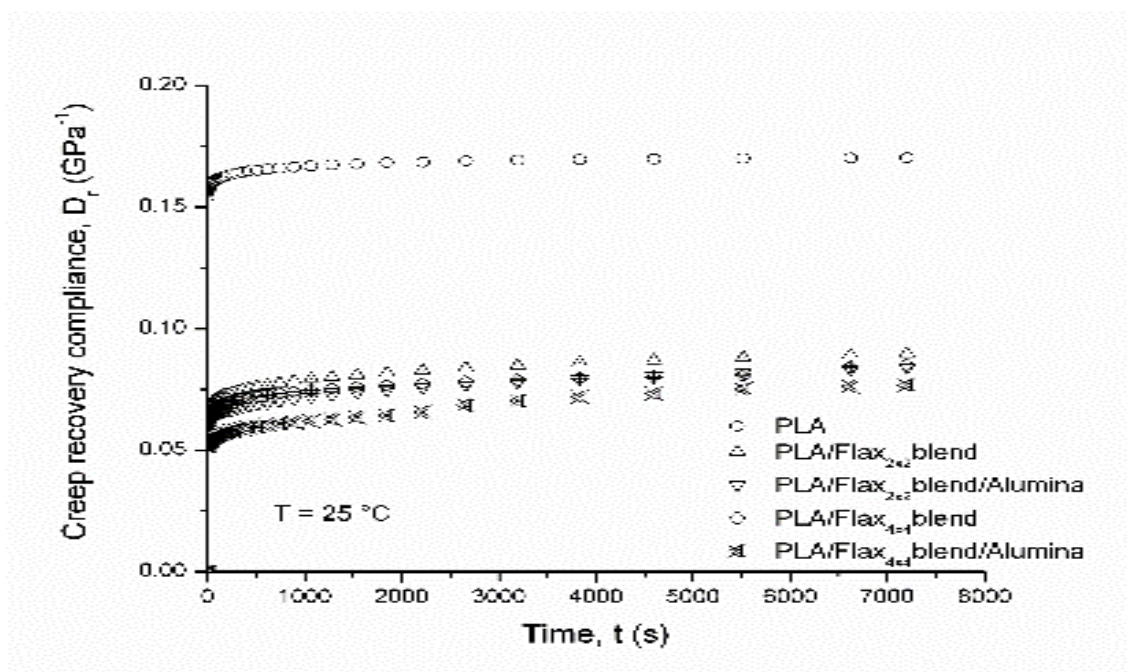
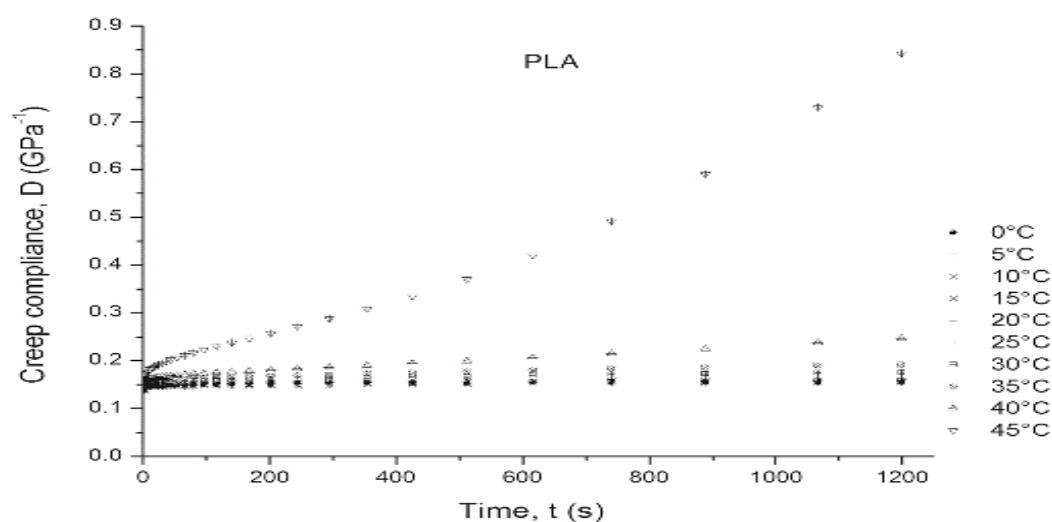


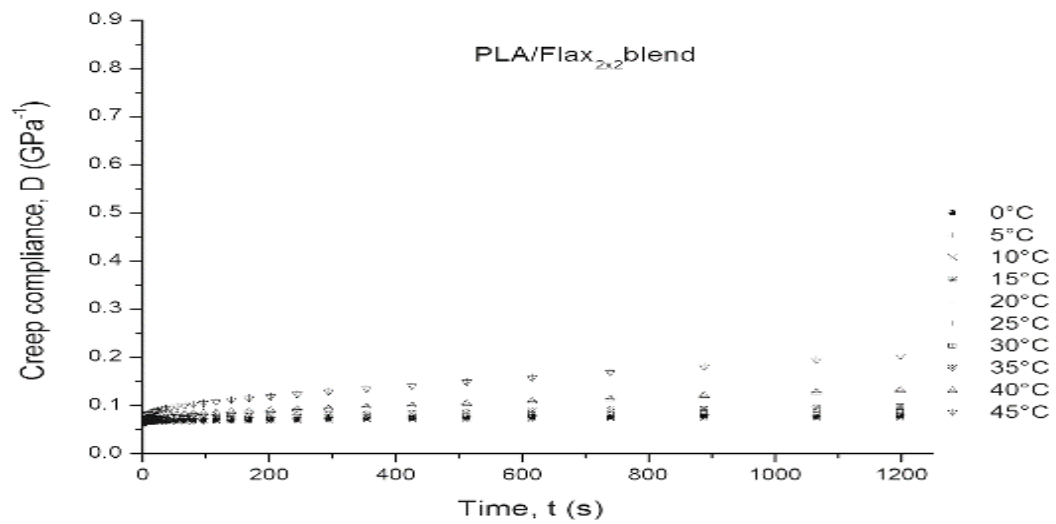
Figure 78: Creep a) and creep recovery compliance b) of the PLA, PLA/flax blends and PLA/flax/alumina composites at $T=25\text{ °C}$.

Generally, creep compliance depends on the polymer composite structure and test temperature. Figures 79a-c, demonstrate the effects of increased temperature on the creep response of PLA, PLA/ flax2x2 blend and PLA/ flax2x2/alumina composite. It is interesting to note that the PLA and composites indicated a relative small creep in the low temperature range of 0-35°C. This is probably due to the fact that the amorphous molecular structure of PLA was difficultly susceptible to untangle and slip the polymer chains. Similar for crystalline structure of PLA still had a stronger and denser bond. This effect was strongly suppressed in the alumina-containing system due to decrease the mobility of the amorphous segments. Note that the high level of PLA crystallinity and PLA based systems [31], strong constraining effects of the limited amorphous regions between the crystals are also expected to occur. Observations of the testing temperature higher than 35°C clearly indicated increase the creep resistance of PLA/flax2x2 blend as a result of decreased polymer–flax interfacial strengths. It is notice that the creep resistance increased remarkably with the incorporation of alumina particles and flax compared to the PLA at the whole test temperature. The reduction of creep compliance can be explained by considering the delay of a crystalline rotation and amorphous separation mechanisms due to the increment of restrict with fibrous and alumina reinforcements. This is in qualitative agreement with the DMA results of figure 82.

a)



b)



c)

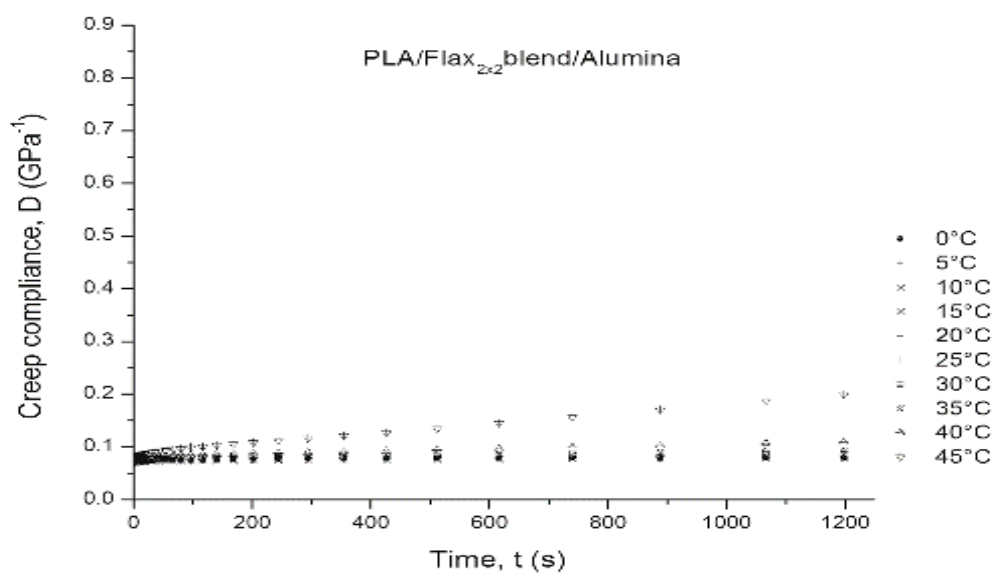


Figure 79: Effect of temperature on the creep compliance of the PLA a) PLA/flax2x2 blend b) and PLA/flax2x2/alumina composite c).

From the creep master curves, the creep compliances of PLA, PLA/flax2x2 blend and PLA/ flax2x2/alumina composite were measured at different temperatures and shifted according to the following the time-temperature superposition (TTS) principle. The related shift factor (aT) used for the generation of the creep master curve is $aT = D(t,$

$T)/(D(t, T_{ref}))$. A reference temperature ($T_{ref} = 5^{\circ}\text{C}$) was used for this superposition (shifting) process. The shift factors were determined for each curve using the related software package of the DMA device (Rheology Advantage Data Analysis). Accordingly, for the time dependency of the creep compliance master curves we have adapted the Findley power law equation in Ref. [120]:

$$D_F = D_{F0} + D_{F1} * t^n \quad (40)$$

Where n is a stress independent constant, D_{F0} is the time-independent compliance, and D_{F1} is the coefficient of the time-dependent term.

Master curves of the creep compliance against time created at a reference temperature of 5°C are shown in figure 80 for the PLA, PLA/flax2x2 blend and PLA/flax2x2/alumina composite. Note that the creep compliance master curve provided a useful prediction of the creep over time for all systems up to approx. 1.25×10^7 h. For the resulting creep compliance vs. time master curves, the Findley power law was adapted. The related curves showed a good agreement between the experimental and the simulated results, according to the Findley power law. However, the power law model may show considerable deviation from the initial experimental result of PLA while for longer time duration the calculated data provided a prediction of good fits within the initial and steady state creep of the PLA/flax2x2 blend and PLA/flax2x2/alumina composite.

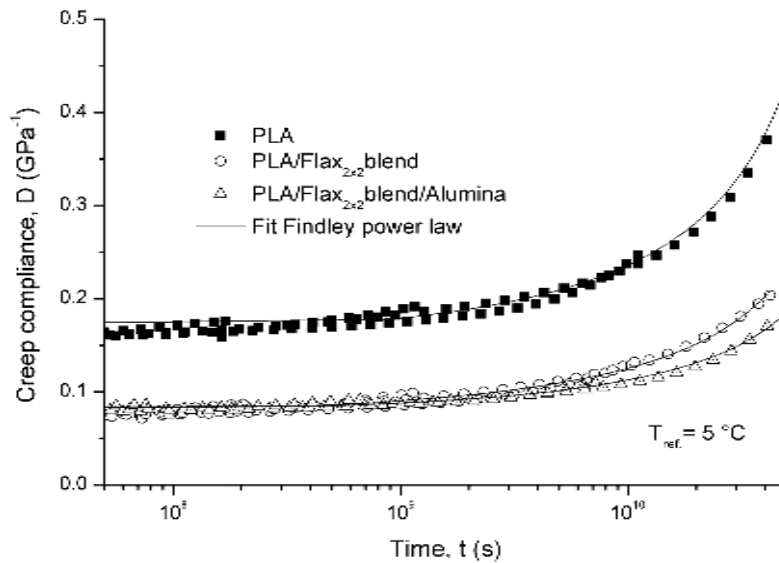


Figure 80: Creep master curves (compliance vs. time) constructed by considering the TTS and selecting $T_{ref} = 5^{\circ}\text{C}$ and their fitting by the Findley power law equation.

Thermogravimetric analysis

Thermal stability is critical for a composite material in many applications. Thermal degradation of composites is a cumulative phenomenon of matrix and nanoparticles and may increase the thermal stability of a matrix. Figure 80 shows the traces of the actual weight loss as a function of temperature for the PLA, PLA/flax blends and PLA/flax/alumina composites. One can see that the thermal degradation of all PLA exhibited a step-like transition from low to high temperatures. Reinforcements with flax reduce the onset of thermal degradation compared to the pure PLA. However, incorporation of alumina particles enhanced the thermal resistance of the PLA/Flax blend. The actual weight loss of the PLA/flax/alumina composites (32%) as reaching 370°C, was beyond that of the PLA/flax blends (16%). Note that the effect of flax reinforcing structures on the TGA value was marginal.

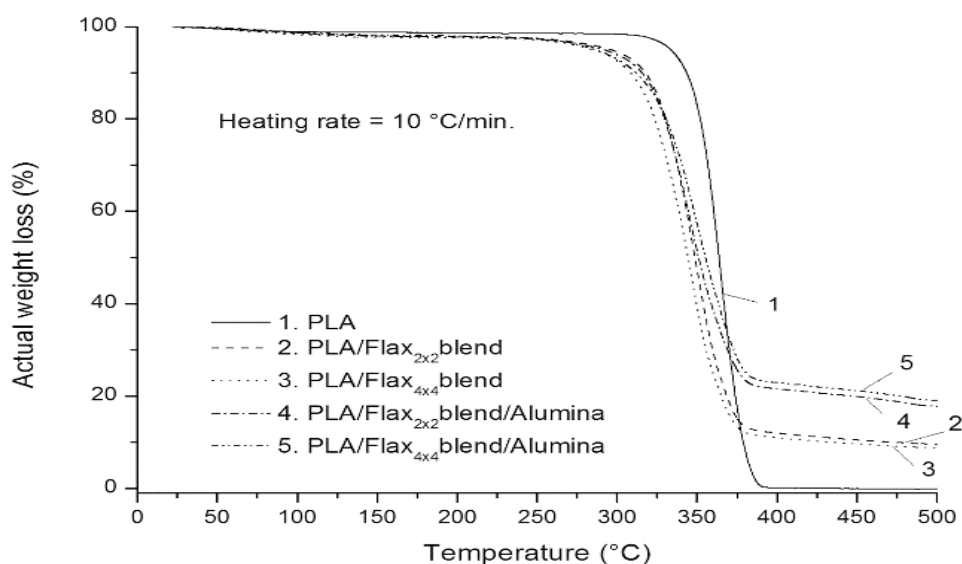


Figure 81: Actual weight loss versus temperature for the PLA, PLA/flax blends and PLA/flax/alumina composites.

Dynamic mechanical response

DMTA spectra in form of storage modulus (E') and loss factor ($\tan \delta$) as function of temperature are demonstrated in figure 82. It can be seen in this figure that the blends with 40 vol.% of flax_{2x2} and flax_{4x4} exhibited higher stiffness than the PLA. For example, the storage modulus of PLA/flax_{4x4} blend was increased by approx. 100% compared to the neat PLA. It can be observed that the E' of PLA and PLA/flax blends below the glass transition temperature (T_g) was almost constant and increased slightly above 100°C,

due to the cold crystallization of the amorphous PLA. This cold crystallization phenomenon was typical of PLA. A similar trend has been reported for the micro- and nanofibrillated cellulose-reinforced PLA composites [31, 115]. It is interesting to note that the stiffness values of the PLA/flax_{4x4} blend were markedly higher than that of the PLA/flax_{2x2} blend in the whole temperature range. This is due to the composites character of flax weave style 4x4. However, the incorporation of alumina particles resulted in increase in the storage modulus at least below T_g of PLA, compared to that of the PLA/flax blends. This indicated the reinforcing effect of the nanoparticles leading to increased stiffness. The plots of $\tan \delta$ vs. T in figure 82 reveal the T_g of PLA at approx. 60°C. Filling with flax and alumina particles was accompanied with a shift in the T_g of PLA towards higher temperature. This can be confirmed to the effects of the fibrous and alumina reinforcement with reduced molecular chain mobility.

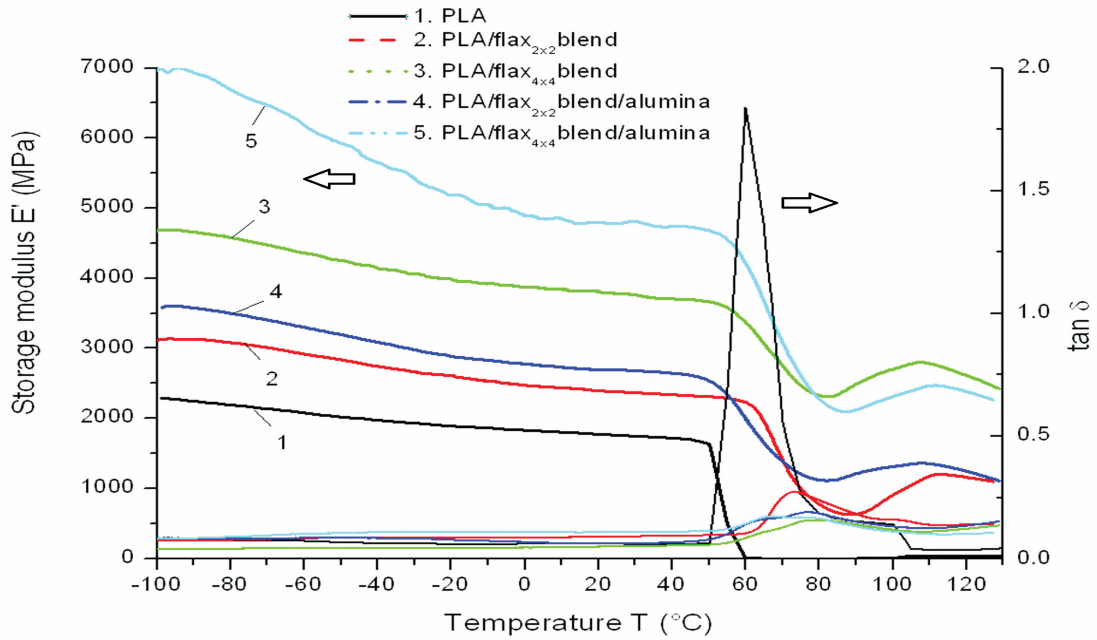


Figure 82: E' and $\tan \delta$ vs. T traces for the PLA, PLA/flax blends and PLA/flax/alumina composites.

In order to obtain a deeper insight into interfacial adhesion effect of the flax and alumina reinforced PLA systems on the temperature, the applicability of the conversion method from the modulus to the creep compliance based on the correspondence principle of a linear viscoelastic material [33], has been investigated. Creep compliance is defined as the inverse quantity of modulus by the following equation:

$$D' - iD'' = \frac{1}{E' + iE''} = \frac{E'}{(E')^2 + (E'')^2} - i \frac{E''}{(E')^2 + (E'')^2} \quad (41)$$

where D' and E' are the real, and D'' , E'' are the imaginary parts of creep compliance and modulus, respectively.

The following relationship between storage creep compliance and the modulus is given by:

$$D' = \frac{E'}{(E')^2 + (E'')^2} \quad (42)$$

The storage creep compliance as a function of temperature for PLA, PLA/flax2x2 blend and PLA/flax2x2/alumina composite are depicted in figure 83. The reinforcing effect of flax and alumina particles, which reduced the creep compliance, was obvious in this figure. Recall, the increase of the creep resistance was because of the development of an interphase between PLA–flax and PLA–alumina in which the molecular mobility was reduced. DMTA spectra indicated that T_g of the PLA affected by the flax and alumina particles. The related change in T_g maybe traced to the limited interphase formation with reduced molecular mobility.

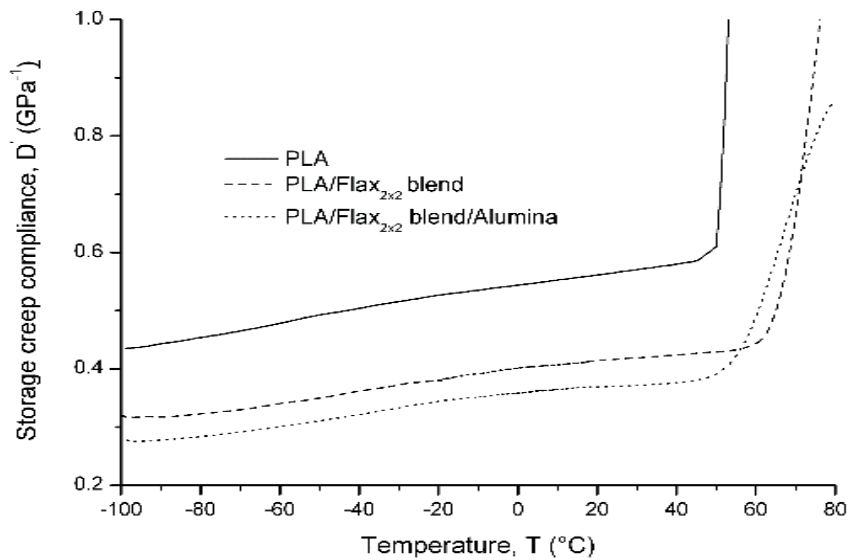


Figure 83: Conversion from the modulus to creep compliance for the PLA, PLA/flax2x2 blend and PLA/flax2x2/alumina composite.

Conclusion

In this work we have examined the effect of composite structures, viz. flax2x2 twill and flax4x4 hopsack, in a PLA/flax/alumina nanocomposites. The alumina particles were introduced via a nanospraying technique. The morphology, water absorption, impact, creep, thermal and mechanical properties of the PLA-based systems were studied. The diameter range of flax filaments was in between 15 and 25 μm and displayed fiber lumina. The alumina particles were homogeneously distributed but still partly aggregation dispersed in the composites according to SEM investigations. Flax reinforcement in PLA matrix increased the water uptake. Incorporation of alumina particles decreased the water uptake compared to the flax composites. The impact energy and stiffness value of PLA/flax blends was markedly higher than that of PLA. However, the impact results reflected the effects of composite structures. The presence of alumina particles was associated with a reduction in the maximum force peak of impact test. Incorporation of alumina particles enhanced storage modulus and the creep resistance compared to the PLA/flax blends but slightly incremented thermal resistance. Clear trend in the effect of composite structures was found in the stiffness but not in the thermal behaviour. The creep master curves could be well described by the Findley power law model. Moreover, the applicability of the conversion method from the modulus to the creep compliance could describe the development of an interfacial adhesion of the flax and alumina reinforced PLA systems in function of temperature. A benefit of this proposed nano-spraying technique is a very effective process being simple and cost efficient for producing multi-phase hybrid biocomposites.

4.5 Poly(hydroxybutyrate-co-hydroxyvalerate)/sisal natural fiber/clay composites

State of the Art

Nowadays, the polymers from renewable resources such as Poly(hydroxybutyrate-co-hydroxyvalerate)(PHBV) and polylactide (PLA) are gaining ground over conventional petroleum based matrices. Among the various available PHBVs and PLAs have potential to be used in bio-base polymer composites [53, 109, 121] because of environmental problems related to their disposal as well as concerns over petroleum availability for the productions of e.g. polypropylene, polyethylene. Note that PHBV is a Polyhydroxyalkanoates (PHAs) family widely used in the potential applications in food packaging and biomedical, due to its good biocompatibility, biodegradability, however the widespread

application was limited due to its narrow processing window and poor mechanical properties [122-123]. Natural fibers have been receiving considerable attention as substitutes for synthetic fiber reinforcement. The addition of natural fiber reinforcement can dramatically improve selected properties of the related biopolymers [64, 109]. Džalto J. et al. [64] reported for the green composites that the mechanical performance of furan biopolymer was enhanced by flax fiber textiles reinforced the furan matrix. In the recent years, PHBV is often reinforced with the natural fibers, such as cellulose, abaca kenaf and bamboo to improve the mechanical properties (e.g. impact, stiffness and strength properties). Sanjeev et al. [124] reported on achieving the biocomposites with superior properties by combining the PHBV/Bamboo fiber. The results showed that the bamboo fiber reinforced PHBV composites was able to improve tensile properties of PHBV. The stiffness of PHBV composites at 40 wt.% of bamboo fiber enhanced by 175% compared with neat PHBV. The significantly improved properties were attributed to the length and distribution of bamboo fibers. Qian [125] demonstrated the improved mechanical properties of PHBV/Bamboo pulp fiber (BPF) using a surface modification of fibers of the polymeric diphenylmethane diisocyanate (pMDI) as a coupling agent and the grafted maleic anhydride (MA) as a compatibilizer. Both pMDI and MA can be improved the interfacial adhesion between BPF and PHBV. The results of related PHBV/BPF composites showed that the tensile, flexural and modulus increased substantially.

Currently most studies on natural fibers as reinforcement and the development of hybrid composites with particular regard to its different applications are concerned on the fundamental understanding of their mechanical and barrier behavior [55]. Recently, Siengchin et al. was pointed out that flax reinforcements of different composite structures may play a role as a controlling factor to optimize the mechanical properties of the hybrid PP and HDPE composites [126]. Furthermore, nanofillers such as carbon nanotubes, silica, layered silicate and clay have attracted great attention in the past decades for the production of composites based on engineered and bio-polymers [127-129].

The goal of this work was to demonstrate the feasibility of the fabrication of PHBV reinforced with unmodified and modified sisal fiber using hot compression technique. Note that sisal is a plant which can generate revenue from production to farmers in Thailand. Issue such fibers of sisal will be left to waste or are used with low economic values. This is important to increase the value of sisal output. This project is therefore to introduce the concept of short and long fiber sisal reinforced PHBV polymer. A further aim of this work was to check the effect of the fiber size and clay particles on the impact and mechanical properties of hybrid composites. The dispersion of sisal fiber in PHBV was assessed by optical microscope and scanning electron microscopy (SEM).

Materials and preparation of composites

PHBV in a fine powder form was provided by Ningbo Tianan Biologic Material Co.,Ltd. and was used as polymeric matrix for all composite systems. Its melt flow index (MFI) of PHBV was 4.35 g/10 min (190°C, 2.16 kg). The density was 1.25 g/cm³ and the glass transition (T_g) was 5°C. The sisal fibers were supplied by Hupkapong Agricultural Co-operative Ltd. Silane (Bis(triethoxysilylpropyl)tetrasulfide) was purchased from local commercial sources. Nanoclay was supplied by Polymer Innovation Co.,Ltd.

Prior to treatment, the untreated sisal fibers were washed with water the fibers were dried in an oven at 60°C for 2 h. A solution of 3 vol.% of silane coupling agent (Bis(triethoxysilylpropyl)tetrasulfide) was prepared in acetone. Sisal fibers were immersed in the solution for 24h. The treatment of sisal fibers were removed from the solution and dried in oven at 60°C for 24h.

Prior to the composites processing, the fibers were cut into the length of 5 mm (long fiber - l) and 0.25 mm (short fiber - s). Note that the diameter of sisal fiber was in the range of 200-400 µm. To avoid moisture, the PHBV and sisal fiber were dried at 80°C and 60°C for 24h and 6 h, respectively. The PHBV/sisal fiber/clay composites were mixed by tumbling in a sealed bag and then mixing occurred in a hot compression molded at 180°C into 3mm thick plates under a pressure of 2500 psi. The duration of compression molding was 10 min. The recipe of composites was listed in Table 14. Note that the proposed of using PHBV powder and continue with hot press technique is an effective process being simple and cost efficient for producing thermoplastic hybrid composites.

Table 14: Recipe and designation of the biocomposites systems.

Materials	Matrix (wt.%)	Sisal fibers (wt.%)		Silane (vol.%)	Clay (wt.%)
		0.25mm (S)	5mm (L)		
PHBV	100	-	-	-	-
PHBV/sisal (S/L)	95	5	5	-	-
PHBV/sisal (S/L)	90	10	10	-	-
PHBV/sisal (S/L)	80	20	20	-	-
PHBV/sisal (S/L)	70	30	30	-	-
PHBV/treated sisal (S/L)	80	20	20	3	-
PHBV/clay	95	-	-	-	5
PHBV/sisal/clay (S/L)	75	20	20	-	5
PHBV/treated sisal/clay (S/L)	75	20	20	3	5

Characterization and testing

Morphology detection

The fracture surface was subjected to scanning electron microscopy (SEM) inspection in a JSM 5400 device of Jeol (Tokyo, Japan). The surface was gold coated prior to SEM inspection performed at low acceleration voltage.

Tensile response

Tensile test was performed on dumbbell-shaped specimens (DIN-ISO-527) on a Zwick 1474 (Ulm, Germany) universal testing machine. Tests were run at room temperature at $v=2$ mm/min crosshead speed and the related stress-strain curves were registered.

Water absorption

Water absorption of the composites was investigated over a period of 30 days. The composites were cut into specimens (20x20 mm²) and then, they were immersed in water in a bath at room temperature. Weight gains were recorded by periodic removal of the specimens from the water bath and weighing on a balance. The percentage gain at any time t (M_t) as a result of moisture absorption was calculated from the following equation:

$$M_t = \frac{W_w - W_d}{W_w} \cdot 100\% \quad (43)$$

where W_d and W_w denote the weight of dry material (initial weight of materials) and weight of materials after exposure to water absorption, respectively.

Impact response

The impact resistance was determined on notched Charpy test specimens according to EN ISO 179-1 and using a universal testing machine with a single swing of a pendulum energy of 25 J. Five specimens were tested and at least three replicate specimens were presented as an average of tested specimens. The Charpy impact strength of notched specimens, a_{cN} , was calculated with the following equation:

$$a_{cN} = w \times 10^3 / h \times b_N \quad (44)$$

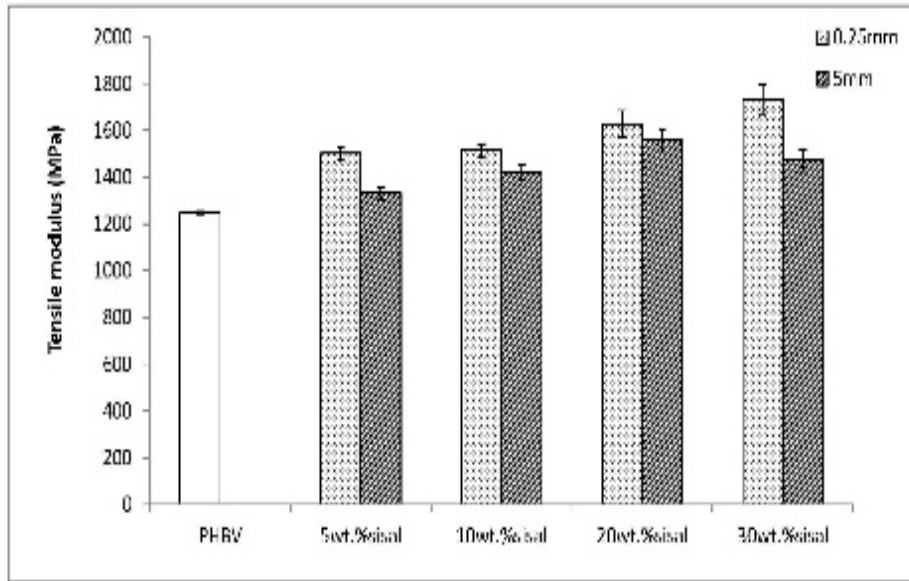
where; w is the corrected energy absorbed by the specimen in joules, h is the thickness of the test specimen in millimeters, b_N is the remaining width at the notch base of the test specimen in millimeters.

Results and discussion

Tensile response

The tensile modulus and tensile strength data of PHBV composites containing sisal fibers are showed in figures 84a and 84b, respectively. One can recognize that the tensile modulus of the PHBV composites can be improved with sisal fiber loading. For example, incorporation of 10 wt.% of short and long sisal fiber in PHBV matrix, the stiffness increased by 21% and 14% respectively. Especially, at 20 wt.% of short and long sisal fiber loading increased up to 30% and 25% respectively, compared to the neat PHBV. A possible explanation of the increased the stiffness of composites can be ascribed to dispersion of sisal fibers in the PHBV matrix, which lead to the distribution and transfer of stress from matrix to fiber. One can clearly recognize that the short sisal fiber reinforced PHBV composites provided higher modulus compared to the long sisal fiber/composites. According to the reported by Sanjeev et al. that the tensile properties of natural fiber/PHBV composites influenced on different factors such as length, distribution, orientation of fibers and their interfacial bond strength with matrix [125]. Considering the fact that the thickness of tensile specimen itself contained lower than the length of long sisal fiber. The reduction of modulus can be assigned to some reordering of the long fiber reinforcement during hot pressing. This suggestion is in accord with experimental results achieved mostly on the fiber orientations. Note that the dispersion stage of short fiber reinforcement was better occurred. Whereas, the tensile strength of PHBV composites decreased with addition of sisal fiber (cf. figure 84b). This can be attributed to the related of fiber contents and the poor adhesion between sisal fiber which lead to low transferred stress from the matrix to the stronger fibers. Moreover, agglomeration of high fiber content leads to a decrease in composite strength due to PHBV matrix cracking.

a)



b)

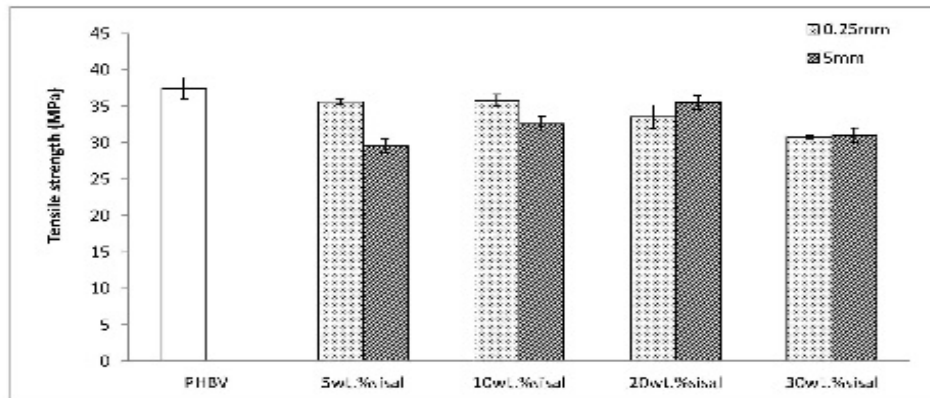
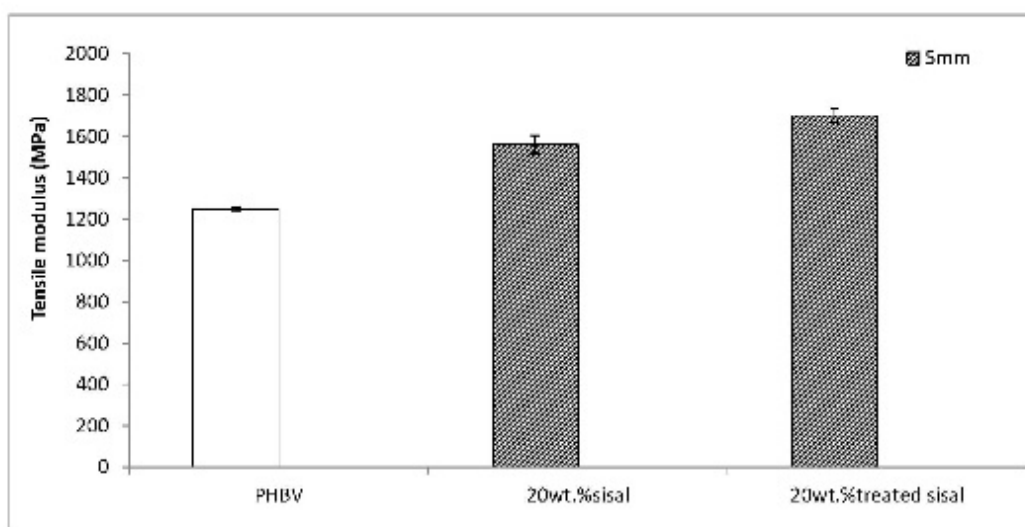


Figure 84: Effect of sisal fiber contents on tensile modulus a) and tensile strength b).

It has been reported that by adding silane may improve an interfacial interaction of natural fiber polymer composites [130]. This is in accordance with our tensile test observation of PHBV/sisal composites as shown in figures 85a and 85b, the addition of 20 wt.% of silane treated sisal increased the tensile stiffness and tensile strength of PHBV composites by 10% and 5% respectively, compared to untreated one. This could be attributed to good adhesion between treated fiber and PHBV (cf. figure 97). Note that the mobility of PHBV molecule chains may be restrained by the silane.

a)



b)

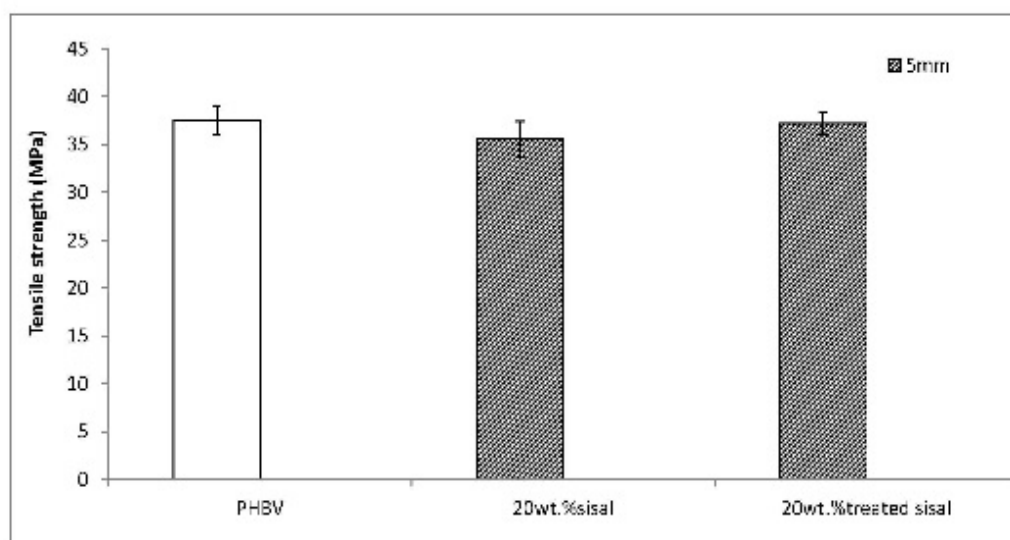
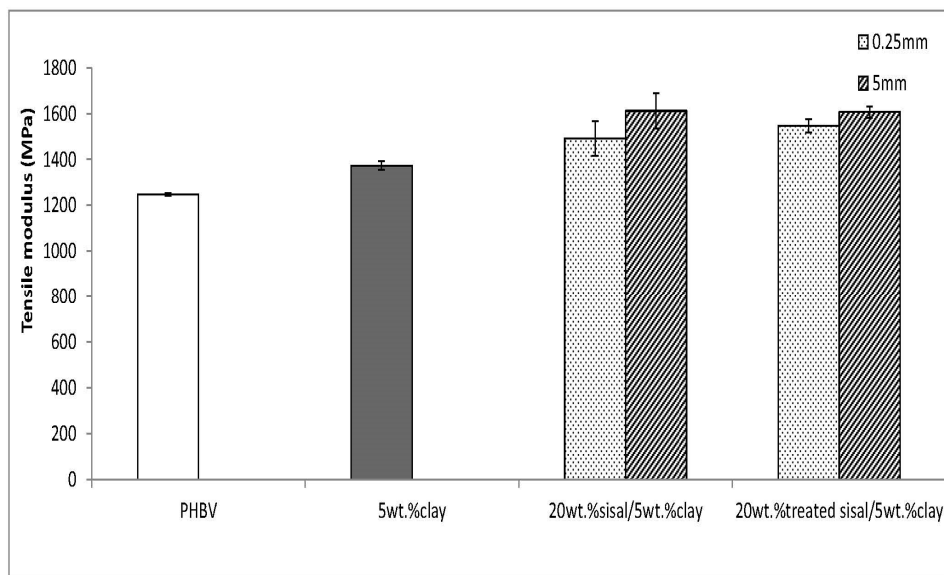


Figure 85: Effect of silane on tensile modulus a) and tensile strength b).

Tensile modulus and tensile strength data of PHBV composites and hybrid with addition of clay particles are showed in figures 86a and 86b. Tensile modulus of PHBV/sisal/clay hybrid composites of short and long fiber increased 20% and 30% respectively, compared to the neat PHBV. An additional of clay particles was reduced in tensile stiffness and strength compared to the PHBV/20 wt.% of short and long sisal fiber composites. A decrease of tensile modulus can be attribute to the incomplete dispersion of clay agglomerate into the PHVB matrix. However, the effect of silane treatment indicated slightly an increase in tensile modulus of PHBV/sisal/clay hybrid composites.

a)



b)

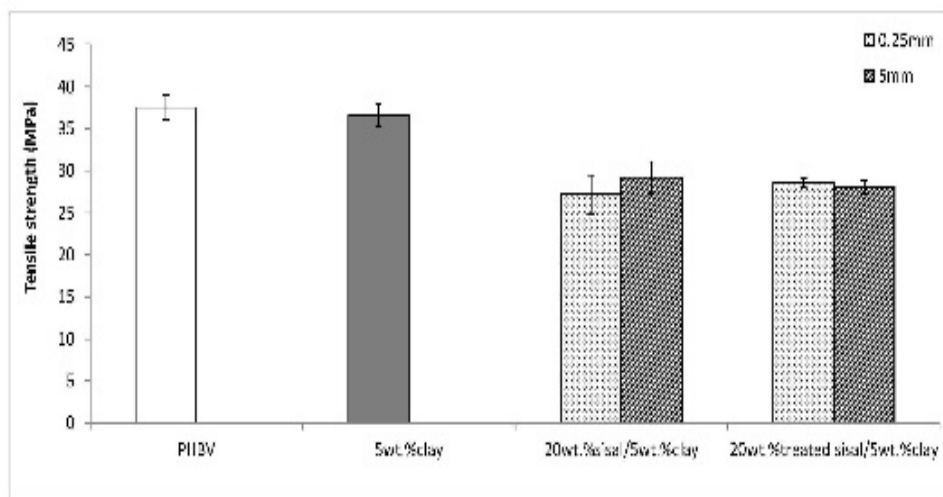


Figure 86: Tensile modulus a) and tensile strength b) of sisal fiber/PHBV and hybrid composites.

Impact strength

Generally, the notched Izod impact strength test can be measured the energy to propagate existing crack which depends on various factors like morphology, fiber-matrix adhesion, toughness and defects, in the packing of polymer composites. The impact strength of short and long sisal fiber reinforced PHBV composites as a function of fiber content and silane is demonstrated in figure 87. One can see that impact strength of all PHBV composites increased with increasing sisal fiber content. Note that fiber content increased an interface on the crack path and high energy was consumed. Impact strength of short sisal fiber/PHBV composites increased steadily with fiber loading. For PHBV composite containing 30 wt.% sisal fiber, the impact strength improved by 36% compared to the neat PHBV. The most interesting result is that impact strength of PPHBV composites was strongly affected by the long fiber of sisal and increased dramatically. As expected, the sisal fiber reinforcement leads to increased stiffness and impact strength. It is usually accepted that the fiber length domains first cavitate provoking locally a stress transition in impact mechanical terms. This supports the development of fiber length entanglement and superimposed the stretching of the amorphous and entangled chains occurs with considerable all increasing the impact strength. Due the stress concentration effects of fiber agglomerates which cannot be released by matrix-related events owing to inhomogeneous fiber dispersion. Stress concentration induces fiber/matrix debonding, causing the tensile strength. For example, at 30 wt.% long sisal fiber reinforced PHBV improved up to 800% compared to the neat PHBV. However, addition of silane did not significantly an increase in impact strength at all composites (cf. fig. 86). Furthermore, impact strength data of PHBV composites and hybrid composites with addition of clay particles are shown in figure 88. The effect of clay particles dispersion on the impact strength value was marginal.

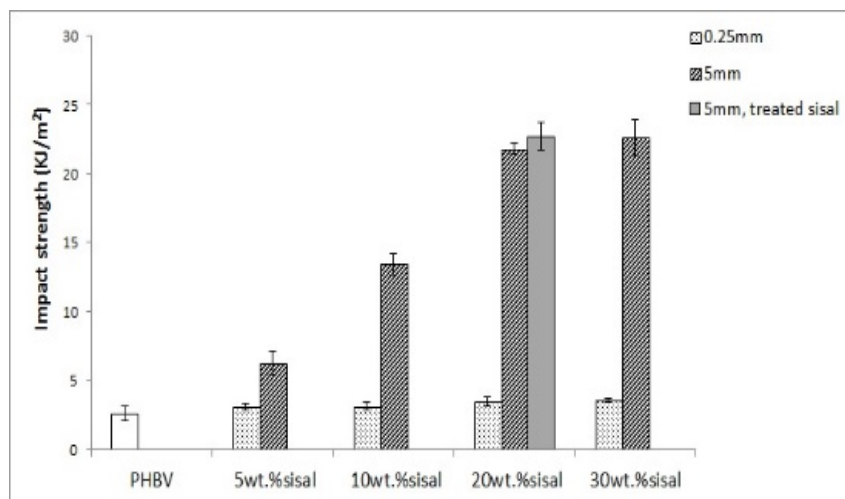


Figure 87: Effect of sisal fiber contents and silane on impact strength.

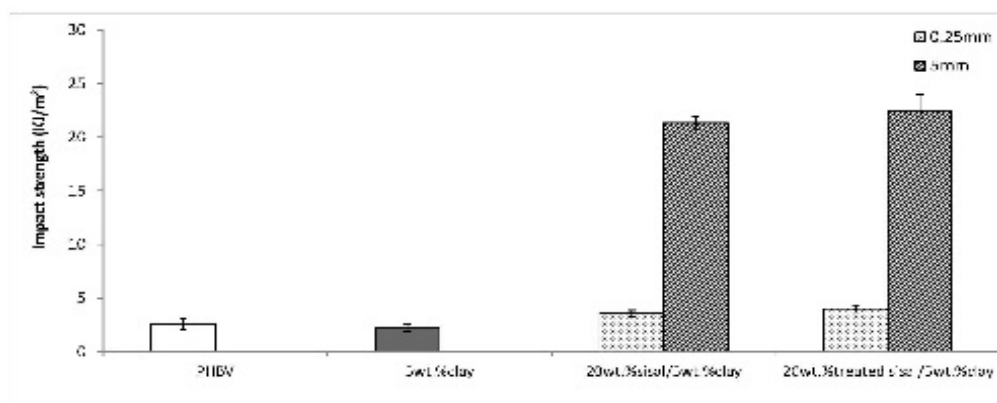


Figure 87: Impact strength of sisal fiber/PHBV and hybrid composites systems.

Hardness resistance

Hardness value of sisal fiber reinforced PHBV composites is summarized in figure 89. Hardness value of short sisal fiber composites increased steadily with increasing fiber loading. For the PHBV/30 wt.% short sisal composite, the hardness enhanced by 5% compared to the neat PHBV whereas, the hardness value of long sisal fiber composites decreased with fiber loading. It has to be clarified that this behavior is probably due to the energy transfer from PHBV matrix to sisal fiber. Figure 90 is shown an increase hardness value of PHBV composites with silane treated sisal fiber. The PHBV/3 vol.% silane/20 wt.% of short and long sisal fiber composites increased by 3% and 4%, respectively compared to untreated sisal fiber. This may be linked with some effects this behavior is due to the sisal fiber dispersion into PHBV matrix and also an improve in adhesion

of related PHBV composites as similar result reported for starch-grafted-polypropylene/kenaf fibers composites in ref.[131]. On other hand, Addition of clay particles did not significantly improve hardness values of PHBV/sisal composites at all as the results are shown in figure 91.

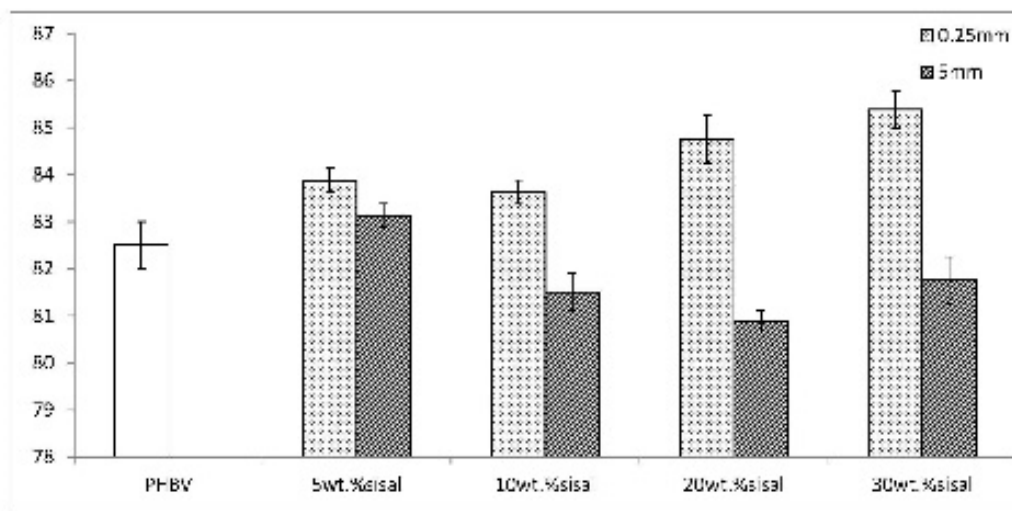


Figure 88: Effect of fiber contents on hardness.

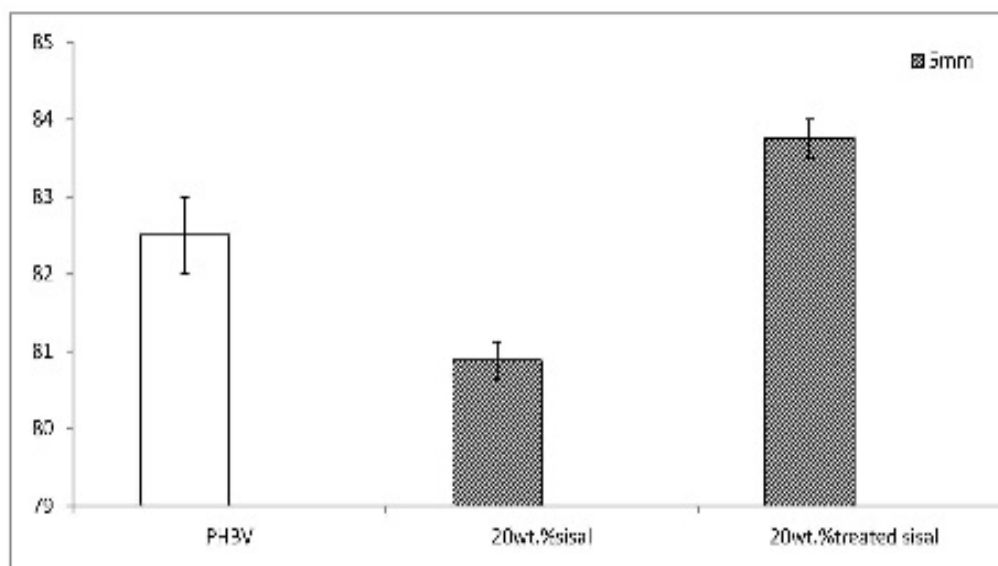


Figure 89: Effect of silane on hardness.

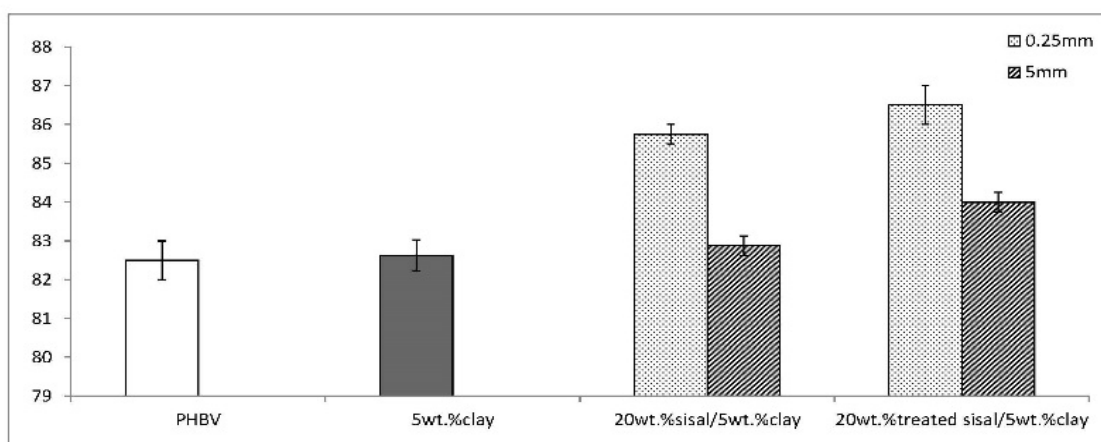


Figure 90: Hardness of sisal fiber/PHBV and hybrid composites systems.

Water absorption

Water absorption as a function of time for the PHBV/ containing different amounts of sisal fiber composites is demonstrated in figure 92. One can recognize that the water sorption behavior was considered to depend on sisal fiber content. The neat PHBV recorded water absorption value at 0.8% upon 350 hours. The PHBV/sisal composites exhibited remarkably large amount of water absorption. Especially, the water absorption of PHBV/30 wt.% of short sisal fiber composites at first 72 and 350 hours increased by 4% and 7% respectively. Note that the long sisal fiber/PHBV composites increased by 11% and 14% respectively compared to the neat PHBV. This was attribute due to the chemical nature of cellulose contents in sisal fiber. The water absorption of PHBV/3vol.% treated silane composites is shown in figure 93. It is interesting to note that water absorption of PHBV/sisal composites decreased. This can be well explained that the hydrophilic of sisal fibers was reduced by incorporation of silane which improved compatibility and adhesion of PHBV/sisal composites. Figure 94 displays the water absorption behavior of PHBV/sisal composites and hybrid systems. The PHBV/clay composite recorded water absorption value at 1.2% upon 350hr. Note that the incorporation of silane and clay particles in the PHBV/sisal composites was reduced slightly the water absorption. One may conclude that the water absorption was decreased by adding all nanoparticles. Fick's law in equation 44 is adopted also to calculate the diffusion coefficient (D) of the water absorption values. The calculation of diffusion coefficient is shown in Table 15. The D of the PHBV/sisal composites decreased with additional of clay particles. This may be linked with an incorporation of silane and clay particles. The results suggested that D may be sensitive to the nanoparticles barrier effect. It has also been observed by Becker

O. et al. [83] that these nanoparticles reacted with water lead to decrease the rate of diffusion.

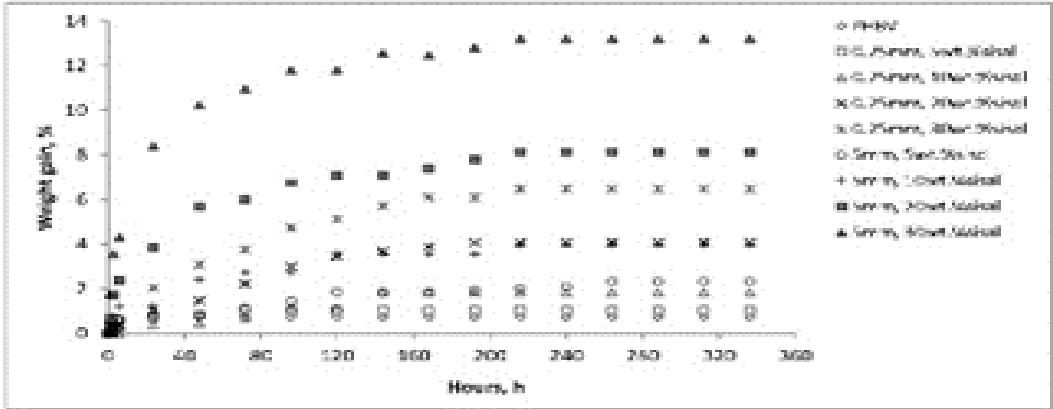


Figure 91: Water absorption of different sisal contents.

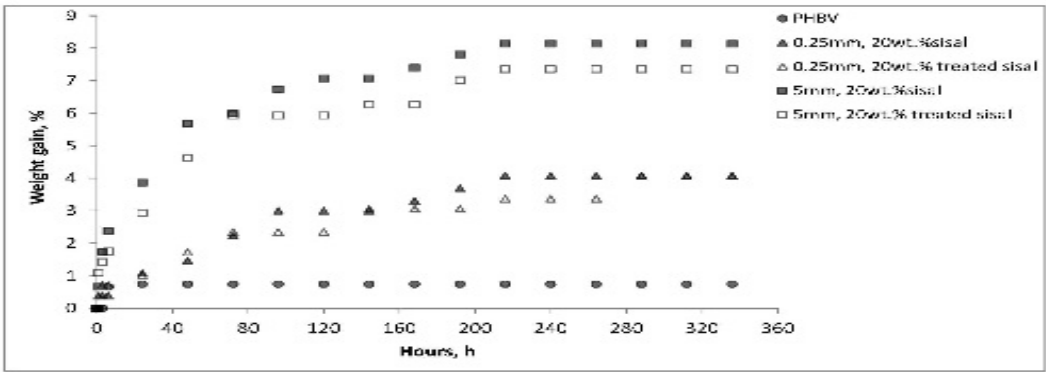


Figure 92: Water absorption of treated and untreated sisal fiber.

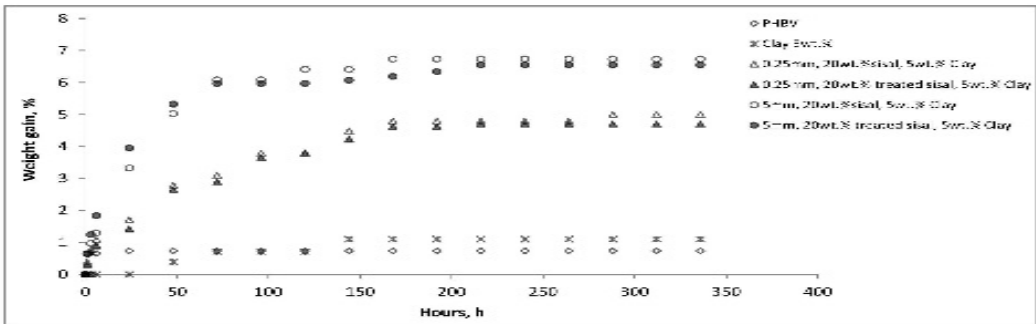


Figure 93: Water absorption of PHBV/sisal composites and hybrid systems.

Table 15: Calculated the diffusion coefficient (D).

	D (mm ² /hr.)	R ²
PHBV	3.976E-03	0.779
clay 5wt. %	4.276E-03	0.913
0.25mm, 5wt. % sisal	4.142E-03	0.866
0.25mm, 10wt. % sisal	4.251E-03	0.844
0.25mm, 20wt. % sisal	4.295E-03	0.963
0.25mm, 30wt. % sisal	4.453E-03	0.996
0.25mm, 20wt. % treated sisal	2.691E-03	0.968
0.25mm, 20wt. % sisal, 5wt. % clay	4.302E-03	0.99
0.25mm, 20wt. % treated sisal, 5wt. % clay	4.267E-03	0.994
5mm, 5wt. % sisal	2.798E-03	0.958
5mm, 10wt. % sisal	3.551E-03	0.964
5mm, 20wt. % sisal	4.172E-03	0.933
5mm, 30wt. % sisal	5.096E-03	0.9
5mm, 20wt. % treated sisal	3.641E-03	0.908
5mm, 20wt. % sisal, 5wt. % clay	4.648E-03	0.916
5mm, 20wt. % treated sisal, 5wt. % clay	4.504E-03	0.856

Morphology

SEM images of the fracture surfaces for the impact specimen can be seen in figures 95 a-c. It possible to see overview of PHBV composites system studied. One can observed that most of sisal fibers were pull-out from PHBV matrix. For the 5 wt. % of long fiber sisal composite was also aligned and dispersed in the PHBV matrix, (cf. figure 95b) Note that the sisal fibers were in form of single fiber and indicated that the fibers had not been damaged after compression process. Due to the incompatibility between sisal fiber and PHBV matrix, some gaps can be observed in figure 95c. The gaps were also formed mainly due to the hydrophilic characteristic of the sisal fibers and the high reactivity of the PHBV with a moisture. Note that, the incompatibility of fiber/matrix interfaces was reduced the mechanical properties as in above results. Furthermore, an addition of silane treated sisal fiber was well embedded in PHBV matrix (cf. figure 96) which could be increased interfacial adhesion of the sisal fiber/PHBV composites. Affected by this way, the stiffness, impact and hardness properties can be increased due to the development of debonding PHBV molecule chains and sisal fiber pull-out. In order to confirm the modified sisal fiber with silane, the SEM sample was subjected to an EDAX analysis. Figure 97 shows EDAX images of the corresponding PHBV/modified sisal fibercomposites. For selected different spots of sample, an elemental analysis was performed. EDAX revealed the major constituents of silane. These findings confirm that the sisal fiber was coated by silane. Note that the energy absorption was reduced when a crack

grows through the clay agglomeration and the crack can be accreted. Although impact strength was sacrificed in the related structure PHBV composites.

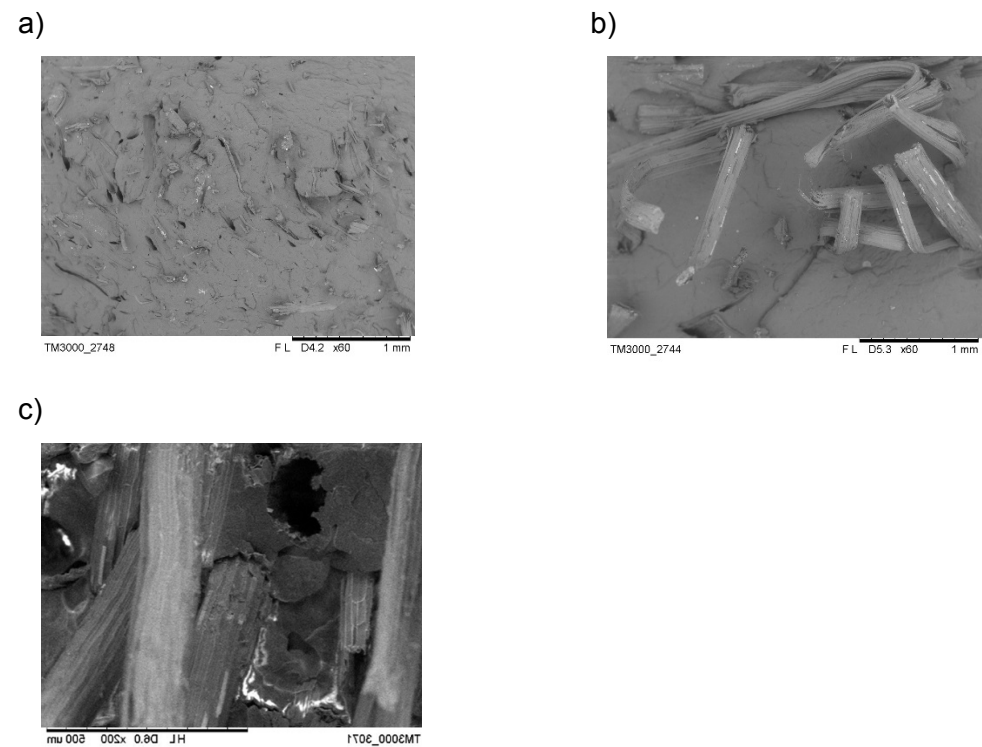


Figure 94: SEM images of PHBV with 5 wt.% short sisal fiber a), long sisal fiber b) and with 20 wt.% long sisal fiber composites c).

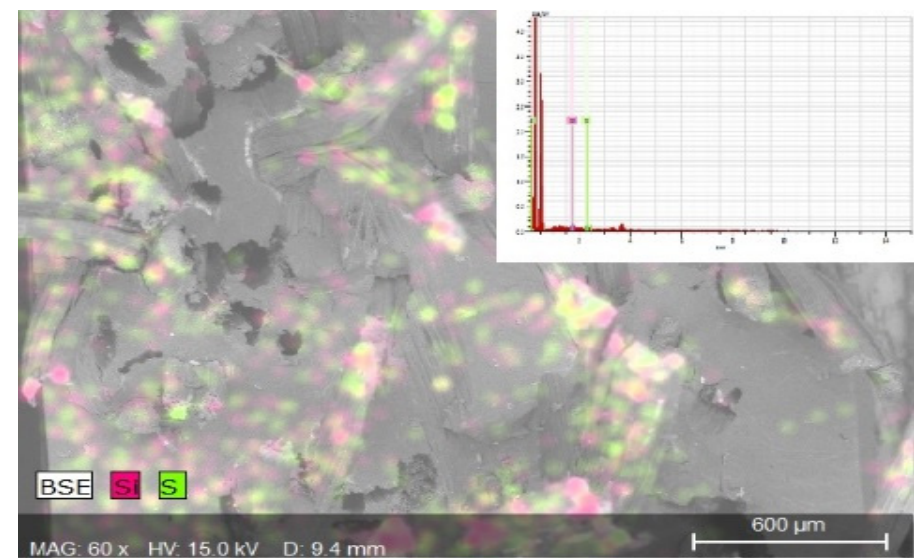


Figure 95: EDAX image of surfaces of the modified sisal fiber/PHBV composite.

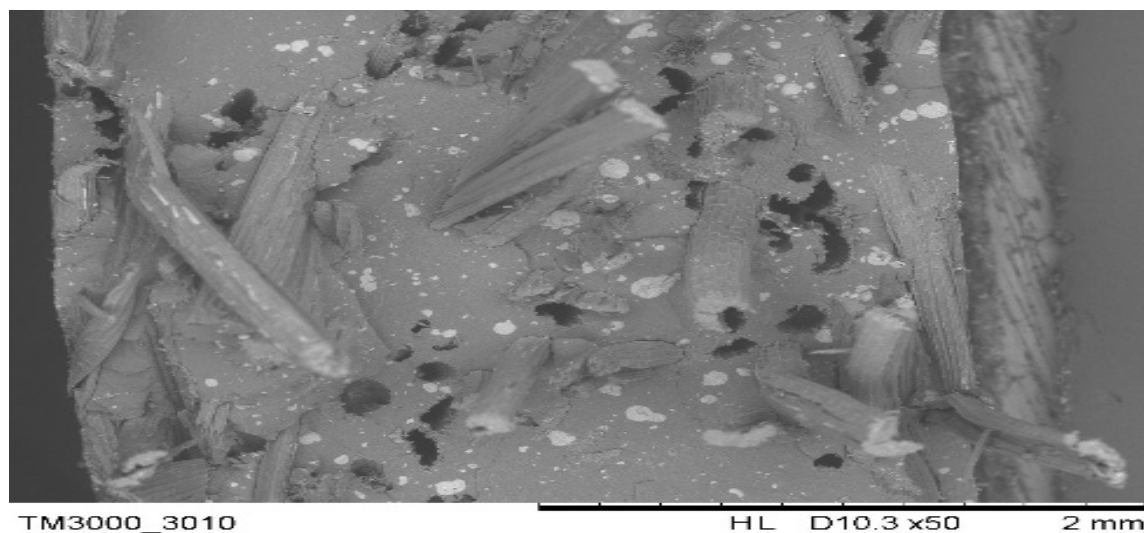


Figure 96: SEM image of PHBV/modified sisal fiber/clay hybrid composite.

Conclusion

The objective of this work was to study the effect of proportions of sisal fibers (short sisal fiber of 0.25 mm and long sisal fiber of 5 mm) reinforced PHBV composites and hybrid with addition of nano-clay particles on the mechanical properties such as tensile, impact and hardness properties. The preliminary results showed that especially, impact strength of 20 wt.% long sisal fiber/PHBV composites increased by 750% compared to the neat PHBV. Sisal fiber dispersion was well and still aligned in PHBV matrix as shown in SEM images. The tensile modulus of PHBV composites at 20 wt.% for short and long sisal fiber increased slightly by 20% and 18% respectively. Furthermore, the tensile strength of 20 wt.% of silane treated long fiber also was enhanced 10%. The hardness of 20 wt.% short sisal fiber/PHBV composites improved by 4% compared to neat PHBV. Note that the embedded of short fiber was better than long fiber in PHBV matrix. Moreover, the silane treated fiber also improved the hardness of composites. This indicated that the sisal fiber dispersed well into PHBV matrix and associated with a strong interfacial bonding between sisal fiber and PHBV matrix. Incorporation of clay particles into the PHBV/sisal fiber composites resulted in considerable an increase of the hardness and water resistance. The reduction in tensile and impact properties was attributed to the agglomeration of clay in the PHBV hybrid composites.

5 References

- [1] Bhargava, A.K.: Engineering materials Polymers, Ceramics and Composites, New Delhi: Prentice Hall of India Private Limited, Vol. 2 (2005).
- [2] Gibson Ronald, F.: Principles of composite material mechanics, Detroit, Michigan, McGraw-Hill, Inc. (1994).
- [3] Mohanty, A.K., Misra, M., Drzal, L.T.: Natural fibers, biopolymers, and biocomposites, ISBN 0-8493-1741-X, (2005).
- [4] Vroman, I., Tighzert, L.: Biodegradable polymers. *Materials* 2 (2009), pp. 307-344.
- [5] Kabir, M.M., Wang, H., Lau, K.T., Cardona, F.: Chemical treatments on plant-based natural fibre reinforced polymer composites: An overview. *Composites: Part B* 43 (2012), pp. 2883–2892.
- [6] Huda, M.S., Drzal, L.T., Mohanty, A.K., Misra, M.: Chopped glass and recycled newspaper as reinforcement fibers in injection molded poly(lactic acid) (PLA) composites: A comparative study. *Composites Science and Technology* 66 (2006), pp. 1813–1824.
- [7] John, M.J., Thomas, S.: Biofibres and biocomposites. *Carbohydrate Polymers* 71 (2008), pp. 343–364.
- [8] Wambua, P., Ivens, J., Verpoest, I.: Natural fibres: can they replace glass in fibre reinforced plastics. *Composites Science and Technology* 63 (2003), pp. 1259–1264.
- [9] Arbelaiz, A., Fernandez, B., Cantero, G., Llano-Ponte, R., Valea, A., Mondragon, I.: Mechanical properties of flax fibre/polypropylene composites. Influence of fibre/matrix modification and glass fibre hybridization. *Composites: Part A* 36 (2005), pp. 1637–1644.
- [10] Li, X. Lope, G., Tabil, Panigrahi, S.: Chemical Treatments of Natural Fiber for Use in Natural Fiber-Reinforced Composites: A Review. *Canada, Springer* 15 (2007), pp. 25-33.
- [11] Vainionpää, S., Rokkanen, P., Törmälä, P.: Surgical applications of biodegradable polymers in human tissues. *Progress in Polymer Science* 14(1989), pp. 679-716.
- [12] Manninen, M.J., Päivärinta, U., Pätäälä, H., Rokkanen, P., Taurio, R., Tamminmäki, M., Törmälä, P.: Shear strength of cancellous bone after osteotomy fixed with absorbable self-reinforced polyglycolic acid and poly-L-lactic acid rods. *Journal of Materials Science: Materials in Medicine* 3(1992), pp. 245-251.

- [13] Auras, R., Harte, B., Selke, S.: An overview of polylactides as packaging materials. *Macromolecular Bioscience* 4(2004), pp. 835-864.
- [14] Dangtungee, R., Petcharoen, K., Pinijsattawong, K., Siengchin, S.: Investigation of the rheological properties and die swell of polylactic acid/nanoclay composites in a capillary rheometer. *Mechanics of Composite Materials* 47(2012), pp. 663-670.
- [15] Fortunati, E., Armentano, I., Iannoni, A., Kenny, J.M.: Development and thermal behavior of ternary PLA matrix composites. *Polymer Degradation and Stability* 95(2010), pp. 2200-2206.
- [16] Kumar, R., Yakabu, M.K., Anandjiwala, R. D.: Effect of montmorillonite clay on flax fabric reinforced poly lactic acid composites with amphiphilic additives. *Composites Part A: Applied Science and Manufacturing* 41(2010), pp. 1620-1627.
- [17] Graupner, N., Herrmann, A.S., Müssig, J.: Natural and man-made cellulose fibre-reinforced poly(lactic acid) (PLA) composites: An overview about mechanical characteristics and application areas. *Composites Part A: Applied Science and Manufacturing* 40(2009), pp. 810-821.
- [18] Ochi, S.: Mechanical properties of kenaf fibers and kenaf/PLA composites. *Mechanics of Materials* 40(2008), pp. 446-452.
- [19] Bledzki, A.K., Jazzkiewicz, A., Scherzer, D.: Mechanical properties of PLA composites with man-made cellulose and abaca fibres. *Composites Part A: Applied Science and Manufacturing* 40(2009), pp. 404-412.
- [20] Roussi r, F., Baley, C., Godard, G., Burr, D.: Compressive and tensile behaviours of PLLA matrix composites reinforced with randomly dispersed flax fibres. *Applied Composite Materials* 19(2012), pp. 171-188.
- [21] Siengchin, S., Pohl, T., Medina, L., Mitschang, P.: Structure and properties of flax/polylactide/alumina nanocomposites. *Journal of Reinforced Plastics and Composites* 32, pp. 23–33.
- [22] Bax, B., Müssig, J.: Impact and tensile properties of PLA/Cordenka and PLA/flax composites. *Composites Science and Technology* 68(2008), pp. 1601-1607.
- [23] Das, K., Ray, D., Banerjee, I., Bandyopadhyay, N.R., Sengupt, S., Mohanty, A.K., Misra, M.: Crystalline morphology of PLA/clay nanocomposite films and its correlation with other properties. *Journal of applied polymer science* 118(2010), pp. 143-151.
- [24] Mulinari, D.R., Voorwald, H.J.C., Cioffi, M.O.H., Silva, M.L.C.P., Cruz, T.G., Saron, C.: Sugarcane bagasse cellulose/HDPE composites obtained by extrusion. *Composites Science and Technology* 69(2009), pp. 214-219.

- [25] Gomes, A., Matsuo, T., Goda, K., Ohgi, J.: Development and effect of alkali treatment on tensile properties of curaua fiber green composites. *Composites Part A: Applied Science and Manufacturing* 38(2007), pp. 1811-1820.
- [26] Arbelaiz, A., Cantero, G., Fernández, B., Mondragon, I., Ganán, P., Kenny, J.M.: Flax fiber surface modifications: Effects on fiber physico mechanical and flax/polypropylene interface properties. *Polymer Composites* 26(2005), pp. 324-332.
- [27] Kowalczyk, M., Piorkowska, E., Kulpinski, P., Pracella, M.: Mechanical and thermal properties of PLA composites with cellulose nanofibers and standard size fibers. *Composites Part A: Applied Science and Manufacturing* 42(2011), pp. 1509-1514.
- [28] Mohanty, S., Verma, S.K., Nayak, S.K.: Dynamic mechanical and thermal properties of MAPE treated jute/HDPE composites. *Composites Science and Technology* 66(2006), pp. 538-547.
- [29] Shaw, M.T., MacKnight, W.J.: *Introduction to polymer viscoelasticity*. John Wiley & Sons. New York (2005).
- [30] Siengchin, S.: Ph.D. Dissertation. IVW Schriftenreihe Band 82. A.K. Schlarb (Hrsg.). Kaiserslautern (2008).
- [31] Suryanegara, L., Nakagaito, A.N., Yano, H.: The effect of crystallization of PLA on the thermal and mechanical properties of microfibrillated cellulose-reinforced PLA composites. *Composites Science and Technology* 69(2009), pp. 1187-1192.
- [32] Siengchin, S., Karger-Kocsis, J., Thomann, R.: Alumina-filled polystyrene micro- and nanocomposites prepared by melt mixing with and without latex precompounding: Structure and properties. *Journal of applied polymer science* 105(2007), pp. 2963-2972.
- [33] Ferry, J.D.: *Viscoelastic Properties of Polymers*. Wiley & Sons. New York (1980).
- [34] Heinemann, M., Fritz, H.G.: *Polylactid-Struktur. Eigenschaften and Anwendungen*. Stuttgart. Plastic Congress. 19(2005).
- [35] Xie, Y., Hill, C.A.S., Xiao, Z., Militz, H., Mai, C.: Silane coupling agents used for natural fiber/polymer composites: A review. *Composites Part A: Applied Science and Manufacturing* 41(2010), pp. 806–819.
- [36] Hong, C.K., Kim, N., Kang, S.L., Nah, C., Lee, Y.S., Cho, B.H.: Mechanical properties of maleic anhydride treated jute fibre/polypropylene composites. *Plastics, Rubber and Composites* 37(2008), pp. 325–330.
- [37] Liu, Q., Hughes, M.: The fracture behaviour and toughness of woven flax fibre reinforced epoxy composites. *Composites Part A: Applied Science and Manufacturing* 39(2008), pp. 1644–1652.

- [38] Schuermann, H.: Konstruieren mit Faser-Kunststoff-Verbunden. Berlin Heidelberg New York. Springer (2007).
- [39] Bodros, E., Pillin, I., Montrelay, N., Baley, C.: Could biopolymers reinforced by randomly scattered flax fibers be used in structural applications. *Composites Science and Technology* 67(2007), pp. 462–470.
- [40] Naik, R.A.: Failure Analysis of Woven and Braided Fabric Reinforced Composites. *Journal of Composite Materials* 29(1995), pp. 2334-2363.
- [41] Siengchin, S.: Impact, Thermal and Mechanical Properties of High Density Polyethylene/Flax/SiO₂ Composites: Effect of Flax Reinforcing Structures. *Journal of Reinforced Plastics and Composites* 31(2012), pp. 959-966.
- [42] Siengchin, S., Pipes, R.B.: Rheological and Dynamic Mechanical Thermal Properties of Epoxy Composites reinforced with Single- and Multiwalled Carbon Nanotubes. *Mechanics of Composite Materials*. 47(2012), pp. 609-616.
- [43] Steeg, M.: Prozesstechnologie fuer Cyclic Butylene Terephthalate im Faser-Kunststoff-Verbund, In: Prof. Dr.-Ing. Peter Mitschang (Hrsg.): IVW Schriftenreihe Band 90. Kaiserslautern: Institut fuer Verbundwerkstoffe GmbH (2010).
- [44] Dittenber, B. D., GangaRao, H.V.S.: Critical review of recent publications on use of natural composites in infrastructure. *Composites Part A: Applied Science and Manufacturing* 43(2012), pp. 1419–1429.
- [45] Ku, H., Wang, H., Pattarachaiyakoo, N., Trada, M.: A review on the tensile properties of natural fiber reinforced polymer composites. *Composites Part B: Engineering* 42(2011), pp. 856–873.
- [46] Anuar, H., Zuraida, A., Kovacs, J. G., Tabi, T.: Improvement of Mechanical Properties of Injection-Molded Polylactic Acid–Kenaf Fiber Biocomposite. *Journal of Thermoplastic Composite Materials* 25(2012), pp. 153-164.
- [47] Lee, S.Y., Kang, I.A., Doh, G.H., Yoon, H.G., Park, B.D., Wu, Q.: Thermal and Mechanical Properties of Wood Flour/Talc-filled Polylactic Acid Composites: Effect of Filler Content and Coupling Treatment. *Journal of Thermoplastic Composite Materials* 21(2008), pp. 209-223.
- [48] Zhao, Y., Qiu, J., Feng, H., Zhang, M., Lei, L., Wu, X.: Improvement of tensile and thermal properties of poly(lactic acid) composites with admicellar-treated rice straw fiber. *Chemical Engineering Journal* 173(2011), pp. 659– 666.
- [49] George, J., Bhagawan, S.S., Thomas, S.: Effects of environment on the properties of low-density polyethylene composites reinforced with pineapple-leaf fiber. *Composites Science and Technology* 58(1998), pp. 1471–85.

- [50] Huda, M.S., Drzal, L.T., Mohanty, A.K., Misra, M.: The effect of silane treated and untreated-talc on the mechanical and physico-mechanical properties of poly(lactic acid)/newspaper fibers/talc hybrid composites. *Composites Part B: Engineering* 38(2007), pp. 367–379.
- [51] Siengchin, S., Sinpayakun, P., Suttiruengwong, S., Asawapirom, U.: Effect of nanofiller aspect ratio on the stress relaxation and creep response of toughened POM composites. *Mechanics of Composite Materials* 46(2010), pp. 341-348.
- [52] Paessler, M., Schledjewski, R.: Effect of ring winding technology on nol ring testing and accompanying characteristics. *ECCM 14. Budapest. Hungary* (2010).
- [53] Lee, S.H., Wang, S.: Biodegradable polymers/ bamboo fiber biocomposite with bio-based coupling agent. *Composites Part A: Applied Science and Manufacturing* 37(2006), pp. 80-91.
- [54] Karger-Kocsis, J., Siengchin, S.: Single-Polymer Composites Concepts, Realization and Outlook: Review. *KMUTNB International Journal of Applied Science and Technology* 7(2014), pp. 1-9.
- [55] Teo, P.S., Chow, W.S.: Water vapour permeability of poly(lactic acid)/chitosan binary and ternary blends. *KMUTNB International Journal of Applied Science and Technology* 7(2014), pp. 23-27.
- [56] Gu, S.Y., Zhang, K., Ren, J., Zhan, H.: Melt rheology of polylactide/ poly(butyl- enesadipate-co-terephthalate) blends. *Carbohydrate Polymers* 74(2008), pp. 79–85.
- [57] Wang, R., Wang, C.H., Jiang, Z.H.: Biodegradability of flax oil fibers reinforced with poly(lactic acid) composites. *Journal of Fiber Bioengineering and Informatics* 3(2010), pp. 75-79.
- [58] Oksman, K., Skrifvars, M., Selin, J.F.: Natural fibres as reinforcement in polylactic acid (PLA) composites. *Composites Science and Technology* 63(2003), pp. 1317–1324.
- [59] Song, Y.S., Lee, J.T., Ji, D.S., Kim, M.W., Lee, S.H., Ryou, Y.J.: Viscoelastic and thermal behavior of woven hemp fiber reinforced poly(lactic acid) composites. *Composites Part B: Engineering* 43(2012), pp. 856-860.
- [60] John, M.J., Anandjiwala, R.D.: Chemical modification of flax reinforced polypropylene composites. *Composites Part A: Applied Science and Manufacturing* 40(2009), pp. 442–448.
- [61] Sdrobis, A., Darie, R.N.: Low density polyethylene composites containing cellulose pulp fibers. *Composites Part B: Engineering* 43(2012), pp. 1873–1880.

- [62] Arrakhiz, F.Z., Achaby, M.E., Malha, M.: Mechanical and thermal properties of natural fibers reinforced polymer composites: Doum/low density polyethylene. *Materials & Design* 43(2013), pp. 200–205.
- [63] Wu, C.S.: Utilization of peanut husks as a filler in aliphatic aromatic polyesters: Preparation, characterization, and biodegradability. *Polymer Degradation and Stability* 97(2012), pp. 2388–2395.
- [64] Džalto, J., Medina, L.A., Mitschang, P.: Volumetric interaction and material characterization of flax/furan bio-composites. *KMUTNB International Journal of Applied Science and Technology* 7(2014), pp. 11–21.
- [65] Minkova, L., Peneva, Y., Tashev, E., Filippi, S., Pracella, M., Magagnini, P.: Thermal properties and microhardness of HDPE/clay nanocomposites compatibilized by different functionalized polyethylenes. *Polymer Testing* 28(2009), pp. 528–533.
- [66] Swain, S.K., Isayev, A.I.: Effect of ultrasound on HDPE/clay nanocomposites: Rheology, structure and properties. *Polymer* 48(2007), pp. 281–289.
- [67] Faruk, O., Matuana, L.M.: Nanoclay reinforced HDPE as a matrix for wood-plastic composites. *Composites Science and Technology* 68(2008), pp. 2073–2077.
- [68] Khumalo, V. M., Karger-Kocsis, J., Thomann, R.: Polyethylene/synthetic boehmite alumina nanocomposites: Structure, thermal and rheological properties. *EX-PRESS Polymer Letters* 4(2010), pp. 264–274.
- [69] Khumalo, V. M., Karger-Kocsis, J., Thomann, R.: Polyethylene/synthetic boehmite alumina nanocomposites: structure, mechanical, and perforation impact properties. *Journal of Materials Science* 46(2011), pp. 422–428.
- [70] Siengchin, S., Karger-Kocsis, J., Apostolov, A.A., Thomann, R.: Polystyrene-fluorohectorite nanocomposites prepared by melt mixing with latex precompounding: Structure and mechanical properties. *Journal of Applied Polymer Science* 106(2007), pp. 248–254.
- [71] Panthapulakkal, S., Law, S., Sain, M.: Enhancement of processability of rice husk filled high-density polyethylene composite profiles. *Journal of Thermoplastic Composite Materials* 18(2005), pp. 445–458.
- [72] Li, X., Tabil, L.G., Oguocha, I.N., Panigrahi S.: Thermal diffusivity, thermal conductivity, and specific heat of flax fiber-HDPE biocomposites at processing temperatures. *Composites Science and Technology* 68(2008), pp. 1753–1758.
- [73] Liu, H., Wua, Q., Zhang, Q.: Preparation and properties of banana fiber-reinforced composites based on high density polyethylene (HDPE)/Nylon-6 blends. *Bioresource Technology*. 100(2009), pp. 6088–6097.

- [74] Li, Q., Matuana, L.M.: Effectiveness of maleated and acrylic acid-functionalized polyolefin coupling agents for HDPE-wood-flour composites. *Journal of Thermoplastic Composite Materials* 16(2003), pp. 551-564.
- [75] Choudhury, A.: Isothermal crystallization and mechanical behavior of ionomer treated sisal/HDPE composites. *Materials Science and Engineering A*. 491(2008), pp. 492–500.
- [76] Siengchin, S., Karger-Kocsis, J., Psarras, G. C., Thomann, R.: Polyoxymethylene/polyurethane/alumina ternary composites: Structure, mechanical, thermal and dielectric properties. *Journal of Applied Polymer Science* 110(2008), pp. 1613–1623.
- [77] Cheung, H.Y., Ho, M.P., Lau, K.T., Cardona, F., Hui, D.: Natural fibre-reinforced composites for bioengineering and environmental engineering applications. *Composites Part B: Engineering* 40(2009), pp. 655–663.
- [78] John, B., Varughese, K.T., Oommen, Z., Potschke, P., Thomas, S.: Dynamic mechanical behavior of high density polyethylene/ ethylene vinyl acetate copolymer blends: the effects of blend ratio, reactive compatibilization, & dynamic vulcanization. *Journal of Applied Polymer Science* 87(2003), pp. 2083–2099.
- [79] Vaisman, L., Gonza'lez, M.F., Marom, G.: Transcrystallinity in brominated UHMWPE fiber reinforced HDPE composites: morphology and dielectric properties. *Polymer* 44(2003), pp. 1229–1235.
- [80] Siengchin, S., Karger-Kocsis, J.: Mechanical and stress relaxation behavior of santoprene® thermoplastic elastomer/boehmite alumina nanocomposites produced by water-mediated and direct melt compounding. *Composites Part A: Applied Science and Manufacturing* 41(2010), pp. 768-773.
- [81] Siengchin, S., Abraham, T.N., Karger-Kocsis, J.: Structure–stress relaxation relationship in polystyrene/fluorohectorite micro- and nanocomposites. *Mechanics of Composite Materials* 44(2008), pp. 495-504.
- [82] Gornicka, B., Prociow, E.: Polyester and Polyesterimide Compounds with Nanofillers for Impregnating of Electrical Motors. *Acta Physica Polonica A* 115(2009), pp. 842-845.
- [83] Becker, O., Varley, R.J., Simon, G.P.: Thermal stability and water uptake of high performance epoxy layered silicate nanocomposites. *European Polymer Journal* 40(2004), pp. 187–195.
- [84] Chow, W.S.: Water absorption of epoxy/glass fiber/organo-montmorillonite nanocomposites. *eXPRESS Polymer Letters*. 1(2007), pp. 104–108.

- [85] Hepworth, D.G., Hobson, R.N., Bruce, D.M., Farrant, J.W.: The use of unretted hemp fibre in composite manufacture. *Composites Part A: Applied Science and Manufacturing* 31(2000), pp. 1279–1283.
- [86] Sain, M., Suhara, P., Law, S., Bouilloux, A.: Interface modification and mechanical properties of natural fiber–polyolefin composite products. *Journal of Reinforced Plastics and Composites* 24(2005), pp. 121–130.
- [87] Sun, Z.Y., Han, H.S., Dai, G.C.: Mechanical properties of injection-molded natural fiber-reinforced polypropylene composites: Formulation and compounding processes. *Journal of Reinforced Plastics and Composites* 29(2010), pp. 637–650.
- [88] Albano, C., Ichazo, M., Gonzalez, J., Delgado, M., Poleo, R.: Effects of filler treatments on the mechanical and morphological behaviour of PP+ wood Flour and PP+sisal fibre. *Material Research Innovations* 4(2001), pp. 284–293.
- [89] Lei, Y., Wu, Q., Yao, F., Xu, Y.: Preparation and properties of recycled HDPE/natural fiber composites. *Composites Part A: Applied Science and Manufacturing* 38(2007), pp. 1664–1674.
- [90] Rosso, P., Ye, L., Friedrich, K., Sprenger, S.: A Toughened Epoxy Resin by Silica Nanoparticle Reinforcement. *Journal of Applied Polymer Science* 100(2006), pp. 1849–1855.
- [91] Tsai, J.L., Cheng, Y.L.: Investigating Silica Nanoparticle Effect on Dynamic and Quasi-static Compressive Strengths of Glass Fiber/Epoxy Nanocomposites. *Journal of Composite Materials* 43(2009), pp. 3143–3155.
- [92] Siengchin, S., Karger-Kocsis, J.: Structure, mechanical, and fracture properties of nanoreinforced and HNBR-toughened polyamide 6. *Journal of Applied Polymer Science* 123(2012), pp. 897–902.
- [93] George, J., Bhagawan, S.S., Thomas, S.: Thermo-gravimetric & dynamic mechanical thermal analysis of pineapple fibre reinforced polyethylene composites. *Journal of thermal analysis* 47(1996), pp. 1121–1140.
- [94] Bledzki, A.K., Faruk, O., Sperber, V.E.: Cars from Bio-Fibres. *Macromolecular Materials and Engineering* 291(2006), pp. 449–457.
- [95] <http://www.presseportal.de/story.htx>
- [96] Zampaloni, M., Pourboghrat, F., Yankovich, S.A., Rodgers, B.N., Moore, J., Drzal, L.T., Mohanty, A.K., Misra, M.: Kenaf natural fiber reinforced polypropylene composites: A discussion on manufacturing problems and solutions. *Composites Part A: Applied Science and Manufacturing* 38(2007), pp. 1569–1580.
- [97] Wambua, P., Ivens, J., Verpoest, I.: Natural fibres: Can they replace glass fibre reinforced plastics? *Composites Science and Technology* 63(2003), pp. 1259–1264.

- [98] Prashantha, K., Soulestin, J., Lacrampe, M.F., Claes, M., Dupin, G., Krawczak, P.: Multi-walled carbon nanotube filled polypropylene nanocomposites based on masterbatch route: Improvement of dispersion and mechanical properties through PP-g-MA addition. *eXPRESS Polymer Letters*. 2(2008), pp. 735–745.
- [99] Abraham, T.N., Wanjale, S., Siengchin, S., Karger-Kocsis, J.: Dynamic mechanical and perforation impact behavior of all-PP composites containing beta-nucleated random PP copolymer as matrix and stretched PP homopolymer tape as reinforcement: Effect of draw ratio of the tape. *Journal of Thermoplastic Composite Materials* 24(2011), pp. 377-388.
- [100] Chiu, W.Y., Fang, S.J.: Mechanical properties and morphology of crosslinked PP/PE blends and PP/PE/propylene–ethylene copolymer blends. *Journal of Applied Polymer Science* 30(1985), pp. 1473–1489.
- [101] Haque, M., Hasan, M., Islam, S., Ali, E.: Physico-mechanical properties of chemically treated palm and coir fiber reinforced polypropylene composites. *Biore-source Technology*. 100(2009), pp. 4903–4906.
- [102] Van de Velde, K., Kiekens, P.: Influence of fiber Surface Characteristics on the Flax/Polypropylene Interface. *Journal of Thermoplastic Composite Materials* 14(2001), pp. 244–260.
- [103] Van de Velde, K., Kiekens, P.: Development of a flax/polypropylene composite with optimal mechanical characteristics by fiber and matrix modification. *Journal of Thermoplastic Composite Materials* 15(2002), pp. 281–300.
- [104] Zhong, Y., Poloso, T., Hetzer, M., Kee, D.: Enhancement of wood/polyethylene composites via compatibilization and incorporation of organoclay particles. *Polymer Engineering & Science* 47(2007), pp. 797–803.
- [105] Kord, B.: Effect of nanoparticles loading on properties of polymeric composite based on hemp fiber/polypropylene *Journal of Thermoplastic Composite Materials* 25(2012), pp. 793-806.
- [106] Najafi, A., Kord, B., Abdi, A., Ranaee, S.: The impact of the nature of nanoclay on physical and mechanical properties of polypropylene/reed flour nanocomposites. *Journal of Thermoplastic Composite Materials* 25(2012), pp. 717-727.
- [107] Arbelaiz, A., Fernandez, B., Ramos, J.A., Retegi, A., Llano-Ponte, R., Mondragon, I.: Mechanical properties of short flax fibre bundle/polypropylene composites: Influence of matrix/fibre modification, fibre content, water uptake and recycling. *Composites Science and Technology* 65(2005), pp. 1582–1592.

- [108] Siengchin, S., Rungsardthong, V.: HDPE reinforced with nanoparticle, natural and animal fibers: Morphology, thermal, mechanical, stress relaxation, water absorption and impact properties. *Journal of Thermoplastic Composite Materials* 26(2013), pp. 1025–1040.
- [109] Siengchin, S., Dangtungee, R.: Effect of woven flax structures on morphology and properties of reinforced modified polylactide composites. *Journal of Thermoplastic Composite Materials* 26(2013), pp. 1424–1440.
- [110] Siengchin, S., Haag, R., Sinpayakun, P.: A Review of creep resistance of nano - scale reinforcing thermoplastics. *Asian International Journal of Science and Technology* 2(2009), pp. 15-20.
- [111] Pegoretti, A., Kolarik, J., Slouf, M.: Phase structure and tensile creep of recycled poly(ethylene terephthalate)/short glass fibers/impact modifier ternary composites. *eXPRESS Polymer Letter* 3(2009), pp. 235-244.
- [112] Mohanty, A.K., Misra, M., Drzal, L.T.: Sustainable bio-composites from renewable resources: opportunities and challenges in the green materials world. *Journal of Polymers and the Environment* 10(2002), pp. 19-26.
- [113] Scaffaro, R., Morreale, M., Re, G.L., Mantia, F.P.: Degradation of Mater-Bi®/wood flour biocomposites in active sewage sludge. *Polymer Degradation and Stability* 94(2009), pp. 1220-1229.
- [114] Chou, P.M., Mariatti, M., Zulkifli, A., Sreekantan, S.: Evaluation of the flexural properties and bioactivity of bioresorbable PLLA/PBSL/CNT and PLLA/PBSL/TiO₂ nanocomposites. *Composites Part B: Engineering* 43(2012), pp. 1374-1381.
- [115] Haq, M., Burgueno, R., Mohanty, A.K., Misra, M.: Hybrid bio-based composites from blends of unsaturated polyester and soybean oil reinforced with nanoclay and natural fibers. *Composites Science and Technology* 68(2008), pp. 3344–3351.
- [116] Ganesh, V.K., Naik, N.K.: Failure behavior of plain weave fabric laminates under on-axis uniaxial tensile loading: III- Effect of fabric geometry. *Journal of Composite Materials* 30(1996), pp. 1823–1856.
- [117] Gupta, A., Raghavan, J.: Parametric study of the effect of microstructure on creep of plain weave composites. *Composites Part A: Applied Science and Manufacturing* 42(2011), pp. 511–520.
- [118] Varghese, S., Gatos, K.G., Apostolov, A.A., Karger-Kocsis, J.: Morphology and mechanical properties of layered silicate reinforced natural and polyurethane rubber blends produced by latex compounding. *Journal of Applied Polymer Science* 92(2004), pp. 543–551.

- [119] Leu, Y.Y., Chow, W.S.: Kinetics of water absorption and thermal properties of poly(lactic acid)/organomontmorillonite/poly(ethyleneglycol) nanocomposites. *Journal of Vinyl and Additive Technology* 17(2011), pp. 40-47.
- [120] Findley, W.N., Lai, J.S., Onaran, K.: Creep and relaxation of nonlinear viscoelastic materials. Dover Publications: New York. (1989).
- [121] Siengchin, S.: Reinforced Flax mat/modified Polylactide (PLA) Composites: Impact, Thermal and Mechanical Properties. *Mechanics of composite Materials* 50(2014), pp. 257-266.
- [122] de Koning, G.J.M., Lemstra.: Crystallization phenomena in bacterial poly[(R)-3-hydroxybutyrate]: 2. Embrittlement and rejuvenation. *Polymer* 34(1993), pp. 4089-4094.
- [123] Amass, W., Amass, A., Tighe, B.: A review of biodegradable polymers: uses, current developments in the synthesis and characterization of biodegradable polyesters, blends of biodegradable polymers and recent advances in biodegradation studies. *Polymer International* 47(1998), pp. 89-144.
- [124] Sanjeev, S., Mohanty, K.A., Tomohiko, S., Yoshihiro, T., Hiroyuki, H.: Renewable resource based biocomposites from natural fiber and polyhydroxybutyrate-co-valerate(PHBV) bioplastic. *Composites Part A: Applied Science and Manufacturing* 39(2008), pp. 875-886.
- [125] Qian, J.: Investigation of crystallization of poly(3-hydroxybutyrate-CO-3-hydroxyvalerates) and their bamboo fiber reinforced composites. Master Thesis. Department of Civil and Environmental Engineering, Washington state university (2006).
- [126] Siengchin, S., Dingtungee, R.: Polyethylene and polypropylene hybrid composites based on nano silicon dioxide and different flax structures. *Journal of Thermoplastic Composite Materials* 27(2014), pp. 1428-1447.
- [127] Zhao, H., Cui, Z., Wang, X., Turng, L.S., Peng, X.: Processing and characterization of solid and microcellular poly(lactic acid)/polyhydroxybutyrate-valerate (PLA/PHBV) blends and PLA/PHBV/Clay nanocomposites. *Composites Part B: Engineering* 51(2013), pp. 79-91.
- [128] Javadi, A., Srithep, Y., Lee, J., Pilla, S., Clemons, C., Gong, S., Turng, L.S.: Processing and characterization of solid and microcellular PHBV/PBAT blend and its RWF/nanoclay composites. *Composites Part A: Applied Science and Manufacturing* 41(2010), pp. 982-990.
- [129] Majeed, K., Jawaid, M., Hassan, A., Bakar, A.A., Abdul Khalil, H.P.S, Salema, A.A., Inuwa, I.: Potential materials for food packaging from nanoclay/natural fibres filled hybrid composites. *Materials and Design* 46(2013), pp. 391-410.

- [130] Li, X., Tabil, L.G., Panigrahi, S.: Chemical Treatments of Natural Fiber for Use in Natural Fiber-Reinforced Composites: A review. *Journal of Polymers and the Environment* 15(2007), pp. 25-33.
- [131] Hamma, A., Kaci, M., Mohd Ishak, Z.A., Pegoretti, A.: Strach-grafted-polypropylene/kenaf fibres composites part 1: Mechanical performances and viscoelastic behavior. *Composites Part A: Applied Science and Manufacturing* 56(2014), pp. 328-335.

PERSONAL INFORMATION

Name:	Suchart Siengchin
Date and Place of Birth:	13.11.1971 - Bangkok, Thailand
Nationality:	Thai

EDUCATION

1995 – 1996	Preparation course for foreign students (University of Applied Sciences Giessen/Friedberg), Germany
1996 – 1999	Mechanical Engineering, accomplished by the German degree “Diplom-Ingenieur” at the University of Applied Sciences Giessen/Friedberg, Hessen, Germany
2000 - 2002	Master of Science in Polymer Technology at the University of Applied Sciences Aalen, Baden-Wuerttemberg, Germany
2002 - 2004	Master of Science in Material Science at the Erlangen-Nürnberg University, Bayern, Germany
2005 - 2008	Doctor of Philosophy in Engineering (Dr.-Ing.) at the Institute for Composite Materials, University of Kaiserslautern, Rheinland-Pfalz, Germany
09/2008 - 01/2009	Postdoctoral Research Assistant in the Institute for Composite Materials, University of Kaiserslautern, Rheinland-Pfalz, Germany
01/2009- 07/2009	Postdoctoral Research Assistant in the School of Materials Engineering, Purdue University, West Lafayette, Indiana, USA
09/2011- 04/2012	Guest Researcher at the Institute for Composite Materials, University of Kaiserslautern, Rheinland-Pfalz, Germany

EXPERIENCE

- Lecturer at Production Engineering Department, The Sirindhorn International Thai-German Graduate School of Engineering (TGGS), King Mongkut's University of Technology North Bangkok, Thailand
Period of time: 01/10/09 – Today
- PE-Coordinator at Production Engineering Department, The Sirindhorn International Thai-German Graduate School of Engineering (TGGS), King Mongkut's University of Technology North Bangkok, Thailand
Period of time: 01/02/11 – 31/05/12
- Deputy Director for Research and academic Affair, The Sirindhorn International Thai-German Graduate School of Engineering (TGGS), King Mongkut's University of Technology North Bangkok, Thailand
Period of time: 01/06/12 – 14/11/12
- Vice President for Research and Academic Promotion, King Mongkut's University of Technology North Bangkok, Thailand
Period of time: 14/11/12 – Today

